

REPUBLIC OF CAMEROON

Peace - Work – Fatherland

MINISTRY OF PUBLIC WORKS

Publics National Advanced School of
Public Works

DEPARTMENT OF CIVIL
ENGINEERING



REPUBLIQUE DU CAMEROUN

Paix-Travail-Patrie

MINISTERE DES TRAVAUX PUBLICS

ECOLE NATIONALE SUPERIEURE
DES
TRAVAUX PUBLICS

DEPARTEMENT DU GENIE CIVIL



UNIVERSITÀ
DEGLI STUDI
DI PADOVA

NON-LINEAR STATIC AND LINEAR DYNAMIC ANALYSIS FOR
REINFORCED CONCRETE BUILDING AS COMPLEMENTARY
METHODS OF ANALYSIS AND DESIGN

*A thesis submitted in partial fulfilment of the requirements for the degree of Master of
Engineering (MEng) in civil Engineering*

Curriculum: **Structural engineering**

Presented by:

TATCHA KANKEU Yvan Loïc

Student number: **15TP20933**

Supervised by:

Prof. Carmelo MAJORANA

Co-supervised by:

Dr. Eng. Guillaume Hervé POH'SIE

Eng. Giuseppe CARDILLO

Members of jury:

President: **Prof. Carmelo MAJORANA**

Examiner: **Dr. Giscard Desting NIMPA**

Reporter: **Dr. Eng. Guillaume Hervé POH'SIE**

*Academic year
2019-2020*

DEDICATION

Dedicated to my parents KANKEU Fernand Désiré and KANKEU Brigitte Camille and to all my family in gratitude for all the support you have given me for the success of my studies and my achievements, for your presence and for all the love you give me every day.

ACKNOWLEDGEMENTS

This thesis is the fruit of the combined efforts of several individuals who contributed either directly or indirectly to its elaboration. It is therefore with gratitude that I address my sincere thanks to:

- **The President of the jury** for the honour of accepting to preside this jury;
- The **Examiner** of this jury for accepting to bring his criticisms and observations to ameliorate this work;
- My supervisors Prof. Eng. **Carmelo MAJORANA**, Dr Eng. **Guillaume Hervé POH'SIE** and Eng. **Giuseppe CARDILLO** for all the guidance, the advices and the patience provided to me during this work;
- Pr. **NKENG George ELAMBO** and Dr **BWEMBA Charles** for all their academic and administrative support during these five years spent at NASPW in this MEng program in partnership with University of Padua;
- Pr. **MBESSA Michel**, the Head of Department of Civil Engineering for tutoring and valuable advices;
- **All the teaching and administrative staff** of University of Padova and NASPW for their good quality of teaching and the motivation they developed in us to continue our studies;
- **All my classmates and my friends** of the 6th batch of MEng in The NASPW who were source of motivation and tenacity;
- My parents Mr **KANKEU Fernand Desiré** and Mrs **KANKEU NGOUANWOU Brigitte Camile** for the trust that they place in me and the efforts made for the accomplishment of this degree;
- My late grandparents Mr **YOUMBI Evariste** (2017) and Mrs **MADJO Antoinette** (2019) in memory of them;
- My brothers and sisters, **Gladys, Dorice, Romeo, Mégane, Annaëlle** and **Jovic**. Their presence, encouragement and support have been indispensable to this work;
- All the family, especially the **KANKEU** family, the **FONKOU** family, **KUITCHE TAKAM** and the **WABO** family for their encouragement, dedication and financial support during all these years;
- All my friends who have encouraged me throughout my school career and who continue to this day;
- All the people who, from near or far, helped me with all their heart to carry out this work.

GLOSSARY

LIST OF ABBREVIATIONS

3D	Three Dimensions
ASCE	American Society of Civil Engineers
ATC	Applied Technology Council
CCSZ	Central Cameroon Shear Zone
CP	Collapse Prevention
CQC	Complete Quadratic Combination
CVL	Cameroon Volcanic line
DCH	High Ductility Class
DCM	Medium Ductility Class
EN	European Norm
FEMA	Federal Emergency Management Agency
IO	Immediate Occupancy
LS	Life Safety
MDOF	Multiple Degree of Freedom
MPR	Mass participation ratio
NSP	Non-linear Static Procedure
PBE	Performance Base Engineering
RC	Reinforced Concrete
SAP	Structural Analysis Program
SEAOC	Structural Engineers Association of California
SDOF	Single Degree of Freedom
SLS	Service Limit State
SRSS	Square Root of Sum of Squares
SSI	Soil-Structure Interaction
SSZ	Sanaga Shear Zone
ULS	Ultimate Limit State

LIST OF SYMBOLS

A	Area of the cross section
A_c	Area of the concrete cross section
A_{min}	Minimum section area

A_s	Area of the steel reinforcement section
A_{sw}	Cross sectional area of the shear reinforcement
$C_{min,b}$	Minimum cover due to bond requirement
$C_{min,dur}$	Minimum cover due to environmental conditions
C_{min}	Minimum concrete cover
E	Young Modulus
E	Seismic action
E_m^*	Actual deformation energy
F_b	Shear force
\bar{F}	Normalized force
G1k	Structural load of the building
G2k	Non-structural load apply on the building
H	Total height of the building
I	Moment of inertia
K_s	Subgrade coefficient
MEd	Design bending moment
MRd	Resisting moment
MSd	Soliciting bending moment
M_t	Total mass of the superstructure
NEd	Design axial force
NRd	resisting axial force
L_p	Plastic hinge length
S	Soil factor
$S_d(T)$	Design response spectrum
$S_e(T)$	elastic response spectrum
S_r	Recovery area of the column
VEd	Design shear force
VRd,C	Design shear resistance of the member without shear reinforcement
a_g	Design ground acceleration
b	Width of the element
c	Concrete cover
d	Effective height of the section
d_r	Design inter-storey drift

dt	Target displacement
e	Eccentricity
f_{cd}	Design resisting strength of the concrete
f_{ctm}	Tensile strength of the concrete
f_{yd}	Design yielding strength of the steel
f_{yk}	Characteristic yield strength
f_{ywd}	Design yield strength of the shear reinforcement
m_i	Mass in the i -th storey;
n_r	Number of surfaces in contact
q_0	Basic value of the behaviour factor
$s_{l,max}$	Maximum longitudinal spacing
$s_{t,max}$	Maximum transversal spacing
g	Spectral acceleration
Φ_i	Normalized displacement
q	Behaviour factor
s	Spacing of the stirrups
t	Breadth of the support
x	Neutral Axis Position
$\Delta C_{dur,add}$	Add reduction of minimum cover for use of additional protection
$\Delta C_{dur,st}$	Reduction of minimum cover for use of stainless steel
$\Delta C_{dur,\gamma}$	Additive safety element
φ_{ef}	Effective creep ratio
γ	Specific weight
γ_c	Partial factor for concrete
γ_s	Partial safety factor for steel
$\Psi_{E,i}$	Combination coefficient for variable action
λ	Slenderness
λ_{lim}	Limit value of slenderness
σ_c	Stress in the concrete
σ_s	Stress in the reinforcement
ξ	viscous damping
Γ	Transformation factor

ABSTRACT

In order to respond to the emerging trend of performance-based design approaches and to improve design efficiency, the main objective of this thesis is to analyse the elastic and inelastic behaviour of reinforced concrete buildings under the effect of a weak earthquake, using linear dynamic analysis and non-linear static analysis, in order to predict its response for better design. This objective is achieved by using as a case study an existing 6-storey building located in Cameroon at the ENSTP of Yaoundé in the Centre region. A linear static analysis is first carried out on this building to determine its behaviour under vertical loading, i.e., solicitations and deflections, which are then used to design its structural elements. In order to show the limitations of this static design, a modal response spectrum analysis is performed to determine its elastic behaviour and elastic response when subjected to a relatively very weak earthquake taken according to the French standard. It appears that this building undergoes large displacements, the inter-storey drifts exceed the limit prescribed by Eurocode 8, the loads are enormous compared to what the structure can support, showing that this structure is not resistant. A new design is therefore carried out, taking into account its response to this earthquake. The result is an increase in the reinforcement and concrete cross-sections of the structural elements resulting in a reduction in the elastic response of the building in terms of storey displacement, which this time is within the limit prescribed by Eurocode 8. In order to determine its non-linear behaviour when subjected to the same seismic loading, a non-linear static analysis or pushover is applied to the redesigned building to determine its capacity curve and to deduce its ductility and target displacement. The latter is used to determine the maximum seismic loading that the building receives which allows the optimization of its structural elements. The results obtained show that when the building is designed as a non-linear system, part of the seismic load it receives is dissipated, which is demonstrated by the fact that the displacements of the floors, the inter-storey drifts and even the stresses on the structural elements are very low compared to those obtained when the building is considered perfectly elastic.

Keywords: Behaviour, capacity curve, ductility, response, target displacement, inter-storey drifts.

RESUME

Afin de répondre à la tendance émergente des approches de conception basées sur la performance et d'améliorer l'efficacité de la conception, l'objectif principal de ce mémoire est d'analyser le comportement élastique et inélastique des bâtiments en béton armé sous l'effet d'un faible tremblement de terre, en utilisant l'analyse dynamique linéaire et l'analyse statique non linéaire, afin de prédire sa réponse pour une meilleure conception. Cet objectif est atteint en utilisant comme étude de cas un bâtiment existant de 6 étages situé au Cameroun à l'ENSTP de Yaoundé dans la région Centre. Une analyse statique linéaire est d'abord effectuée sur ce bâtiment pour déterminer son comportement sous chargement vertical, c'est-à-dire les sollicitations et les déflexions, qui sont ensuite utilisées pour concevoir ses éléments structurels. Afin de montrer les limites de cette conception statique, une analyse modale spectrale est effectuée pour déterminer son comportement élastique et sa réponse élastique lorsqu'il est soumis à un séisme relativement très faible pris selon la norme française. Il apparaît que ce bâtiment subit de grands déplacements, les dérives inter-étages dépassent la limite prescrite par l'Eurocode 8, les charges sont énormes par rapport à ce que la structure peut supporter, montrant que cette structure n'est pas résistante. Une nouvelle conception est donc réalisée, en tenant compte de sa réponse à ce séisme. Le résultat est une augmentation du ferrailage et des sections de béton des éléments structuraux, ce qui entraîne une réduction de la réponse élastique du bâtiment en termes de déplacement d'étage, qui se situe cette fois dans la limite prescrite par l'Eurocode 8. Afin de déterminer son comportement non linéaire lorsqu'il est soumis à la même charge sismique, une analyse statique non linéaire ou Pushover est appliquée au bâtiment reconçu pour déterminer sa courbe de capacité et en déduire sa ductilité et son déplacement cible, ce dernier est utilisé pour déterminer la charge sismique maximale que le bâtiment reçoit, ce qui permet l'optimisation de ses éléments structuraux. Les résultats obtenus montrent que lorsque le bâtiment est conçu comme un système non linéaire, une partie de la charge sismique qu'il reçoit est dissipée, ce qui est démontré par le fait que les déplacements des étages, les dérives inter-étages et même les efforts sur les éléments structurels sont très faibles par rapport à ceux obtenus lorsque le bâtiment est considéré comme parfaitement élastique.

Mots clés : Comportement, courbe capacité, ductilité, réponse, déplacement cible, dérives entre étages.

LIST OF FIGURES

Figure 1. 1. Non-linear behavior of concrete and steel reinforcement.....	4
Figure 1. 2. Coignet Reinforced Concrete System.....	4
Figure 1. 3. Francois Coignet House, First House in reinforced concrete, built in 1853.....	5
Figure 1. 4. Concrete-Steel Rod Detailing, Hannebique System (1892)	5
Figure 1. 5. The first building in Paris constructed by Francois Hennebique built in 1893	6
Figure 1. 6. The Leland Stanford Jr. Museum in San Francisco (USA)	6
Figure 1. 7. Idealization of a SDOF structure	9
Figure 1. 8. Effective earthquake force: horizontal ground motion	10
Figure 1. 9. Mass-spring idealisation (5 degrees of freedom).....	11
Figure 1. 10. Finite element idealization of a 5-storey building (5 degrees of freedom).....	11
Figure 1. 11. Collapse of the Tacoma Narrows Bridge (1940)	15
Figure 1. 12. Heavily damaged buildings in Mexico City, 1985. (Image by David Tenenbaum)	15
Figure 1. 13. Failure that can occur when the p-delta effect is not taken into account (Mall Parking Structure Collapsed Sideways After 1994 Northridge Earthquake).....	17
Figure 1. 14. Performance objectives suggested by SEAOC (1995)	18
Figure 1. 15. Visualization of performance levels. (Personal communication with R. Hamburger.)	19
Figure 1. 16. Flow chart depicting the nonlinear dynamic analysis process (Improvement of Nonlinear Static Seismic Analysis Procedures, FEMA 440, June 2005).....	21
Figure 1. 17. Flow chart depicting the process followed in nonlinear static procedures (Improvement of Nonlinear Static Seismic Analysis Procedures, FEMA 440, June 2005)	22
Figure 1. 18. Matrix depicting possible inelastic seismic analysis procedures for various structural models (Improvement of Nonlinear Static Seismic Analysis Procedures, FEMA 440, June 2005)	22
Figure 1. 19. Seismicity map of Cameroon (Eloumala et al, 2014)	25
Figure 1. 20. Spatial distribution of seismic events in Cameroon (Eloumala et al, 2014).....	26
Figure 1. 21. Seismic mapping of Cameroon (https://thinkhazard.org/fr/report/45-cameroon/EQ_01/07/2021_at_19_h16)	27
Figure 2. 1. Shape of the horizontal elastic response spectrum (EN 1998-1)	32
Figure 2. 2. Illustration of the concrete cover on the section of a structural element	36

Figure 2. 3. Reduction of bending moment at the support (DJEUKOUA Laure, 2018).....	38
Figure 2. 4. Cross-section of beam.....	38
Figure 2. 5. Neutral axis	39
Figure 2. 6. Stress and strain distribution.....	39
Figure 2. 7. Section with biaxial bending.....	49
Figure 2. 8. Example of rectangular design chart (R. S. Narayanan and A. Beeby, Designer’s Guide to EN1992-1-1 and EN1992-1-2).....	50
Figure 2. 9. Column section	50
Figure 2. 10. Capacity curve	60
Figure 2. 11. Levels of damage described by a capacity curve.....	60
Figure 2. 12. Hinge location at the column and beam.....	61
Figure 2. 13. Force–deformation relationship of a typical plastic hinge.....	62
Figure 2. 14. Bilinear idealisation of the pushover curve of equivalent SDOF system	65
Figure 2. 15. Determination of the target displacement for the equivalent SDOF system	67
Figure 2. 16. Soil modelling by a linear springs system: (a) concentrated spring (b) distributed springs (Davidovici et al, 2013)	68
Figure 3. 1. Structural plan from RDC to storey 5 of the case study	72
Figure 3. 2. Repartition of building.....	72
Figure 3. 3. Beam selected for design	76
Figure 3. 4. Static schemes of beam study	77
Figure 3. 5. Load combinations.....	77
Figure 3. 6. Bending moment diagrams for 9 load combinations on the beam.....	78
Figure 3. 7. Shear force diagrams for 9 load combinations on the beam.....	78
Figure 3. 8. Envelope curve of the bending moment on the beam.....	79
Figure 3. 9. Envelope curve of shear force on the beam	79
Figure 3. 10. Design curve of the beam	79
Figure 3. 11. Verifications of the section under bending moment	80
Figure 3. 12. Verifications of the section under shear force	80
Figure 3. 13. Bending moment diagrams for SLS combination.....	81
Figure 3. 14. Envelope curve of SLS bending moment	81
Figure 3. 15. Concrete stress limitation.....	81
Figure 3. 16. Reinforcement stress limitation	82
Figure 3. 17. Most stressed columns in terms of bending moment.....	84

Figure 3. 18. Axial force diagrams for 15 combinations of loads in columns of row J-10.....	84
Figure 3. 19. Shear force diagrams V_{y-y} for 15 combinations of column J-10 in the y direction	84
Figure 3. 20. Shear force diagrams V_{x-x} for 15 combinations of column J-10 in the x-direction	85
Figure 3. 21. Bending moment diagrams M_{y-y} around Y for 15 combinations of loads in columns of row J-10.....	85
Figure 3. 22. Bending moment diagrams M_{x-x} around X for 15 combinations of loads in columns of row J-10.....	85
Figure 3. 23. Envelop curve of Axial force in column J-10.....	86
Figure 3. 24. Envelope curve of Shear forces V_{y-y} along Y in column J-10	86
Figure 3. 25. Envelope of Bending moment M_{y-y} around Y in columns J-10.....	86
Figure 3. 26. Envelope of Bending moment M_{x-x} around X in columns J-10.....	86
Figure 3. 27. Checking the columns with M-N interaction diagrams along the x-direction...	88
Figure 3. 28. Checking the columns with M-N interaction diagrams along the y-direction...	88
Figure 3. 29. Building modelling	89
Figure 3. 30. Natural Periods of the building for each vibration Mode	90
Figure 3. 31. Modal participating mass ratio.....	90
Figure 3. 32. First vibration mode of the structure, Translation along y.....	91
Figure 3. 33. Second vibration mode of the structure, Translation along x	91
Figure 3. 34. Third vibration mode of the structure, Torsion around z.....	91
Figure 3. 35. Cumulative Modal mass participating ratios	92
Figure 3. 36. The Response spectrum of earthquake motion	93
Figure 3. 37. Combination of seismic action.....	94
Figure 3. 38. Determination of acceleration of structure at the ground	94
Figure 3. 39. Acceleration of the structure at the level of the ground.....	95
Figure 3. 40. Deformed shape of the structure in the X-Z view.....	96
Figure 3. 41. Deformed shape of the structure in the Y-Z view.....	96
Figure 3. 42. The reference vertical element for determining the storeys displacement	97
Figure 3. 43. Storey displacement in the x direction.....	97
Figure 3. 44. Storey displacement in the y direction.....	97
Figure 3. 45. Inter-storeys drifts.....	98
Figure 3. 46. Envelope curve of solicitations on the beams of frame 10 of block A.	98
Figure 3. 47. New envelope curve of bending moment of the beam	99

Figure 3. 48. New envelope curve of Shear of the beam	99
Figure 3. 49. Comparison of seismic bending moment and the resisting moment of the statically designed beam	99
Figure 3. 50. Comparison of seismic Shear force and the resisting Shear of the statically designed beam	100
Figure 3. 51. Envelope curve of bending moments on column row L-4.....	100
Figure 3. 52. Envelope curve of Axial force on the columns of row L-4 due to seismic combinations load	101
Figure 3. 53. Envelope curve of Shear force on the columns of row L-4 due to seismic combinations load	101
Figure 3. 54. Envelope curve of Bending moment around y direction on the columns of row L-4 due to seismic combinations load	101
Figure 3. 55. Envelope curve of Bending moment around x direction on the columns of row L-4 due to seismic combinations load	101
Figure 3. 56. Control of new columns in the M-N interaction diagram of statically designed columns in the x-direction.....	102
Figure 3. 57. Control of new columns in the M-N interaction diagram of statically designed columns in the y-direction.....	102
Figure 3. 58. Verification of the new section under bending moment due to static and dynamic loading.....	103
Figure 3. 59. Verification of the new section under Shear force due to static and dynamic loading.....	103
Figure 3. 60. Checking the new columns with M-N interaction diagrams along the x-direction	105
Figure 3. 61. Checking the new columns with M-N interaction diagrams along the y-direction	105
Figure 3. 62. Shear verification on column row L-4	106
Figure 3. 63. Natural Periods of the new structure for each vibration Mode	106
Figure 3. 64. Deformed shape of the structure in the X-Z view.....	107
Figure 3. 65. Deformed shape of the structure in the Y-Z view.....	108
Figure 3. 66. New storey displacement in the x direction.....	108
Figure 3. 67. New storey displacement in the y direction.....	108

Figure 3. 68. New inter-storey drifts	109
Figure 3. 69. Foundation plan	109
Figure 3. 70. Modelling of structure with spring constraints	110
Figure 3. 71. Natural periods of the building with different base constraints	110
Figure 3. 72. Envelope curve of storey displacement in the x direction	111
Figure 3. 73. Envelope curve of storey displacement in the y direction	111
Figure 3. 74. Inter-storey drift in the x direction	111
Figure 3. 75. Inter-storey drift in the y direction	112
Figure 4. 1. Structural model of the building with affected plastic hinge	113
Figure 4. 2. Definition of the properties of the hinge for beams	114
Figure 4. 3. Definition of the properties of the hinge for columns	114
Figure 4. 4. Capacity curve in the x direction of the building	115
Figure 4. 5. Capacity curve in the y direction of the building	115
Figure 4. 6. State of the building at the fifth registration of analysis in the x direction	116
Figure 4. 7. State of the building at the tenth registration of analysis in the x direction	117
Figure 4. 8. State of the building at the seventeenth registration of analysis in the x direction	117
Figure 4. 9. State of the building at the twentieth registration of analysis in the x direction	118
Figure 4. 10. State of the building at the seventy-seventh registration of analysis in the x direction	118
Figure 4. 11. State of the building at the seventh registration of analysis in the y direction	119
Figure 4. 12. State of the building at the eleventh registration of analysis in the y direction	119
Figure 4. 13. State of the building at the Sixteenth registration of analysis in the y direction	119
Figure 4. 14. Idealized bilinear capacity curve in the x direction of Equivalent SDOF system	120
Figure 4. 15. Idealized bilinear capacity curve in the y direction of Equivalent SDOF system	121
Figure 4. 16. Solicitation on the beams of frame 10 when the load is in the positive x-direction	122
Figure 4. 17. Optimal envelop curve of bending moment of beams	122
Figure 4. 18. Optimal envelop curve of shear force of beams	123

Figure 4. 19. Bending moment verification of the designed beam using non-linear static analysis.....	123
Figure 4. 20. Shear verification of the designed beam using non-linear static analysis	124
Figure 4. 21. Bending moment on columns of frame 10 when the load is in the positive x and y direction.....	124
Figure 4. 22. Optimal axial forces diagram of the columns in row 4-L.....	125
Figure 4. 23. Optimal shear force V_{y-y} diagram of the columns in row 4-L in the y- direction	125
Figure 4. 24. Optimal shear force V_{x-x} diagram of the columns in row 4-L in the x-direction	125
Figure 4. 25. Optimal bending moment M_{y-y} diagram of the columns in row 4-L in the y- direction.....	125
Figure 4. 26. Optimal bending moment M_{x-x} diagram of the columns in row 4-L in the x- direction.....	126
Figure 4. 27. Verification of the M-N interaction in the x direction of the columns	127
Figure 4. 28. Verification of the M-N interaction in the y direction of the columns	127
Figure 4. 29. Shear verification on column row 4-L	127
Figure 4. 30. The inter-storeys drift	128
Figure 4. 31. Capacity curve of the building in the x direction.....	128
Figure 4. 32. Capacity curve of the building in the y direction.....	129
Figure 4. 33. First plastic mechanism in the x-direction	129
Figure 4. 34. First plastic mechanism in the y-direction	130

LIST OF TABLES

Table 1. 1. Past Seismic events in Cameroon (Plan national de contingence Cameroun, 2011)	28
Table 2. 1. Basic value of the behaviour factor, q_0 , for systems regular in elevation	33
Table 2. 2. Value of β	51
Table 2. 3. Values of modulus of subgrade reaction for different type of soil	69
Table 3. 1. Concrete characteristics	73
Table 3. 2. Reinforcement characteristics	74
Table 3. 3. structural permanent load	74
Table 3. 4. Non-structural permanent load at storey level due to slab	75
Table 3. 5. Non-structural permanent load due to wall and exterior cladding	75
Table 3. 6. Non-structural permanent loads at roof level	75
Table 3. 7. Deflection control	82
Table 3. 8. Preliminary design of columns	83
Table 3. 9. Longitudinal reinforcement of columns	87
Table 3. 10. Verification of minimum and maximum quantity of steel	87
Table 3. 11. Selected Mode	92
Table 3. 12: The base shear	95
Table 3. 13. Section of new columns with longitudinal reinforcement	104
Table 3. 14. Verification of minimum and maximum quantity of steel	104
Table 3. 15. The new useful mode of vibration	107
Table 4. 1. Weight and normalized displacement of each storey	120
Table 4. 2. Determination of the target displacement	121
Table 4. 3. Optimised column section with longitudinal reinforcement	126
Table 4. 4. Verification of minimum and maximum quantity of steel	126

TABLE OF CONTENTS

DEDICATION	I
ACKNOWLEDGEMENTS	II
GLOSSARY	III
ABSTRACT	VI
RESUME.....	VII
LIST OF FIGURES.....	VIII
LIST OF TABLES	XIV
TABLE OF CONTENTS	XV
GENERAL INTRODUCTION	1
CHAPITRE 1 : LITTERATURE REVIEW.....	2
INTRODUCTION	2
1.1. REINFORCED CONCRETE BUILDING	2
1.1.1. Material	2
1.1.2. Brief history of reinforced concrete building design	4
1.2. ANALYSIS OF REINFORCED CONCRETE BUILDINGS	7
1.2.1. Linear analysis	7
1.2.2. Non-linear analysis	16
1.3. EARTHQUAKE IN CAMEROUN	25
1.3.1. Seismic region in Cameroon	25
1.3.2. Recent seismic events in Cameroon	27
CONCLUSION	28
CHAPITRE 2 : METHODOLOGY	29
INTRODUCTION	29
2.1. SITE RECOGNITION	29
2.2. SITE VISIT	29
2.3. DATA COLLECTION	29
2.4. CODES AND STANDARDS	29
2.5. EVALUATION PROCEDURE OF ACTIONS OF THE BUILDING	30
2.5.1. Permanent action.....	30

2.5.2. Variable action	30
2.5.3. Combination of action.....	34
2.6. MATERIAL, DURABILITY AND CONCRETE COVER	35
2.7. LINEAR STATIC ANALYSIS	36
2.7.1. Design of beam	36
2.7.2. Design of columns	46
2.8. LINEAR DYNAMIC ANALYSIS	54
2.8.1. The modal analysis	54
2.8.2. The Multi-modal response spectrum analysis.....	55
2.9. NON-LINEAR STATIC ANALYSIS.....	58
2.9.1. Principle and purpose of analysis	59
2.9.2. Description of analysis.....	59
2.9.3. Method of analysis	61
2.9.4. The capacity curves.....	64
2.9.5. Target displacement	64
2.10. SOIL-STRUCTURE INTERACTION	67
2.10.1. Evaluation of the footing section	68
2.10.2. Evaluation of the stiffness for each footing class	68
CONCLUSION	69
CHAPITRE 3 : LINEAR ANALYSES AND INTERPRETATION OF RESULTS.....	70
INTRODUCTION	70
3.1. GENERAL PRESENTATION OF THE SITE	70
3.1.1. Geology and relief.....	70
3.1.2. Climate and hydrology.....	71
3.2. PRESENTATION OF THE PROJECT	71
3.2.1. Geometry of the building	71
3.2.2. Architectural and structural plan.....	71
3.2.3. Material properties	72
3.3. LINEAR STATIC ANALYSIS AND DESIGN	74
3.3.1. Action on the building	74
3.3.2. Durability and concrete cover	75
3.3.3. Design of beam	76
3.3.4. Design of column.....	83

3.4. LINEAR DYNAMIC ANALYSIS	89
3.4.1. Modal analysis	89
3.4.2. Response spectrum analysis.....	93
3.4.3. Redesign and new building response	102
3.4.4. When taking into account soil-structure interaction	109
CONCLUSION	112
CHAPITRE 4 : PUSHOVER ANALYSIS AND INTERPRETATION OF RESULTS	113
INTRODUCTION	113
4.1. MODELLING OF THE STRUCTURE.....	113
4.2. LATERAL LOAD PATTERN	114
4.3. RESULTS OF THE PUSHOVER ANALYSIS	115
4.3.1. Capacity curve	115
4.3.2. Plastic mechanism.....	116
4.4. TARGET DISPLACEMENT	120
4.5. OPTIMIZATION OF THE STRUCTURAL ELEMENT	122
4.5.1. Beams.....	122
4.5.2. Columns	124
4.6. THE INTER-STOREY DRIFTS	128
4.7. WHEN TAKING INTO ACCOUNT SOIL-STRUCTURE INTERACTION	128
CONCLUSION	130
GENERAL CONCLUSION	131
BIBLIOGRAPHY	133
APPENDIX	136
APPENDIX A. TABLES FOR METHODOLOGY	136
APPENDIX B. STRUCTURAL AND ARCHITECTURAL PLAN	140
APPENDIX C. DETAILING OF STRUCTURAL ELEMENTS.....	142
APPENDIX C1. Detailing of the beam	142
APPENDIX C2. Detailing of column	145

GENERAL INTRODUCTION

Recently, following repeated building collapses in Cameroon, building safety has become a topic of considerable interest. In Europe and America, engineers are now opting for performance-based designs to improve the performance and life span of buildings, ensure their safety and minimise the risk of collapse due to natural disasters such as earthquakes.

In Cameroon, most existing reinforced concrete buildings are designed for vertical loads only, which does not provide any safety against possible earthquakes. In view of the recent seismic events of 2002 and 2005 that shook some localities in the southern and central regions of the country, it is important to realise that this disaster, even if the probability is low, can happen again and damage buildings that were designed without taking this into account. Measures must therefore be taken for new and existing buildings to avoid or limit their damage. Hence the importance of this study which analyses the elastic and inelastic behaviour of reinforced concrete buildings under the effect of an earthquake using linear dynamic and non-linear static analysis procedures to predict their responses for better design.

In order to achieve this objective, this study, focused on three main analyses including linear static analysis and linear dynamic analysis for the elastic response and nonlinear static analysis for the inelastic response, is divided into 4 chapters. The first chapter, which is the literature review, presents the seismic regions of Cameroon, the importance and the work done on the evaluation of the behaviour of reinforced concrete structures using these three types of analysis. The second chapter, the methodology, presents the procedures and methods that will be used to carry out these different analyses and the last two chapters present respectively the results and interpretations of the linear analysis and those of the non-linear static analysis.

CHAPITRE 1 : LITTERATURE REVIEW

Introduction

Several scientists and civil engineers such as Anil K. Chopra, Rakesh K. Goel, Ray W. Cough and Joseph Penzien have revolutionised structural engineering by studying the dynamic and static behaviour of structures in the elastic and inelastic domains. This chapter is devoted to the study of the work carried out on the evaluation of the behaviour of reinforced concrete structures by using linear dynamic analysis and non-linear static analysis. A brief description of the seismic regions and recent earthquakes in Cameroon is presented for the application of these analyses on a real concrete building in Cameroon.

1.1. Reinforced concrete building

After the discovery of reinforced concrete in 1867, the explosion of reinforced concrete construction was born, houses built in reinforced concrete, buildings, bridges, retaining walls, etc. When we spoke about construction, we immediately had the word concrete in our mouths because it is a material very resistant in compression, easy to handle and can take any shape we want to give it.

1.1.1. Material

Reinforced concrete is a composite building material made of concrete and steel rebars that combines the complementary mechanical properties of these materials (good compressive strength of concrete and good tensile strength of steel).

1.1.1.1. Concrete

Concrete is a building material composed of cement, fine aggregate (sand) and coarse aggregate mixed with water, which hardens over time. Concrete is widely regarded as the most popular building material, as it offers a variety of benefits through its properties.

a. Mechanical properties

This material works well in compression, and knowledge of its mechanical properties is essential for the design of structures. Quite often, many concrete professionals consider that the essential characteristic of hardened concrete is its mechanical strength in compression at a given age (28 days). The tensile and flexural strength of concrete is much lower than its compressive strength, as shown in **Figure 1.1 a)**, concrete is not resistant in tension.

b. Durability

Concrete is the most widely used material in the world, mainly due to its durability and strength, it can withstand almost any climate and is resistant to erosion, rot and rust, which means it requires minimal maintenance. It can outlast wood and other common building materials and its strength improves over time.

c. Sustainability

Concrete is environmentally friendly throughout the construction process, from raw material production to demolition. This certainly contributes to its popularity as a building material, now that the building culture is moving towards more sustainable and environmentally friendly construction.

d. Malleability

Concrete is malleable when wet and solid when hardened, making it extremely versatile. As concrete can be poured, it can be moulded into any desired shape. For this reason, concrete is commonly used for foundations, roads and bridges.

1.1.1.2. Steel rebars

Reinforcing steel bar has long been used as a reinforcing agent for concrete. It is made from a combination of different permits and steel grades. The outside of each steel bar has ridges. These ridges allow the concrete to adhere to the rebar so that it does not slip inside the slab. It has several properties that make it an excellent choice for reinforcing concrete structures.

a. Mechanical properties

This material works very well in compression and tension as shown in **figure 1.1. b)**. But in reinforced concrete elements, its main role is to resist bending and shearing forces, the concrete already plays the role of resisting compression.

b. Thermal properties

The modulus of thermal expansion of steel reinforcement is very similar to that of concrete. Due to the similarity of concrete and steel thermal properties additional stresses or deflections are not introduced upon heating the concrete structure.

c. Strength retention

Under heating from fire, steel is able to withstand high temperatures before strength and ductility properties change. Many concrete structures that have been subjected to fire can be rehabilitated using the existing reinforcing steel

d. Joining

Steel reinforcement can be joined using welding or couplers that have strengths similar to that of the reinforcing steel.

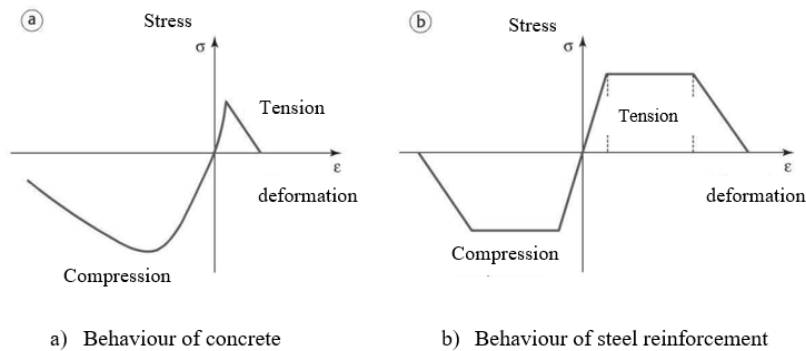


Figure 1. 1. Non-linear behavior of concrete and steel reinforcement

1.1.2. Brief history of reinforced concrete building design

The use of binders in construction began 2000 years ago with the Romans, who used quicksilver. In 1845, the French gardener Joseph-Louis Lambot had the idea of using wire and mortar to make orange tree boxes and tanks (in 1845), and then a boat (in 1849). This was the discovery of the use of steel as reinforcement, marking the creation of reinforced concrete and its use in building construction.

1.1.2.1. The progress of the design in Europe

In 1867, the French industrialist **Francois Coignet**, published a book describing many applications and uses of reinforced concrete.

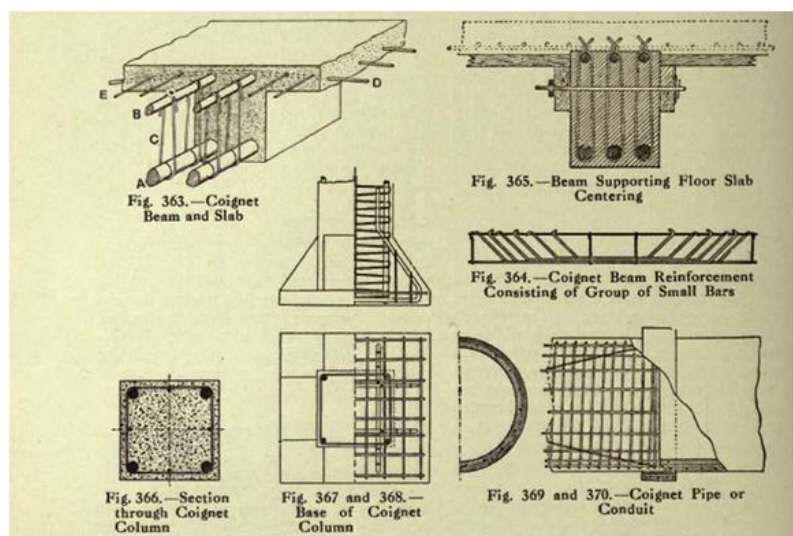


Figure 1. 2. Coignet Reinforced Concrete System



Figure 1. 3. Francois Coignet House, First House in reinforced concrete, built in 1853

Between 1891 and 1894, several European researchers published theories and test results, including Professor Moller (Germany), Robert Wunsch, 1884 (Hungary - builder), Josef Melan 1892, (Austria - professor/engineer, the inventor of the Melan system (dragon bridge), the German G. A. Wayss, the first engineer who developed a theory and then provided formulas and design methods, the Frenchman François Hennebique who made in 1892 the first reinforced concrete slab and demonstrated the usefulness of stirrups to strengthen beams against shear (see **Figure 1.4**).

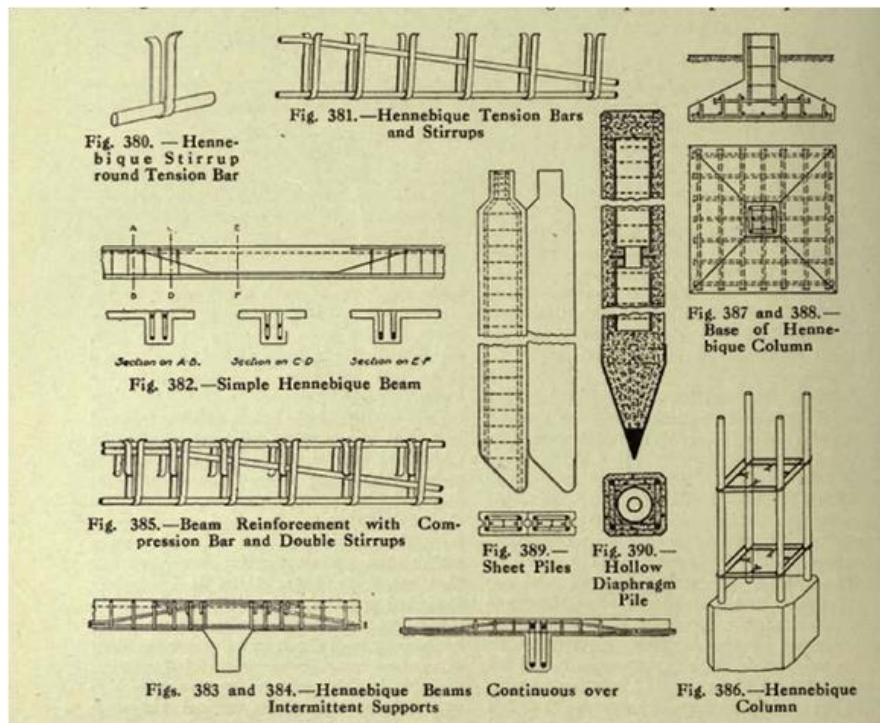


Figure 1. 4. Concrete-Steel Rod Detailing, Hannebique System (1892)



Figure 1. 5. The first building in Paris constructed by Francois Hennebique built in 1893

Around 1976, in order to harmonise construction techniques and to facilitate the free access of companies to the markets, the Eurocodes were developed. They will be the main means of designing building structures and civil engineering works. The Eurocodes programme was completed in 2005 and contains 60 codes grouped into 10 families, from Eurocode 0 to Eurocode 9.

1.1.2.2. The progress of the design in America

In the United States, the pioneers were **Thaddeus Hyatt**, who conducted experiments on reinforced concrete beams in the 1850s. However, Hyatt's experiments remained unknown until 1877, when his work was published privately. **Ernest L. Ransome** was the first to use and patent the deformed (twisted) bar in 1884. In 1890, Ransome built the Leland Stanford Jr. Museum in San Francisco, a two-storey, 95-metre-long reinforced concrete building. Since that time, the development of reinforced concrete in the United States has been rapid.

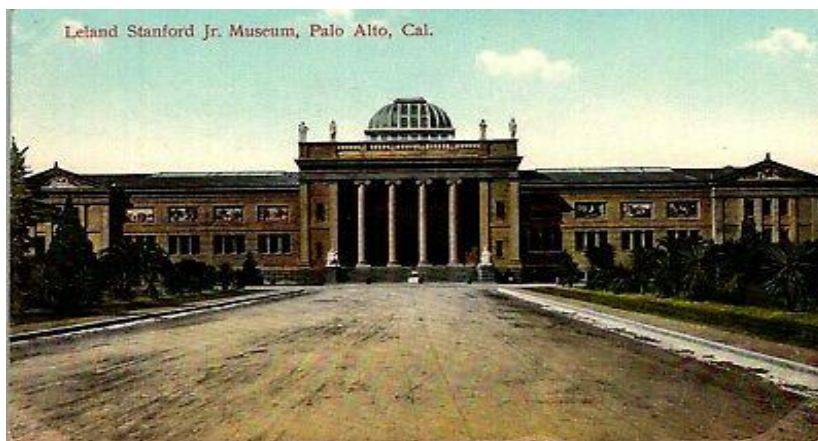


Figure 1. 6. The Leland Stanford Jr. Museum in San Francisco (USA)

In 1904, the American Concrete Institute (ACI) Foundation was established to promote progress, innovation and collaboration in the concrete industry through strategic investments in research, grants and ideas.

In 1906, with the damage caused by the San Francisco, California earthquake (magnitude 7.9), engineers conducted extensive research and revised design methodology, thus beginning earthquake engineering with elastic dynamic analysis and later inelastic analysis.

1.2. Analysis of reinforced concrete buildings

A reinforced concrete building is a combination of structural and non-structural elements. The structural elements are the load-bearing elements of the structure, the elements that participate in its resistance, without them the building does not exist. All of these elements combined form the skeleton of the building. They are made up of columns, beams, slabs, walls, if there are any, and foundations. The non-structural elements are secondary elements which do not participate directly or almost not directly in the resistance of the structure. We have among other things the filling walls, the covers of roof, etc.

There are different approaches to analyse a reinforced concrete building depending on its importance and the actions to which it is or will be subjected.

1.2.1. Linear analysis

To perform the Linear analysis, some assumptions have to be made:

- The deformations remain in the elastic domain (small deformation)
- The stiffness of elements is constant;
- The changes of geometry due to displacement are assumed to be small and therefore, can be ignored;
- Original or undeformed state is use as the reference state.

Depending of the action, we can perform static or dynamic analysis.

1.2.1.1. Linear static analysis

Linear static analysis (LSA) is the basic form of analysis done to study about the response of a building. This analysis is one where a linear relationship exists between the applied forces and displacements. In practice, this applies to structural problems where the stresses remain in the linear elastic range of the material used. In a linear static analysis, the stiffness matrix of the model is constant, and the solution process is relatively short compared to a non-linear analysis on the same model, the structural analysis incorporates only linear elastic materials and small

deformation theory, buckling phenomena are not included in the model but are assessed through examination of the output. Inertial forces are not considered.

In structural design, linear static analysis is used to determine the stresses on structural elements when they are subjected to loads, usually static loads. Static analysis is very important, as it is the basis for all other analyses, and is simple to perform. For a first estimation, linear static analysis is often used before performing a full non-linear analysis and is also often used in linear dynamic analysis.

1.2.1.2. Linear dynamic analysis

Dynamic analysis is carried out when the structure is likely to be loaded by a dynamic action such as earthquake, wind actions, etc.

a. Dynamic behaviour

A mechanical vibration is the motion of a particle or a body which oscillates about a position of equilibrium. It generally results when a system is displaced from a position of stable equilibrium and tends to return to this position under the action of restoring forces (either elastic forces, as in the case of a mass attached to a spring, or gravitational forces, as in the case of a pendulum).

i. Free vibration

A structure is said to be undergoing free vibration when it is disturbed from its static equilibrium position and then allowed to vibrate without any external dynamic excitation. In this case the dynamic properties (period, frequency, mode shape) of the system are said to be “natural”. Because the system is linear, these dynamic properties are independent of the initial displacement and velocity.

ii. Forced vibration

When an external force is applied to the system, the resulting motion is described as a forced vibration. The external force can be a periodic force, in this case the motion is called harmonic or periodic vibration.

Depending on the characteristics of the system studied and the external environment of the system, the motion can be with or without damping. In reality there is no system without damping, all vibration is actually damped to some degree. The reinforced concrete buildings are damped systems and their damping factor is about 5%.

b. Degree of freedom system

The degree of freedom is the possibility for a given system to undergo a translation or a rotation. In principle an element of system has 6 degrees of freedom in space, 3 translations in planes and 3 rotations with respect to the 3 axes of space. The bonds suppress the degrees of freedom. Under earthquake, the structures are considered as deformable and all the oscillating masses which compose them (construction elements) can possibly keep their 6 degrees of freedom. The nature of the elements and their connections will condition the relevance of the degrees of freedom taken into account during an analysis.

i. Single-Degree-Of-Freedom (SDOF) system

Each element of the real structure contributes to the inertia (mass), stiffness and energy dissipation (damping) properties of the structure. To facilitate the study of its dynamic behaviour, a structure can be idealized as a finite element by a set of masses (representing all the mass of the structure) connected together by frame or bar elements (representing the stiffness of the structure) to which dampers (representing the damping of the structure) have been added (see **Figure 1.7 a**). The same system can be idealized by a system of mass (representing all the mass of the structure) and spring (representing the stiffness of the structure) with a damper if the system is damped (see **figure 1.7 b**).

The number of independent displacements required to define the displacement positions of all the masses relative to their initial position is called the number of degrees of freedom (DOF) for dynamic analysis (lateral displacement). When the dynamism of the system allows only one independent displacement defining the displacement of all masses, the system is called single degree of freedom (SDOF) system (see **figure 1.7**). The idealization allows to easily determine the dynamic properties of the structure through the establishment of its equation of motion.

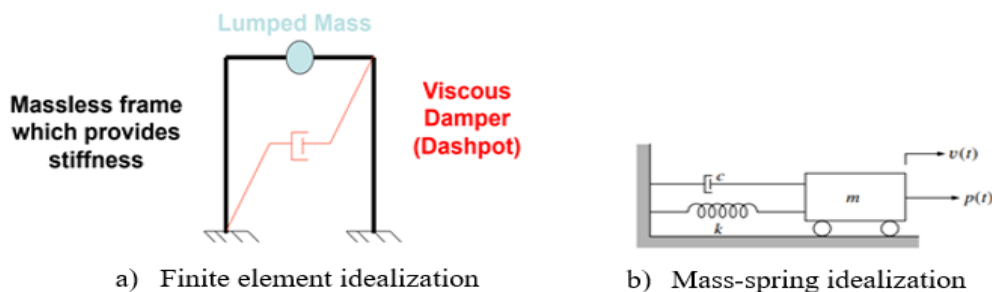


Figure 1. 7. Idealization of a SDOF structure

The equation of motion is a mathematical equation describing the motion of a physical object. In general, the equation of motion includes the acceleration of the object as a function

of its position, velocity, mass and any variables affecting any of these. There are several methods to determine it, among which, Newton's second law and the method of conservation of mechanical energy of the system.

1) For undamped free vibration of SDOF system

The equation of motion is:

$$\ddot{u}(t) + \frac{k}{m}u(t) = 0 \tag{1.1}$$

Where:

$u(t)$ and $\ddot{u}(t)$ are the displacement and the acceleration of the system respectively;

k is the rigidity of the system;

m is the total mass of the system.

The solution of equation (1.1) allows to obtain the natural dynamic properties of the SDOF system such as natural period T and frequency ω given by equation (1.2), and the mode shape Φ defined by equation (1.3).

$$\omega^2 = \frac{k}{m} , \quad T = 2\pi\sqrt{\frac{m}{k}} \tag{1.2}$$

$$\Phi(k - m\omega^2) = 0 \tag{1.3}$$

2) For damped free vibration of SDOF system

$$\ddot{u}(t) + c\dot{u}(t) + \frac{k}{m}u(t) = 0 \tag{1.4}$$

Where c is the damped coefficient and $\dot{u}(t)$ the velocity of the system

3) For undamped forced vibration

$$m\ddot{u}(t) + ku(t) = F(t) \tag{1.5}$$

Where $F(t)$ is the force that excites the system, this force can be the load due to seismic action.

The seismic action transmits to the base of the structure an action in the form of acceleration which acts on the building in the form of an inertial force $P_{eff}(t)$.

$$F(t) = P_{eff}(t) = -m\ddot{u}_g(t) \tag{1.6}$$

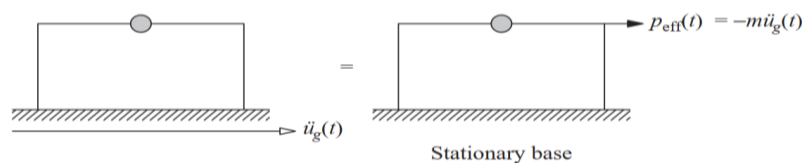


Figure 1. 8. Effective earthquake force: horizontal ground motion

ii. Multiple degree of freedom system

In the case of MDOF, the dynamism of the system allows many independent displacements defining the movements of all masses. This case perfectly represents buildings of more than 1 level subjected to a dynamic load.

The idealization of these systems is done in the same way as the SDOF system, a finite element model consisting of superposed frame elements representing the stiffness of each floor and masses representing the masses of each level (see **figure 1.10**). A mass-spring model consisting of several springs in series, each spring representing the stiffness of each floor (see **figure 1.9**).

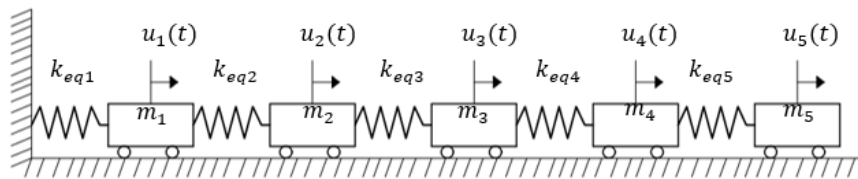


Figure 1. 9. Mass-spring idealisation (5 degrees of freedom)

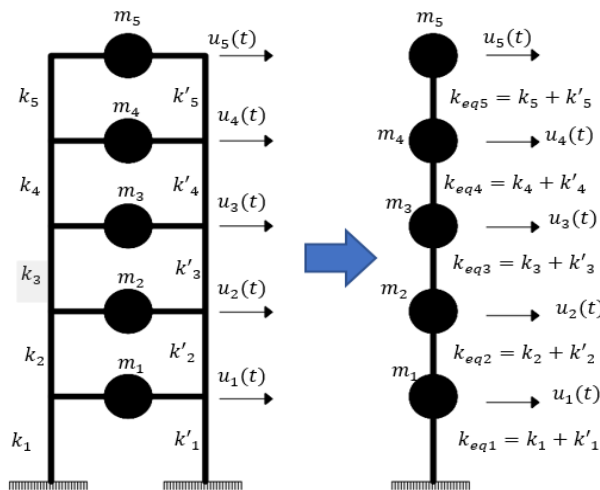


Figure 1. 10. Finite element idealization of a 5-storey building (5 degrees of freedom)

The equation of motion of the MDOF system, as well as the SDOF, can be determined using the second law of Newton or the law of conservation of mechanical energy.

Idealization assumes that a structure behaves like a harmonic oscillator with one or more degrees of freedom, allowing to establish the equation of motion of the structure and thus to determine its dynamic characteristics such as period and frequency and shape modes (simple modal analysis). But the idealization of this certain building does not allow to observe or to study correctly its dynamic behaviour, for that a more detailed idealization in 3 dimensions is necessary and the process allowing to study the dynamic behaviour in this case is the Modal analysis.

c. Modal analysis

Modal analysis is an indispensable tool in understanding the dynamics behaviour of structures, how structures and objects vibrate and how they resist to applied forces. Modal analysis is the process of determining the inherent dynamic characteristics of a system in forms of natural frequencies, damping factors and mode shapes, and using them to formulate a mathematical model for its dynamic behaviour. (Jimin He, and Zhi-Fang Fu, in *Modal Analysis*, 2001). Modal analysis methods are relatively recent investigative methods, which have been implemented to establish and/or improve the knowledge of the dynamic model of real structures. The modal analysis will allow the calculation of eigenvalues and their associated values (eigen pulses, eigenfrequencies or eigen periods), precision, eigenvectors, participation coefficients and participating masses for the study of the structure's vibrations (free or excited).

i. Brief background of Modal analysis

In the history of modal analysis, the conception of modes of vibration dates back to the 18th century and the pioneering studies and debates of Daniel and John Bernoulli, Euler and d'Alembert (see Kline 1990) who, while studying the problem of the vibration of a stretched string, invented the notion of modal contributions of form that constitute the set of observed oscillations. This revolutionary vibrational knowledge for the time, as well as a systematic treatment and practical extensions of the themes of modal analysis, more focused on continuous systems, first appeared in a very concerted way in Lord Rayleigh's landmark book "Theory of Sound" (1877).

Much later, today, the term modal analysis is used in a different context in engineering parlance, depending on the engineering domain and application, ranging from simple eigenvalue analysis, which recovers the frequencies and shapes of normal modes, to complex experimental identification of dynamic properties. Its typical definition, closest to earthquake engineering, refers to the set of theoretical tools and operations used to simplify the calculation of the dynamic response of a very large extended structural system under a generic time-dependent load. A much broader picture of modal analysis encompassing, in addition to the above aspects, a vast experimental background that makes an invaluable contribution to the understanding, improvement and control of structures, relates mainly to mechanical engineering. This latter overview was first captured in a very holistic way by the publication of a seminal book by **Ewins** (*Modal Testing, Theory and Practice*, 1984), which was subsequently followed by similar influential titles such as those by his students **Maia et al.** (*Theoretical and Experimental Modal Analysis*, 1997) and **Jimin He** and **Zhi-Fang Fu** (*Modal analysis*, 2001). Professor **John Biggs** (*Introduction to Structural Dynamics*, 1964), Professor **Ray W. Clough**

“Nonlinear static and linear dynamic analysis for reinforced concrete building as complementary method of analysis and design”

Master in civil engineering defended by: TATCHA KANKEU Yvan Loïc, NASPW Yaoundé, 2019-2020

and civil engineer **Joseph Penzien** (*Dynamic of structure*, 1993), and **Anil K. Chopra** (*Dynamic of structure, theory and application to earthquake engineering*, 1995) have contributed immensely in the application and understanding of this analysis.

ii. The importance of modal analysis

Modal analysis is an important tool for identifying and solving structural vibration problems. It identifies the natural frequencies, damping coefficients and mode shapes of the structure that allow the determination of common vibration problems when an excitation function interacts with the natural frequency of the structure. When the excitation force is known to coincide with one of the natural frequencies found in the modal analysis, the structure can be redesigned or modified to move the natural frequency away from the excitation frequency. Structural elements can be added to increase the stiffness of the structure or the mass can be increased or decreased. By doing this, the excitation frequency will no longer fall on the natural frequency of the structure. These techniques can be applied to move the natural frequencies away from the frequency of the excitation force.

1.2.1.3. Elastic seismic analysis

In general, linear procedures are applicable when the structure is expected to remain nearly elastic for the level of ground motion of interest or when the design results in nearly uniform distribution of nonlinear response throughout the structure. There are several methods for elastic seismic analysis, the simplest is Modal response spectrum analysis.

a. Modal response spectrum analysis

In earthquake engineering, after studying the modal analysis of a structure to determine the modes of vibration and the natural frequencies of the structure, we apply what is called “the modal response spectrum analysis.”

The response spectrum analysis is a linear dynamic analysis method that measures the contribution of each natural mode of vibration to indicate the maximum probable seismic response of a structure considered essentially elastic. It gives an overview of the dynamic behaviour by measuring the acceleration, velocity or pseudo-spectral displacement as a function of the structural period for a given history and damping level.

b. The purpose of modal response spectrum analysis

The modal response spectrum analysis is a very important in earthquakes engineering, this analysis method allows to obtain the response of a structure to dynamic loading and to get a better insight into the performance of the building and the requirements of the structure not only in terms of shear at the base, but also in terms of shear in the floors and moment in the

building. In a very simple way, in addition to the deformations of the structure, it allows to determine the solicitations that are created on the structure due to the dynamic load. The modal response spectrum analysis allows a clear understanding of the contributions of the different vibration modes.

1.2.1.4. Limit of elastic analysis

Although elastic analysis gives a good indication of the elastic capacity of structures and shows where deformation may occur first, it cannot account for the redistribution of forces during the progressive deformation that follows and predict its failure mechanisms, or detect the possibility and location of any premature failure.

1.2.1.5. Practical example for dynamic analysis

There are several examples of disasters where a prior accurate modal analysis could have prevented loss of lives and property

a. Tacoma Narrows Bridge Disaster of 1940

The Tacoma Narrows Bridge was built in Washington state in the 1930s and opened to traffic on July 1, 1940. It spans the Puget Sound from Gig Harbor to Tacoma, which is 40 miles south of Seattle. The canal is about a mile wide where the bridge crosses the Sound. Thin and slender, it was the third longest suspension bridge in the world at the time, with a length of 5,959 feet or about 1,820 m. On November 7, high winds buffeted the area and the bridge swayed considerably. The first failure came at about 11 a.m. The bridge rocked back and forth wildly. Even though the bridge towers were made of strong structural carbon steel, the bridge proved no match for the violent movement, and collapsed.

Investigations Following the collapse, it was revealed that engineers had not properly considered the aerodynamic forces that were at play at this location during a period of high winds. At the time of construction, these forces were not routinely considered by engineers and designers, and later tests revealed that the bridge was vulnerable to wind-generated vibrations. When the bridge was subjected to high winds from a certain direction, the frequency oscillations increased to the point that collapse was inevitable.



Figure 1. 11. Collapse of the Tacoma Narrows Bridge (1940)

b. Mexico City Earthquake of 1985

Another concrete example is the 19 September 1985 earthquake in Mexico City. This powerful 8.1 magnitude earthquake killed more than 10,000 people, injured another 30,000 and left a quarter of a million people homeless. The energy released by the earthquake was equivalent to 1114 nuclear detonations, and the quake was felt as far away as Los Angeles, more than 800,000 km away. Until the 1950s, there were no earthquake codes. It was only in the late 1950s and 1970s that earthquake codes were developed and introduced for building construction. Despite this, none of these safety measures could cope with a magnitude 7.0 event.

During the earthquake, most of the 6-15 storey towers collapsed, resulting in huge losses of life and property. An analysis of the building debris was carried out, and it was found that buildings under 6 or over 15 storeys were not damaged as much, while 9-storeys buildings were completely reduced to rubble. Two explanations have been put forward to explain the impact of the earthquakes, the duration of the tremor and the resulting resonance with the frequency of the lake bed. In other words, the resonance frequency of the 6-15 storey structures coincided almost exactly with the frequency of the earthquake.



Figure 1. 12. Heavily damaged buildings in Mexico City, 1985. (Image by David Tenenbaum)

“Nonlinear static and linear dynamic analysis for reinforced concrete building as complementary method of analysis and design”

Master in civil engineering defended by: TATCHA KANKEU Yvan Loïc, NASPW Yaoundé, 2019-2020

1.2.2. Non-linear analysis

During the past decade, significant progress has been made in performance-based engineering methods that rely on nonlinear analysis procedures. Explicitly, a Non-linear analysis is an analysis where a nonlinear relation holds between applied forces or response and displacements. Some important technical phenomena can only be evaluated on the basis of a non-linear analysis like progressive damage behaviour due to long term severe loads, collapse or buckling of structures due to sudden overloads (blast, earthquake, etc). For some structures (e.g., cables), non-linear phenomena must be included in the analysis, even for service load calculations. The need for nonlinear analysis has increased in recent years due to the need for use of optimized structures, use of new materials, addressing safety-related issues of structures more rigorously. The corresponding benefits can be most important.

1.2.2.1. The source of non-linearity

Nonlinear effects in concrete building can originate from geometrical nonlinearity's (i.e., large deformations), material nonlinearity's (i.e., elasto-plastic material), and contact.

a. Material nonlinearity

Non-linearity of materials implies the non-linear behaviour of a material as a function of current strain, strain history, strain rate, temperature, pressure, etc. When materials enter the region beyond their elastic limits, they no longer behave linearly, many phenomena can occur, permanent deformations, cracking, beam rotations, energy dissipation, etc.

b. Geometric nonlinearity

In analyses involving geometric nonlinearity, changes in geometry as the structure deforms are considered in formulating the constitutive and equilibrium equations. In structural design, the best known geometric non-linearity is the P-Delta analysis, which is a force follower approach because as the deflection increases, we have to re-test the additional forces generated by the P-delta effects. A P-Delta analysis is not simple, its effects will be very negative if neglected.



Figure 1. 13. Failure that can occur when the p-delta effect is not taken into account (Mall Parking Structure Collapsed Sideways After 1994 Northridge Earthquake)

c. Constraint and Contact Nonlinearity

Constrained non-linearity in a system can occur if kinematic constraints are present in the model. The kinematic degrees of freedom of a model can be constrained by imposing restrictions on its motion.

1.2.2.2. Performance concept and non-linear response

With the exception of special high-performance structures and structures with special protection systems, it is generally not economically feasible to design a structure to remain fully elastic for ground motions representative of the maximum risk level considered in high-seismicity regions. Therefore, some nonlinear behaviour must be anticipated during design and analysis.

Building performance can be expressed in multiple ways. In building design practice today, the most common approach is to define a series of performance objectives. A performance objective is a statement of the expected building performance conditioned on it having been subjected to a particular loading. For example, Tall Buildings Initiative TBI (2010) recommends that a tall building be designed to satisfy the following two performance objectives:

- The building shall have a small probability of life-threatening collapse given that it has been subjected to rare earthquake ground shaking defined as the Maximum Considered Earthquake (MCE) shaking level
- The building shall have a small probability of damage requiring repair given that it has been subjected to more frequent ground shaking defined as the Service Level Earthquake (SLE) shaking level.

The concept of discrete performance objectives became firmly established in the 1990s with the introduction of the Vision 2000 Committee report on performance-based seismic design of buildings (SEAOC, 1995) and the development of performance-based assessment procedures for existing buildings (ATC 40, 1996; FEMA 273, 1997). **Figure 1.14** illustrates the performance objectives suggested in SEAOC (1995), but using performance level designations of ASCE 41 (which supersedes FEMA 273). For the Basic objective, which would apply to the vast majority of buildings, the performance objectives would be:

- Operational for Frequent shaking;
- Immediate Occupancy for Occasional shaking,
- Life Safety for Rare shaking;
- And Collapse Prevention for Very Rare shaking

Proposed return periods for these different shaking levels are shown in parentheses. For more critical structures, higher performance objectives were suggested (**Figure 1.14**).

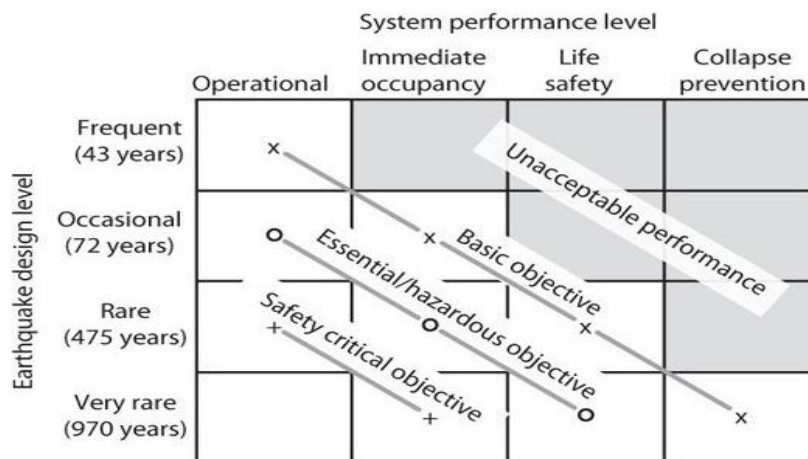


Figure 1.14. Performance objectives suggested by SEAOC (1995)

Non-linear analysis involves relating performance levels to the physical condition of the building as it is subjected to increasing lateral deformation. **Figure 1.15** illustrates three performance levels introduced in FEMA 273 (1997) and continued in ASCE 41 (2013).

a. Immediate Occupancy (IO)

This performance level corresponds to a state in which some damage may have occurred, but after cosmetic repairs the structure can be occupied and functional. The structure experience light damages, there is no permanent drift, the building retains original strength and stiffness substantially and minor cracks in facades, partitions and ceilings and structural elements appear.

b. Life Safety (LS)

It is a term used to define a performance state with a “comfortable” margin below the collapse state. The building suffers moderate general damage, all floors of the structure retain residual strength and stiffness, load-bearing elements are functioning. However, the structure suffers some permanent drift, the partitions are damaged, the concrete beams suffer significant damage and shear cracks. Minor cracks develop in the columns.

c. Collapse Prevention (CP)

It is a point in the response just prior to onset of collapse. The building is severely damaged, the structure retains little residual rigidity and strength. The building is experiencing large permanent drifts, and is close to collapse. Major cracks develop in ductile elements, non-ductile columns experience splice failures and limited cracking, and short columns are severely damaged.

Figure 1.15 implies that performance states are a function of the deformations imposed on the structural and non-structural systems.

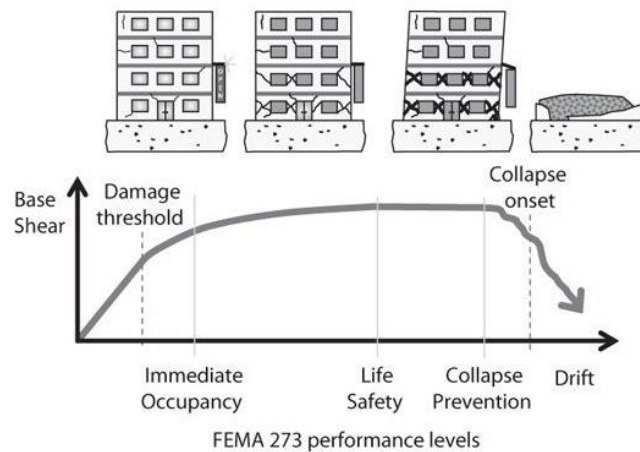


Figure 1. 15. Visualization of performance levels. (Personal communication with R. Hamburger.)

Building performance should be defined by the performance of the building system as a whole. It can be difficult, however, to quantify performance metrics for building systems. Therefore, as a practical matter, a common practice is to define system performance based on the performance of individual structural (or non-structural) components that compose the building system. In effect, the building performance is defined as being equal to the worst performance of any of the components of the building. This approach, which is adopted in ASCE 41, tends to be a very conservative approach.

The preceding discussion emphasizes the current approach of gauging performance using structural engineering metrics, such as displacement, story drift, floor acceleration, inelastic deformation, and component forces, all compared with values that are considered acceptable. It is also feasible to translate these engineering metrics into damage states, and from there into consequences such as casualties, repair costs, and downtime. This approach is not commonly applied today, but the capabilities exist and are occasionally applied for special buildings.

1.2.2.3. Overview of Non-linear analysis in earthquake engineering

Practicing engineer use nonlinear analysis procedures for the seismic evaluation and design of upgrades of existing building and other structures, as well as design of new construction. The practical objective of nonlinear seismic analysis is to predict the expected behaviour of the structure in the future earthquake shaking, i.e., estimate the magnitude of the inelastic deformations and distortions. This has become increasingly important with the emergence of Performance-Based Engineering (PBE) as a technique for seismic evaluation and design (ATC, 1996; BSSC, 2000). PBE uses the prediction of performance to inform decisions regarding safety and risk. For this purpose, PBE characterizes performance primarily in terms of expected damage to structural and non-structural components and contents.

The generic process of nonlinear analysis is similar to conventional linear procedures in that the engineer develops a model of the building or structure, which is then subjected to a representation of the anticipated seismic ground motion. The results of analysis are predictions of engineering demand parameters within the structural model that are subsequently used to determine performance based on acceptance criteria. The engineering demand parameters normally comprise global displacements (e.g., roof or other reference point), story drifts, story forces, component distortions, and component forces.

1.2.2.4. Option for Non-linear analysis

Various combinations of structural model types and characterizations of seismic ground motion define a number of options for inelastic analysis. The selection of one option over another depends on the purpose of the analysis, the anticipated performance objectives, the acceptable level of uncertainty, the availability of resources, and the sufficiency of data. In some cases, applicable codes and standards may dictate the analysis procedure.

The primary decision is whether to choose non-linear analysis over more conventional linear elastic analysis. In general, linear procedures are applicable when the structure is expected to remain nearly elastic for the level of ground motion of interest or when the design results in nearly uniform distribution of nonlinear response throughout the structure. In these

cases, the level of uncertainty associated with linear procedures is relatively low. As the performance objective of the structure implies greater inelastic demands, the uncertainty with linear procedures increases to a point that requires a high level of conservatism in demand assumptions and/or acceptability criteria to avoid unintended performance. Inelastic procedures facilitate a better understanding of actual performance. This can lead to a design that focuses upon the critical aspects of the building, leading to more reliable and efficient solutions.

Nonlinear dynamic analysis using the combination of ground motion records with a detailed structural model theoretically is capable of producing results with relatively low uncertainty (see **Figure 1.16**). In nonlinear dynamic analyses, the detailed structural model subjected to a ground motion record produces estimates of component deformations for each degree of freedom in the model and higher-level demands (element distortions, story drifts, roof displacement) derive directly from the basic component actions. At each level of intensity, the multiple time histories produce a distribution of results in terms of a selected engineering demand parameter.

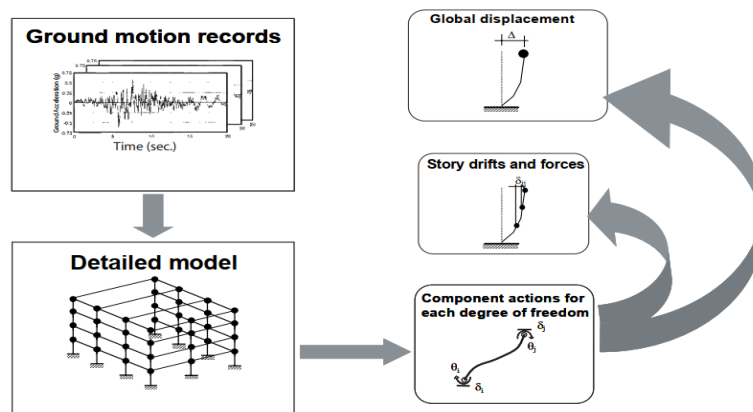


Figure 1. 16. Flow chart depicting the nonlinear dynamic analysis process (Improvement of Nonlinear Static Seismic Analysis Procedures, FEMA 440, June 2005)

Nonlinear static procedures (NSPs) convert MDOF models to equivalent SDOF structural models and represent seismic ground motion with response spectra as opposed to ground-motion records (see **Figure 1.17**). They produce estimates of the maximum global displacement demand. Story drifts and component actions are related subsequently to the global demand parameter by the pushover or capacity curve that was used to generate the equivalent SDOF model. This is similar to simplified nonlinear dynamic analyses using SDOF models. In contrast to the use of simplified dynamic analyses using multiple ground motion records, the use of nonlinear static procedures implies greater uncertainty due to the empirical procedures used to estimate the maximum displacement. This is true even if spectra representative of the

multiple ground motion records is used in the nonlinear static analysis. **Figure 1.18** summarizes the relationship among the normal options for inelastic seismic analysis procedures with respect to the type of structural model and characterization of ground motion. Also noted in the figure is the relative uncertainty associated with each option. The actual uncertainty inherent in any specific analysis depends on a number of considerations.

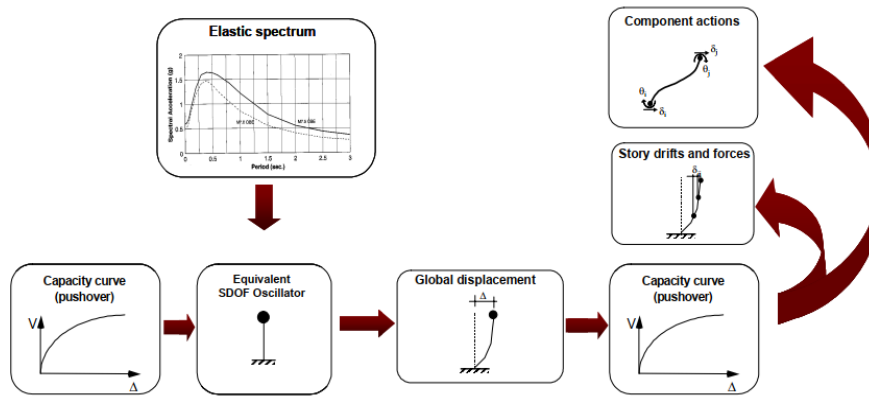


Figure 1. 17. Flow chart depicting the process followed in nonlinear static procedures (Improvement of Nonlinear Static Seismic Analysis Procedures, FEMA 440, June 2005)

		GROUND MOTION	
		Corresponding response spectra	Multiple records
STRUCTURAL MODEL	Detailed		Dynamic analysis
	Equivalent MDOF	Multi-mode pushover analysis (MPA)	Simplified MDOF dynamic analysis
	Equivalent SDOF	Nonlinear static procedures (NSP's)	Simplified SDOF dynamic analysis
		high	low
RELATIVE UNCERTAINTY			

Figure 1. 18. Matrix depicting possible inelastic seismic analysis procedures for various structural models (Improvement of Nonlinear Static Seismic Analysis Procedures, FEMA 440, June 2005)

1.2.2.5. Non-linear static analysis

Nonlinear static analysis or Pushover analysis is an approximate analysis method in which the structure is subjected to monotonically increasing lateral forces with an invariant height-wise distribution until a target displacement is reached. It consists of a series of sequential elastic analysis, superimposed to approximate a force-displacement curve of the overall

“Nonlinear static and linear dynamic analysis for reinforced concrete building as complementary method of analysis and design”

Master in civil engineering defended by: TATCHA KANKEU Yvan Loïc, NASPW Yaoundé, 2019-2020

structure. It has been developed over the last twenty years and has become the preferred analysis procedure for the design and evaluation of seismic performance, as the procedure is relatively simple and considers post-elastic behaviour.

a. Brief background of current Non-linear static procedure

With the introduction of performance-based seismic evaluation guidelines (e.g., FEMA 440 and ATC-40, FEMA 2005 and ATC 1996, respectively) and design standards (e.g., Eurocode 8, CEN 2005), approximate nonlinear static procedures (NSPs) have become popular in engineering practice as effective tools for estimating seismic demands under a given performance limit state. In many projects, they have replaced the more complex and expensive nonlinear dynamic analysis. Nowadays, there are many nonlinear static procedures recommended by the codes, which can be divided into two broad categories. The first category of NSPs consists of the Capacity Spectrum Method (CSM), suggested by Freeman et al. (1975 and 1998) and implemented in the ATC-40 guidelines (1996), and the equally innovative N2 method, introduced by Fajfar et al. (1988 and 2000) and later included in Eurocode 8 (CEN, 2005). These proposals are characterized by their simplicity and generally consider a first mode and/or uniform load distributions in the calculation of the pushover/capacity curve. The second category includes the more recent proposals by Chopra and Goel (2002 and 2004) on a modal pushover analysis (MPA), Kalkan and Kunnath (2006) who propose an adaptive modal combination procedure (AMCP), and Casarotti et al. (2007) who introduce the adaptive capacity spectrum method (ACSM). All of these methods have improvements over their predecessors, such as the inclusion of the contribution of higher modes and the consideration of progressive damage.

b. Purpose of pushover analysis

When used in the right conditions, this method provides access to the information needed to conduct a relevant capacity analysis:

- Estimation of the deformations demands for elements that have to form elastically in order to dissipate the energy imparted to the structure;
- Estimation of the consequences of the strength deterioration of individual elements on behaviour of the structural system.
- Rational assessment of the ductility of the building;
- Identification of the elements that provide ductility;

- Demonstration of how progressive building failure actually occurs and identification of critical regions where deformation demands are expected to be high and the final failure mode;
- Observation of stress flows in the structure and their evolution with the appearance of non-linearities;
- Possibility of evaluating the residual capacity of a structure for a given earthquake, in relation to a defined limit state.

c. Limitation of pushover analysis

i. Response quantity of interest

Nonlinear static pushover procedures are useful to estimate peak displacement response in conjunction with the use of “equivalent” SDOF systems. They appear to be reliable for the design and evaluation of low-rise buildings. However, MDOF effects associated with the presence of significant higher-mode response in relatively tall frame buildings, can significantly affect inter-story drifts, plastic hinge rotations, story shears, and overturning forces and other response quantities. The contribution to inter-story drifts stems directly from the higher mode shapes being more tortuous and therefore having a greater contribution to inter-story drift. Consequently, estimates of inter-story drift based on a first mode pushover analysis is prone to be inaccurate as the number of stories and period increases. Pushing to a target displacement will not necessarily develop the maximum inter-story drifts in each story because the maximum values in each story do not occur simultaneously, and the sum of the individual maximum inter-story drifts may be twice the peak roof displacement, depending on the mechanism that develops (Krawinkler). Some evidence suggests that pushovers tend to overestimate weak story drifts.

ii. Structural system type

Shear walls and frames have different higher-mode periods relative to their fundamental modal periods. These systems have characteristically different percentages of mass participating in the first and higher modes and develop characteristically different types of mechanisms. As noted previously, NSPs do not predict story forces reliably, and more sophisticated analytical techniques may be required for systems sensitive to these parameters.

iii. Inelastic mechanism

Forces associated with response in other modes may influence the development of an inelastic mechanism, and thus, pushover analyses may not always identify the governing mechanism (Krawinkler and Seneviratna, 1998).

1.3. EARTHQUAKE IN CAMEROUN

Earthquake, also called a seism, can therefore be defined as a violent shaking of the ground resulting from a sudden release of energy accumulated by the contraction of the rocks, propagating from the earth's crust to its surface through waves called seismic waves.

1.3.1. Seismic region in Cameroon

Cameroon spans the area between latitude 2°N to 13°N and longitude 08°E to 16°E. It corresponds to a complex which includes the Congo Craton in the South and the major geological feature in Central Africa called “Cameroon Volcanic Line”, uprising from the West in the Gulf of Guinea to the North (Eloumala et al. 2014). Eloumala Onana, Mouzong Pemi and Ateba Bekoa, in the review “Crustal Structure and Seismogenic Zone of Cameroon: Integrated Seismic, Geological and Geophysical Data”, define a seismic region is a zone where a given seismo-tectonic structure is active. It is determined on the basis of detailed geological studies of the zone, as well as consistent and comprehensive historical and instrumental data on seismic events to support the results. Several types of seismic region model have been identified. Each model is adopted and assumed to have homogeneous seismicity, as the seismic activity is scattered over a large area with no well identified point or specific fault location to justify a point or plane seismic source. Here, the tectonic characteristics of each zone and the density of the spatial distribution of seismic events are used to delineate Cameroon into four main seismic source regions, illustrated in **Figures 1.19** and **1.20**.

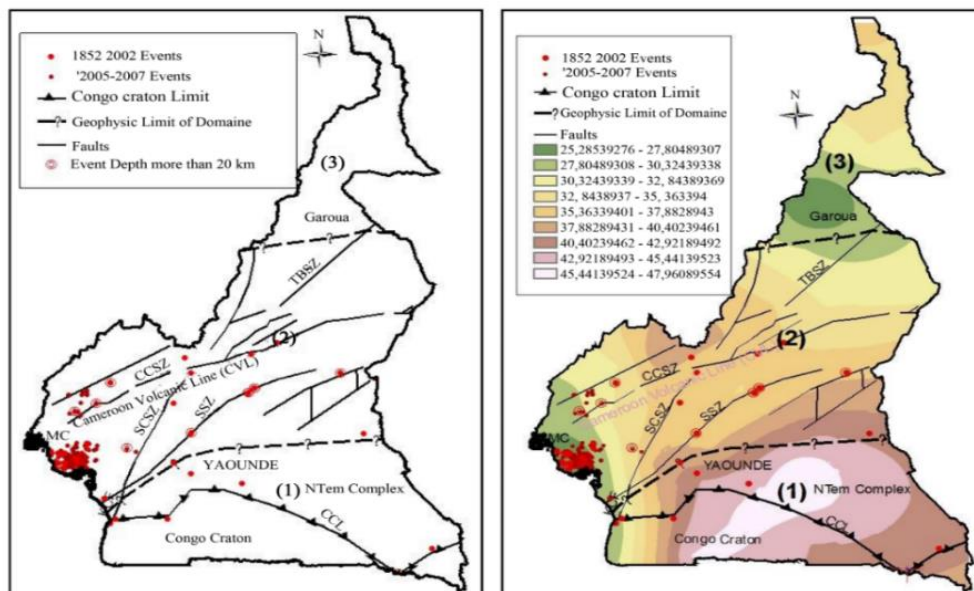


Figure 1. 19. Seismicity map of Cameroon (ELOUMALA et al, 2014)

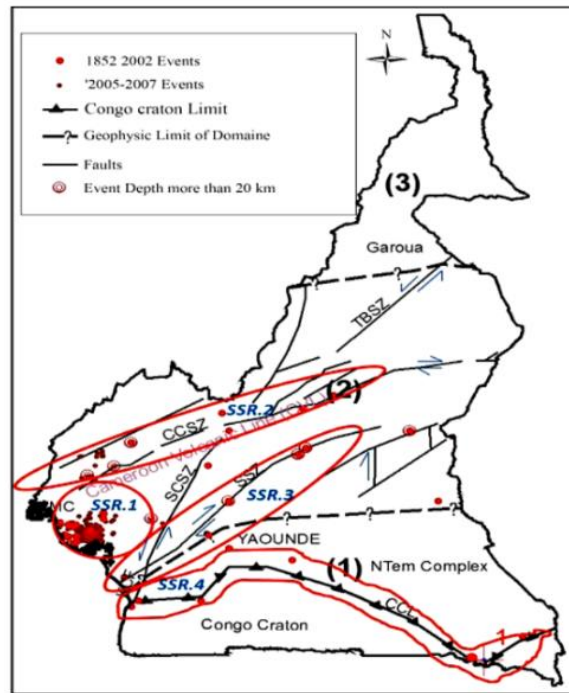


Figure 1. 20. Spatial distribution of seismic events in Cameroon (Eloumala et al, 2014)

a. The Seismic Source Region I

It corresponds to the area of “Mount Cameroon” volcano, in South-West Cameroon. From data recorded by temporary seismic network, 93.4 % of events are located in this Region. The seismic activity in this region is related to the magmatic activity and the maximum magnitude recorded in the source region is 4.4 Mb; this suggests a weak seismicity.

b. The Seismic Source Region II

It is also located in the South West region, in the North of mount Cameroon. In contrary to the “Seismic Source Region I”, “Source Region II” is affected by southern segments faults of “Central Cameroon Shear Zone” (CCSZ). The maximum magnitude recorded is 5.1 Mb, this might suggest a week to moderate seismicity.

c. The Seismic Source Region III,

Located in Central Cameroon, along Fault called “Sanaga Shear Zone” (SSZ). The maximum magnitude recorded in this source region was 5.8 Mb. Although this might suggest a moderate seismicity, the parameter of SSZ with average depth of 33 km and length of 900 km, convinced us that it is an important seismogenic area.

d. The Seismic Source Region IV,

It follows the northern boundary of Congo Craton. Although most events are shallow and have weak magnitude, this characteristic event shows that segment faults of this source region can generate large earthquakes.

The global seismicity map of Cameroon given in the **figure 1.21** shows the degree of seismicity in each region if an earthquake occurs.

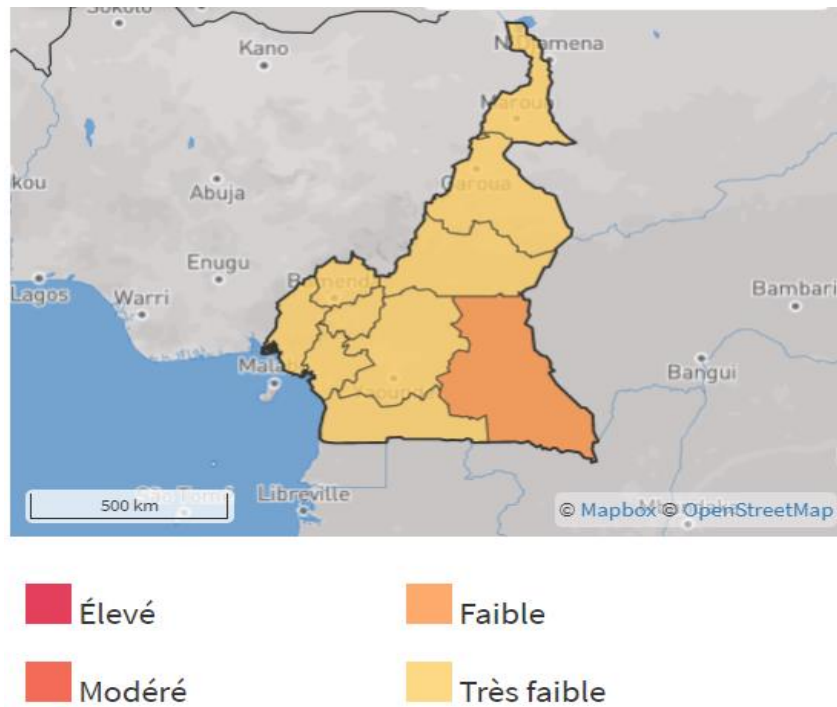


Figure 1. 21. Seismic mapping of Cameroon (https://thinkhazard.org/fr/report/45-cameroon/EQ_01/07/2021 at 19 h16)

1.3.2. Recent seismic events in Cameroon

Cameroon experienced its last recorded earthquakes in 2005 and 2002. On July 23rd 2002, the earthquake occurred in the kribi region, and according to Ntepe et al. (2002), the analysis of this earthquake revealed a magnitude of $3.6 \pm 0.4M$. Also, the preliminary seismic risk assessment has identified the town of Kribi as the riskiest area in the southern region.

On march 19th 2005, earthquake occur in many cities of country as Douala, Yaoundé, Monatélé in the Lékié subdivision, Ebebda in the neighbourhood of Sanaga river. This earthquake did not cause significant material and human damage but caused a slight crack on the buildings, the most important was found in the town of Ebebda, located near the “seismic source region III”, along the Sanaga shear zone. **Table 1.1** illustrates the past to recent earthquake recorder in Cameroon.

Table 1. 1. Past Seismic events in Cameroon (Plan national de contingence Cameroun, 2011)

Date	Locality concerned	Fault involved	Magnitude (Richter scale)	Damage-observations
1991	Lolodorf	Mbalmayo	6	High potential risk
1913	Akonolinga	Sanaga	5.1	High potential risk
1945	Ouessou	Centre Cameroon	5.6	High potential risk
1969	Yoko	Centre Cameroon	4.6	High potential risk
1983	Maga	Centre Cameroon	4.1	Building's destruction
1987	Tibati	Centre Cameroon	4.8	Damage recorded
1987	Kribi	Eseka-Kribi	4	High potential risk
2002	Kribi	Eseka-Kribi	-	Damage recorded
2005	Monatéfé	Sanaga	4.4	High potential risk

Conclusion

The objectives of this chapter were to present the seismic regions of Cameroon and the different analyses and designs that can be carried out on a building subjected to an earthquake. It was found that Cameroon has 4 seismic source regions distributed in the central, southern, coastal and western parts of the country. The most recent earthquakes observed were in 2002 in the locality of Kribi in the southern region and in 2005 in the locality of Monatéfé in the central region. In order to prevent and avoid major damage to buildings, engineers have developed a number of analyses and designs that take these seismic events into account. Our focus has been on linear dynamic analysis and non-linear static analysis which are analyses capable of predicting the behaviour and the elastic or inelastic response of structures to earthquakes. The methodology for the application of these analyses on a real building in Cameroon is discussed in the next chapter.

CHAPITRE 2 : METHODOLOGY

Introduction

Since the creation of reinforced concrete, several techniques and methods have been developed to analyse and design reinforced concrete buildings. This study focuses on three analyses, the linear static analysis, the linear dynamic analysis and the non-linear static analysis, which will be presented in detail in this chapter along with the case study application, the standards used and the types of materials and actions that will be considered.

2.1. Site recognition

For a good study of the building, it is necessary to know its environment. This requires a site recognition, which is done by a field trip or documentary research, in order to know the location of the site, climate, hydrology and socio-economic parameters of the region.

2.2. Site visit

The aim of this activity is to provide an overall description of the building based on site observations and to present its use category, dimensions, floor plans and elevation configuration.

2.3. Data collection

There are two types of data to collect, structural data and geotechnical data. The structural data is related to the structural plan of each level where we can identify the position of the structural elements, i.e., beams, columns, slabs, etc and the characteristics of the materials used. The geotechnical data are those extracted from the in situ and laboratory tests carried out on the site. For this project, we did not have the possibility to have the geotechnical data, so those that will be used in the following will be assumptions made from constructions around our building.

2.4. Codes and standards

It is a set of rules that specify the standards for design. Around the world, several design codes are used depending on the continent, country or region where we are. For this study, we will work with the European Standard or European Norms (Eurocodes), drafted and maintained by CEN (European Committee for Standardization).

Depending of the type of structure, the used of the structure, the actions on the structures, the construction material, etc, there are different Eurocodes, each code divided in many parts. For this study we will use:

- EN 1990 or Eurocode 0: basis of structural design;
- EN 1991 or Eurocode 1 : Actions on structures ;
- EN 1992 or Eurocode 2: Design of concrete structures;
- EN 1998 or Eurocode 8: Design of structures for earthquake resistance.

2.5. Evaluation procedure of actions of the building

EN 1990 classify the action by their variation in time.

2.5.1. Permanent action

Generally represented by the letter G, there are:

- Permanent structural loads represented by G1, that are the self-weight of structural elements obtained by multiplying the specific weight of concrete by the section of the elements;
- Permanent non-structural load represented by G2, that represent the weight of the non-structural given by Eurocode 1.

2.5.2. Variable action

EN 1990 define variable action as an action for which the variation in magnitude with time is neither negligible nor monotonic. There are imposed loads on building floors, beam and roofs, wind actions or snow loads and seismic action (depending of the site location). In this study we study the effects of imposed load and seismic action, we neglect the effect of wind.

2.5.2.1. Imposed load

Imposed loads are those arising from occupancy. It includes the normal use by people, the furniture and moveable objects and others. EN 1991 classifies building into different use categories and each category has a correspond imposed load. **Table A. 2** of Appendix A shows the classification of buildings in the use categories and **Table A. 1** of Appendix A shows the imposed load for each category.

2.5.2.2. Seismic action

Within the scope of EN 1998 the earthquake motion at a given point on the surface is represented by an elastic ground acceleration response spectrum, henceforth called an “elastic response spectrum”

a. The horizontal elastic response spectrum

The horizontal seismic action is described by two orthogonal components assumed as being independent and represented by the same response spectrum. For the horizontal components of the seismic action, the elastic response spectrum $S_e(T)$ is defined by the following expressions:

$$0 \leq T \leq T_B : S_e(T) = a_g \cdot S \left[1 + \frac{T}{T_B} \cdot (\eta \cdot 2,5 - 1) \right] \quad (2.1)$$

$$T_B \leq T \leq T_C : S_e(T) = a_g \cdot S \cdot \eta \cdot 2,5 \quad (2.2)$$

$$T_C \leq T \leq T_D : S_e(T) = a_g \cdot S \cdot \eta \cdot 2,5 \left[\frac{T_C}{T} \right] \quad (2.3)$$

$$T_D \leq T \leq 4s : S_e(T) = a_g \cdot S \cdot \eta \cdot 2,5 \left[\frac{T_C T_D}{T^2} \right] \quad (2.4)$$

$S_e(T)$ is the elastic response spectrum;

T is the vibration period of a linear single-degree-of-freedom system;

a_g is the design ground acceleration on type a ground ($a_g = \gamma_1 \cdot a_{gR}$);

a_{gR} is reference acceleration at ground level depending on the seismicity zone (**Table A. 4** of Appendix A and **Figure 1. 21**);

γ_1 is the importance coefficient (see **Table A. 5** of Appendix A);

T_B is the lower limit of the period of the constant spectral acceleration branch;

T_C is the upper limit of the period of the constant spectral acceleration branch;

T_D is the value defining the beginning of the constant displacement response range of the spectrum;

S is the soil factor that depends on the ground type (see **Table A. 6** and **Table A. 7**);

η is the damping correction factor with a reference value of $\eta = 1$ for 5% viscous damping.

$$\eta = \sqrt{10/(5 + \xi)} \geq 0,55 ;$$

ξ is the viscous damping ratio.

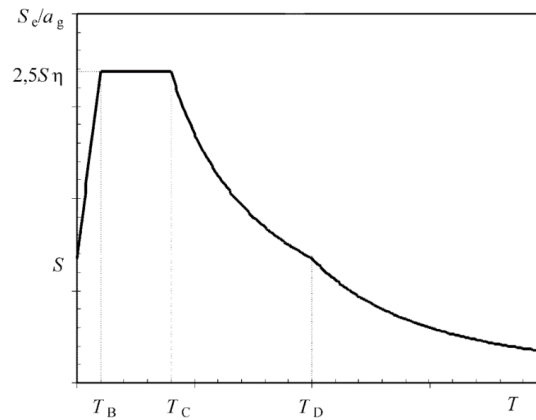


Figure 2. 1. Shape of the horizontal elastic response spectrum (EN 1998-1)

It is important to note that, the values of the periods T_B , T_C and T_D and of the soil factor S describing the shape of the elastic response spectrum depend upon the ground type (see **Table A. 8** and **Table A. 7** of appendix A).

b. Design spectrum for elastic analysis

The capacity of structural systems to resist seismic actions in the non-linear range generally permits their design for resistance to seismic forces smaller than those corresponding to a linear elastic response (EN1998/3.2.2.5 (1)). To avoid explicit inelastic structural analysis in design, the capacity of the structure to dissipate energy, through mainly ductile behaviour of its elements and/or other mechanisms, is taken into account by performing an elastic analysis based on a response spectrum reduced with respect to the elastic one, henceforth called a "design spectrum". This reduction is accomplished by introducing the behaviour factor q .

i. The behaviour factor

The behaviour factor q is an approximation of the ratio of the seismic forces that the structure would experience if its response was completely elastic with 5% viscous damping, to the seismic forces that may be used in the design, with a conventional elastic analysis model, still ensuring a satisfactory response of the structure. The values of the behaviour factor q , which also account for the influence of the viscous damping being different from 5%, are given for various materials and structural systems according to the relevant ductility classes in the various Parts of EN 1998. The value of the behaviour factor q may be different in different horizontal directions of the structure, although the ductility classification shall be the same in all directions. It is defined by equation (2.5)

$$q = q_0 \cdot k_w \tag{2.5}$$

Where:

k_w : is the factor reflecting the prevailing failure mode in structural systems with walls.
 $k_w = 1$ for frame or frame-equivalent dual systems;

q_0 : is the basic value of the behaviour factor, dependent on the type of the structural system and on its regularity in elevation. The basic values of q_0 for the various structural types are given in **Table 2.1**

Table 2. 1. Basic value of the behaviour factor, q_0 , for systems regular in elevation

STRUCTURAL TYPE	DCM	DCH
Frame system, dual system, coupled wall system	$3,0\alpha_u/\alpha_1$	$4,5\alpha_u/\alpha_1$
Uncoupled wall system	3,0	$4,0\alpha_u/\alpha_1$
Torsionally flexible system	2,0	3,0
Inverted pendulum system	1,5	2,0

With α_u/α_1 is a multiplication factor.

ii. The design spectrum

For the horizontal components of the seismic action the design spectrum, $S_d(T)$, shall be defined by the following expressions:

$$0 \leq T \leq T_B : S_d(T) = a_g \cdot S \left[\frac{2}{3} + \frac{T}{T_B} \cdot \left(\frac{2,5}{q} - \frac{2}{3} \right) \right] \quad (2.6)$$

$$T_B \leq T \leq T_c : S_d(T) = a_g \cdot S \cdot \frac{2,5}{q} \quad (2.7)$$

$$T_c \leq T \leq T_D : S_d(T) \begin{cases} = a_g \cdot S \cdot \frac{2,5}{q} \cdot \left[\frac{T_c}{T} \right] \\ \geq \beta \cdot a_g \end{cases} \quad (2.8)$$

$$T_D \leq T : S_d(T) \begin{cases} = a_g \cdot S \cdot \frac{2,5}{q} \cdot \left[\frac{T_c T_D}{T^2} \right] \\ \geq \beta \cdot a_g \end{cases} \quad (2.9)$$

a_g , S , T_B , T_c and T_D are defined in section 2.3.2.2. a;

$S_d(T)$ is the design spectrum;

Q is the behaviour factor;

β is the lower bound factor for the horizontal design spectrum. The recommended value is 0,2.

2.5.3. Combination of action

EN1990 gives the following combinations of loads depending on whether the verification is for the ultimate limit state (ULS) or the serviceability limit state (SLS).

2.5.3.1. The combination of action for ULS design

In general terms, for persistent and transient design situations, the combination of action can be taken as:

$$\sum_{j \geq 1} \gamma_{G,j} G_{k,j} + \gamma_{Q,1} Q_{k,1} + \sum_{i > 1} \gamma_{Q,i} \psi_{0,i} Q_{k,i} \quad (2.10)$$

Where:

- $G_{k,j}$ is the characteristic value of the permanent action j;
- $Q_{k,1}$ is the characteristic value of the leading variable action 1;
- $Q_{k,i}$ is the characteristic value of the accompanying variable action I;
- ψ is the combination factors that is function of the use category of the building, the factor for combination value of a variable action, see **Table A. 3** of Appendix A

The coefficients $\gamma_{G,j}$ and $\gamma_{Q,i}$ are partial factors which minimize the action which tends to reduce the solicitations and maximize the one which tends to increase it. The recommended values preconized by the EN1990 for the structural and geotechnical (STR and GEO) verifications are:

$$\gamma_{G,j}(\text{sup}) = 1,35 \quad \gamma_{G,j}(\text{inf}) = 1$$

$$\gamma_{Q,1} = 1,5 \text{ for unfavorable condition and } 0 \text{ for favorable}$$

$$\gamma_{Q,i} = 1,5 \text{ for unfavorable condition and } 0 \text{ for favorable}$$

2.5.3.2. The combination of action for SLS verification

The combinations of actions for serviceability limit states are defined symbolically by the following expressions:

- **The characteristic or rare combination**, normally used for irreversible limit states;

$$\sum_{j \geq 1} G_{k,j} + Q_{k,1} + \sum_{i > 1} \psi_{0,i} Q_{k,i} \quad (2.11)$$

- **The Frequent combination**, normally used for reversible limit states;

$$\sum_{j \geq 1} G_{k,j} + \psi_{1,1} Q_{k,1} + \sum_{i > 1} \psi_{1,i} Q_{k,i} \quad (2.12)$$

- **Quasi-permanent combination**, normally used for long-term effects and the appearance of the structure.

$$\sum_{j \geq 1} G_{k,j} + \psi_{1,1} Q_{k,1} + \sum_{i > 1} \psi_{2,i} Q_{k,i} \quad (2.13)$$

2.5.3.3. Seismic combination

The fundamental combination between the seismic action and the other loads (permanents and variables) is given by equation (2.14)

$$\sum_{j \geq 1} G_{k,j} + E + \sum_{i \geq 1} \psi_{2,i} Q_{k,i} \quad (2.14)$$

In order to take into account, the propagation of the seismic action in all directions 3 main directions x, y, z of space, we will carry out combinations of the seismic action according to these directions. Let E_x, E_y be the seismic forces in the X, Y, directions respectively, we neglect the effect of seismic forces in z direction. The different combinations of loading of the seismic action are presented by equations (2.15) and (2.16)

$$\pm E_x \pm 0.3E_y \quad (2.15)$$

$$\pm 0.3E_x \pm E_y \quad (2.16)$$

2.6. Material, Durability and Concrete cover

The material is reinforced concrete made of concrete and steel (rebar and stirrups). EN 1992 states that the durability of a structure shall meet the requirements of serviceability, strength and stability throughout its design working life, without significant loss of utility or excessive unforeseen maintenance. The required protection of the structure shall be established by considering its intended use, design working life, maintenance program and actions.

Adequate concrete cover is required to ensure adequate bond and to protect the reinforcement from corrosion and damage. The necessary cover depends on the grade of concrete, the exposure of the beam, and the required fire resistance. EN 1992 defines it as being the distance between the surface of the reinforcement closest to the nearest concrete surface (including links and stirrups and surface reinforcement where relevant) and the nearest concrete surface as we can see in **Figure 2. 2**

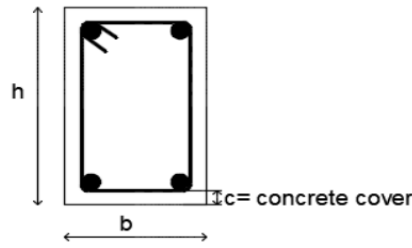


Figure 2. 2. Illustration of the concrete cover on the section of a structural element

The nominal concrete cover is the minimum concrete cover C_{min} plus an allowance in design for deviation ΔC_{dev} , (see equation (2.17))

$$C_{nom} = C_{min} + \Delta C_{dev} \quad (2.17)$$

ΔC_{dev} is the allowance in design for deviation with a recommended value of 10 mm

C_{min} is the minimum concrete cover defined in equation (2.18)

$$C_{min} = \max(C_{min,b}; C_{min,dur} + \Delta C_{dur,\gamma} - \Delta C_{dur,st} - \Delta C_{dur,add}; 10mm) \quad (2.18)$$

$C_{min,b}$ is the minimum cover due to bond requirement, equal to the diameter of the bars or the equivalent diameter in the case of bundled bars (see **Table A. 9** of Appendix A);

$\Delta C_{dur,\gamma}$ additive safety element with a recommended value equal to 0;

$C_{min,dur}$ the minimum cover due to environmental conditions which depends of the exposure and the structural class of the building (see **Table A. 10**);

$\Delta C_{dur,st}$ reduction of minimum cover for use of stainless steel, without specifications, the recommended value is 0;

$\Delta C_{dur,add}$ reduction of minimum cover for use of additional protection, without specifications, the recommended value is 0.

2.7. Linear static analysis

This section presents the analysis and design steps of the structural elements of the study building when it is subjected to static actions.

2.7.1. Design of beam

Beams are horizontal members that span columns. Beams support the loads from slabs, other beams, walls, and sometimes columns. They transfer the loads to the columns supporting them. Beams can be simply supported, continuous, or cantilevered and can be designed as rectangular, square, T-shaped, and L-shaped sections.

Reinforced concrete beam design consists primarily of producing member details which will adequately resist the ultimate bending moments, shear forces and torsional moments. At the same time serviceability requirements must be considered to ensure that the member will behave satisfactorily under working loads. It is difficult to separate these two criteria, hence the design procedure consists of a series of interrelated steps and checks. These steps may be condensed into three design basic stages.

2.7.1.1. The preliminary analysis

The preliminary analysis consists first of all in the preliminary design of the beam section which consists in determining its depth h and width b , with the help of the pre-dimensioning relations.

- For simply supported beams

$$h \geq \frac{L}{14} \text{ and } b \cong 0,5 h \quad (2.19)$$

- For cantilevered beams

$$h \geq \frac{L}{18} \text{ and } b \cong 0,5h \quad (2.20)$$

- For embedded beam

$$h \geq \frac{L}{20} \text{ and } b \cong 0,5h \quad (2.21)$$

Secondly, we determine the solicitation due to the loads acting on the beam (here we will just have bending moment and shear force). From the combinations of loading used, we will have different solicitations diagrams, which will allow us to represent the envelope curve. The software SAP 2000 (version 22) will help us to determine the solicitations of each loading combination. Then, using the software Microsoft EXCEL, we will establish the envelope curve of each type of stress present on the beam.

2.7.1.2. Detailed analysis and design of reinforcement

This stage consists in designing the beam at ultimate limit state using the solicitation and the section from previous stage.

a. Design for bending moment

The longitudinal reinforcement of the beam is the main element that resists the bending moment acting on the beam. It is therefore natural to use the bending moment diagram of the beam to determine the amount of reinforcement required. But the diagram used is not exactly the one obtained from the RDM methods; it is the so-called design diagram which is a transformation of the RDM diagram.

i. The design diagrams

From the previous stage, the bending moment envelope curve of a beam or a continuous beam has been obtained. Section 5.3.2.2 in the EN 1992-1-1 prescribes a reduction of a bending moment at the support by a factor ΔM_{Ed} . For continuous beams, the value of the reduction, is function of the connection between the beam and the support as shown in **Figure 2. 3**.

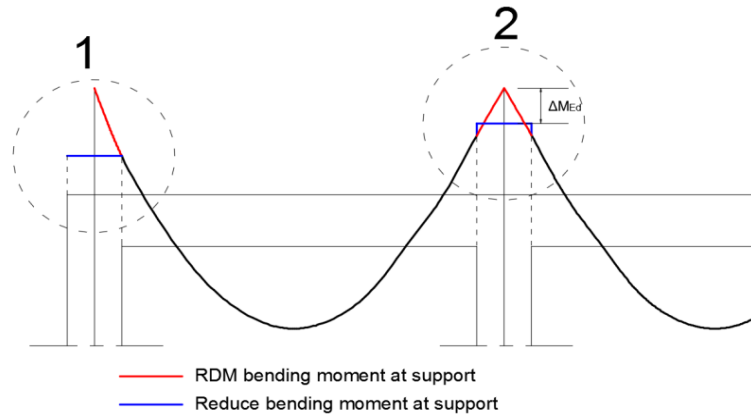


Figure 2. 3. Reduction of bending moment at the support (DJEUKOUA Laure, 2018)

$$\Delta M_{Ed} = F_{Ed,sup} \cdot \frac{t}{8} \tag{2.22}$$

$F_{Ed,sup}$ is the design support reaction;

t is the breadth of the support.

ii. The longitudinal steel reinforcement

When a concrete beam undergoes a bending generated by the bending moment, the lower fibre of the beam undergoes a traction in span and the upper fibre undergoes the same thing in support, but the concrete alone resists very badly to the traction. To alleviate this problem, we insert on these parts the steels reinforcement because resists very well to the traction. The quantity of steel required will be determined from the study of the section (see **figure 2.4**) of the beam and following procedure:

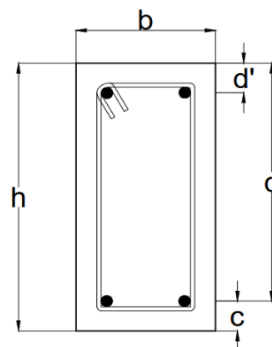


Figure 2. 4. Cross-section of beam

1) Determination of X_{lim}

The neutral axis is the boundary between the tension and compression zones of the beam section (see figure 2.5) it depends of the properties of the section and material of section.

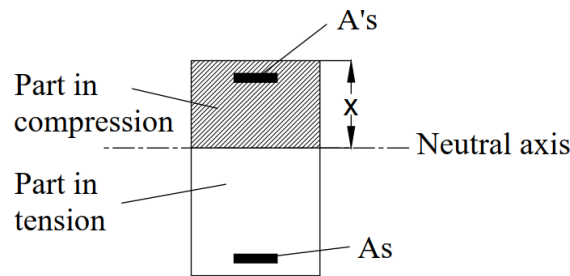


Figure 2. 5. Neutral axis

X_{lim} , the neutral axis limit, is when the concrete has reached its compressive strength and the steel has reached its yield strength. It is obtained using the equation (2.23)

$$X_{lim} = \frac{\epsilon_{cu}}{\epsilon_{cu} + \epsilon_{yd}} \cdot d \tag{2.23}$$

ϵ_{cu} is the ultimate strain of concrete;

ϵ_{yd} is yield stain of steel;

d is the effective depth (see Figure 2. 4)

2) The determination of the limit of the resisting bending moment ($M_{Rd,lim}$) of the section

It is given by equation (2.24)

$$M_{Rd,lim} = F_c \cdot Z_{lim} \tag{2.24}$$

Where F_c is the resultant of the compression stresses and Z_{lim} the inner lever arm (distance between the resultant of compression stress and the tension stress in the section) show in Figure 2. 6 and defined by equation (2.25) and (2.26)

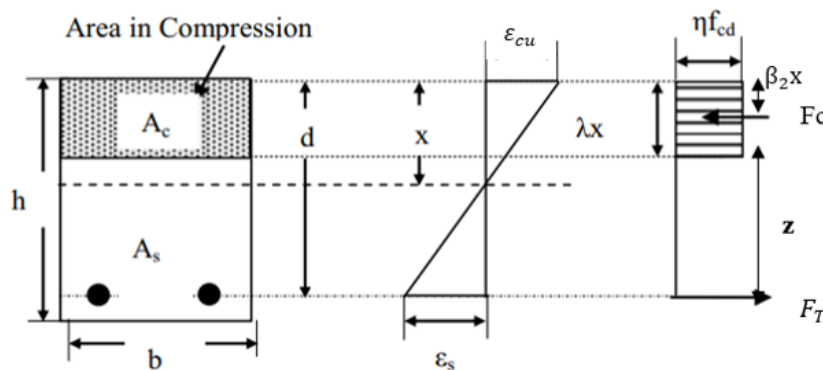


Figure 2. 6. Stress and strain distribution

$$F_c = f_{cd} \cdot \beta_1 \cdot X_{lim} \cdot b \quad (2.25)$$

$$Z_{lim} = d - \beta_2 \cdot X_{lim} \quad (2.26)$$

f_{cd} the design compressive strength of concrete;

β_1 the ratio between the area of the parabola-rectangle diagram at certain deformation and the area of rectangle at the same deformation, $\beta_1 = \lambda \cdot \eta = 0.8$;

β_2 the position factor, $\beta_2 = \frac{\lambda}{2} = 0.4$

3) Determination of the section of longitudinal reinforcement

- If $M_{Rd,lim} > M_{Ed}$

The reinforcement is need only on the lower fibre of the section (As). First the neutral axis of the section undergoing the bending moment M_{Ed} is determined using equation (2.27)

$$x = \frac{d}{2\beta_2} - \sqrt{\left(\frac{d}{2\beta_2}\right)^2 - \frac{M_{Ed}}{\beta_1 \cdot \beta_2 \cdot b \cdot f_{cd}}} \quad (2.27)$$

Finally, A_s is obtained by using (2.28)

$$A_s = \frac{M_{Ed}}{f_{yd} \cdot z} \quad (2.28)$$

M_{Ed} the bending moment of the section;

z the lever arm shown in **Figure 2. 6** and defined like equation (2.26)

- If $M_{Rd,lim} \leq M_{Ed}$

The reinforcement is need both in the lower (As) and in the upper fibre (As') of the section. (Or increase the cross section of beam to have the first case). First, ΔM_{Ed} is determined using equation (2.29)

$$\Delta M_{Ed} = M_{Ed} - M_{Rd,lim} \quad (2.29)$$

Secondly, we determine A'_s given by (2.30)

$$A'_s = \frac{\Delta M_{Ed}}{f_{yd} \cdot (d - d')} \quad (2.30)$$

Finally, A_s is done by (2.31)

$$A_s = \frac{M_{Rd,lim}}{f_{yd} \cdot z_{lim}} + A'_s \quad (2.31)$$

b. Design for shear

To resist the shear force, the beam needs transverse steel reinforcement, also called stirrups. EN 1992 presents two methods of analysis and design for shear, the standard method and the variable inclination method of stirrups. We will use the standard method whose procedure is the following:

1) Determined the design shear resistance of the member without shear reinforcement

$V_{Rd,c}$

$$V_{Rd,c} = \min \left\{ \left[C_{Rd,c} \cdot k (100 \cdot \rho_l \cdot f_{ck})^{\frac{1}{3}} + k_1 \cdot \sigma_{cp} \right] b_w \cdot d \right. \\ \left. (V_{min} + k_1 \cdot \sigma_{cp}) b_w \cdot d \right. \quad (2.32)$$

f_{ck} is the Characteristic cylinder compressive strength in MPa

$$k = 1 + \sqrt{\frac{200}{d}} \leq 2.0 \text{ with } d \text{ in mm}$$

$$\rho_l = \frac{A_{sl}}{b_w \cdot d} \leq 0.02$$

A_{sl} is the area of the tensile reinforcement

b_w is the smallest width of the cross-section in the tensile area (mm)

$$\sigma_{cp} = \frac{N_{Ed}}{A_c} < 0.2 \text{ (MPa)}$$

N_{Ed} is the axial force in the cross-section due to loading in N ($N_{Ed} > 0$ for compression).

A_c the area of concrete cross section in mm^2

The recommended value of $C_{Rd,c}$ is $\frac{0,18}{\gamma_c}$, k_1 is 0.15 and V_{min} is $0,035 \cdot k^{\frac{3}{2}} \cdot f_{ck}^{\frac{1}{2}}$

2) The value obtained is then compared to the design shear force V_{Ed} of the section considered resulting of the external loading

- **If $V_{Ed} \leq V_{Rd,c}$**

No shear reinforcement is required. However, minimum shear reinforcement and maximum spacing must be provided. It is given by (2.33) and (2.34)

$$\frac{A_{sw,min}}{s} = \frac{0,08 \cdot f_{ck}^{0,5} \cdot b_w}{f_{yk}} \quad (2.33)$$

$$s_{max} = \min \left(0,8 \cdot d ; \frac{3 \text{stirrups}}{m} \right) \quad (2.34)$$

- **If $V_{Ed} > V_{Rd,c}$**

Shear reinforcement should be provided and we can determine the area of the shear reinforcement and their spacing using (2.35)

$$\frac{A_{sw}}{s} = \frac{V_{Ed}}{0,9 \cdot d \cdot f_{ywd}} \quad (2.35)$$

f_{ywd} is the design yielding strength of the shear reinforcement;

A_{sw} is the cross-sectional area of the shear reinforcement;

s is the spacing of the stirrups.

2.7.1.3. Serviceability Limit State (SLS) verification

The serviceability limit state is the verification or design to ensure that a structure is comfortable and usable. This includes vibration and deflection (movement), as well as cracking and stress limitation. These are conditions that are not strength-based but which may nevertheless make the structure unsuitable for its intended use, for example, it may cause discomfort to occupants under common conditions. EN 1992-1 for the design of a reinforced concrete section provides three SLS verifications, stress limitation, cracking and deflection.

a. Stress limitation

According to EN1992, the compressive stress in the concrete shall be limited in order to avoid longitudinal cracks, micro-cracks or high levels of creep, where they could result in unacceptable effects on the function of the structure. the characteristic combination and the quasi-permanent combination of loads are used for this verification; quasi permanent is usually use for long term effects. The stress value is function of the modular ratio in short terms and long terms expressed in equation (2.36) and (2.37) respectively.

$$n_0 = \frac{E_S}{E_C} \quad (2.36)$$

$$n_\infty = n_0(1 + \varphi_L \cdot \rho_\infty) \quad (2.37)$$

Where $\varphi_L = 0.55$ for shrinkage of concrete and the parameter $\rho_\infty = 2 \div 2.5$.

The procedure for this verification is as follows:

1) Determination of the position of the neutral axis of the uncracked concrete section.

The position of neutral axis is given by equation (2.38)

$$x = \frac{n(A_s + A'_s)}{b} \cdot \left[-1 + \sqrt{\frac{2b(A_s \cdot d + A'_s \cdot d')}{n(A_s + A'_s)^2}} \right] \quad (2.38)$$

Where A'_s and A_s , are the upper and lower steel reinforcement inside the section respectively.

d , d' and b are the geometrical characteristics of the section presented in Figure 2. 4

2) Determination of the moment of inertia of the uncracked section.

The moment of inertia is given by (2.39)

$$I = \frac{bx^3}{3} + nA'_s(x - d')^2 + nA_s(d - x)^2 \quad (2.39)$$

3) Determination of the stress in concrete and in steel

The stress in concrete is given by (2.40)

$$\sigma_c = \frac{M}{I} \cdot x \quad (2.40)$$

The stress in steel (for A_s and A'_s) is given by (2.41) for stress in A_s and (2.42) for stress in A'_s .

$$\sigma_s = n \cdot \frac{M}{I} \cdot (d - x) \quad (2.41)$$

$$\sigma'_s = n \cdot \frac{M}{I} \cdot (x - d') \quad (2.42)$$

4) Verification

This is the last step of the procedure that consist to verify the stress limitation on steel and on concrete.

$$\sigma_c \leq 0,6 f_{cm} \quad \text{for characteristic combination of loads;}$$

$$\sigma_c \leq 0,45 f_{cm} \quad \text{for quasi permanent combination of loads;}$$

$$\sigma_s \leq 0,8 f_{yk} \quad \text{for characteristic combination of loads.}$$

b. Deflection control

The general requirement is that neither the efficiency nor the appearance of a structure should be affected by deflections that will occur during its lifetime. Deflections should not exceed those that can be absorbed by other connected elements such as partitions, glazing, cladding, services or finishes. The limitations necessary to meet the requirements will vary

considerably depending on the nature of the structure and its loads, but for reinforced concrete the following can be considered as reasonable guides:

- 1) The final deflection of a beam, slab or cantilever should not exceed $span/250$
- 2) That part of the deflection which takes place after the application of finishes or fixing of partitions should not exceed $span/500$ to avoid damage to fixtures and fittings.

Deflections should be calculated under the action of the quasi-permanent load combination, assuming this loading to be of long-term duration. This is a reasonable assumption as deflection will be affected by long-term effects such as concrete creep, while not all of the variable load is likely to be long-term and hence will not contribute to the creep effects. To keep it simple we will just check the short-term deformability and the procedure is following:

1) Determination of the deflection f_1 of the section in the elastic state

It is given by equation (2.43), and for it is considered that the neutral axis of the section is equal to half the height of the section in this case.

$$f_1 = \frac{5}{384} \cdot \frac{Fed \cdot l^4}{EI} \quad (2.43)$$

Fed is load due to the quasi-permanent combination load;

L is length of span;

E is the young modulus of concrete

I is the moment of inertia of the section for neutral axis $x = \frac{h}{2}$, given by equation (2.44)

$$I = \frac{bh^3}{12} + n \cdot A'_s \left(\frac{h}{2} - d' \right)^2 + n \cdot A_s \left(d - \frac{h}{2} \right)^2 \quad (2.44)$$

With the homogenization coefficient n given by (2.36).

2) Determination of the deflection f_2 of the section in plastic state

For this purpose, the neutral axis x is determined using the static moment equilibrium of the section, so x is determined by solving the second-degree equation (2.45)

$$\frac{bx^2}{2} + n \cdot A'_s(x - d') - n \cdot A_s(d - x) = 0 \quad (2.45)$$

After determine x, I and f_2 is determine using (2.39) and (2.46) respectively.

$$f_2 = \frac{5}{384} \cdot \frac{Fed \cdot l^4}{EI} \quad (2.46)$$

3) Determination of the total deflection f

It is given by the (2.47)

$$f = f_1 \cdot \beta \left(\frac{M_{cr}}{M} \right)^2 + f_2 \left[1 - \beta \left(\frac{M_{cr}}{M} \right)^2 \right] \quad (2.47)$$

Where M_{cr} is the cracking moment (2.48) and $\beta = 1$ for short term loading.

$$M_{cr} = \frac{f_{ctm} \cdot bh^2}{6} \quad (2.48)$$

4) Check if the total deflection f is less than the deflection limit for short term effect given by (2.49)

$$f_{lim} = \frac{l}{250} \quad (2.49)$$

c. Crack control

Cracking is normal in reinforced concrete structures subjected to bending, shearing, torsion or tension resulting from either direct loading or imposed stresses or strains, but it should be limited to a degree that does not impair the proper functioning or durability of the structure or render its appearance unacceptable.

Cracks may also arise from other causes such as plastic shrinkage or expansive chemical reactions in hardened concrete, but we will not consider these in this work.

EN1992 defines two methods to control cracking. The first method, called the simplified method, is used to determine:

- The maximum diameter of the longitudinal bars to be used to avoid limit cracking.

To do this **Table A. 13** of Appendix A which presents the maximum diameter of the longitudinal bars as a function of the stress acting on these bars is used and the maximum crack width.

Once determined, it is sufficient to calculate the adjusted maximum bar diameter using equation (2.50)

$$\phi_s = \phi_s^* \cdot \frac{f_{ct,eff}}{2.9} \cdot \frac{k_c h_{cr}}{8(h-d)} \quad (2.50)$$

This value must be greater than the diameters of the longitudinal reinforcement we used to form the beam.

- The maximum spacing between the longitudinal bars.

Here **Table A. 14** from Appendix A is used. it shows the maximum spacing between the longitudinal reinforcements according to their stresses and the maximum crack width.

The maximum crack width is determined using **Table A. 12** in Appendix A. It depends on the exposure class of the building and the type of load combination at SLS.

The second method, called the analytical method, directly determines the crack width of the beam and then compares this value with the maximum crack width. For this analysis we will use the first method.

2.7.2. Design of columns

The columns in a structure carry the loads from the beams and slabs down to the foundations, and therefore they are primarily compression members, although they may also have to resist bending forces due to the continuity of the structure. Columns have two axes, and bending can occur on one or both the axes. The bending action may produce tensile stresses on part of the cross section of the column. Despite the tensile forces acting on columns, they are generalized as compressive members because compressive forces dominate in the column design.

2.7.2.1. Preliminary analysis

The preliminary static analysis consists first in the preliminary design of the column which consists in determining the dimension of its section.

In seismic area, the preliminary design of the column considers that 60% of the concrete resistance is used to take over the axial force. Then we can estimate the minimum area section of the column using equation (2.51)

$$N_{Rd} = 0,6 \cdot f_{cd} \cdot A_c \geq N_{Ed} \quad (2.51)$$

A_c is the area of column section.

N_{Ed} is the axial load computed using the recovery area of the column.

After determining the minimum area, we can assume a column section considering this minimum area.

The second part of the analysis consists in determining the solicitations on the columns, for this purpose, a modelling of the building is necessary (see section 2.8.1.1.) and will be carried out in the software SAP 2000(version 22). A series of loading combinations will be carried out on the building in order to obtain the maximum solicitations on the columns. The Excel software will allow us to analyse the data received and to generate the solicitation diagrams. But before obtaining the maximum solicitations, a modal analysis (see section 2.8.1.) Will be carried out on the building in order to validate the sections of the columns and to check if any modelling errors have been made.

2.7.2.2. Column classification

After determining the cross-section of the column, it is necessary to classify it i.e., determine whether it is a short or a slender column. To do this, we determine the slenderness ratio of the column and compared it to its limit value λ_{lim} . The slenderness ratio λ of a column bent about an axis is given by equation (2.52)

$$\lambda = \frac{l_0}{i} = \frac{l_0}{\sqrt{(I/A)}} \quad (2.52)$$

l_0 is the effective height of the column;

i is the radius of gyration about the axis considered;

I is the second moment of area of the section about the axis;

A is the cross-sectional area of the column.

EN 1992 places an upper limit on the slenderness ratio of a single member below which second order effects may be ignored. This limit is given by equation (2.53)

$$\lambda_{lim} = 20 \cdot A \cdot B \cdot C / \sqrt{n} \quad (2.53)$$

Where:

$$A = \frac{1}{1 + 0,2 \cdot \varphi_{ef}} \quad (2.54)$$

φ_{ef} is the effective creep ratio (if not known A can be taken as 0.7)

$$B = \sqrt{1 + 2 \cdot w} \quad (2.55)$$

$$w = \frac{A_s f_{yd}}{A_c f_{cd}} \quad (2.56)$$

If not known B can be taken as 1.1

$$C = 1,7 - r_m \quad (2.57)$$

$$r_m = \frac{M_{01}}{M_{02}} \quad (2.58)$$

If r_m not known then C can be taken as 0.7

$$n = \frac{N_{Ed}}{A_c f_{cd}} \quad (2.59)$$

N_{Ed} the design ultimate axial load in the column;

M_{01} and M_{02} are the first order moments at the end of the column with $|M_{01}| \leq |M_{02}|$

2.7.2.3. The longitudinal reinforcements

The longitudinal reinforcements resist the bending moment acting along the column. Since the column is also subjected to an axial force, we cannot use here the method used to determine the longitudinal reinforcements of the beam. For columns, there are several methods for determining the amount of this longitudinal reinforcement depending on whether the column is slender or not. The simplest method is the **Design Charts Method**, that considers a symmetric distribution of longitudinal reinforcement ($A_s=A_s'$).

The first step of the design of longitudinal reinforcement of column is to check whether it is necessary to take into account the interaction of biaxial bending moment or whether the determination of the longitudinal reinforcements will be done separately according to the two main planes x-z and y-z.

If expression (2.60) is satisfied, separate design along the two axes of the section of column are needed, otherwise we have to take into account the interaction of biaxial bending.

$$\frac{e_y}{e_x} \leq 0.2 \quad \text{and} \quad \frac{e_x}{e_y} \leq 0.2 \quad (2.60)$$

e_y and e_x are the first-order eccentricities in the direction of the section dimensions b and h respectively.

a. The separate design

The design will consist of determining the longitudinal reinforcement due to (M_x, N_{ed}) and (M_y, N_{ed}).

M_x and M_y are the bending moments around the x-x and y-y axes of the section (see **Figure 2. 7**) and N_{ed} is the axial force on the section (see **Figure 2. 9**).

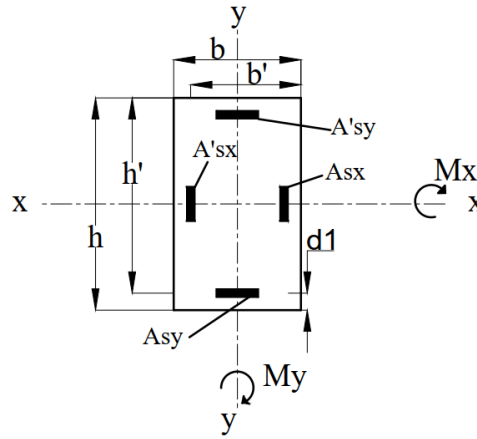


Figure 2. 7. Section with biaxial bending

The procedure for designing a rectangular section as shown in **Figure 2. 7** using the design charts Method, carried out in the same way in the x-z and y-z planes, is as follows:

(1) Determination of the appropriate Design chart

The design chart is a diagram that expresses $\frac{Asf_{yd}}{bh^2f_{cd}}$ as a function of $\frac{N}{bhf_{cd}}$ and $\frac{M}{bh^2f_{cd}}$ (see **Figure 2. 8**).

It is possible to draw your own design chart using equation (2.61) and (2.62) or to use the diagrams that have already been defined.

$$\frac{N}{bhf_{cd}} = \frac{0.56 \cdot s}{h} + \frac{f_{sc} \cdot A_s}{f_{ck} \cdot b \cdot h} + \frac{f_s \cdot A_s}{f_{ck} \cdot b \cdot h} \quad (2.61)$$

$$\frac{M}{bh^2f_{cd}} = \frac{0.56 \cdot s}{h} \left(0.5 - \frac{s}{2h}\right) + \frac{f_{sc} \cdot A_s}{f_{ck} \cdot b \cdot h} \left(\frac{d}{h} - 0.5\right) - \frac{f_s \cdot A_s}{f_{ck} \cdot b \cdot h} \left(\frac{d}{h} - 0.5\right) \quad (2.62)$$

f_s and f_{sc} are the steel stress for steel in compression and steel in tension respectively. They are defined as follow:

- If $\varepsilon_s < \varepsilon_{yd}$, then $f_s = E_s \cdot \varepsilon_s$ (2.63)

- If $\varepsilon_s \geq \varepsilon_{yd}$, then $f_s = f_{yd}$ (2.64)

The predefined diagrams depend on the properties of the cross-section, materials and reinforcement arrangements; therefore, it must first be ensured that the properties of the cross-section and the reinforcement arrangements are consistent with the chosen design diagram. The section properties are the shape of the cross-section (circular or rectangular) and the ratio $d1/h$ for the rectangular section and d/h (See **Figure 2. 8**). The material properties are just to check if the concrete grade f_{ck} is greater or not to 90 MPa.

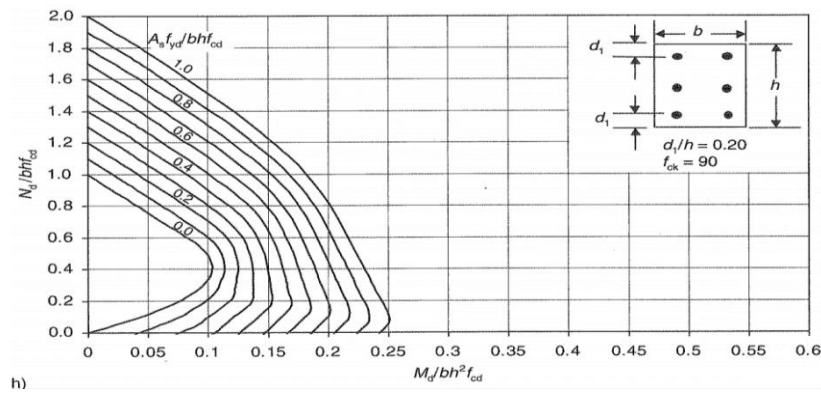


Figure 2. 8. Example of rectangular design chart (R. S. Narayanan and A. Beeby, Designer’s Guide to EN1992-1-1 and EN1992-1-2)

(2) Determination of the point given by equation 2.65

$$\left(\frac{N_{Ed}}{bhf_{cd}}; \frac{M}{bh^2f_{cd}} \right) \tag{2.65}$$

Where:

Ned and M are the axial force on the column and the design Moment respectively on the column.

(3) Determination of the ratio $\frac{Asf_{yd}}{bh^2f_{cd}}$ using the design chart

The point determined in step (2) is represented in the design chart and allows the value of ratio $\frac{Asf_{yd}}{bh^2f_{cd}}$ to be obtained by interpolation with its curves.

(4) Determination of As

With the value of $\frac{Asf_{yd}}{bh^2f_{cd}}$ obtained in step (3), As can be calculated.

For a separate calculation, this procedure is carried out in the X and Y direction with the moments Mx and My respectively. It must also be taken into account that the depth (h) and effective depth (d) of the section changes depending on whether we are on the x or y axis.

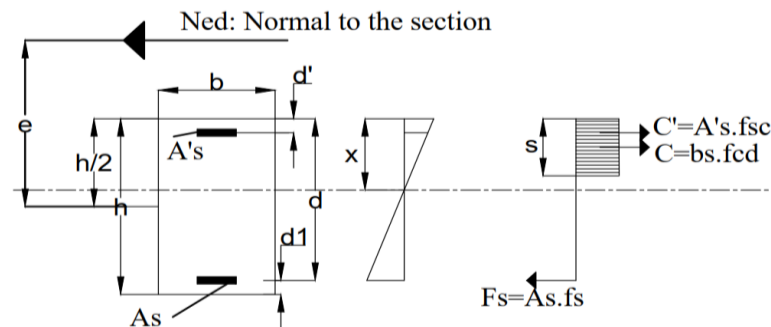


Figure 2. 9. Column section

b. Interaction of biaxial bending

If expression (2.60) is not satisfied, we have to take into account the interaction of the biaxial bending moment.

This approximate method specifies that a column subjected to an ultimate load N_{ed} and moments M_x and M_y in the direction of the x-x and y-y axes respectively (figure 2.7) may be designed for a single axis bending but with an increased moment and subject to the following conditions.

- If $\frac{M_x}{h'} \geq \frac{M_y}{b'}$ the increase single axis design moment is:

$$M'_x = M_x + \beta \frac{h'}{b'} \times M_y \tag{2.66}$$

- If $\frac{M_x}{h'} < \frac{M_y}{b'}$ the increase single axis design moment is:

$$M'_y = M_y + \beta \frac{b'}{h'} \times M_x \tag{2.67}$$

The dimensions h' and b' are defined in **Figure 2. 7** and β is specified in **Table 2. 2** and can be obtained using equation (2.68)

$$\beta = 1 - \frac{N_{Ed}}{bhf_{ck}} \tag{2.68}$$

After obtaining the design moment (can be M'_x or M'_y but not both), the determination of longitudinal reinforcement is carried out in the same way as described in section **2.7.2.3. a.**

Table 2. 2. Value of β

$\frac{N_{Ed}}{bhf_{ck}}$	0	0.1	0.2	0.3	0.4	0.5	0.6	≥ 0.7
β	1	0.9	0.8	0.7	0.6	0.5	0.4	0.3

c. Minimum and maximum longitudinal reinforcement

The recommended value for the minimum and maximum longitudinal area of reinforcement following EN1992-1 is given by equation (2.69) and (2.70) respectively.

$$A_{s,min} = \max\left(\frac{0.1N_{Ed}}{f_{yd}}; 0.002 \cdot A_c\right) \tag{2.69}$$

$$A_{s,max} = 0.4 \cdot A_c \tag{2.70}$$

The design chart method is an approximate method to determine the amount of longitudinal reinforcement in a column section. But to ensure its effectiveness, it is necessary to check the section design by the M-N interaction diagram.

2.7.2.4. The M-N interaction diagram

The M-N interaction diagram is a diagram that shows all the limit situations that can determine the failure of the section, beyond this limit, the failure occurs. It is specific to each section and is determined by the calculation of 6 significant points. Each point is formed by the couple $(N_{Rd}; M_{Rd})$, the procedure for establishing it, considering a rectangular cross-section **Figure 2. 7**, is as follows:

N_{Rd} and M_{Rd} are the resisting axial force and the resisting moment of the cross-section respectively.

(1) First point

The section is assumed to be completely in tension; therefore, the concrete does not react. We impose $\varepsilon_s = \varepsilon_{ud}$ and $\varepsilon'_s > \varepsilon_{yd}$

We have:

$$N_{Rd} = -A_s \cdot f_{yd} - A'_s \cdot f_{yd} \quad (2.71)$$

$$M_{Rd} = A_s \cdot f_{yd} \cdot \left(d - \frac{h}{2}\right) - A'_s \cdot f_{yd} \cdot \left(d' - \frac{h}{2}\right) \quad (2.72)$$

(2) Second point

The section is completely subjected to traction. We impose $\varepsilon_s = \varepsilon_{ud}$ and $\varepsilon_c = 0$.

ε'_s is calculated using equation (2.73)

$$\varepsilon'_s = \varepsilon_{ud} \cdot \frac{d'}{d} \quad (2.73)$$

$$N_{Rd} = -A_s \cdot f_{yd} - A'_s \cdot f'_s \quad (2.74)$$

f'_s is defined according to equation (2.63) and (2.64)

M_{Rd} is calculate using equation (2.72)

(3) Third point

We impose that the failure is due to concrete and the lower reinforcement is yielded. We assume $\varepsilon_s \geq \varepsilon_{yd}$ and $\varepsilon_c = \varepsilon_{cu2}$ and we determine the position of neutral axis and ε'_s using equation.

$$x = d \cdot \frac{\varepsilon_c}{\varepsilon_c + \varepsilon_s} \quad (2.75)$$

$$\varepsilon'_s = \varepsilon_c \frac{x - d'}{x} \quad (2.76)$$

$$N_{Rd} = bs \cdot f_{cd} + A'_s \cdot f_{sc} - A_s \cdot f_{yd} \quad (2.77)$$

f_{sc} is determined using equation (2.63) and (2.64)

$$M_{Rd} = f_{cd} + A'_s \cdot f_{sc} \left(d' - \frac{h}{2} \right) + bs \cdot f_{cd} \left(\frac{h}{2} - \frac{s}{2} \right) + A_s \cdot f_{yd} \left(d - \frac{h}{2} \right) \quad (2.78)$$

(4) Fourth point

We impose that the failure is due to concrete and the lower reinforcement reaches exactly $\varepsilon_s = \varepsilon_{yd}$, the neutral axis x and ε'_s is determine using equation (2.75) and (2.73) respectively. The resisting axial force and the resisting moment is determine using equation (2.77) and (2.78)

(5) Fifth point

We impose that the failure is due to concrete and no strain in A_s ($\varepsilon_s = 0$), then the neutral axis position will be equal to the effective depth of the section and ε'_s is determined using equation (2.73)

$$N_{Rd} = bs \cdot f_{cd} + A'_s \cdot f_{sc} \quad (2.79)$$

$$M_{Rd} = A'_s \cdot f_{sc} \left(d' - \frac{h}{2} \right) + bs \cdot f_{cd} \left(\frac{h}{2} - \frac{s}{2} \right) \quad (2.80)$$

(6) Sixth point

We impose that the section uniformly compressed. We assume $\varepsilon_s = \varepsilon'_s = \varepsilon_c = \varepsilon_{c2}$

$$N_{Rd} = bhf_{cd} + A'_s f_{yd} - A_s \cdot f_{yd} \quad (2.81)$$

M_{Rd} is calculate using equation (2.72)

2.7.2.5. Shear verification

The verification procedure is the same for the beam. The detailing of members prescribed by the EN 1992 imposed a minimum diameter of 6 mm or one quarter the maximum diameter of the longitudinal bars. The maximum spacing of the transverse reinforcement is given by the equation (2.82)

$$S_{cl,max} = \min(20\phi_{l,min}; b; 400mm) \quad (2.82)$$

Where:

$\phi_{l,min}$ is the minimum diameter of the longitudinal bars.

b is the lesser dimension of the column.

This maximum spacing has to be reduced by a factor 0,6 in sections within a distance equal to the larger dimension of the column cross-section above or below the beam.

2.8. Linear Dynamic analysis

Dynamic analysis is an analysis that is carried out when the structure is likely to be loaded by a dynamic action such as earthquake, wind, explosion, etc. The purpose of linear dynamic analysis is to determine the response of the structure to a dynamic action. For a seismic action, there are several methods to obtain this response, the simplest and most popular method is the Modal Response Spectrum Analysis.

The Modal Response Spectrum Analysis is an elastic dynamic analysis method that allows to determine elastically the peak dynamic responses of all significant modes of the structure, using the ordinates of the site dependent design spectrum. The overall response is obtained by statistical combination of the maximum modal contributions. (EC8-2/4.2.1.2-(1)). This method is based on the seismic loading described in the form of a response spectrum and the supposed elastic behaviour of the structure allowing the calculation of eigenmodes or natural modes. It can be applied to any type of structure (irregular buildings, structures at special risk whether regular or irregular), with the exception of those with pronounced geometric non-linearities or mechanical non-linearities (insulators and dampers) and it is carried out in two phases, the modal analysis and the response spectrum analysis.

2.8.1. The modal analysis

Before determining the response of the structure to a seismic action, we must first understand how it vibrates. Modal analysis is indispensable to understand the behaviour of the structure to a dynamic action, it allows us to understand how the structure vibrates by determining its modal properties, which are independent of the earthquake action.

This work can be done by hand considering the equations of MDOF system evoked in section 1.2.1.2. b. ii. , but it will be very long and very delicate. To go quickly, we will perform this analysis using the software SAP 2000 V22.

2.8.1.1. Modelling of the structure

The first and most important part of this analysis is the modelling of the structure, as the model considered has a key role in predicting the dynamic behaviour of the structure. A model that is not well idealized to the real structure will produce results that are not those of the real

structure. Given the modelling errors, numerical errors and discretization errors, it is unnecessary to over-detail a model for the simple purpose of determining the modal properties of the structure. The important elements are those that affect the mass, strength, robustness and deformability of the structure, such as columns and beams modelled by frame elements, shear walls and sometimes slabs modelled by area elements (but these can be omitted if they are not included in the study). In general, non-structural elements do not affect the stiffness and strength of a structure, but there are special cases such as stair and special infills that can significantly affect them and should not be overlooked.

2.8.1.2. Determination of the modal properties

After selecting the calculation assumptions and establishing the calculation model, the modal properties for the system are determined. These properties include:

- The modal circular frequencies, ω , and period, T ;
- The modal shape, Φ ;
- The modal participation factor, Γ ;
- The effective modal mass, m .

The modal properties of the structure determined by modal analysis will allow to estimate the response of the structure under the effect of the earthquake loads.

2.8.2. The Multi-modal response spectrum analysis

The response spectrum analysis will use the elastic response spectrum of the earthquake to estimate the response of the structure for each of the useful vibration modes obtained. It will then be necessary to determine the participation of the various modes in the deformations of the structure, i.e., the modes conditioning the effective deformation, in order to evaluate the inertia forces which can be associated with them for the dimensioning of the structure. The response spectrum analysis consists of the following steps:

- Selection of the useful modes and possibly taking into account the pseudo-mode;
- Determination of the acceleration at the level of the ground;
- Determination of the response of the structure;
- Combination of modal responses;
- Cumulation of the effects of the components of the seismic movement.

2.8.2.1. Selection of the useful modes

After the modal analysis, a number of the structure's eigenmodes are available, known by the eigen periods (or frequencies) and eigenforms, with a precision that decreases towards the

higher modes. The analysis of the vibration modes allows the detection of inaccuracies due to the design of the model.

In practice, only a part of these modes will make a significant contribution to the response of the structure, and it is this set of modes that must be taken into account for the analysis. For common buildings, very often alone, two or three modes have a significant influence on the response to a given direction of the earthquake and, among them, the first mode is largely preponderant; therefore, the number of modes selected should not be less than three. In the general case, the simple examination of eigenforms is not a sufficiently reliable method to make the necessary selection, quantitative criteria are needed to evaluate the importance of each of them, which can be done through the effective modal mass contributions of each mode

The criterion most generally used to validate the selection made on modes is that of effective modal masses. By definition, the modal mass for mode i is the effective mass in the studied earthquake direction, i.e., the one accelerated by the acceleration S_a provided by the response spectrum. The result is a force of inertia equal to the horizontal force specific to the response of the structure in this mode.

The calculation of the vibration modes must be continued up to the spectrum cut-off frequency in each direction studied (33 Hz for structures at normal risk and 25 Hz structures at special risk). To avoid neglecting an important mode, the sum of the effective modal masses for the modes considered must be greater than or equal to 90% of the total mass of the structure.

2.8.2.2. The acceleration of the structure at the ground level

Due to the earthquake motion, the structure will be accelerated according to the modes of vibration it adopts. These accelerations are determined using the design response spectrum. Practically, the periods of the useful modes selected for analysis will be projected into the design response spectrum to determine the corresponding accelerations as a function of the acceleration of gravity, and then converted to acceleration in m/s^2 . For each vibration mode, an acceleration will be determined.

2.8.2.3. The response of the structure

The response of the structure is the set of effects observed on the structure after the action of the seismic load. These effects take several forms and are very varied, the most important are the base shear, the displacements and accelerations of the nodes or storeys, the inter-storey drifts and the internal forces generated on the structural elements (shear force, axial forces, bending moment, torsion).

Since the structure has several vibration modes, there will be a response for each of its vibration modes. The global response of the structure is obtained by a modal combination of each response through the application of the SRSS method or the CQC method described in section 2.8.2.4.

a. The base shear

The base shear is an estimate of the maximum lateral force expected on the base of the structure due to seismic activity for each horizontal direction in which the building is analysed. it is also equal to the sum of the seismic design forces at each level of a building and, in accordance with section 4.3.3.2.2 of EN1998-1, it is determined by the equation (2.83)

$$F_i = S_b(T_{1i}) \cdot M_t \cdot \lambda \tag{2.83}$$

F_i is the shear base in the i direction;

$S_b(T_{1i})$ is the acceleration of the structure at the ground level for the fundamental mode in the i direction;

T_{1i} is the is the fundamental period of vibration of the building for lateral motion in the i direction;

M_t is the total mass of the building, above the foundation or above the top of a rigid basement, it is determined in accordance with equation (2.14)

λ is the correction factor, the value of which is equal to: $\lambda = 0,85$ if $T_{1i} \leq 2 T_C$ and the building has more than two storeys, or $\lambda = 1,0$ otherwise.

b. The internal forces on the structural element

They are determined at ULS. In this state the structure is considered as dissipative characterised by its behaviour coefficient q which is determined from equation (2.5)

c. The displacement and the inter-storey drift

The displacement of the structure due to the earthquake is determined at SLS. In this state, the behaviour of the structure is assumed to be ideally elastic, i.e., the structure is considered to be non-dissipative. In this case, its behaviour coefficient is equal to 1. The determination of the displacements will therefore be done with a new design spectrum where q is equal to 1.

The damage limitation requirement is considered to have been satisfied, for buildings having non-structural elements of brittle materials attached to the structure, if the inter-storey drifts are limited in accordance with equation (2.84)

$$d_r \cdot v \leq 0.005h \tag{2.84}$$

dr is the design inter-storey drift

h is the storey height

v is the reduction factor which takes into account the lower return period of the seismic action associated with the damage limitation requirement. The recommended values of v are 0,4 for importance classes III and IV and v = 0,5 for importance classes I and II

2.8.2.4. combination of modal responses

The modal responses calculated for the different modes are combined in order to reconstruct the full effects of the actual earthquake. there are several methods for combining the modal responses of each mode including:

a. SRSS method

The SRSS method takes the square root of the sum of the squares of the contributions of each mode instead of the sum of all the responses. The maximum acceleration response is obtained using equation (2.85)

$$R_{max} = \sqrt{\sum_{i=1}^n R_i^2} \quad (2.85)$$

b. CQC method

The CQC method takes into account a correlation between two responses according to the difference in the two eigen periods using equation (2.86) for the maximum response:

$$R_{max} = \sqrt{\sum_{i=1}^n \sum_{j=1}^n e_{ij} R_i R_j} \quad (2.86)$$

2.9. Non-linear static analysis

The behaviour of a structure under dynamic loading is complex to predict, especially since the behaviour can no longer be considered as linear. Non-linear static (pushover) analysis is thus used to quantify the resistance of the structure to lateral deformation to verify or evaluate the structural performance of newly designed and existing buildings and to estimate the expected plastic mechanisms and damage distribution. Various techniques have been recommended, including the use of constant lateral force profiles and the use of adaptive and multimodal approaches. Pushover techniques provide useful information about the overall characteristics of the structural system and can be used to identify some (but not necessarily all) of the likely mechanisms. Because the prescribed loading used in pushover analyses cannot

represent the potential range of loading experienced in the dynamic response, the results obtained from pushover analyses represent at best an approximation of the nonlinear behaviour expected to develop in the response to earthquake ground motions.

2.9.1. Principle and purpose of analysis

In summary, the structure is subjected to a series of monotonically increasing horizontal actions in order to derive its behaviour curve, also known as the capacity curve or pushover curve, which reflects the horizontal force required to bring it to increasing levels of deformation until it reaches a failure defined by a number of criteria and limits. The fundamental ingredient of this method is that the vibratory response of the structure is assimilated to that of an equivalent single degree of freedom system. This response is represented by its capacity curve, which is presented as a force-displacement curve where the displacement corresponds to that of a particular point of the structure (e.g., the top of the building where movements are greatest), and the force represents the shear force at the bottom.

As mentioned in section 1.2.2.5. b. , Non-linear static analysis is performed for several purposes, but here, it will be used to estimate the plastic mechanisms, damage distribution of the structure, its ductility and its target displacement in order to optimize the structure.

2.9.2. Description of analysis

Non-linear static analysis or pushover analysis is an approximate method in which the structure is subjected to lateral loads which represent the inertial forces that occur as a result of dynamic loading such as earthquake ground acceleration. These lateral loads increase in a monotonic way until the first plasticity of a structural element is reached (occurrence of plastic hinges), the mathematical model of the structure is modified to take into account the reduced resistance. The lateral loads are applied again until further additional structural elements reach the plastic resistance. This process continues until the structure becomes unstable or until a fixed limit is reached.

Pushover analysis uses a series of sequential elastic analyses, superimposed to approximate a capacity curve or pushover curve described by the base shear versus the displacement at the top of the structure (see **Figure 2. 10**) which is independent to any the dynamic load.

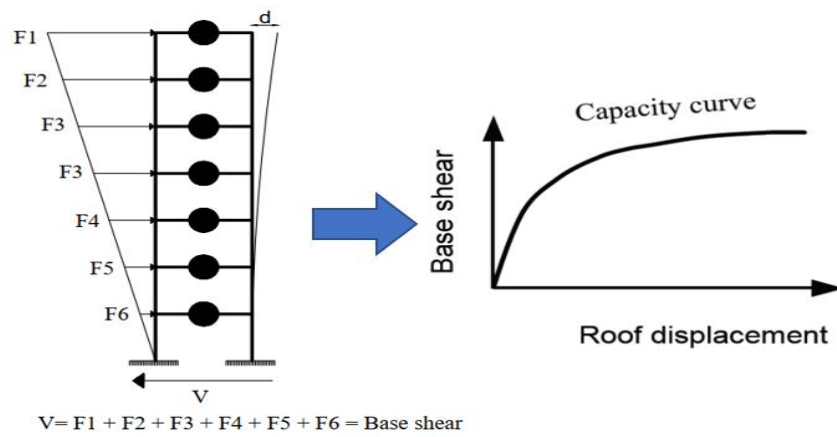


Figure 2. 10. Capacity curve

The capacity curve approximates the way the structure behaves after exceeding the elastic limit and shows that a structure has 4 levels of damage (see **Figure 2. 11**).

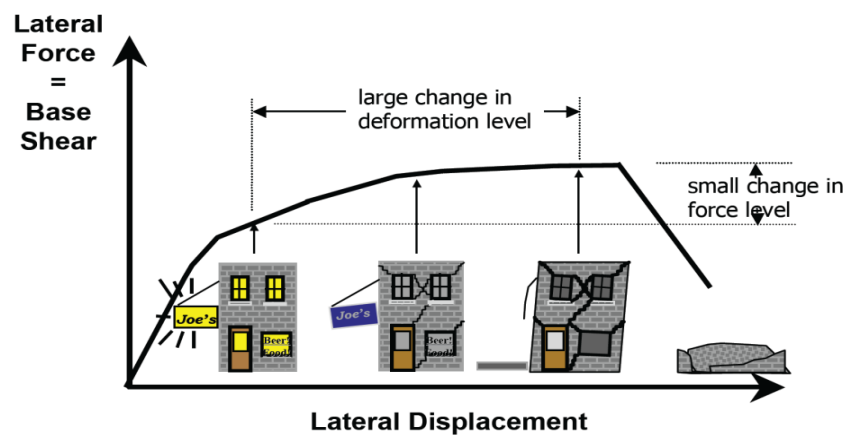


Figure 2. 11. Levels of damage described by a capacity curve

- **First level of damage**

It corresponds to the elastic behaviour of the structure and represents the usual seismic design level. it therefore indicates a state of superficial damage or non-damage.

- **Second level of damage**

It corresponds to a controlled level of damage. the stability of the structure is not at risk, but minor damage is likely to develop.

- **Third level of damage**

It represents an advanced state of damage, with stability at risk. beyond this level, the structure is prone to collapse and will have no resisting capacity.

2.9.3. Method of analysis

The core of the difficulty lies in the assessment of the non-linear behaviour of the structure. The quality of the analysis depends on the reliability of this non-linear behaviour, and is presented in several steps.

2.9.3.1. Modelling of the structure

The analyses will be performed using SAP2000 V22 and a description of the modelling details is provided in the following.

The detailed structural model for non-linear analysis is similar to the linear elastic finite element (component) model described in Section 2.8.1.1. . but with the consideration that the properties of some or all of the components in the model include post-elastic strength and deformation characteristics in addition to the initial elastic properties. These properties are represented on the non-linear model by the addition of plastic hinges to the elastic model.

a. Plastic Hinges

Hinge points are points in a structure where cracking and deformation are expected to occur with relatively higher intensity, so that they exhibit significant flexural (or shear) displacement as the structure approaches its ultimate strength under cyclic loading. These are the locations where transverse diagonal cracks are expected to occur in a real building structure after an earthquake, and are found at both ends of beams and columns. These cracks form at a small distance from the joint, which is where the hinges are supposed to be inserted into the beams and columns of the corresponding analysis model. This distance between the inserted hinges and the joint depends on the cross-sectional characteristics of the elements and a critical insertion length of the hinges called plastic length. **Figure 2. 12** shows the different locations of the plastic hinges.

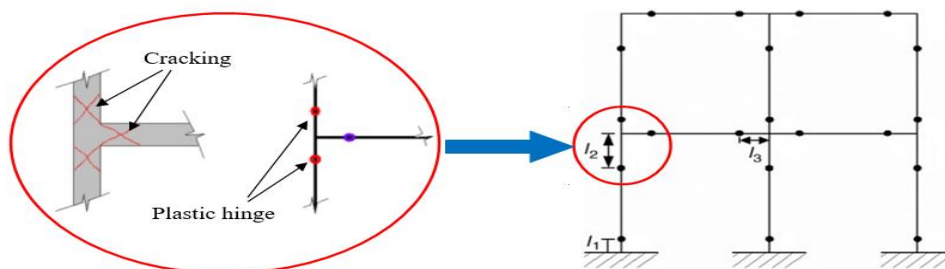


Figure 2. 12. Hinge location at the column and beam

From **Figure 2. 12**, the expression of l_1 , l_2 and l_3 is given by equation (2.87), (2.88) and (2.89) respectively.

$$l_1 = \frac{L_p}{2} \quad (2.87)$$

$$l_2 = H_{Beam} - \frac{L_p}{2} \quad (2.88)$$

$$l_3 = \frac{H_{column}}{2} - \frac{L_p}{2} \quad (2.89)$$

H_{column} is the Column depth;

H_{Beam} is the Beam depth;

L_p is the plastic hinge length given by equation 2.90.

$$L_p = 0.5 H_{beam} \quad (2.90)$$

Equation (2.90) has been implemented by **R. Park** and **T. Paulay** (Reinforced concrete structures, 1975).

b. Properties of Hinges

Hinges are of various types namely, flexural hinges, shear hinges and axial hinges. The first two are inserted into the ends of beams and columns and the last are inserted at either ends of the diagonal struts thus modelled, to simulate cracking of infills during analysis. SAP2000 implements the properties of plastic hinges described in FEMA-356 (or ATC-40). As shown in **Figure 2. 13**, five points marked A, B, C, D and E define the force-deformation behaviour of a plastic hinge. The values assigned to each of these points vary depending on the type of member, material properties, longitudinal and transverse steel content, and the level of axial loading on the member.

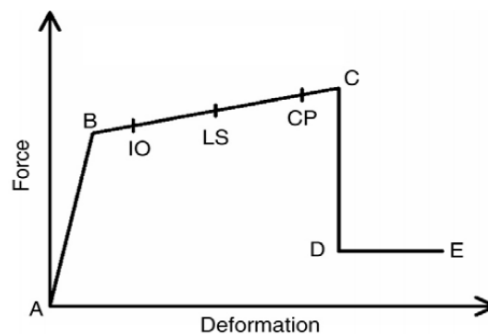


Figure 2. 13. Force–deformation relationship of a typical plastic hinge

- A-B represents the linear elastic range from unloaded state A to its effective yield B;
- B-C represents an inelastic range but linear response of reduced (ductile) stiffness;
- C-D shows a sudden reduction in load resistance followed by a reduced resistance from D to E.

Hinges have non-linear states defined as ‘Immediate Occupancy’ (IO), ‘Life Safety’ (LS) and ‘Collapse Prevention’ (CP) within its ductile range described in section 1.2.2.2.

c. Assignment of the hinges to the elements

Before assigning hinges to elements, it is necessary to define the properties of these hinges which depend on the properties of the element to which the hinges will be assigned. SAP2000 provides 2 types of definition hinge properties:

i. Automatically defined hinge properties

It is defined by the software according to the properties of the element, its behaviour with actions, the axial force behaviour (P), the bending moment behaviour (M), the axial force/moment interaction (P-M) or axial force/biaxial-moment interaction behaviour (P-M-M). It is recommended that M3 hinges be assigned to beams and P-M2-M3 hinges to columns.

ii. User-defined hinge properties

The manual definition of the properties of the hinges requires a moment-curve analysis of each element, which makes the work very tedious, so in this analysis the default-hinges provided by SAP 2000 will be considered.

When automatic or user-defined hinge properties are assigned to a frame element, the program automatically creates a generated hinge property for each hinge.

2.9.3.2. Lateral load pattern

In order to obtain a behaviour of the structure that is as close as possible to reality when subjected to dynamic loading, the distribution of the horizontal incremental action applied on the structure can be presented in different forms:

- a “uniform” pattern, based on lateral forces that are proportional to mass regardless of elevation (uniform response acceleration);
- a “modal” pattern, proportional to lateral forces consistent with the lateral force distribution in the direction under consideration determined in elastic analysis;
- and other simplified distributions depending on the building like rectangular distribution.

Section 4.3.3.4.2.2 of EN 1998-1 states that at least two lateral load distributions should be applied to best represent the dynamic behaviour of the structure. The effects of each distribution modify the capacity curve.

2.9.3.3. Taking into account geometric nonlinearity

Geometric nonlinearity is characterized by P-delta effects and the consideration of large displacements. It is taken into account during the definition of the loads case for the pushover analysis.

2.9.4. The capacity curves

The response of the structure after the application of incremental lateral loads is its behaviour and its different plastic mechanisms. This behaviour is characterised by the so-called capacity curve of the building, which is the relationship between the base shear force and the roof displacement (see **Figure 2. 10**). It is determined for roof displacement values between zero and the value corresponding to at least 150% of the target displacement. In the analysis, the roof displacement is given by a node on the roof, also called the control node. This node should be the one that gives the largest roof displacement, in most cases it is generally at the center of gravity of the roof. This curve is very useful in determining when the structure leaves the elastic domain and begins to behave in a non-linear manner. Again, using this curve, it is possible to determine the peak displacement of the building under a given earthquake, called the target displacement.

2.9.5. Target displacement

The target displacement is the maximum displacement that can be experienced by the structure for a given earthquake. It is determined from the elastic response spectrum. There are several methods of determining target displacement such as the capacity spectrum method of ATC 40 which involves determining the performance point, the coefficient method which uses the coefficients of FEMA 356 and many others. Annex B of EN 1998 presents several steps to determine the target displacement:

1) Transformation of the structure to an equivalent SDOF system.

The mass of an equivalent SDOF system m^* is determined using equation (2.91)

$$m^* = \sum \sum m_i \Phi_i = \bar{F} \quad (2.91)$$

Φ_i : the normalized displacement in such a way that $\Phi_n = 1$, with n the control node;

m_i : the mass in the i-th storey;

\bar{F} : the normalized force.

The transformation factor is given by equation (2.92)

$$\Gamma = \frac{m^*}{\sum m_i \Phi_i^2} = \frac{\sum \bar{F}_i}{\sum \left(\frac{\bar{F}_i^2}{m_i} \right)} \quad (2.92)$$

Then the force F^* and displacement d^* of the equivalent SDOF system are computed using equations (2.93) and (2.94) respectively.

$$F^* = \frac{F_b}{\Gamma} \quad (2.93)$$

$$d^* = \frac{d_n}{\Gamma} \quad (2.94)$$

F_b and d_n are respectively the base shear force and the control node displacement of the MDOF system.

2) Determination of the idealized elasto-perfectly plastic force – displacement relationship

The yield force F_y^* , which represents also the ultimate strength of the idealized system, is equal to the base shear force at the formation of the plastic mechanism. The initial stiffness of the idealized system is determined in such a way that the areas under the actual and the idealized force – deformation curves are equal (see **Figure 2. 14**). Based on this assumption, the yield displacement of the idealised SDOF system d_y^* is determined using equation (2.95).

$$d_y^* = 2 \left(d_m^* - \frac{E_m^*}{F_y^*} \right) \quad (2.95)$$

Where E_m^* is the actual deformation energy up to the formation of the plastic mechanism.

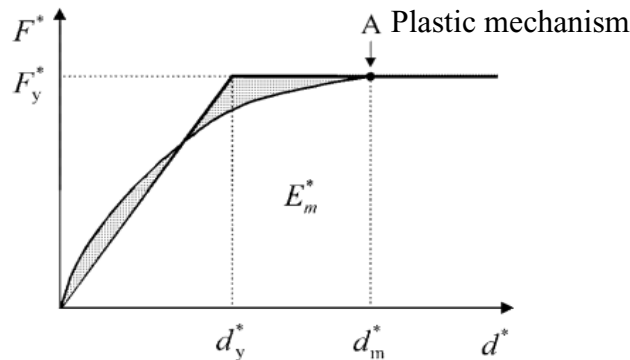


Figure 2. 14. Bilinear idealisation of the pushover curve of equivalent SDOF system

3) Determination of the period of the idealized equivalent SDOF system

The period T^* of the idealized equivalent SDOF system is determined using equation (2.96)

$$T^* = 2\pi \sqrt{\frac{m^* d_y^*}{F_y^*}} \quad (2.96)$$

4) Determination of the target displacement for the equivalent SDOF system

The target displacement of the structure with period T^* and unlimited elastic behaviour is determined using equation (2.97)

$$d_{et}^* = S_e(T^*) \left[\frac{T^*}{2\pi} \right]^2 \quad (2.97)$$

where $S_e(T^*)$ is the elastic acceleration response spectrum at the period T^* .

For the determination of the target displacement d_t^* for structures in the short-period range and for structures in the medium and long-period ranges different expressions should be used as indicated below. The corner period between the short- and medium period range is T_C

- $T^* < T_C$ (Short period range)
 - 1) If $F_y^*/m^* \geq S_e(T^*)$, the response is elastic and thus the target displacement is given by equation (2.98)

$$d_t^* = d_{et}^* \quad (2.98)$$

- 2) If not, the response is nonlinear and the target displacement is given by equation (2.99)

$$d_t^* = \frac{d_{et}^*}{q_u} \left(1 + (q_u - 1) \frac{T_C}{T^*} \right) \geq d_{et}^* \quad (2.99)$$

where q_u is given by equation (2.100)

$$q_u = \frac{S_e(T^*)m^*}{F_y^*} \quad (2.100)$$

- $T^* \geq T_C$ (Medium and long period range)

The target displacement is given by equation (2.101).

The relation between different quantities can be visualized in **Figure 2. 15 a) and b)**.

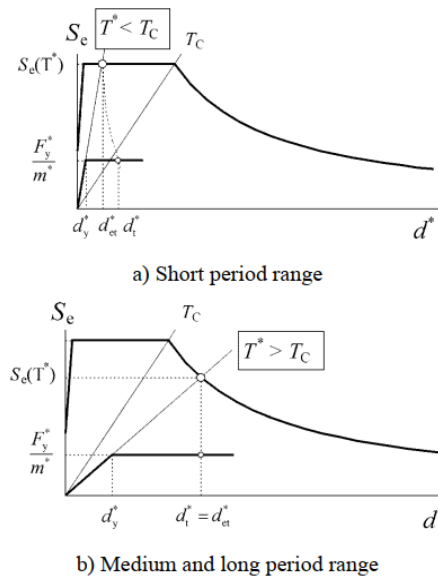


Figure 2. 15. Determination of the target displacement for the equivalent SDOF system

5) Determination of the target displacement for the MDOF system

The target displacement of the MDOF system which corresponds to that of the control node is given by the equation 2.101

$$d_t = \Gamma d_t^* \tag{2.101}$$

2.10. Soil-structure interaction

The soil and the structure interact with each other at all times. This is manifested in the fact that the behaviour and response of a soil, which may be due to one seismic event or another, influences the response of the structure and its behaviour. Conversely, the behaviour of a structure can influence the behaviour of the ground on which it is placed. Thus, it is very important to consider the soil-structure interaction in the analysis of the behaviour of a structure and in the determination of its response to static and dynamic loading. The most commonly used method to represent the soil-structure interaction in the analyses is to use linear springs associated with the structure in the modelling (see **Figure 2. 16**).

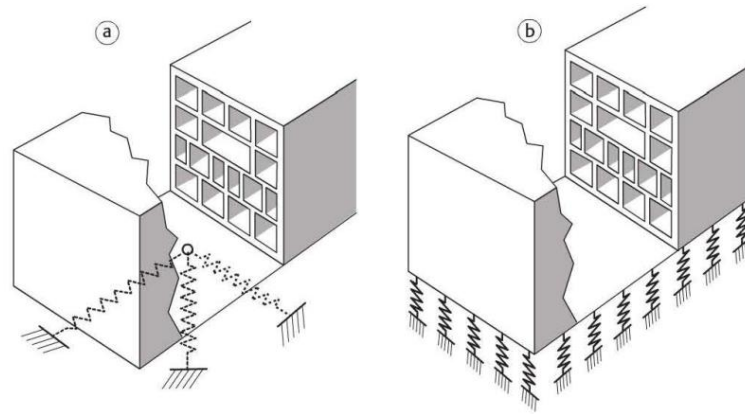


Figure 2. 16. Soil modelling by a linear springs system: (a) concentrated spring (b) distributed springs (Davidovici et al, 2013)

In the present work, we will consider a distributed spring system. The characteristics of these springs being function the soil properties and the interaction surface between the soil and the building, we need first to evaluate the footing sections.

2.10.1. Evaluation of the footing section

Knowing the characteristics of the foundation soil, that are the density ρ , the Elastic modulus E , the Shear modulus G , the Poisson ratio ν , the shear wave velocity V_s , the allowable soil stress can be evaluated. From this stress and the axial forces resulting from the static analysis that can act on each footing, it is possible to determine the minimum cross-sections of each footing by dividing the axial force by the allowable stress.

2.10.2. Evaluation of the stiffness for each footing class

There are different methods and formulations that permit to evaluate de stiffness of the spring that represent the soil in function of the characteristics of the soil. The easiest method is to use the modulus of subgrade reaction of the soil abbreviated **ks**. This coefficient is determined through in-situ tests such as the plate bearing test. Several researchers like Terzaghi have carried out tests on several soils in order to obtain a range of values depending on the type of soil. Table 2.2 shows the different values of **ks** depending on the type of soil.

Table 2. 3. Values of modulus of subgrade reaction for different type of soil

Soil description	Modulus of subgrade reaction (kN/m ² /m)
Humus soil or peat	5000 – 15000
Recent embankment	10000 – 20000
Fine or slightly compacted soil	15000 – 30000
Well compacted sand	50000 – 100000
Very well compacted sand	100000 – 150000
Loam or clay (moist)	30000 – 60000
Loam or clay (dry)	80000 – 100000
Clay with sand	80000 – 100000
Crushed stone with sand	100000 – 150000
Coarse crushed stone	200000 – 250000
Well compacted crushed stone	200000 – 300000

Conclusion

The objective of this chapter was to present the different methods and techniques used for the analysis and design of a reinforced concrete building when it is subjected to the action of vertical loads alone and when it is subjected to a dynamic load such as an earthquake. The main focus is on linear static analysis through column and beam design procedure, linear dynamic analysis through modal analysis and response spectrum analysis, and the nonlinear static analysis through the procedure of determining the capacity curve of the building and its target displacement when subjected to an earthquake. The application of the linear static and linear dynamic analyses to a real case study and the presentation of the results will be the subject of the next chapter.

CHAPITRE 3 : LINEAR ANALYSES AND INTERPRETATION OF RESULTS

Introduction

This chapter presents the application and the results of linear analyses, presented in the methodology, on a real case study. It is mainly structured by the presentation of this case study, its environment and its site, then comes the analysis part divided in two which includes the static linear analysis and the dynamic linear analysis.

3.1. General presentation of the site

Yaoundé, also called the “city of seven hills”, is the political capital of Cameroon. With a population of 4,100,000 in 2019. It is, along with Douala, the most populous city in the country and in the CEMAC zone. Yaoundé is the capital of the Centre region and of the Mfoundi department (the administrative boundaries of the department are the same as those of the department) and is home to most of Cameroon's most important institutions, including the National Advanced School of Public Works (NASPW).

Created in 1970, by decree of the President of the Republic, under the name of National School of Technology (ENAT), it became in 1982 the National Advanced School of Public Works (NASPW) and includes an annex school in BUEA and two Public Works Trade Centres (CMTP) in AKONOLINGA and in GAROUA. The National Advanced School of Public Works is a Public Institution of Technical Vocational Training placed under the supervision of the Ministry of Public Works. It is made up of several buildings, allowing to ensure its good functioning, of which the most recently built building, the new administrative building is the subject of our study.

3.1.1. Geology and relief

The bedrock of Yaoundé is mainly composed of gneiss. This rock is neither porous nor soluble, but it is its discontinuities (faults, diaclases). The hydrogeology is characterized by continuous aquifers, approximately exploitable, overlying fissures or aquifers of aquifer fractures in the bedrock; these types of aquifers are superimposed or isolated. In terms of relief, the terrain rises gently in escarpments from the south-western coastal plain before joining the Adamawa plateau via depressions and granitic massifs. The terrain is characterized by rolling, forested hills, the highest of which have rocky, bare tops.

3.1.2. Climate and hydrology

Yaoundé features a tropical wet and dry climate, with record high temperatures of 36°C , an average of 23.8°C and a record low temperature of 14°C . Primarily due to the altitude, temperatures are not as high as would have been expected for a city located near the equator.

3.2. Presentation of the project

3.2.1. Geometry of the building

The case study is the new administrative building of the national advanced school of public works of Yaoundé. It is built in reinforced concrete and has a total height of 21 m in respect to the ground level and is divided into 7 levels, each level having a height of 3m. The building, mainly offices and meeting rooms (Category B and Class II building according to EN1991-1 and EN 1998 respectively), is irregular in plan and has a total length of 35.5m and a total width of 24m. The structural elements are columns, beams, shear walls and slabs, the slab is a 20 cm thick ribbed slab. The building is divided into 3 blocks separated structurally from each other by separation joint.

The first building block, which we have named block B, is the largest block, it is 31.75 m long and 10 m wide. It has a total of 7 levels, the rooms in this building are offices and meeting rooms. This block is structurally separated from the other two blocks by separation joints. The second building block, named block C, is the smallest block, it has 6 levels. it is the staircase block intended for the circulation between the floors. It is 6 m long and 3.25 m wide and is structurally separated from block B by a separation joint. The last block named block A has 7 levels and includes a hall, a lift shaft with staircases running around it, a mezzanine and a walkway linking it to block A but separated from it structurally by a separation joint, it is 9.75 m long and 10 m wide. All our analysis will focus on block B.

3.2.2. Architectural and structural plan

The architectural plans of the building are presented in appendix B. The structure has the same structural plan from level 1 to level 6, as shown in **Figure 3. 1**. The structural plans of level 7 is presented in appendix B.

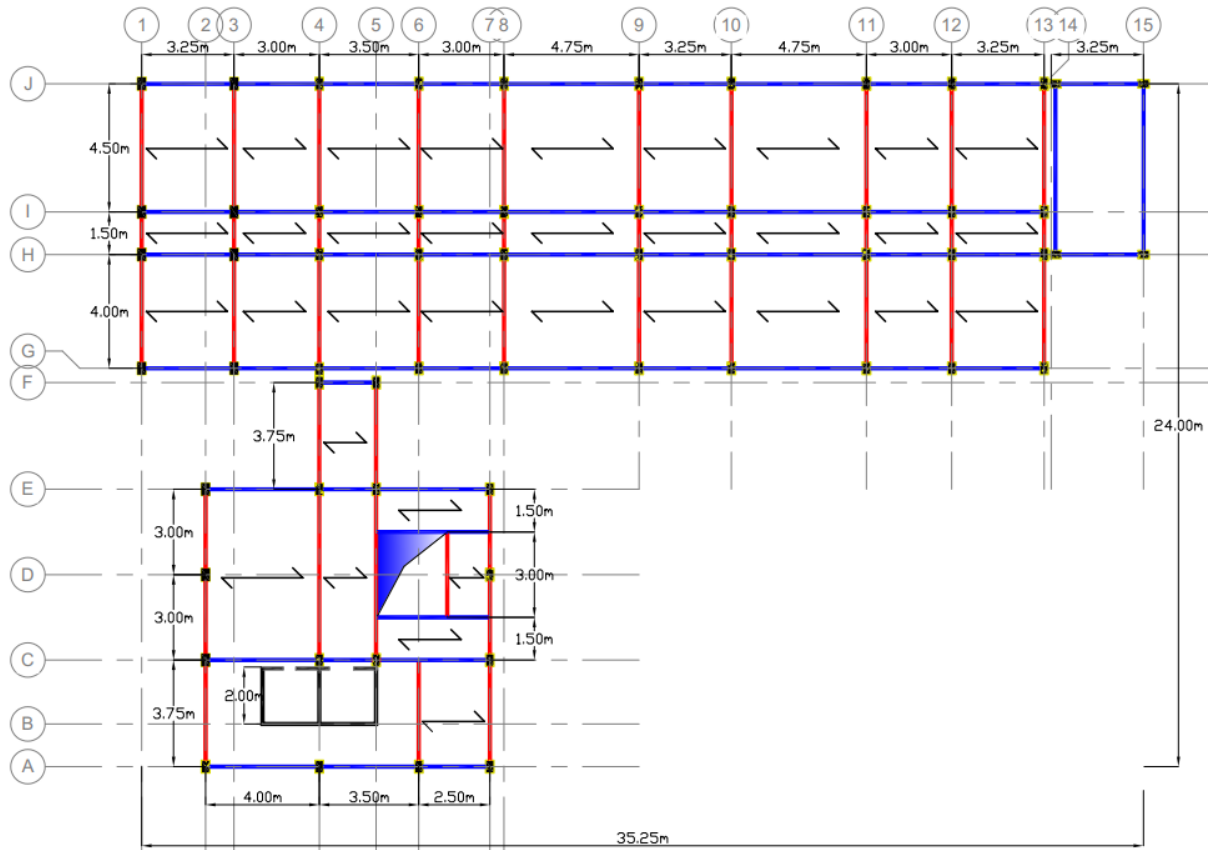


Figure 3. 1. Structural plan from RDC to storey 5 of the case study

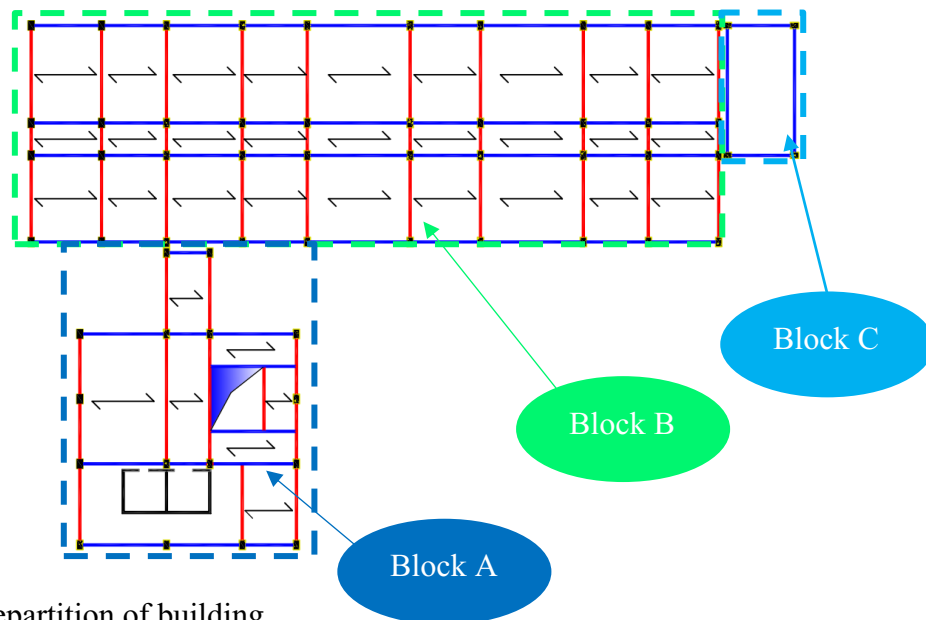


Figure 3. 2. Repartition of building

3.2.3. Material properties

As we said previously, our study is about a reinforced concrete building, this part presents the mechanical properties of concrete and steel used for analysis and the design.

3.2.3.1. Concrete

For the analysis and design, the concrete class chosen is C25/30. **Table 3. 1** give its main characteristics for linear analysis and design of our case study.

Table 3. 1. Concrete characteristics

Property	Value	Unit	Definition
Class	C25/30	-	Concrete class
R_{ck}	30	N/mm ²	Characteristic cubic compressive strength
f_{ck}	25	N/mm ²	Characteristic cylinder compressive strength at 28 days
$f_{cm} = f_{ck} + 8$	33	N/mm ²	Mean concrete compressive strength at 28 days
$f_{ctm} = 0.3 \cdot (f_{ck})^{\frac{2}{3}}$	2.56	N/mm ²	Mean value of axial tensile strength of concrete
γ_c	1.5		Partial safety factor for concrete
α_{cc}	0.85		The coefficient taking account of long-term effects on the compressive strength and of unfavourable effects resulting from the way the load is applied
$E_{cm} = 22 \cdot (f_{cm} / 10)^{0.3}$	31000	N/mm ²	Secant modulus of elasticity
γ	25	kN/m ³	Specific weight of concrete
ϵ_{c2}	2	‰	the strain at reaching the maximum strength
ϵ_{cu2}	3.5	‰	the ultimate strain

3.2.3.2. Steel reinforcement

The longitudinal steel reinforcement adopted is B450C and for transversal reinforcement, we consider steel with a characteristic yield strength of 235 MPa. **Table 3. 2** show the main characteristics of steel reinforcement for linear analysis and design of a structure.

Table 3. 2. Reinforcement characteristics

property	value	unit	definition
class	B450C	-	Longitudinal reinforcement class
γ_s	1.15	-	Partial safety factor of steel
f_{yk}	450	N/mm ²	Characteristic yield strength of longitudinal reinforcement
f_u	540	N/mm ²	Characteristic ultimate strength of longitudinal reinforcement
$\epsilon_s = \epsilon_{yd}$	0.196	%	Yield strain
ϵ_{ud}	6.75	%	Ultimate stain
f_{ywk}	235	N/mm ²	Characteristic yield strength of transversal reinforcement
Es	200000	N/mm ²	Modulus of elasticity
γ	78.5	kN/m ³	Specific weight of steel

3.3. Linear static analysis and design

Linear static analysis consists in analysing the building under vertical static load, i.e., considering only permanent and imposed loads. From this analysis, the solicitations on the structural elements will emerge, which will then be used for their design. The design will be done on the most stressed structural elements.

3.3.1. Action on the building

3.3.1.1. Permanent action

Permanent actions include structural permanent load and non-structural permanent load. The weight of the structure itself i.e., the weight of the structural element (beams, column, slab) constitutes the structural permanent load. All architectural components such as exterior cladding, partitions and ceilings and equipment and static machinery, when permanent fixtures, constitute the non-structural permanent load. **Table 3. 3**, **Table 3. 4**, **Table 3. 5** and **Table 3. 6** present the structural and the non-structural permanent load of the building studied.

- Structural permanent load at storey level and roof level

Table 3. 3. structural permanent load

Nature	Designation	Value	Unit
G1k	Self-weight of slab (16+4)	2.80	kN/m ²

The self-weight of the beams and columns is calculated automatically by the software, while the equivalent self-weight of a 20 cm thick reinforced concrete slab is applied as a dead load on the beams of the structure.

- Non-structural permanent load

Table 3. 4. Non-structural permanent load at storey level due to slab

Nature	Designation	Value	Unit
G2k	screed	0.2	kN/m ²
G2k	tiles	0.6	kN/m ²
G2k	False ceiling	0.5	kN/m ²
Total		1.3	kN/m ²

Table 3. 5. Non-structural permanent load due to wall and exterior cladding

Nature	Designation	Value	Unit
G2k	Partition wall	2.5	kN/m ²
G2k	Exterior cladding	0.18	kN/m ²
Total		2.68	kN/m ²

Table 3. 6. Non-structural permanent loads at roof level

Nature	Designation	Value	Unit
G2k	False ceiling	0.5	kN/m ²
G2k	Metal roofing in zinc, including sheathing and cleats	0.25	kN/m ²
Total		0.75	kN/m ²

3.3.1.2. Imposed load

Because the specific use of the building studied is office, it is classified as category B according to EN 1991-1-1. The imposed load for category B area is between 2 and 3 kN/m². For this study we consider 2.5 kN/m².

The roof is not accessible except for maintenance (category H), so we consider 1 kN/m² for the imposed load on the roof.

3.3.2. Durability and concrete cover

The design working life of this building is 50 years, so the structural class of the building is S4 according to EN 1990. The exposure class is assumed XC1 for all the super structure of

building and XC2 for foundations. Following the procedure of calculation evoked in section 2.6. of the methodology, we obtain:

From equation (2.18), $C_{min} = \max(16; 15 + 0 - 0 - 0; 10 \text{ mm}) = 16 \text{ mm}$

From equation (2.17), $C_{nom} = 16 + 10 = 26 \text{ mm}$

We have the nominal concrete cover equal to 26 mm, we can choose the concrete cover equal or greater than 30 mm for more security and for easy data handling.

3.3.3. Design of beam

The design is carried out on the main beams of the building. For an optimal design, the most solicited beam (beam of line 10) has been considered, the one with the largest area of influence, as shown in **Figure 3. 3**

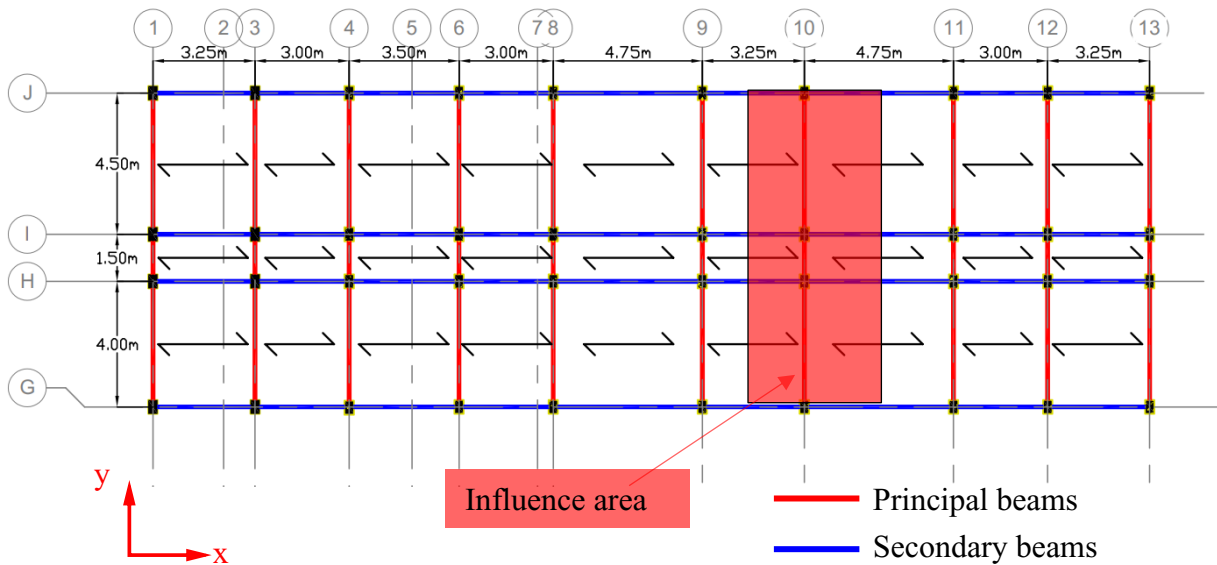


Figure 3. 3. Beam selected for design

3.3.3.1. Preliminary design

Following the procedure evoked in section 2.7.1.1. of the methodology, and considering the beam is simply supported, we obtain:

The longest span of beam in bloc A is 4,5 m, from (2.19) we have

$h \geq \frac{4,5}{14}$ and $b \cong 0,5h$, we choose $h=0,4 \text{ m}$ and $b=0,2 \text{ m}$

3.3.3.2. Static scheme of beam and load combination

The beam to be designed is modelled in a software SAP 2000 v22 as frame element with different restraint at the support. The static schemes of the beam, considered for design, are

shown in **Figure 3. 4** and for these models, nine load combinations are considered for the design of beam at ULS and SLS are presented in **Figure 3. 5**

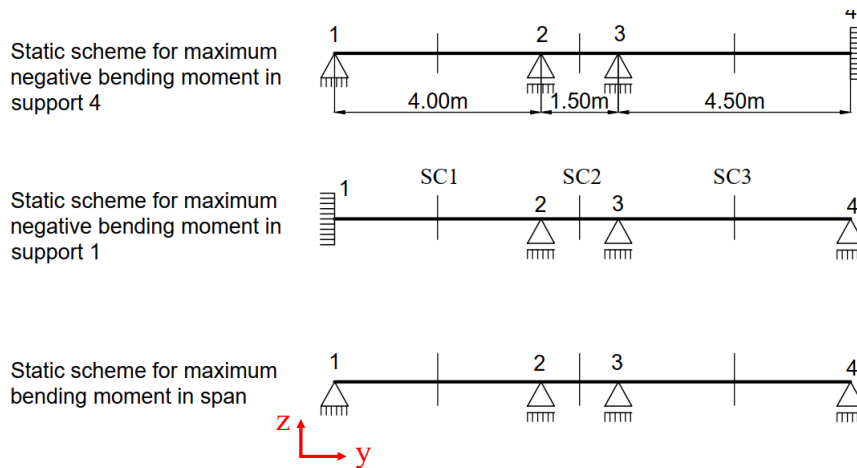


Figure 3. 4. Static schemes of beam study

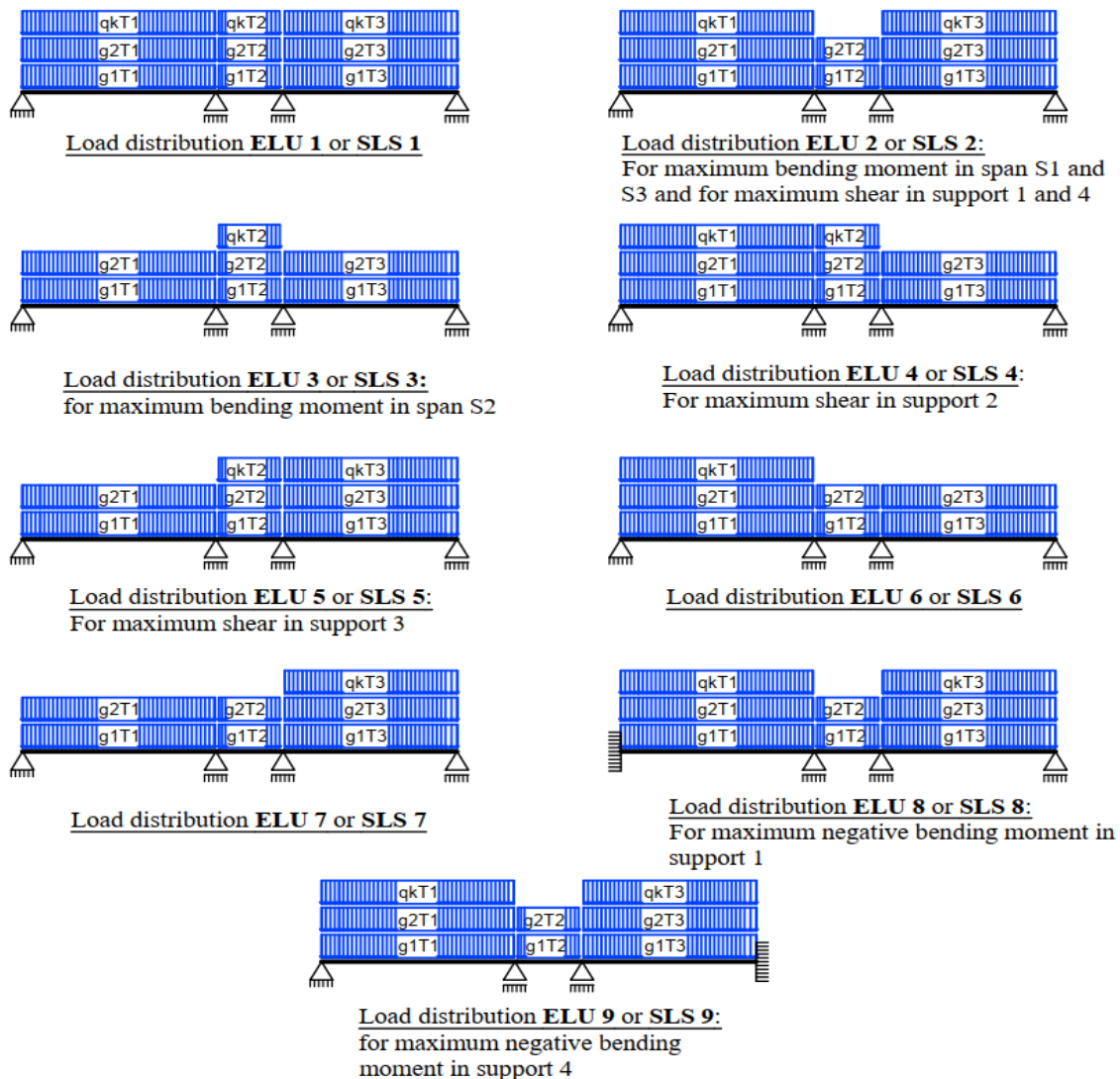


Figure 3. 5. Load combinations

From the different load distribution, solicitations are extracted, the ULS design and the SLS verification can be performed.

3.3.3.3. Ultimate limit state design

a. The internal forces of the beams

The static schemes and loads were implemented in the calculation software SAP2000 v22. The 9 load combinations were defined and the internal forces (bending moment and shear) at each point of the beam were obtained for each of the defined combinations.

The analysis of these results, using Microsoft Excel, allowed to represent the diagrams of these internal forces for each of these combinations (**Figure 3. 6** and **Figure 3. 7**). Again, using Microsoft Excel, the envelope curve of each internal force was obtained and is illustrated by **Figure 3. 8** and **Figure 3. 9**.

Envelope curve is a curve showing the maximum and minimum values of the internal forces from the defined combinations.

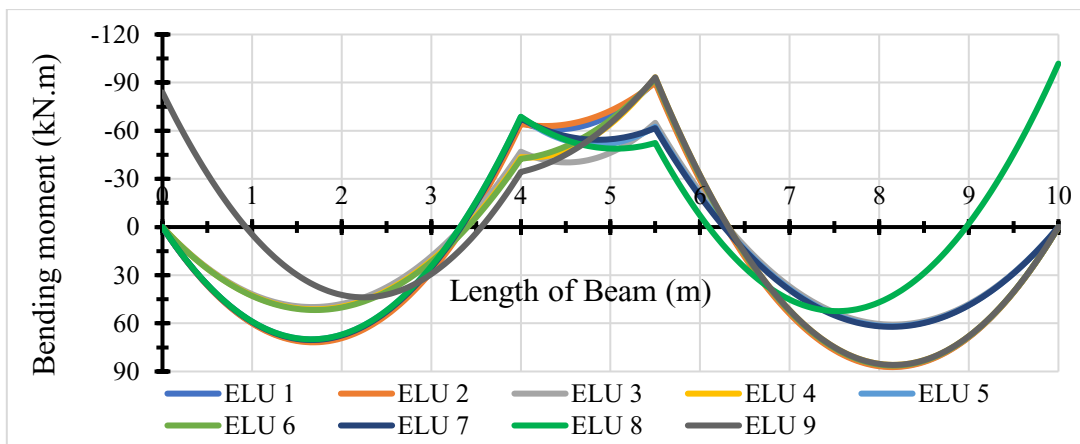


Figure 3. 6. Bending moment diagrams for 9 load combinations on the beam

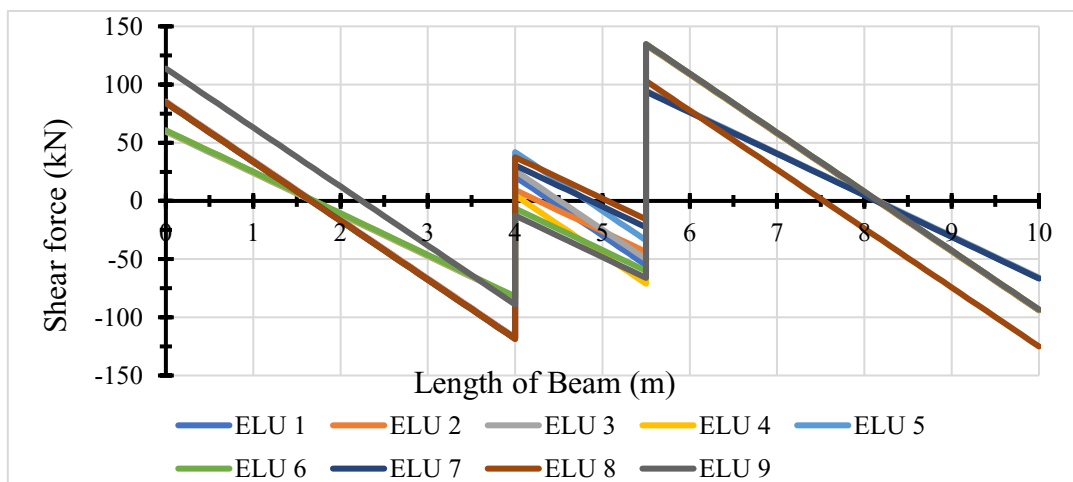


Figure 3. 7. Shear force diagrams for 9 load combinations on the beam

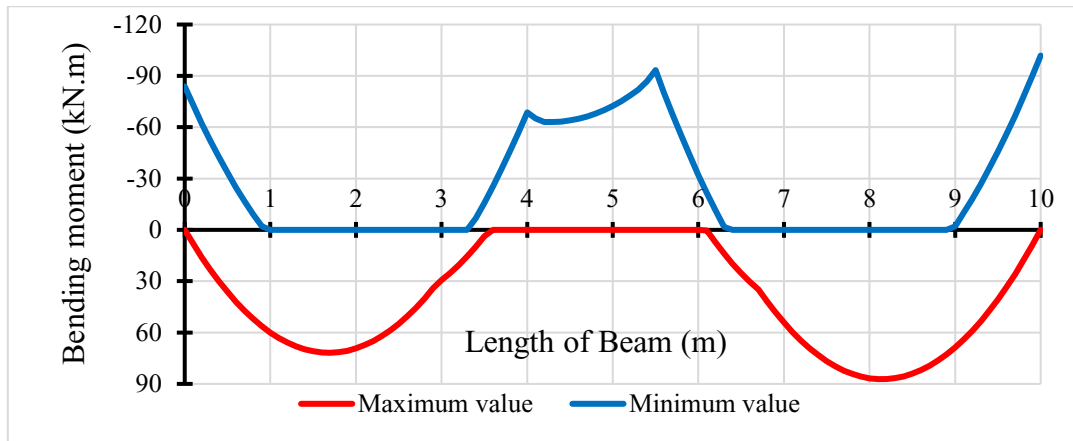


Figure 3. 8. Envelope curve of the bending moment on the beam

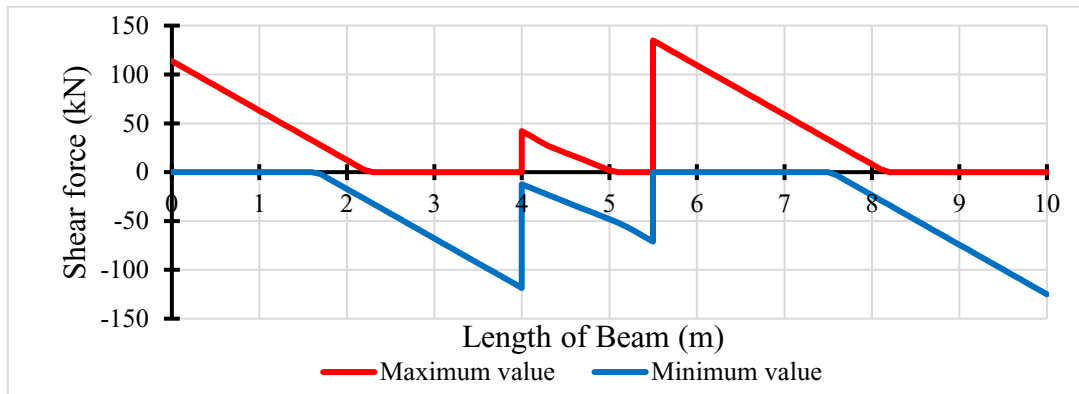


Figure 3. 9. Envelope curve of shear force on the beam

Following the procedure described in section 2.7.1.2. a. i. of the chapter 2, the design curve is obtained (see figure 3.10).

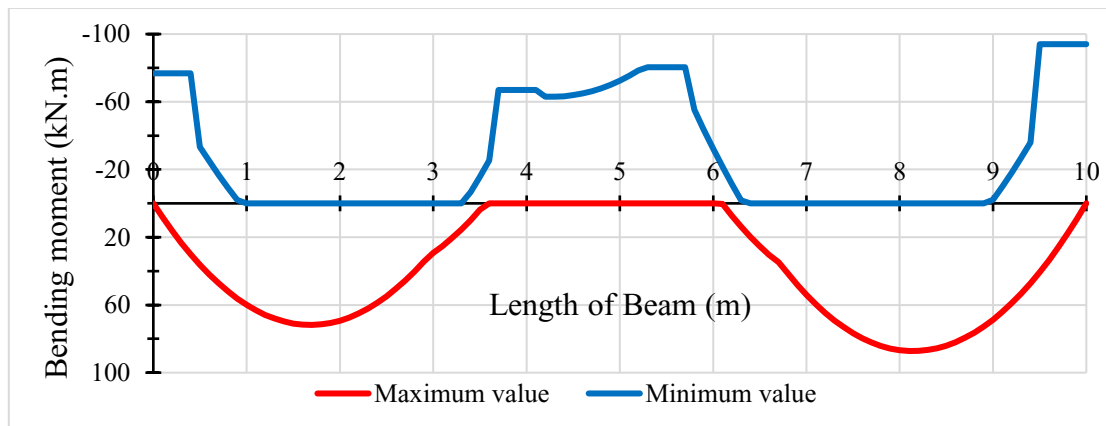


Figure 3. 10. Design curve of the beam

This curve is used to determine the longitudinal reinforcement of the beam according to the procedure described in section 2.7.1.2. a. ii. The distribution of the reinforcement has been plotted in the same diagram as the design moment curve (see Figure 3. 11.) in order to show that at each point of the beam (20 × 40)cm, the resisting moment is greater than the bending moment.

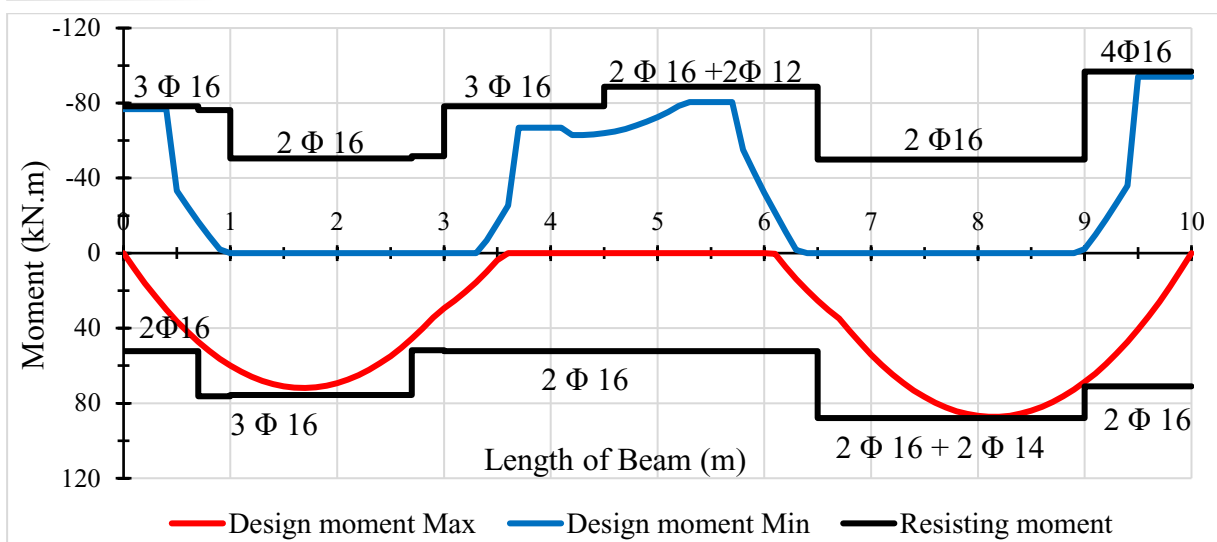


Figure 3. 11. Verifications of the section under bending moment

b. The shear reinforcement

Following the procedure described in section 2.7.1.2. b. for obtaining the shear reinforcement, the distribution of this reinforcement has been plotted in the same diagram as envelope curve of shear (see Figure 3. 12) in order to show that at each point of the beam, the resisting shear is greater than the shear force. The transverse reinforcements are made of $\Phi 8$ and the number of legs of the stirrups is 2.

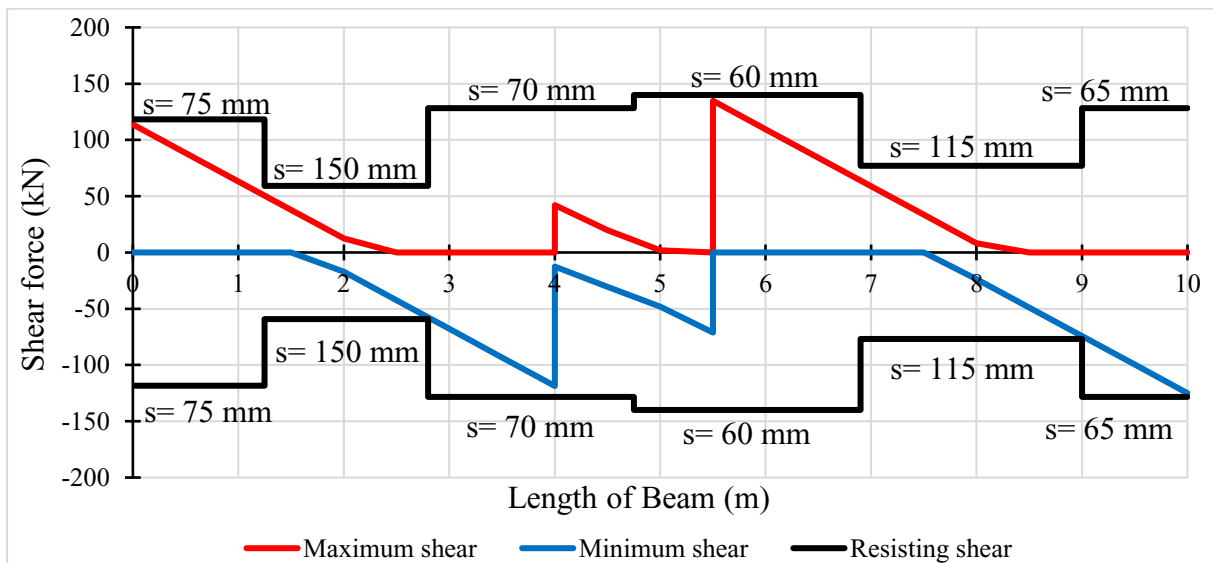


Figure 3. 12. Verifications of the section under shear force

3.3.3.4. Serviceability limit state verifications

The SLS verification was carried out considering the characteristic (or rare) loading condition. The application of this loading was carried out on 7 of the 9 load distributions defined in Figure 3. 5, which allowed to represent the envelope diagram of the bending moment at the rare loading condition presented by **figured 3.13 and 3.14**.

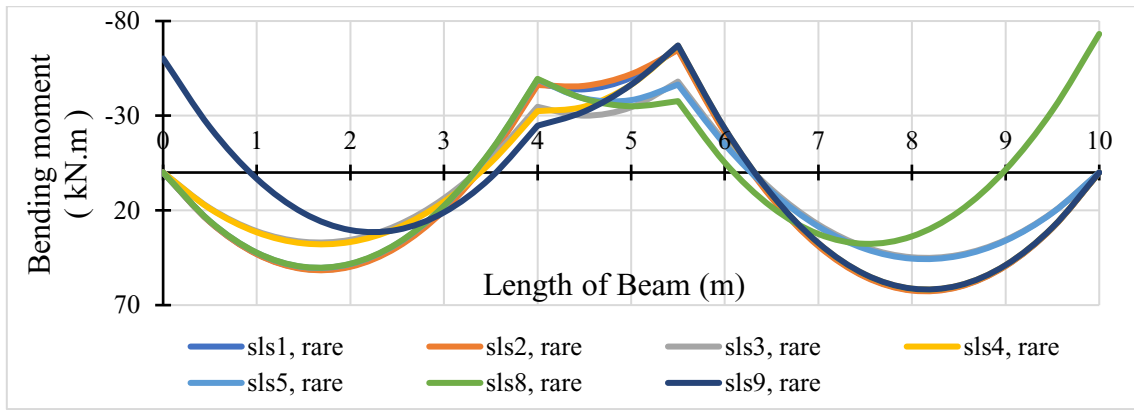


Figure 3. 13. Bending moment diagrams for SLS combination

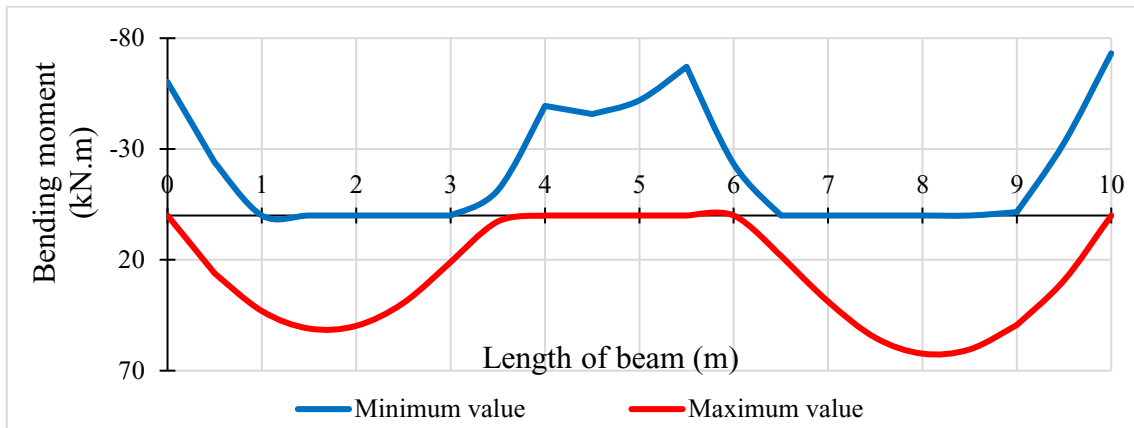


Figure 3. 14. Envelope curve of SLS bending moment

a. Stress limitation

Following the procedure described in section 2.7.1.3. a. , the stress distribution in concrete and in the longitudinal reinforcement is plotted to check the stress limit. They are presented in figure 3.15 and 3.16

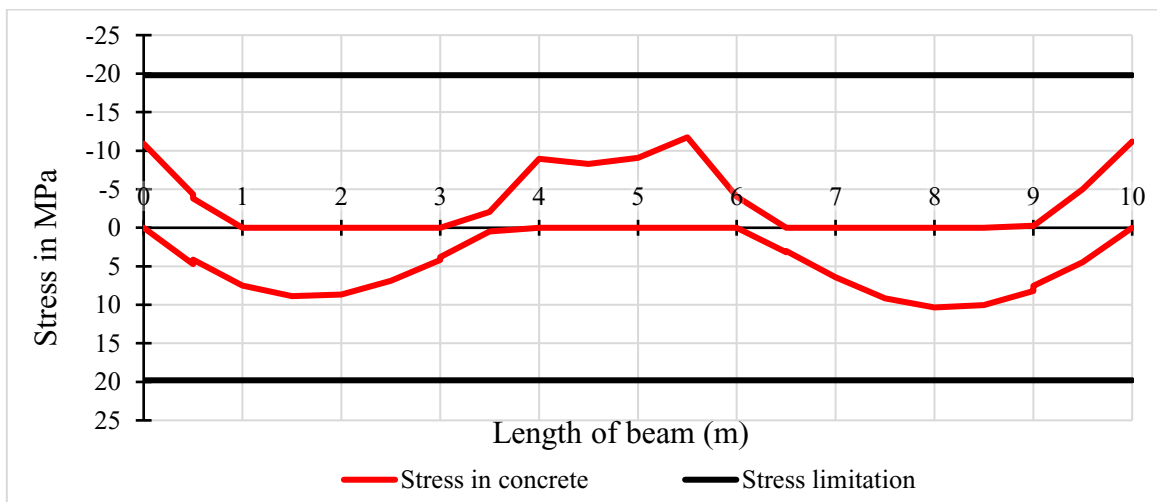


Figure 3. 15. Concrete stress limitation

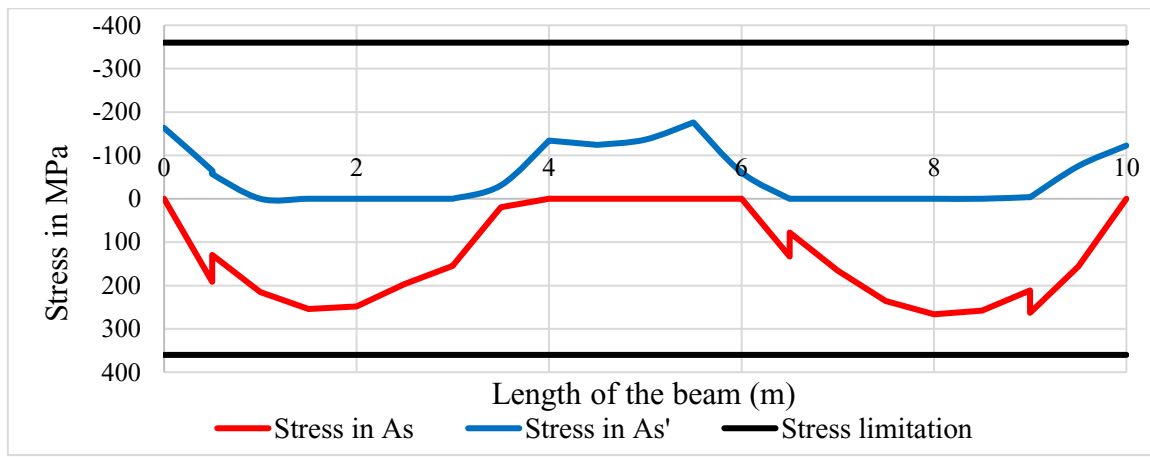


Figure 3. 16. Reinforcement stress limitation

b. Deflection

The deflection verification was carried out in the middle of each span as this is where the maximum deflection is likely to occur. The application of the procedure described in paragraph 2.7.1.3. b. resulted in the deflections in sections Sc1, Sc2 and Sc3 which are presented in Table 3. 7

Table 3. 7. Deflection control

Section	As provided	As' provided	f1 (mm)	f2 (mm)	f (mm)	limit (mm)	Verification
SC1	2 Φ + 2 Φ 14	2 Φ 16	3,05	4,78	4,55	18	Deflection Controlled
SC2	2 Φ 16	3 Φ 16	0,06	0,14	0,13	6	Deflection Controlled
SC3	3 Φ 16	2 Φ 16	4,96	8,59	8,33	16	Deflection Controlled

c. Crack control

Following the procedure of crack control described in section 2.7.1.3. c. of chapter 2, a maximum reinforcement diameter of **20 mm** and a maximum reinforcement spacing of **200 mm** were obtained to control the cracking of the beam at a maximum thickness of **0.4 mm**.

3.3.4. Design of column

3.3.4.1. Preliminary design

Using equation (2.51), the minimum cross-sectional area of the columns in each level was determined. With this minimum area, the column sections were selected, taking into account the slenderness (section 2.7.2.2.). The selected sections are summarized in **Table 3. 8**

Table 3. 8. Preliminary design of columns

Level	Nsd (kN)	Ac, min (mm ²)	a(y) (mm)	b(x) (mm)	A (mm ²)	λ_y	λ_x	λ_{lim}
1	1439,73	78649,41	500	400	200000	25,98	20,78	30,31
2	1176,68	65541,18	400	400	160000	29,05	29,05	29,67
3	927,90	52432,94	400	400	160000	29,05	29,05	37,62
4	686,72	39324,71	400	400	160000	29,05	29,05	50,83
5	456,92	26216,47	400	300	120000	44,72	33,54	57,30
6	232,28	13108,24	300	300	90000	51,64	51,64	84,53
7	90,56	10008,24	300	300	90000	51,64	51,64	216,81

Table 3. 8 shows that λ_x and λ_y are lower than λ_{lim} , so all these columns are classified as short columns. Therefore, the second order effect can be neglected during the design of the longitudinal reinforcement.

3.3.4.2. The internal forces on columns

The static analysis was carried out using the software SAP2000 v22 to determine the internal forces acting on the column. For this analysis we first identified the most stressed columns in the building and then applied load combinations to these columns to obtain the maximum forces. The most stressed columns in terms of bending moment are columns in row J-10 from grid J and 10 shown in **Figure 3. 3** and **figure 3.17**

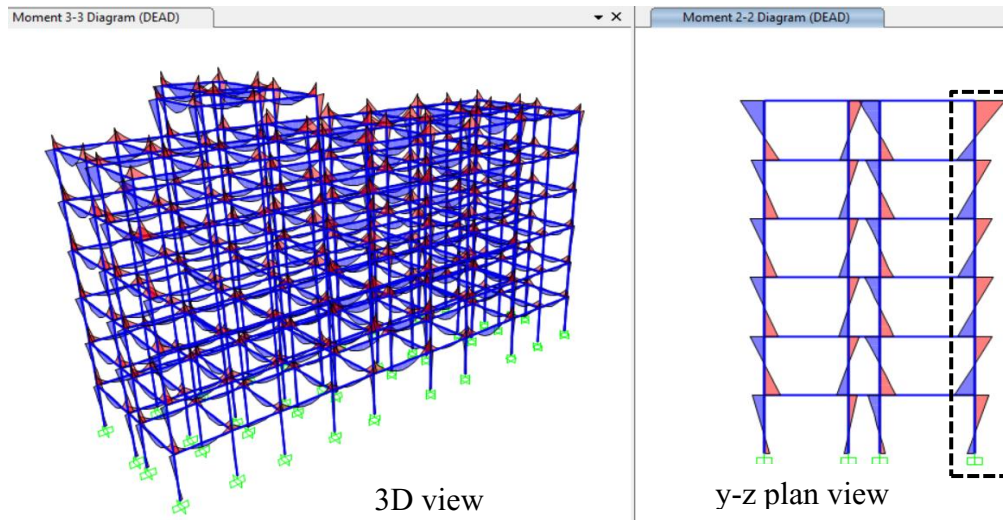


Figure 3.17. Most stressed columns in terms of bending moment

The number of loading combinations considered was 15, and the resulting solicitations were analysed using Excel and plotted. (See figure 3.18 to 3.22)

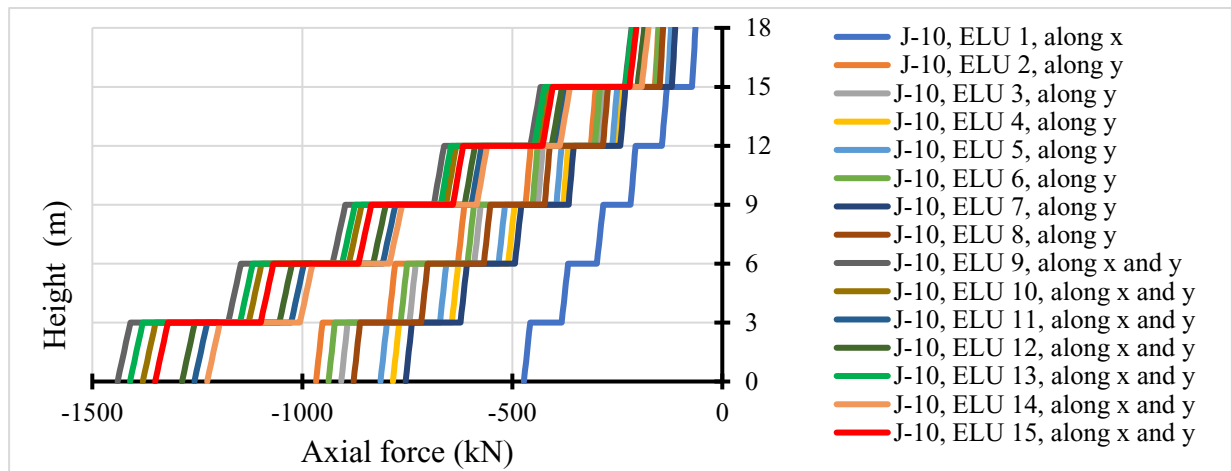


Figure 3.18. Axial force diagrams for 15 combinations of loads in columns of row J-10

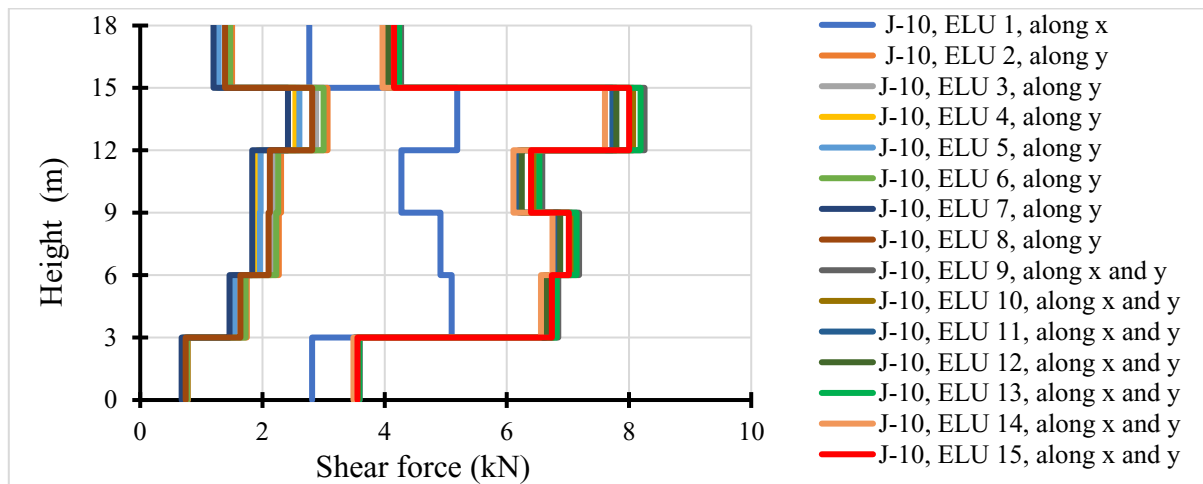


Figure 3.19. Shear force diagrams V_{y-y} for 15 combinations of column J-10 in the y direction

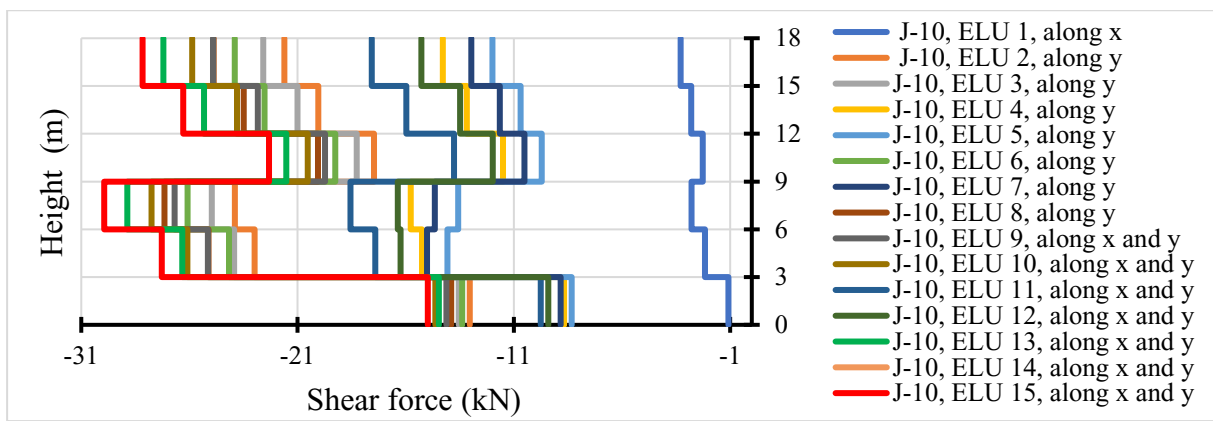


Figure 3. 20. Shear force diagrams V_{x-x} for 15 combinations of column J-10 in the x-direction

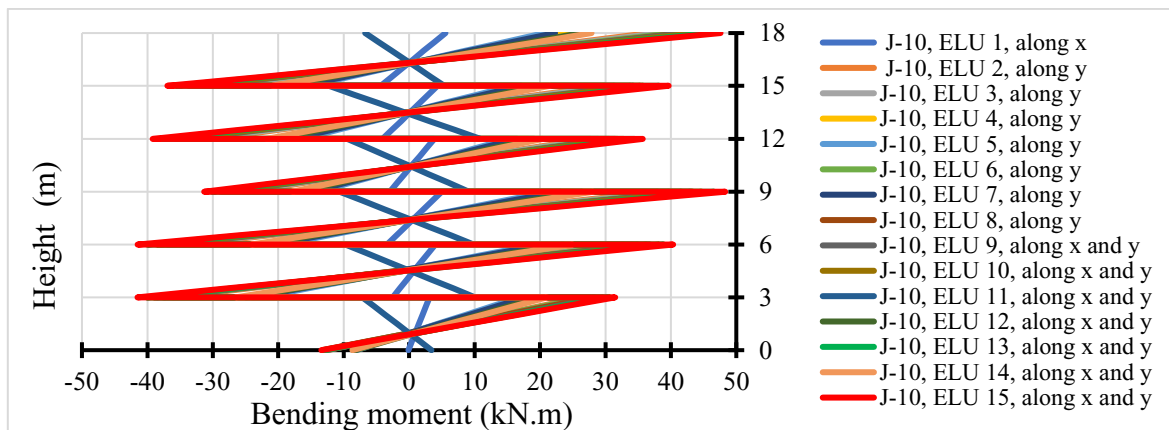


Figure 3. 21. Bending moment diagrams M_{y-y} around Y for 15 combinations of loads in columns of row J-10

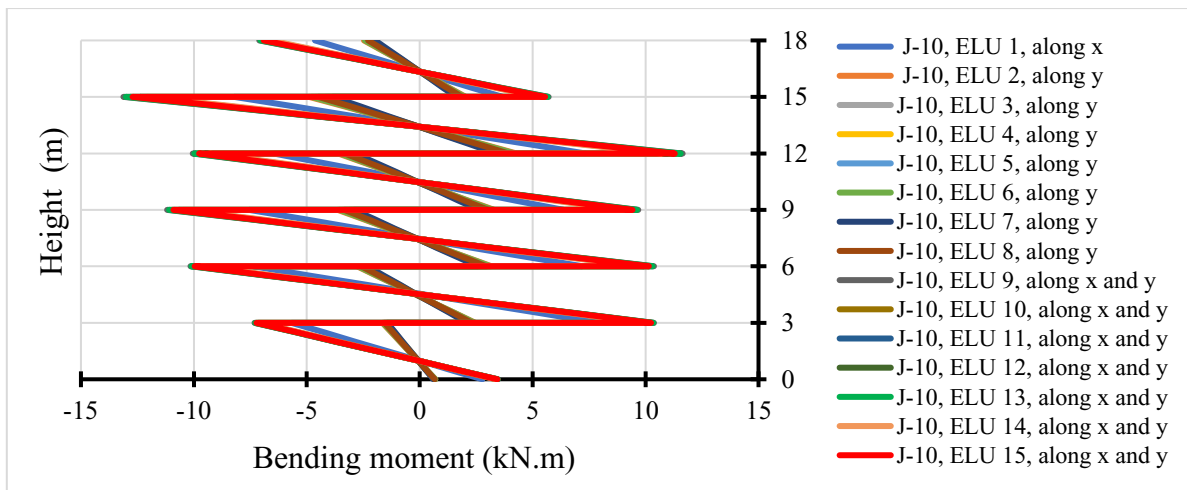


Figure 3. 22. Bending moment diagrams M_{x-x} around X for 15 combinations of loads in columns of row J-10

With these 15 load combinations, we have plotted envelope diagrams for each internal force. (See figure 3.23 to 3.27)

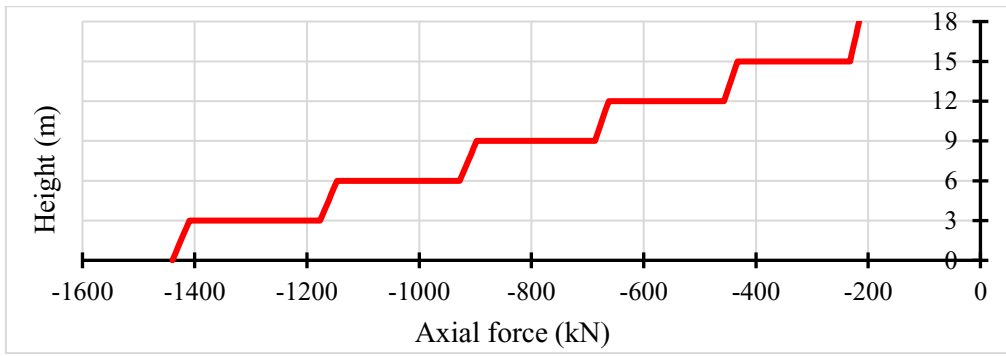


Figure 3. 23. Envelop curve of Axial force in column J-10

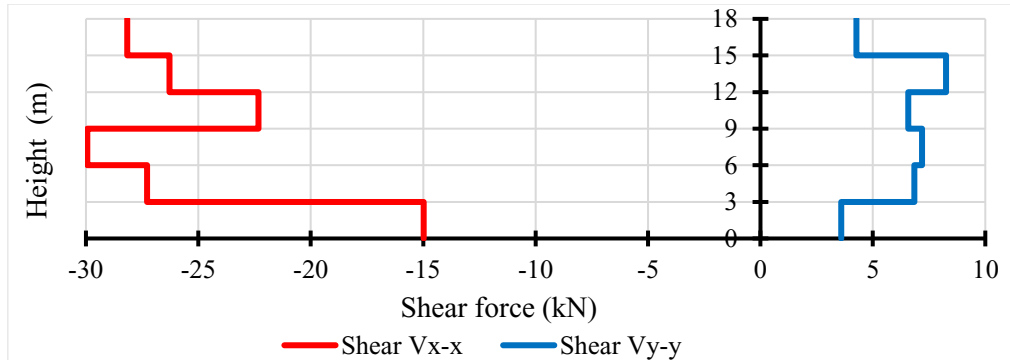


Figure 3. 24. Envelop curve of Shear forces V_{y-y} along Y in column J-10

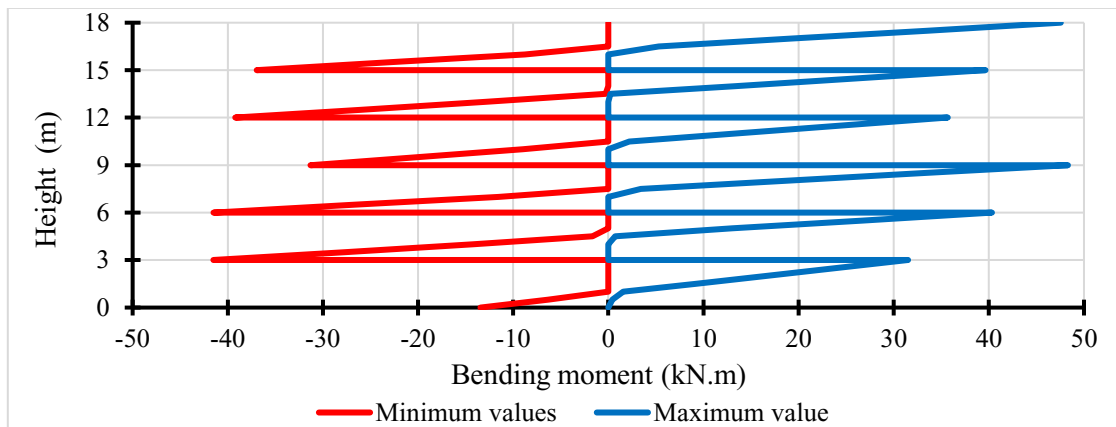


Figure 3. 25. Envelope of Bending moment M_{y-y} around Y in columns J-10

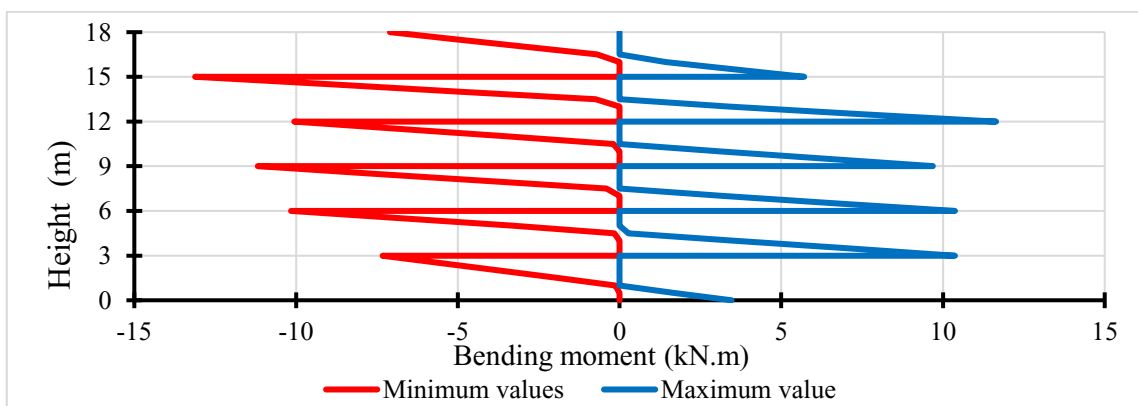


Figure 3. 26. Envelope of Bending moment M_{x-x} around X in columns J-10

3.3.4.3. The longitudinal reinforcements

Following the procedure described in section 2.7.2.3. of the chapter methodology, the longitudinal reinforcement of the columns was determined and summarised in **Table 3.9**

Table 3.9. Longitudinal reinforcement of columns

Level	a	b	dx'	dy'	Asy = Asy'		Asx = Asx'	
	(mm)	(mm)	(mm)	(mm)	(mm ²)	(Φ)	(mm ²)	(Φ)
1	500	400	50	40	456	4 Φ12	456	4 Φ12
2	400	400	40	40	342	3 Φ12	456	4 Φ12
3	400	400	40	40	342	3 Φ12	456	4 Φ12
4	400	400	40	40	342	3 Φ12	456	4 Φ12
5	400	300	40	30	342	3 Φ12	456	4 Φ12
6	300	300	30	30	342	3 Φ12	342	3 Φ12
7	300	300	30	30	342	3 Φ12	342	3 Φ12

Table 3.10. Verification of minimum and maximum quantity of steel

Level	As total		Asmin	Asmax	Verification
	(Φ)	mm ²	mm ²	mm ²	
1	14 Φ 12	1596	400	80000	Checked
2	12 Φ 12	1368	320	64000	Checked
3	12 Φ 12	1368	320	64000	Checked
4	12 Φ 12	1368	320	64000	Checked
5	12 Φ 12	1368	240	48000	Checked
6	10 Φ 12	1140	180	36000	Checked
7	10 Φ 12	1140	180	36000	Checked

After determining the longitudinal reinforcement of the column, it is necessary to check whether the designed columns can withstand the interaction between the bending moment and the axial force without failure. We check this with the help of the M-N interaction diagram.

3.3.4.4. M-N interaction Diagram

The M-N interaction diagram, described in section 2.7.2.4. of columns designed is presented in x and y direction of the columns respectively in **figure 3.28** and **figure 3.29**

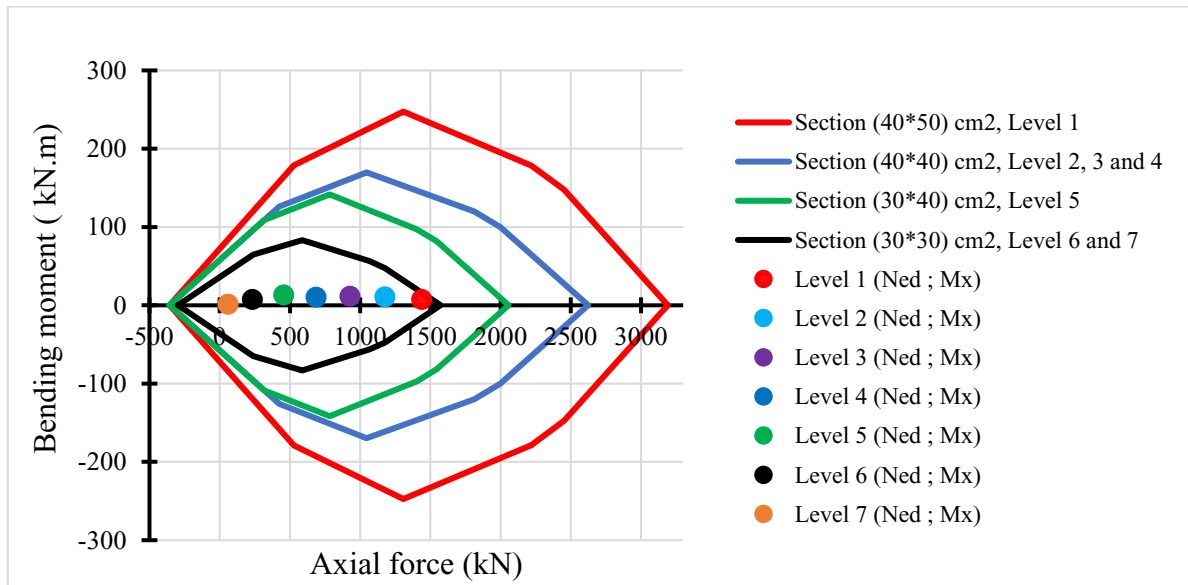


Figure 3. 27. Checking the columns with M-N interaction diagrams along the x-direction

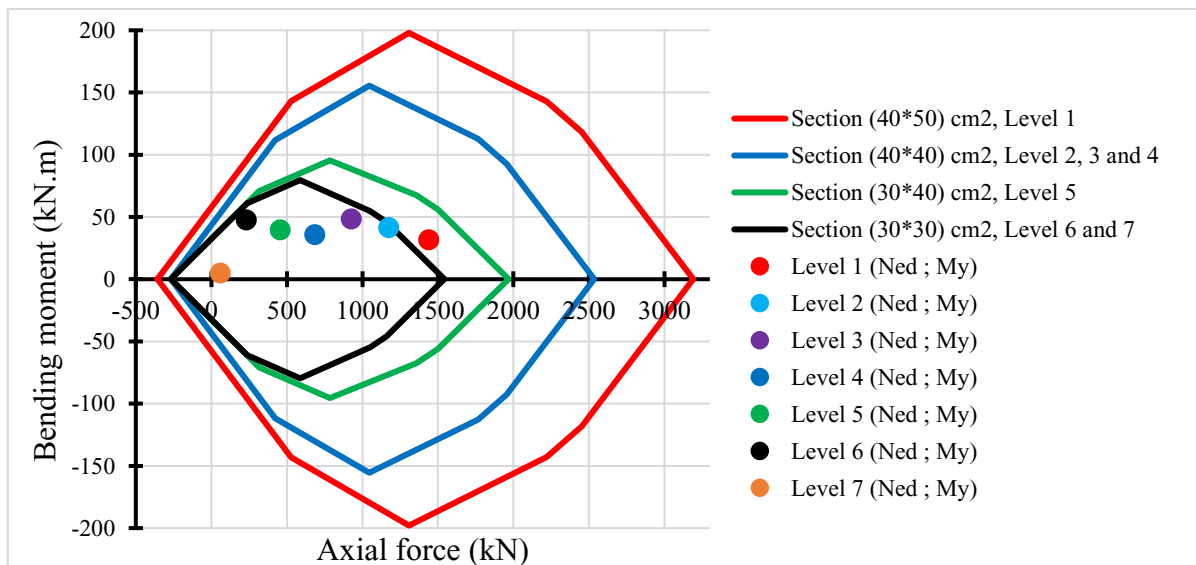


Figure 3. 28. Checking the columns with M-N interaction diagrams along the y-direction

3.3.4.5. Design for shear

The calculation of the shear reinforcement according to the procedure described in section 2.7.1.2. b. for beams shows that the cross-section of columns is capable of withstanding the shear force. Therefore, the minimum area and maximum spacing of the transverse reinforcement is provided. According to section 2.7.2.5. , the transverse reinforcements are made of $\Phi 6$ with maximum spacing of **240 mm**

3.4. Linear dynamic Analysis

Now, the structure is subjected to a seismic force, linear dynamic analysis is required to determine the response of the structure to this seismic action. From this response the solicitations on the structural elements will emerge, which will then be used for their design. The design will be carried out on the most stressed structural elements.

3.4.1. Modal analysis

In order to understand the dynamic behaviour of the building, a modal analysis is performed. We started by defining the building model in the SAP2000 software.

3.4.1.1. Modelling of the building

The modelled building is shown in **Figure 3.29**, the structure consists of vertical and horizontal frame elements representing previously designed columns and beams respectively. The slab and non-structural elements have not been modelled but they are present in the model by their masses which have been distributed on the beams that carry them. A diaphragm was assigned to each floor in order to consider a rigid slab. The soil-structure interaction has not been taken into account so the foundations have been considered embedded.

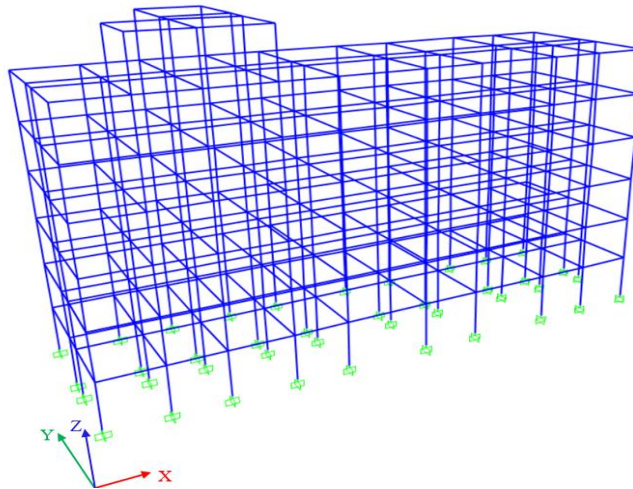


Figure 3. 29. Building modelling

3.4.1.2. Modal properties

For this modelling, which resembles the real building model, we could have thousands and millions of DOFs, which means that we can find as many natural frequencies, but it is not necessary to determine them all. The high frequency modes can be neglected. For this first analysis of the data, we have just extracted the first 16 modes, they are represented in **figure 3.30** depending on their period.

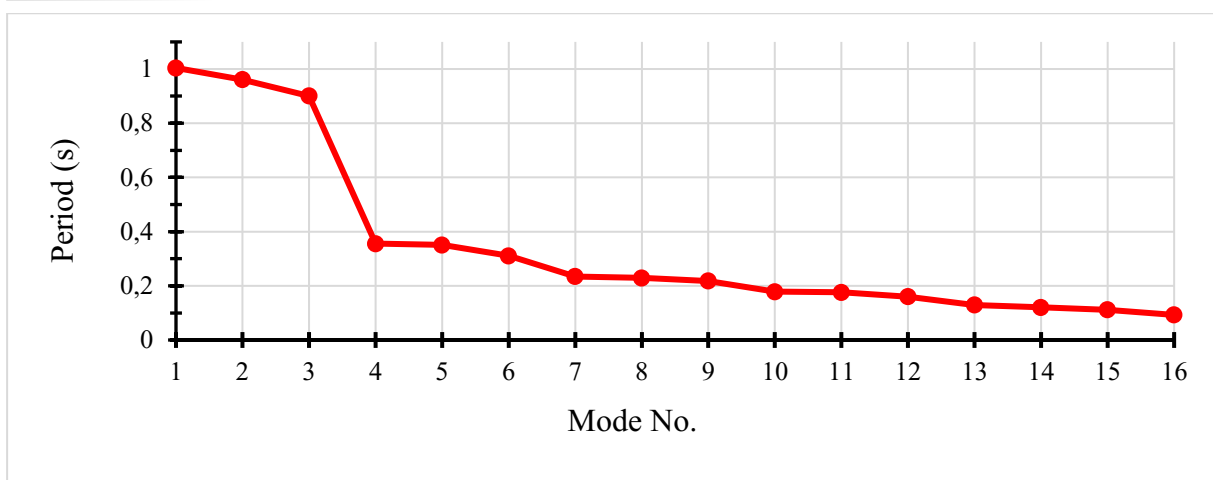


Figure 3. 30. Natural Periods of the building for each vibration Mode

Not all modes participate to the same degree in the deformation of the structure under dynamic loading, the importance of each mode of deformation is determined from the participation factor or its effective modal mass. **Figure 3.31** presents the modal participating mass ratio of each mode in each direction of the building.

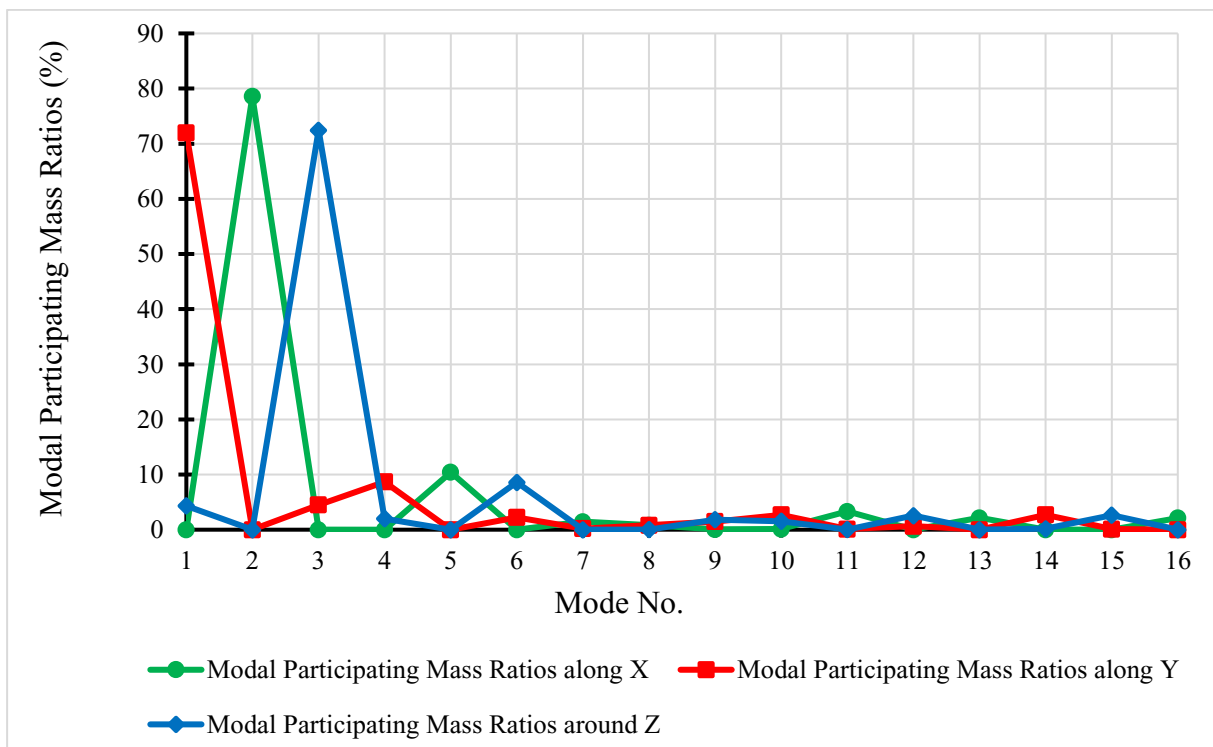


Figure 3. 31. Modal participating mass ratio

The most important modes, i.e., those that have a great influence on the dynamic behaviour of the building, are those with a large modal participating mass ratio (at least 70 %), from **Figure 3.31** we can see that these modes are the 3 first mode. The **figures 3.32 to 3.34** show the shapes of these different modes.

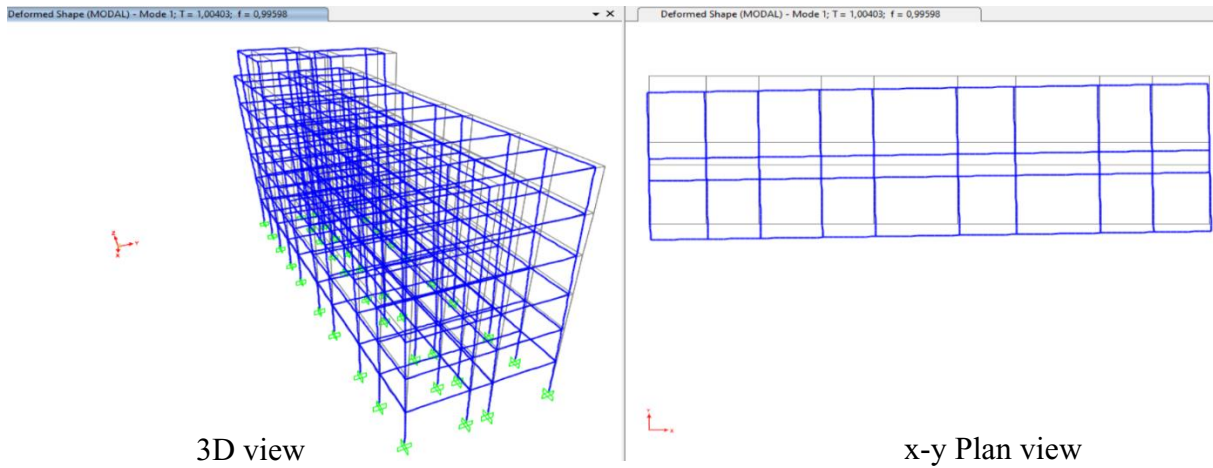


Figure 3.32. First vibration mode of the structure, Translation along y

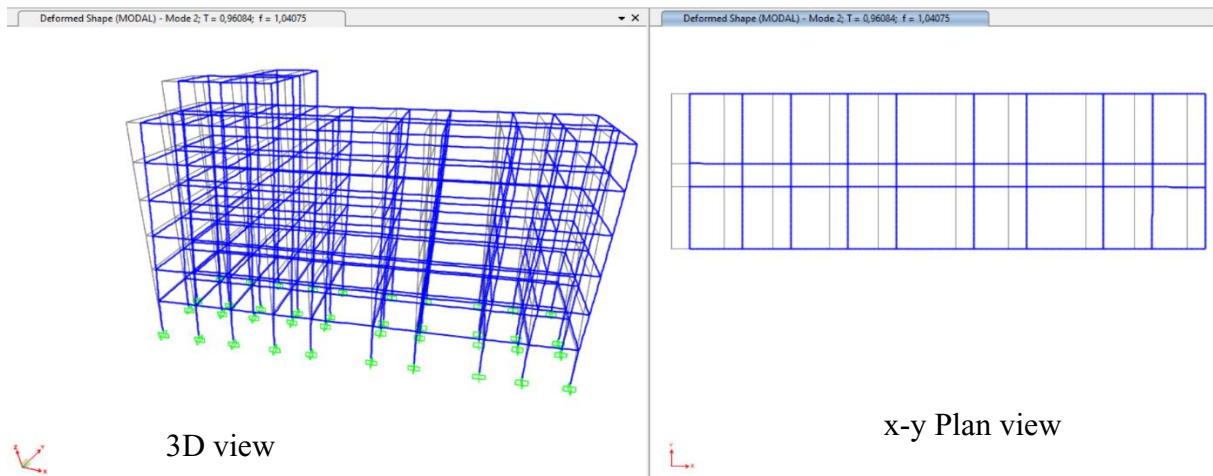


Figure 3.33. Second vibration mode of the structure, Translation along x

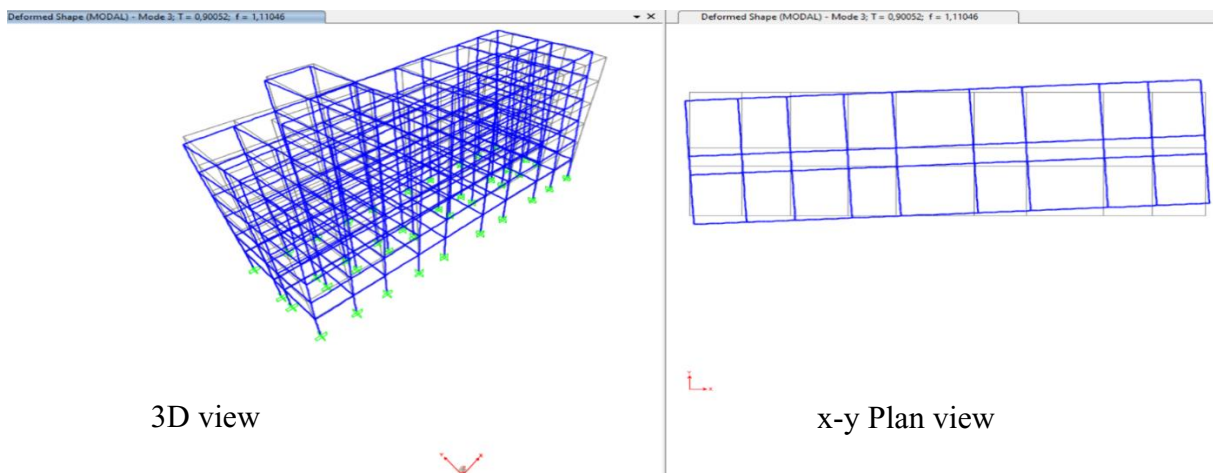


Figure 3.34. Third vibration mode of the structure, Torsion around z

But these modes are not sufficient to have a good response of the structure to a dynamic action because the sum of their effective mass is not higher than 90% of the total mass of the building.

3.4.1.3. Selection of the useful mode

To avoid neglecting an important mode, the sum of the effective modal masses for the modes considered must be greater than or equal to 90% of the total mass of the structure. **Figure 3.35** shows a cumulation of the mass participation ratio of the vibration modes along the x and y directions and around the Z direction. To satisfy this condition in all three directions (along x, y and around z), the minimum number of modes to be considered is 10, the first 10 modes.

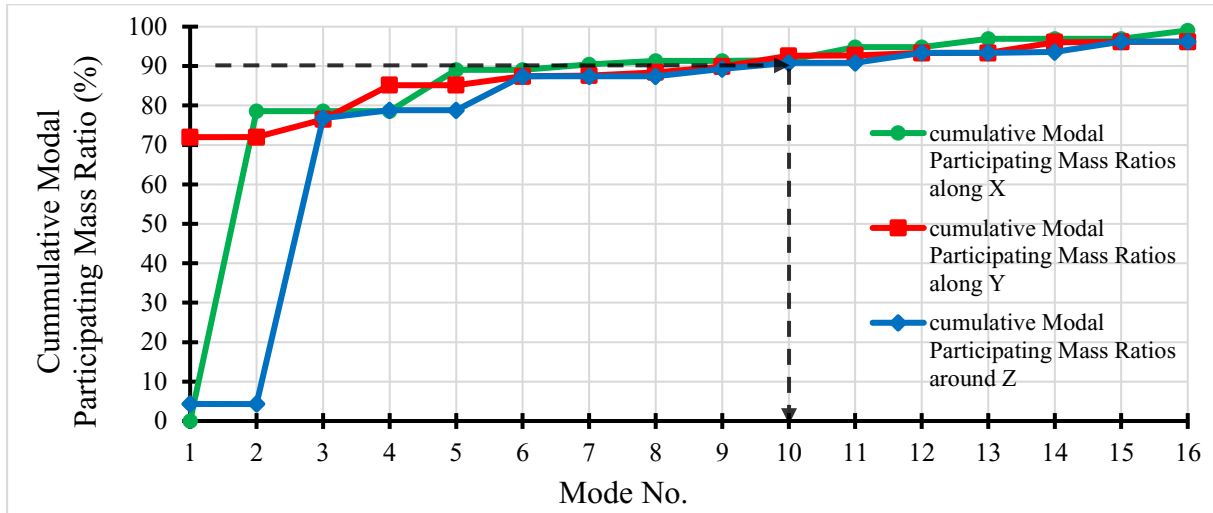


Figure 3. 35. Cumulative Modal mass participating ratios

Table 3.11 shows these first 10 modes, their respective periods and frequencies, and their respective effective modal masses.

Table 3. 11. Selected Mode

Mode	Period (s)	Frequency (Hz)	Modal Participating Mass Ratios (%)		
			in the x direction	in the y direction	around z direction
1	1,0040	0,9960	0,0006	71,9810	4,3210
2	0,9608	1,0408	78,5860	0,0014	0,0029
3	0,9005	1,1105	0,0035	4,5080	72,4650
4	0,3553	2,8148	0,0000	8,6700	2,0010
5	0,3509	2,8501	10,4130	0,0000	0,0003
6	0,3104	3,2219	0,0002	2,2240	8,5920
7	0,2346	4,2631	1,4540	0,2000	0,0025
8	0,2290	4,3669	0,8230	0,8110	0,0230
9	0,2178	4,5916	0,0470	1,4890	1,8410
10	0,1784	5,6053	0,1210	2,7080	1,5490
Sum			91,4483	92,5924	90,7977

These results represent the intrinsic characteristics of the structure and have an important role to play in the evaluation of the response of the structure to the earthquake through the analysis of the response spectrum.

3.4.2. Response spectrum analysis

As mentioned in section 2.8.2. , this part consists of analysing the structure under seismic loading and determining its response.

3.4.2.1. The seismic action

E is the action of the earthquake, it will be represented by its response spectrum, which depends on the class of the building, the class and the acceleration of the ground on which the building stands. Following the procedure described in section 2.5.2.2. the horizontal elastic response spectrum, the design and the non-dissipated response spectrum were constructed and are shown in **figure 3.36**. For this construction, the acceleration of the ground was taken to be 0.4 g according to **Table A. 4** and **Figure 1. 21** in Appendix A and chapter 1 respectively. The soil was assumed to be class C which gave a soil coefficient of **1.15** using in appendix A. From **Table A. 8** the values of the periods TB, TC and TD gave 0.2, 0.6 and 2 respectively

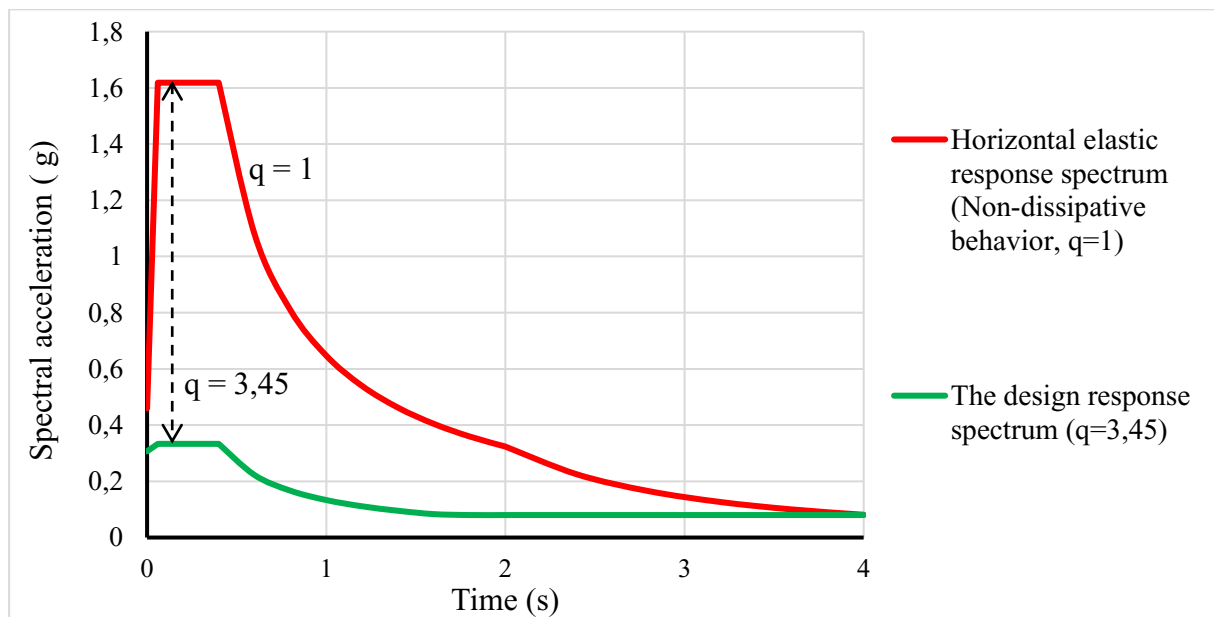


Figure 3. 36. The Response spectrum of earthquake motion

3.4.2.2. Combination of seismic action

Equations (2.15) and (2.16) allow the establishment of 8 seismic load combinations presented in **figure 3.37**.

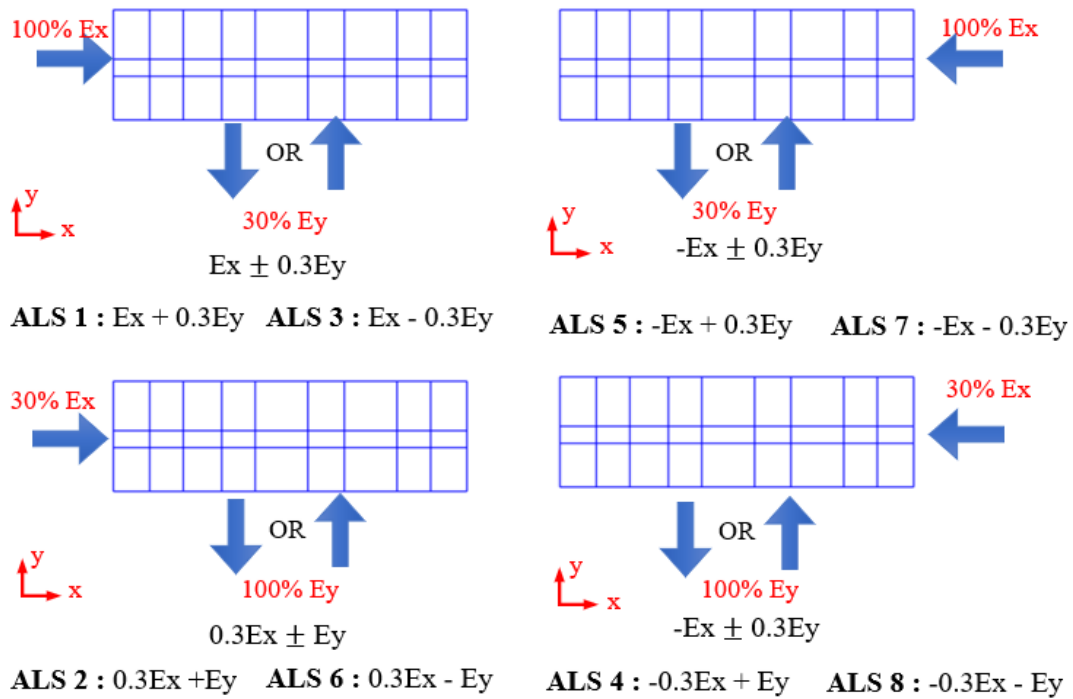


Figure 3.37. Combination of seismic action

All these combinations will be used to evaluate the response of the structure to the ULS and SLS.

3.4.2.3. Acceleration of the structure at the ground level

Following the procedure describe in paragraph 2.8.2.2. of methodology and shown in **Figure 3.38**, the acceleration of the structure at the ground level is determined considering that the structure dissipates the energy. The analysis of the obtained results allowed to plot the acceleration of the structure as a function of the vibration modes presented by **Figure 3.39**

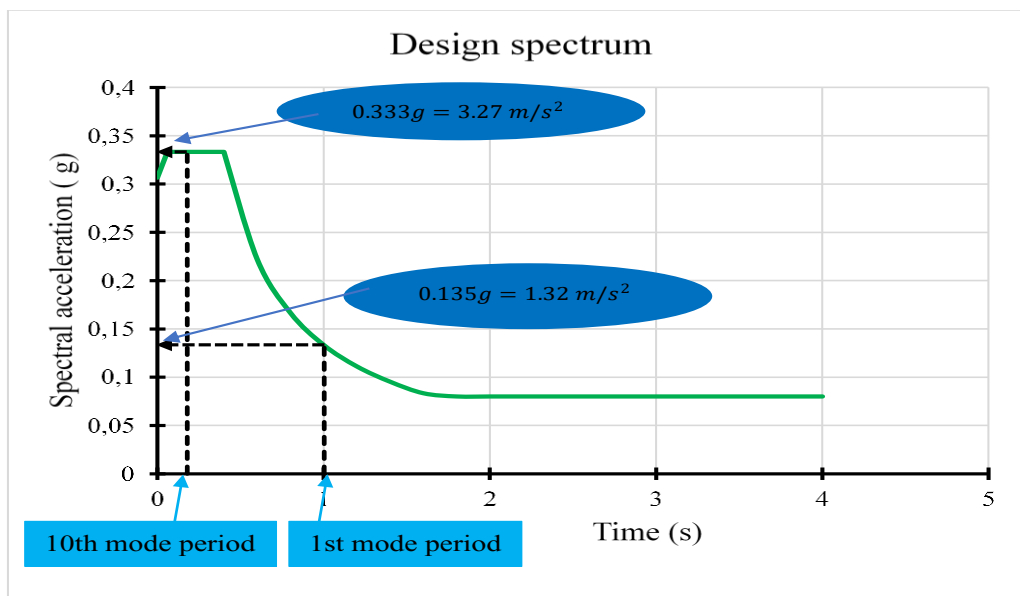


Figure 3.38. Determination of acceleration of structure at the ground

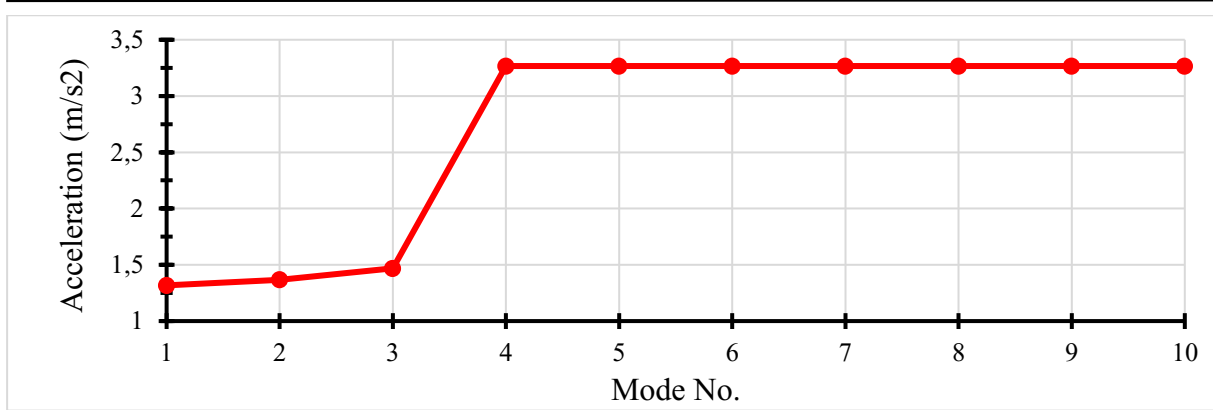


Figure 3. 39. Acceleration of the structure at the level of the ground

3.4.2.4. The response of the structure

The response of the structure to the dynamic load of the earthquake is presented in several forms, we distinguish the base shear, the displacements of the storeys and the solicitations on the structural elements (shear force, axial forces, bending moment, torsion).

a. Base shear of the structure

In accordance with paragraph 2.8.2.3. a. , the base shear is determined for each seismic combination and is presented in table 3.12

Table 3. 12: The base shear

Load case	Base shear (kN)	
	In x direction	In y direction
ALS 1	3844,902	1067,234
ALS 2	1175,912	3482,641
ALS 3	3844,902	-1067,234
ALS 4	-1175,912	3482,641
ALS 5	-3844,902	1067,234
ALS 6	1175,912	-3482,641
ALS 7	-3844,902	-1067,234
ALS 8	-1175,912	-3482,641
Maximum value	3844,902	3482,641
Minimum value	-3844,902	-3482,641

b. Displacement and inter-storey drift of the structure

Using the SLS response spectrum described in paragraph 2.8.2.3. c. and presented in Figure 3. 36, the displacements of the structure were determined. Figures 3.40 and 3.41 show the maximum deformed shape of the structure under different reference planes.

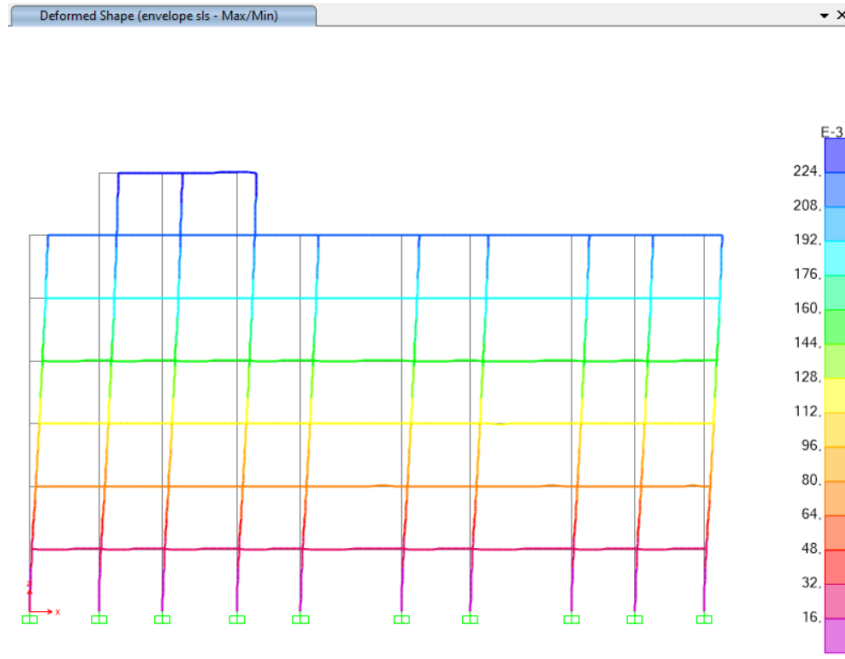


Figure 3. 40. Deformed shape of the structure in the X-Z view

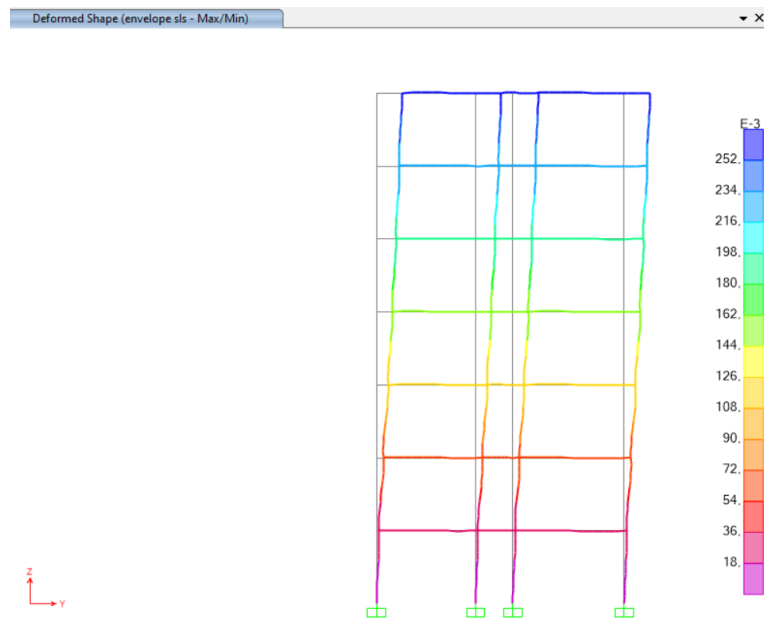


Figure 3. 41. Deformed shape of the structure in the Y-Z view

The displacement value for each point of the same floor of the structure is different. In order to determine the values of the displacements of each storey and the inter-storey drift, we took as reference the vertical element that provided the maximum values, it is presented in Figure 3.42.

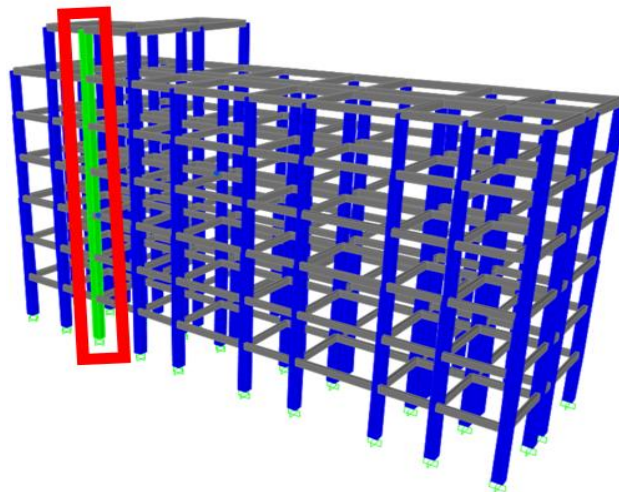


Figure 3. 42. The reference vertical element for determining the storeys displacement
 The collection of the results obtained from this element, for each combination of seismic load presented in **Figure 3. 37**, allowed us to plot the displacement diagram presented by **figure 3.43** and **figure 3.44**, in each direction of the building.

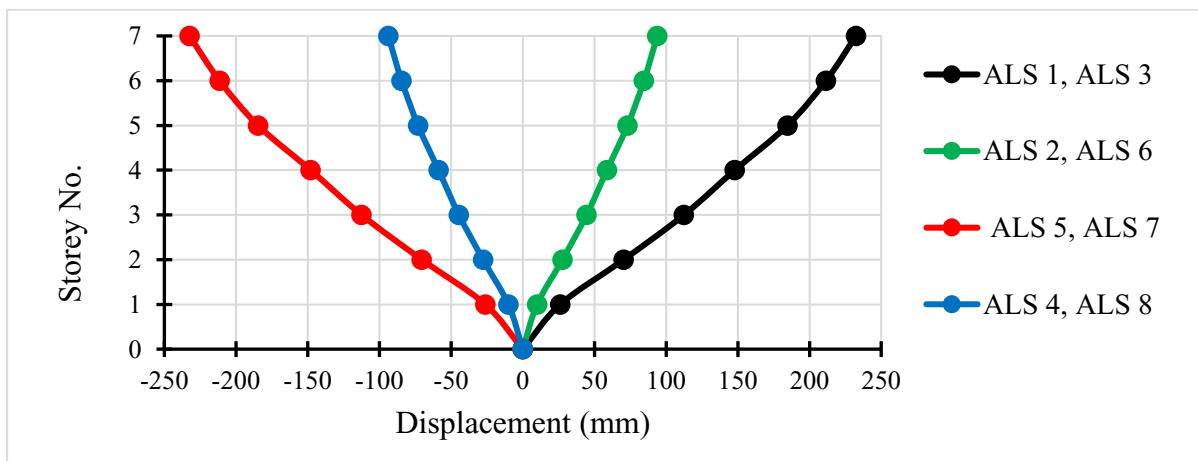


Figure 3. 43. Storey displacement in the x direction

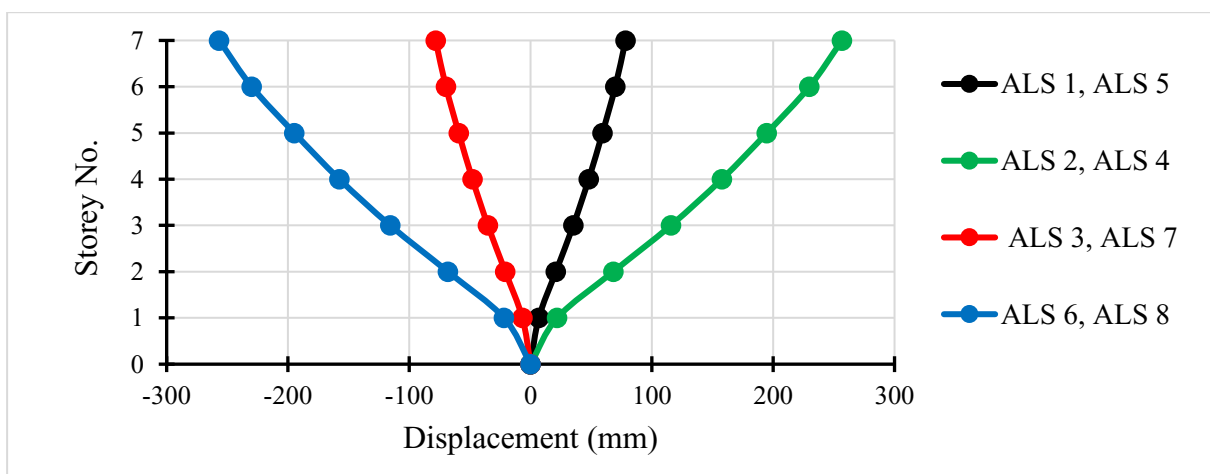


Figure 3. 44. Storey displacement in the y direction

Through these storey displacements, the maximum inter-storey drifts have been determined, plotted and checked (see **figure 3.45**) using the limit inter-storey drift presented by relation (2.84).

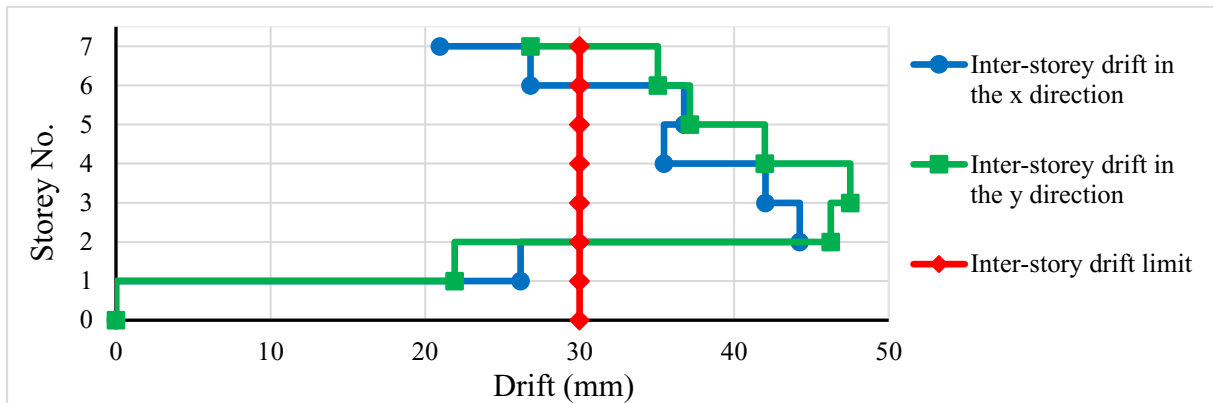


Figure 3. 45. Inter-storeys drifts

It is clear from **figure 3.45** that the inter-storey derivatives do not verify the limits prescribed by the Eurocode which is 30 mm in this case.

c. The new Internal forces on the structural elements

Due to earthquake, there will be new internal forces on beams and columns.

i. Beams

Considering the seismic load combinations described in **Figure 3. 37**, the envelope curves of the internal forces of the building beams have been obtained from the SAP 2000 software and are presented in figure 3.46

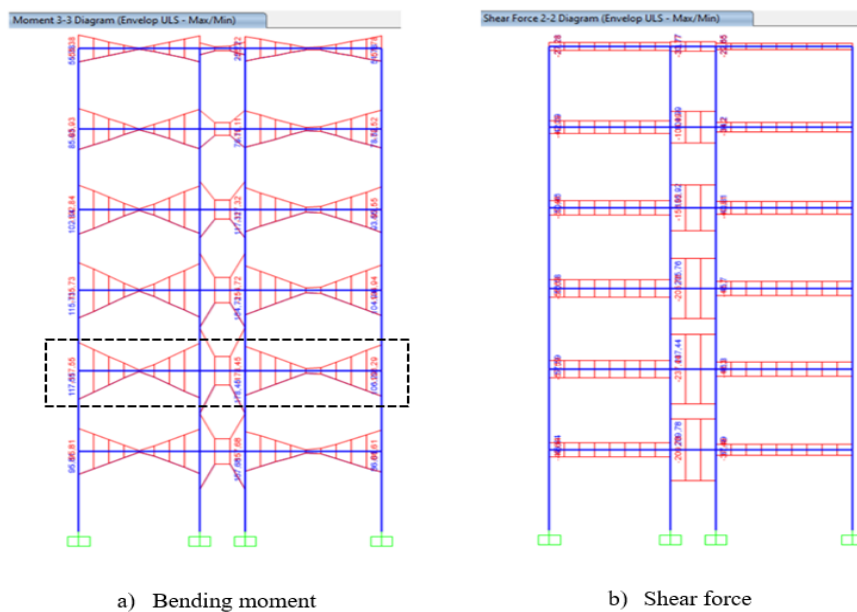


Figure 3. 46. Envelope curve of solicitations on the beams of frame10 of block A.

From these results, the envelope curves of the internal forces of the beam studied in static analysis (**Figure 3. 3**) have been plotted. They are presented in figure 3.47 and 3.48

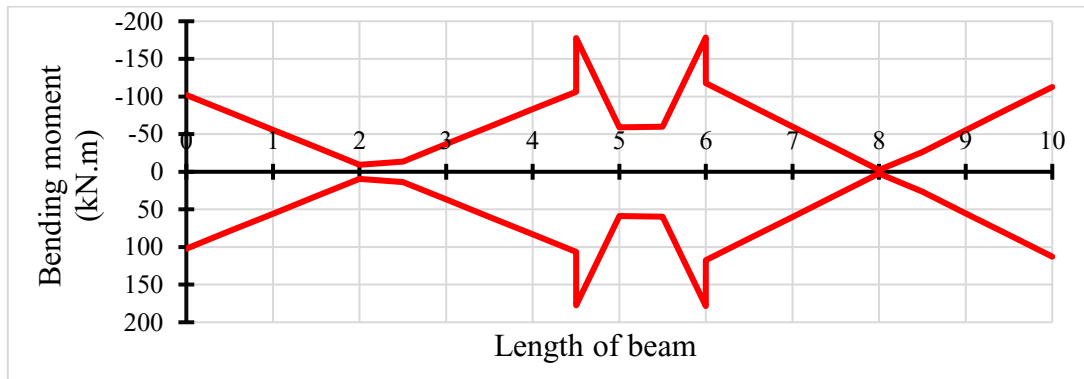


Figure 3. 47. New envelope curve of bending moment of the beam

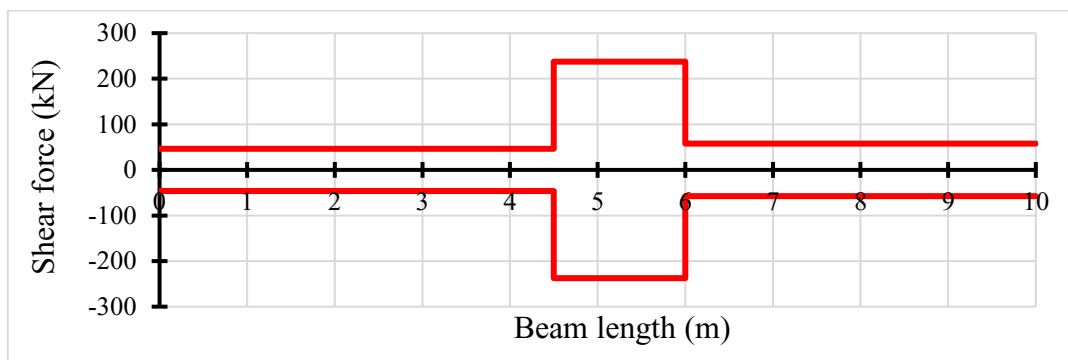


Figure 3. 48. New envelope curve of Shear of the beam

From figure 3.47, the design diagram of the bending moment as described in section 2.7.1.2. a. i. is obtained. The superposition of this diagram with the resisting moment of the previously designed beam (see **figure 3.49**) shows that in some places the bending moment is greater than the resistance of this beam. Therefore, this beam is not able to support the bending moment due to this seismic action.

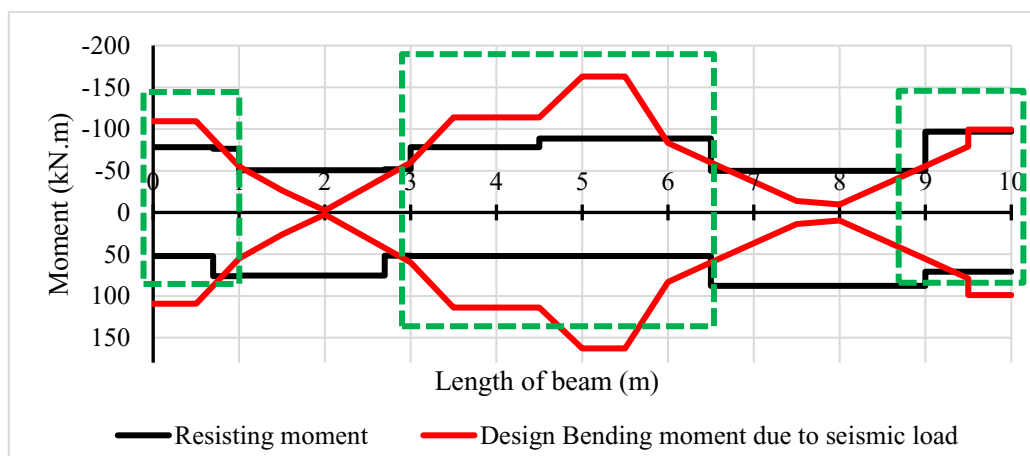


Figure 3. 49. Comparison of seismic bending moment and the resisting moment of the statically designed beam

We have the same thing when we superimpose the shear diagram with the resisting shear (see **figure 3.50**), in some places the beams do not resist the shear.

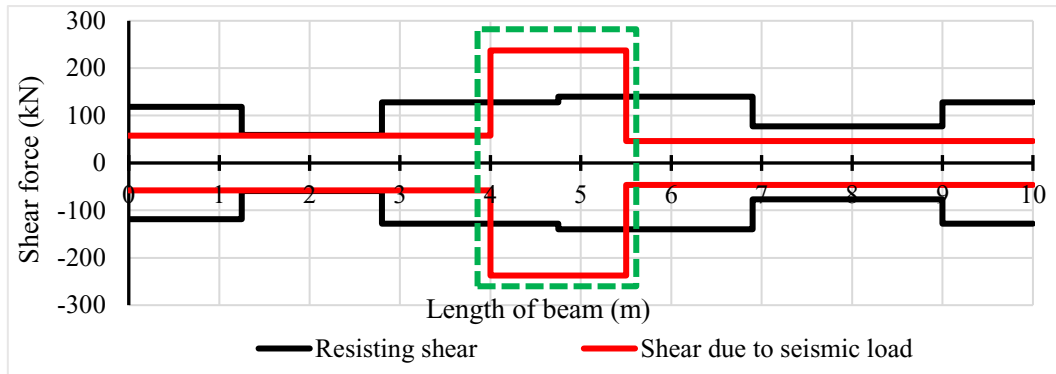


Figure 3. 50. Comparison of seismic Shear force and the resisting Shear of the statically designed beam

All this imply that the design of the beam at these locations must be revised. The simplest solution is to add the longitudinal reinforcement at these locations following the design procedure described in paragraph 2.7.1.2. a. ii. , but the beam will be subjected to excessive stresses and cracks. To solve this problem, the beam cross-section is increased and the reinforcement steels are recalculated taking into account the crack and stress limitation.

ii. Columns

Considering the seismic load combinations described in **Figure 3. 37**, the envelope curves of the internal forces of the column row with the maximum bending moments (see **figure 3.51**) have been plotted. They are presented in figure 3.52 to figure 3.55

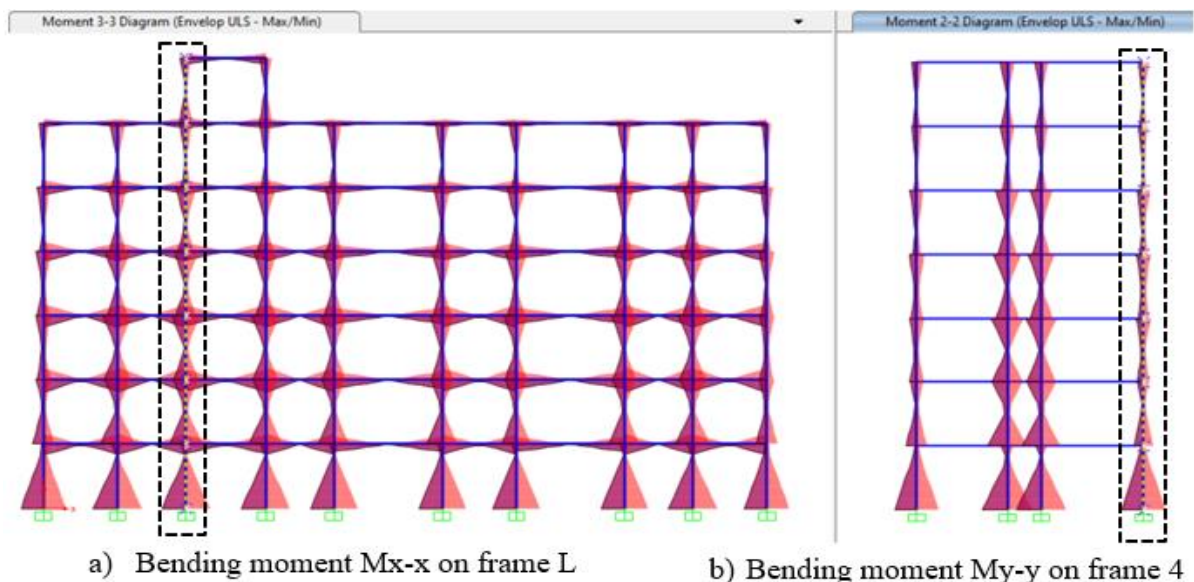


Figure 3. 51. Envelope curve of bending moments on column row L-4

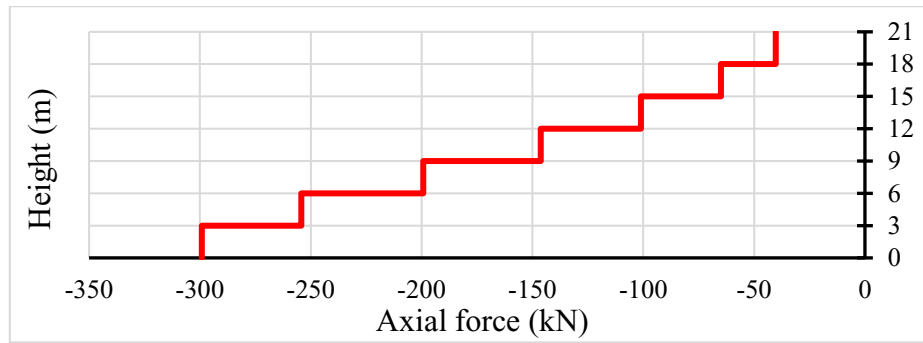


Figure 3. 52. Envelope curve of Axial force on the columns of row L-4 due to seismic combinations load

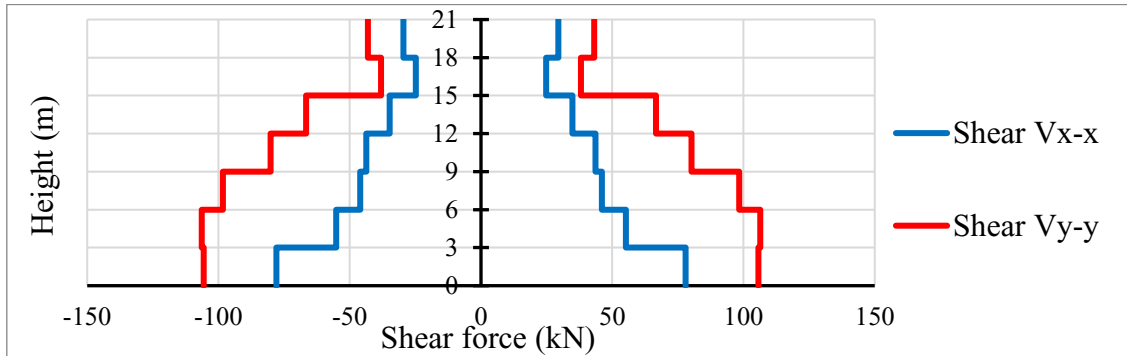


Figure 3. 53. Envelope curve of Shear force on the columns of row L-4 due to seismic combinations load

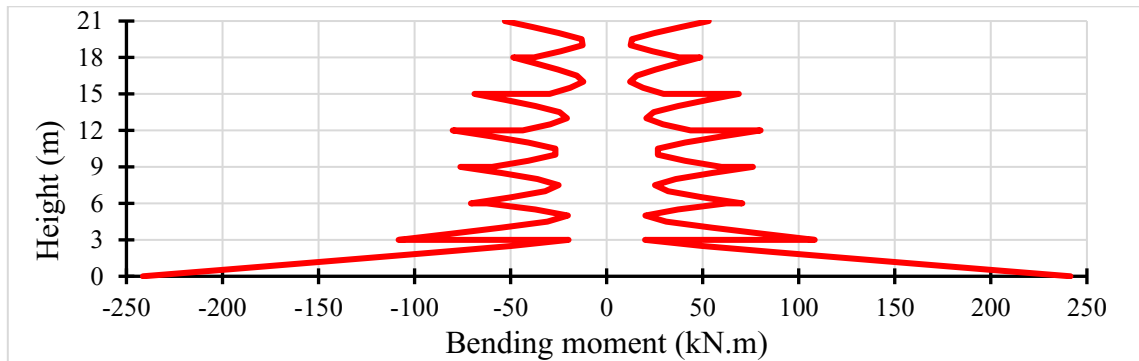


Figure 3. 54. Envelope curve of Bending moment around y direction on the columns of row L-4 due to seismic combinations load

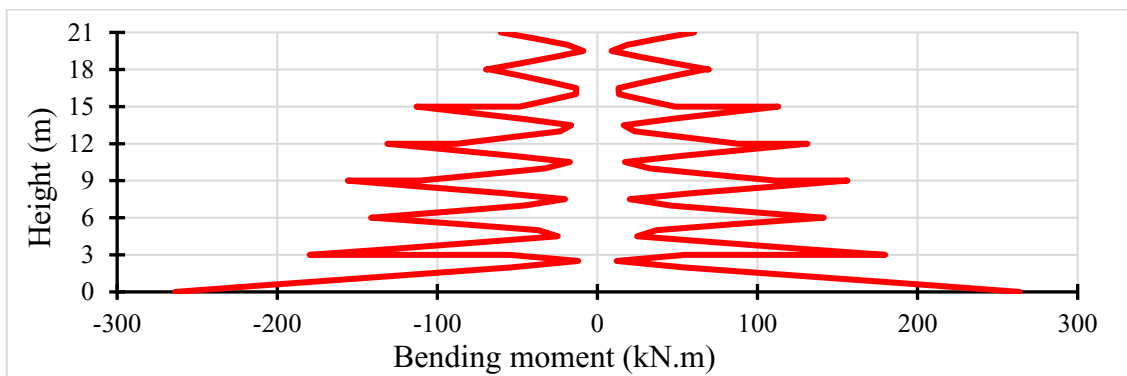


Figure 3. 55. Envelope curve of Bending moment around x direction on the columns of row L-4 due to seismic combinations load

From these internal forces, the columns are checked using the previously designed M-N interaction diagram of the columns. It is shown by **Figure 3. 56** and **3.57**

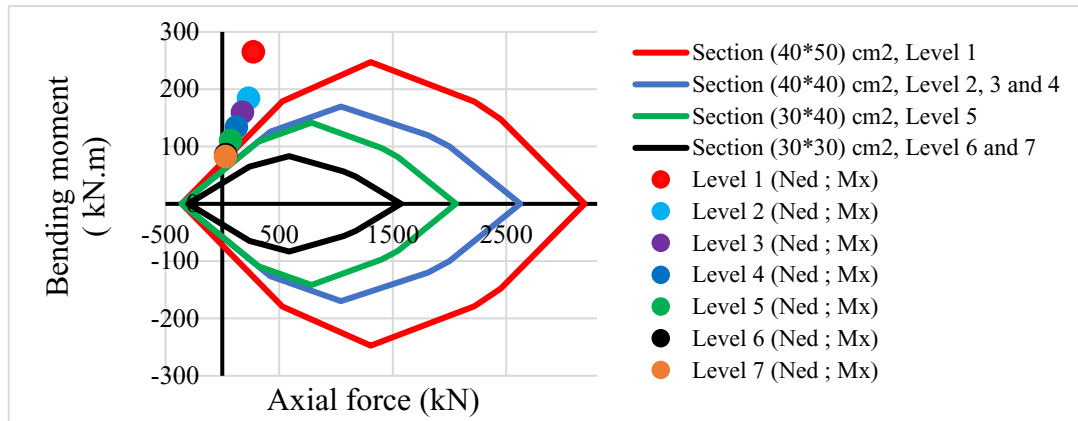


Figure 3. 56. Control of new columns in the M-N interaction diagram of statically designed columns in the x-direction

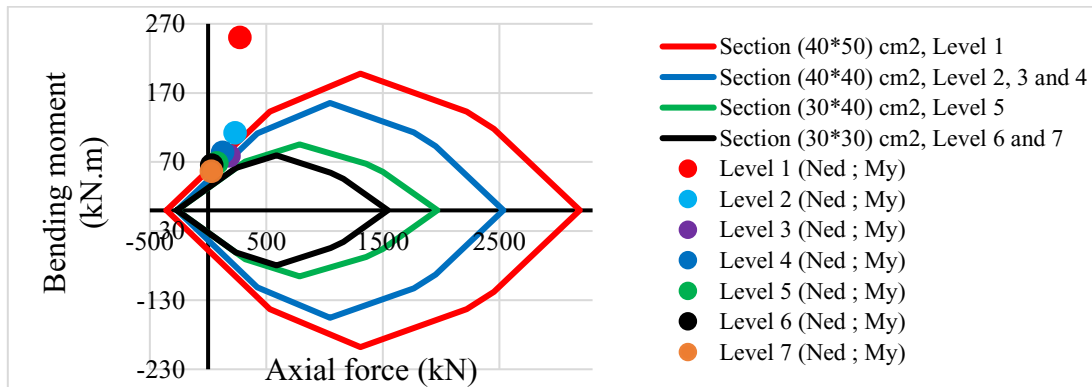


Figure 3. 57. Control of new columns in the M-N interaction diagram of statically designed columns in the y-direction

As can be seen, the solicitation couple (Ned; Med) acting on each column are outside the verification range of the column sections. Therefore, the columns have to be redesigned taking into account the seismic loading.

3.4.3. Redesign and new building response

Previously, it was found that the structural elements of the building were not able to resist the seismic effect and that the building was subject to significant inter-storey drifts exceeding the limit prescribed by the Eurocode. This section will therefore involve redesigning the building and determining its new response.

3.4.3.1. New design Beams

By applying the beam design procedure described in paragraph 2.7.1. , the new beam design resulted in a beam with a cross-section of $(25 \times 50)cm$, the details of which are shown in **figure 3.58** for longitudinal reinforcement and in **figure 3.59** for transversal reinforcement.

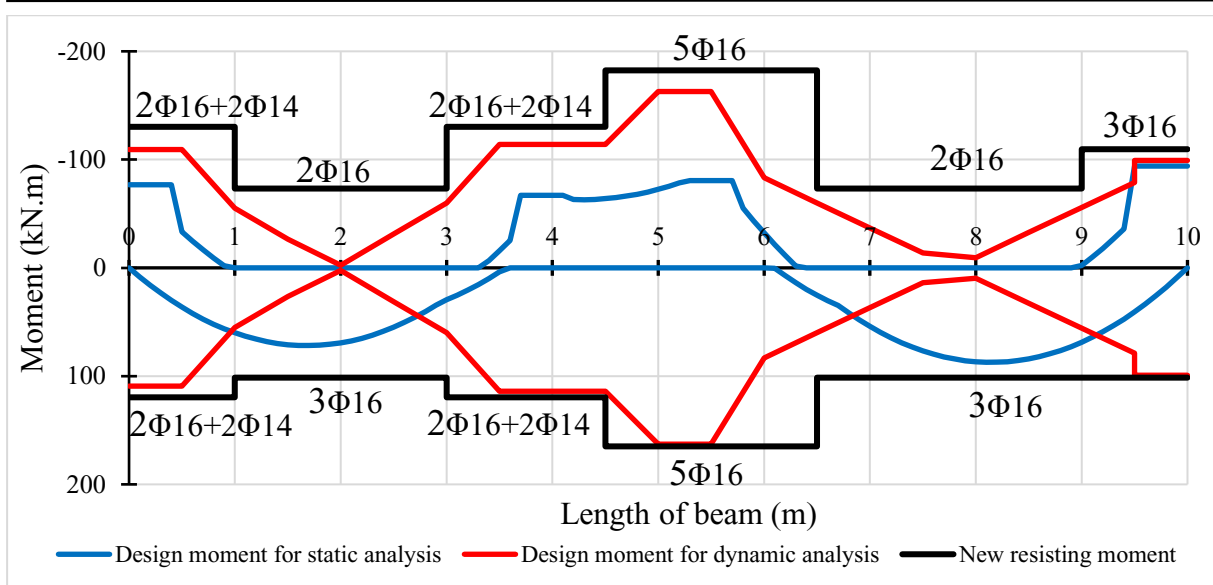


Figure 3. 58. Verification of the new section under bending moment due to static and dynamic loading

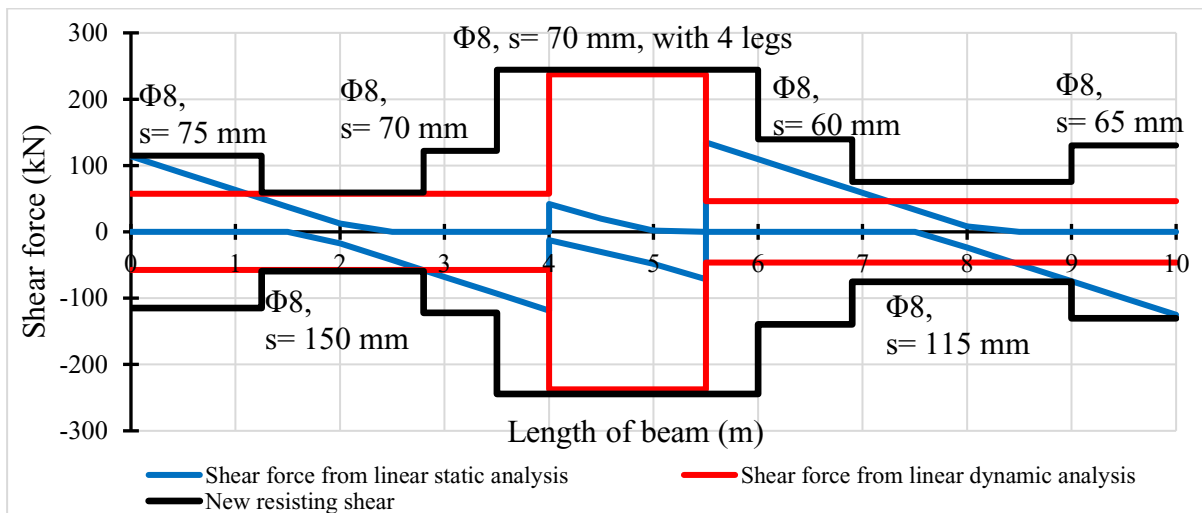


Figure 3. 59. Verification of the new section under Shear force due to static and dynamic loading

3.4.3.2. New design of columns

a. Longitudinal reinforcement

By applying the column design procedure described in section 2.7.2. , the cross-sections and longitudinal reinforcement of the new columns were obtained and are presented in the **table 3.13**

Table 3. 13. Section of new columns with longitudinal reinforcement

level	a	b	dx'	dy'	Asx = Asx'		Asy = Asy'	
	mm	mm	mm	mm	mm ²	Φ	mm ²	Φ
1	500	500	50	50	1530	6Φ18	1530	6Φ18
2	500	500	50	50	1010	5Φ16	808	4Φ16
3	500	500	50	50	1010	5Φ16	808	4Φ16
4	500	400	50	40	770	5Φ14	770	5Φ14
5	500	400	50	40	770	5Φ14	616	4Φ14
6	400	400	40	40	770	5Φ14	616	4Φ14
7	400	400	40	40	770	5Φ14	616	4Φ14

Table 3. 14. Verification of minimum and maximum quantity of steel

Level	As total		Asmin	Asmax	Verification
	(Φ)	mm ²	mm ²	mm ²	
1	22 Φ 18	5610	400	80000	Checked
2	16 Φ 16	3232	320	64000	Checked
3	16 Φ 16	3232	320	64000	Checked
4	18 Φ 14	2772	320	64000	Checked
5	16 Φ 14	2462	240	48000	Checked
6	16 Φ 14	2462	180	36000	Checked
7	16 Φ 14	2462	180	36000	Checked

After determining the longitudinal reinforcement, it is necessary to check whether the newly designed columns can resist the new interaction between the bending moment and the axial force without failure.

b. M-N interaction diagram

The M-N interaction diagram, described in paragraph 2.7.2.4. of columns designed is presented along X and Y axis in **figure 2.60** and **2.61** respectively

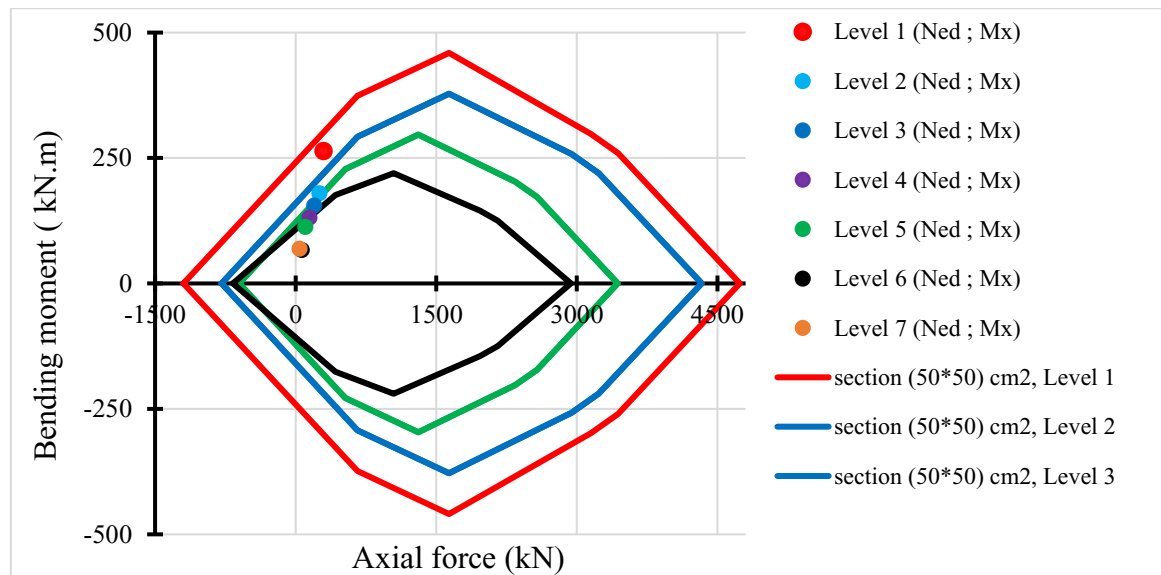


Figure 3. 60. Checking the new columns with M-N interaction diagrams along the x-direction

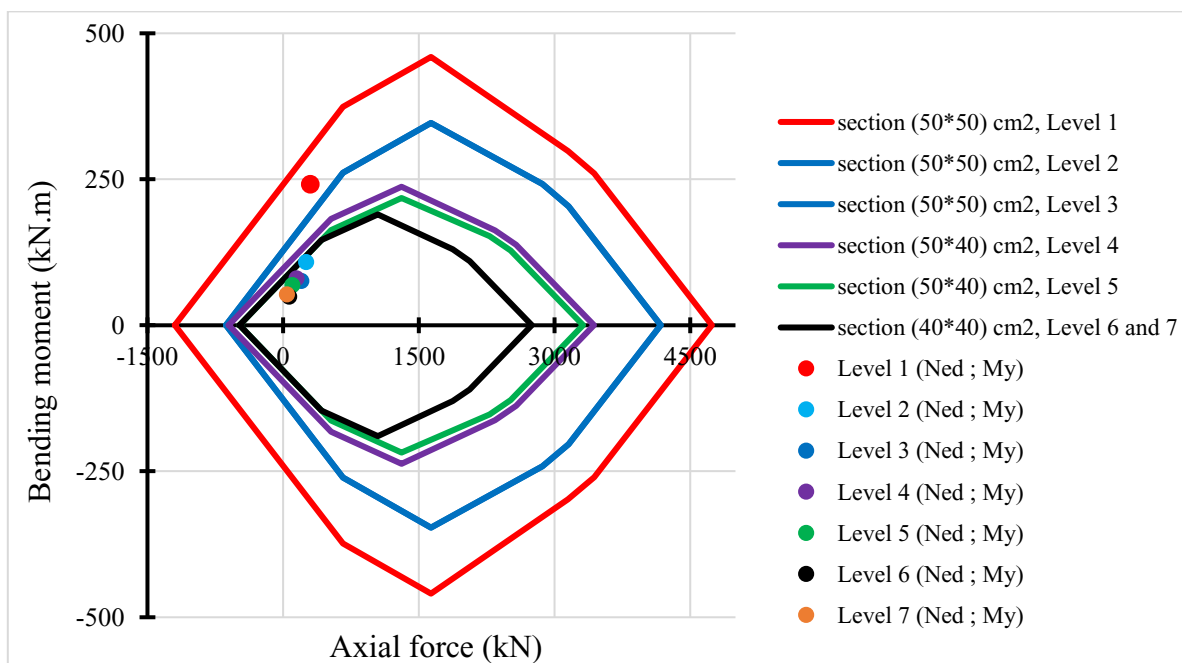


Figure 3. 61. Checking the new columns with M-N interaction diagrams along the y-direction

From these figures, it is clear that the columns are verified for bending and axial force. Now we can design for shear.

c. Shear verification

In the same way as the distribution of the longitudinal reinforcement has changed, the distribution of the shear reinforcement will change depending on the shear force acting on the column. Following the procedure described in section 2.7.2.5. , the new distribution of these shear reinforcement on the column row L-4 is presented in figure 3.62.

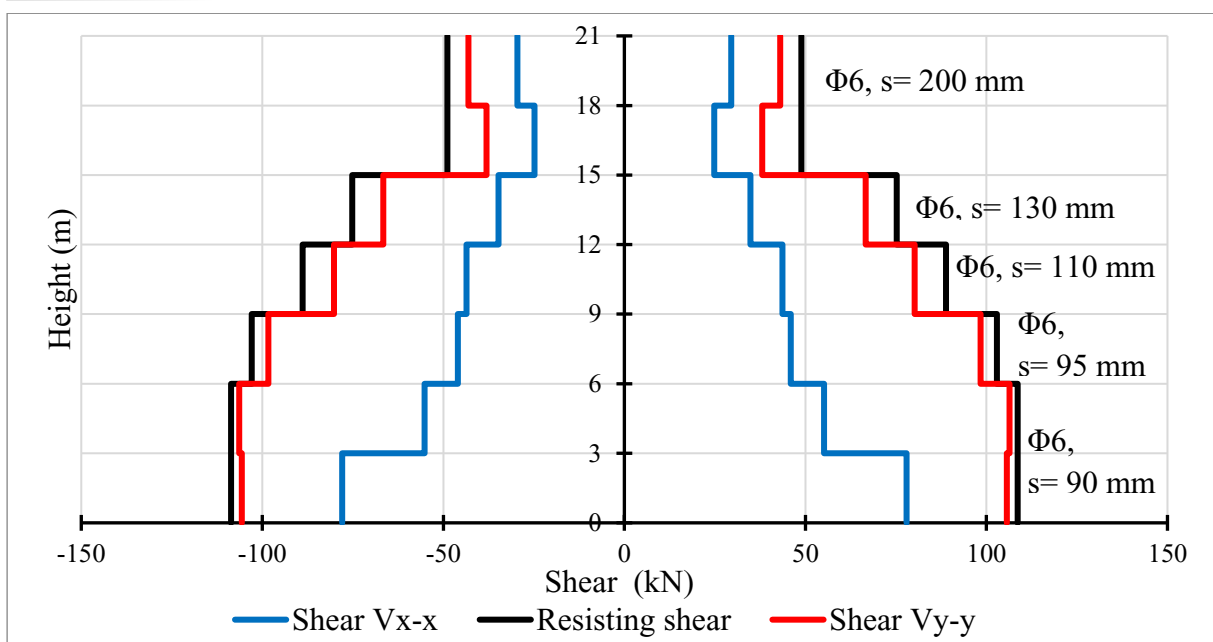


Figure 3. 62. Shear verification on column row L-4

3.4.3.3. The new response of the building

With the new structural element cross-sections obtained, it is necessary to perform another modal response spectrum analysis to check whether the new response of this structure is admissible.

a. The modal properties of the new structure

Another modal analysis was performed on the modelled building with the new column and beam sections obtained from the section 3.4.3.1. and 3.4.3.2. From this analysis the new eigen periods and frequencies of the building were obtained. The figure 3.63 shows the first 16 vibration modes and their eigen periods.

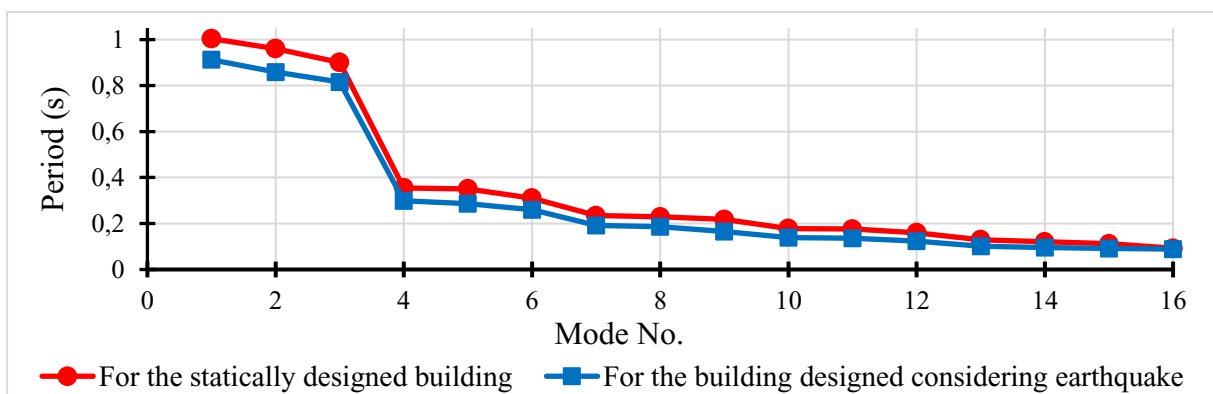


Figure 3. 63. Natural Periods of the new structure for each vibration Mode

The most important vibration modes of this new building are those whose sum of the effective modal masses is higher than 90%. They are presented in the table with their frequencies and effective modal masses.

Table 3. 15. The new useful mode of vibration

Mode	Period (s)	Frequency (Hz)	Modal Participating Mass Ratios		
			in the x direction (%)	in the y direction (%)	around z direction (%)
1	0,9124	1,0958	0,0002	73,2800	3,8960
2	0,8581	1,1648	78,1180	0,0009	0,0050
3	0,8161	1,2253	0,0056	4,0370	73,6240
4	0,2994	3,4019	0,0001	9,1390	1,9250
5	0,2861	3,5191	10,6260	0,0001	0,0004
6	0,2596	3,8591	0,0004	2,4390	9,4490
7	0,1920	5,6684	0,7180	1,4740	0,5430
8	0,1867	5,8395	1,7600	0,8200	0,5760
Sum			91,2284	91,1900	90,0184

These modes will allow the determination of the new displacement and the inter-storey drifts of the building.

b. Displacement and inter-storey drifts

Using the SLS response spectrum described in paragraph 2.8.2.3. c. and presented in **Figure 3. 36**, the new displacements of the structure were determined using SAP 2000. Figures 3.64 and 3.65 show the maximum deformed shape of the structure under different reference planes.

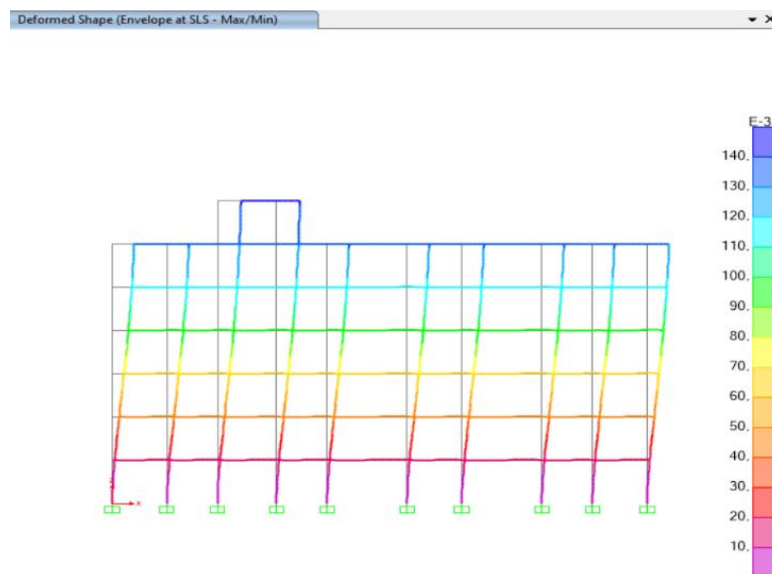


Figure 3. 64. Deformed shape of the structure in the X-Z view

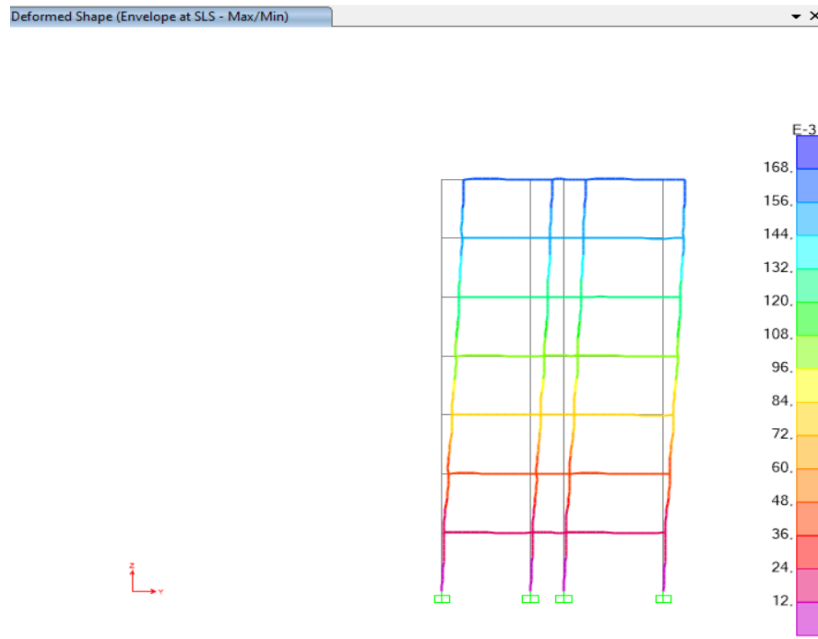


Figure 3. 65. Deformed shape of the structure in the Y-Z view

Using the same vertical element as used in Section 3.4.2.4. b. and shown in Figure 3. 42 to obtain the maximum displacement, the displacements of each storey are plotted and illustrated in Figure 3.66 and 3.67.

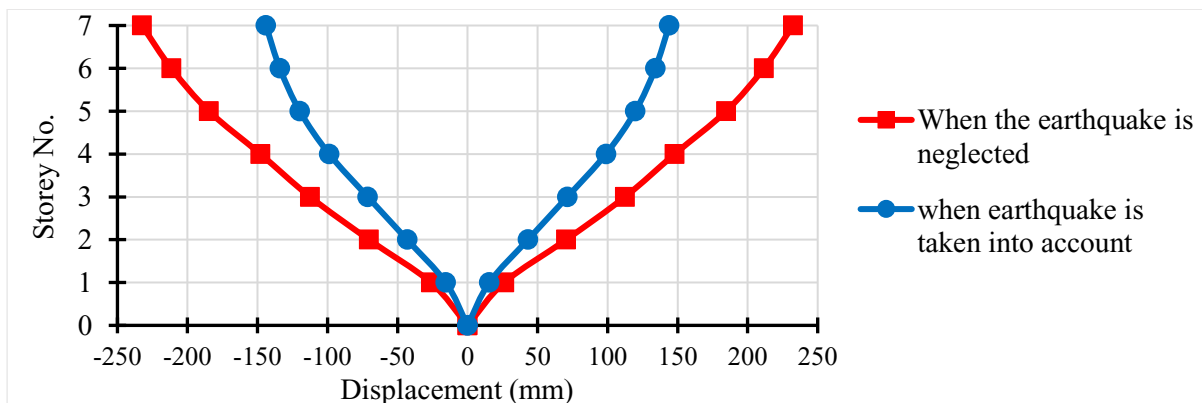


Figure 3. 66. New storey displacement in the x direction

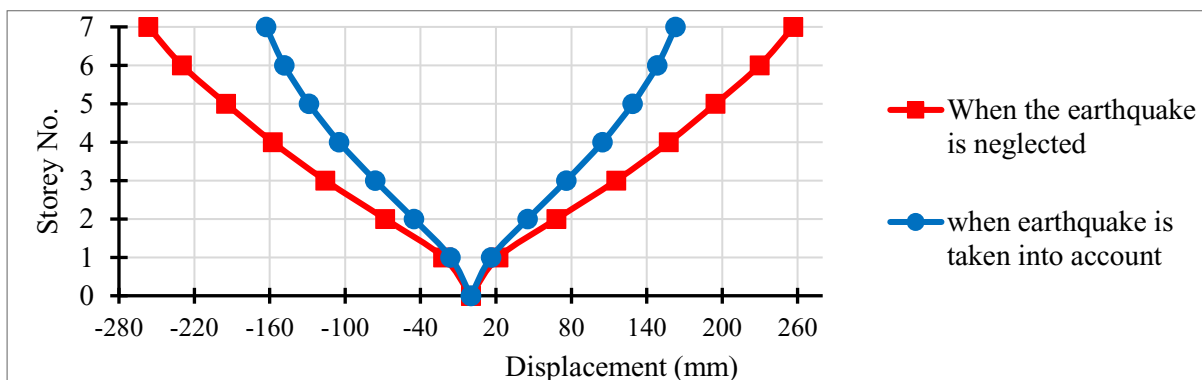


Figure 3. 67. New storey displacement in the y direction

Using these storey displacements, the maximum inter-storey drifts have been determined, plotted and checked as shown in Figure 3.68.

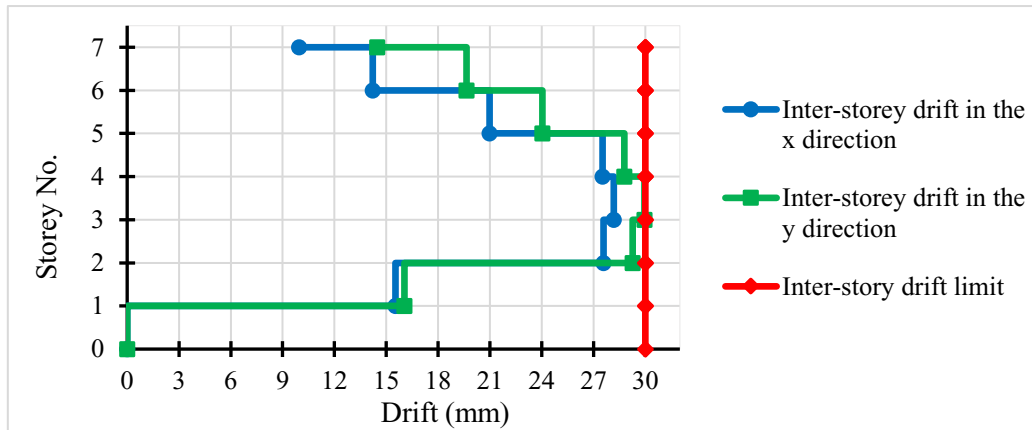


Figure 3. 68. New inter-storey drifts

As it is noted, with the new structural elements considered, the displacements obtained are admissible according to Eurocode 8.

3.4.4. When taking into account soil-structure interaction

Now we want to determine the response of the structure when the soil-structure interaction is taken into account.

3.4.4.1. Classification of footing

The evaluation of the footing cross-section led to two types of footings in the building, isolated footings and combined footings. Some of these footings would normally be off-centre but to simplify the analyses, we have considered them all to be centred on the column and the footings with the largest cross-sections have been assigned to the whole building. The distribution plan of these footings is shown in Figure 3.69.

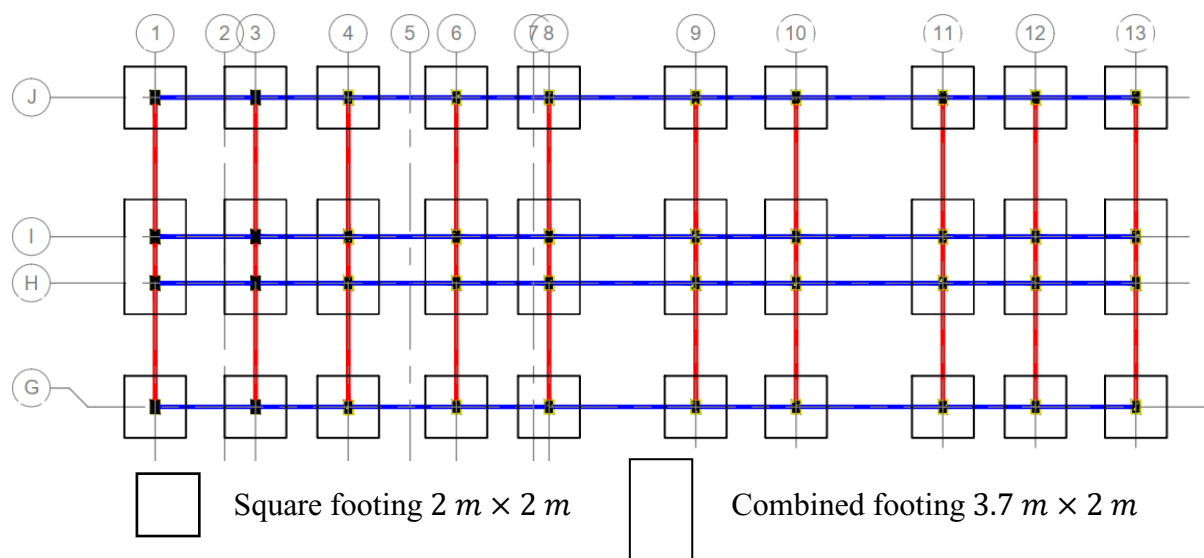


Figure 3. 69. Foundation plan

3.4.4.2. Modelling of the building

The modelling is the same as that shown in **Figure 3. 29** except that here the foundations are represented by shell elements to which springs are assigned to reflect the soil constraints. For this analysis, and according to **Table 2. 3** the modulus of subgrade reaction considered for modelling is 100000 kN/m³ which corresponds to class C soil (see **Table A. 6**). The figure 3.70 present the new modelling of the building.

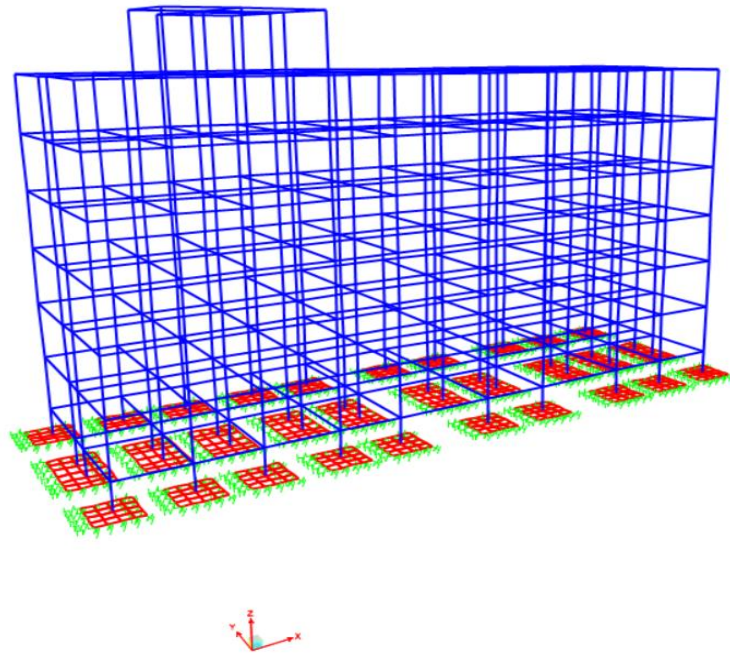


Figure 3. 70. Modelling of structure with spring constraints

3.4.4.3. The Natural period

The modal analysis is first performed on the structure to determine its modal properties, in this case the natural periods were determined and compared (See **figure 3.71**) to the natural periods of the building determined in the section 3.4.1.2. considering the fixed base.

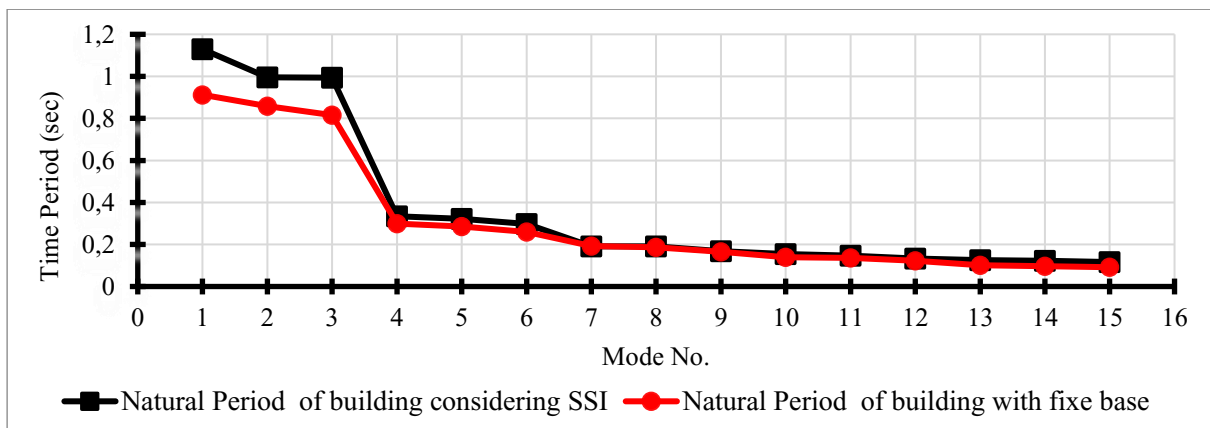


Figure 3. 71. Natural periods of the building with different base constraints

Figure 3.71 shows that for each mode of vibration, the natural period is greater when springs are considered at the base of the structure compared to when the base is fixed. This could lead to a change in the response of the structure when subjected to earthquake.

3.4.4.4. The response of the structure

Displacement of each storey and the inter-storeys drift, shown in figure 3.72, 3.73, 3.74 and 3.75, are the only responses assessed and compared to what we determined in section 3.4.2.4. b.

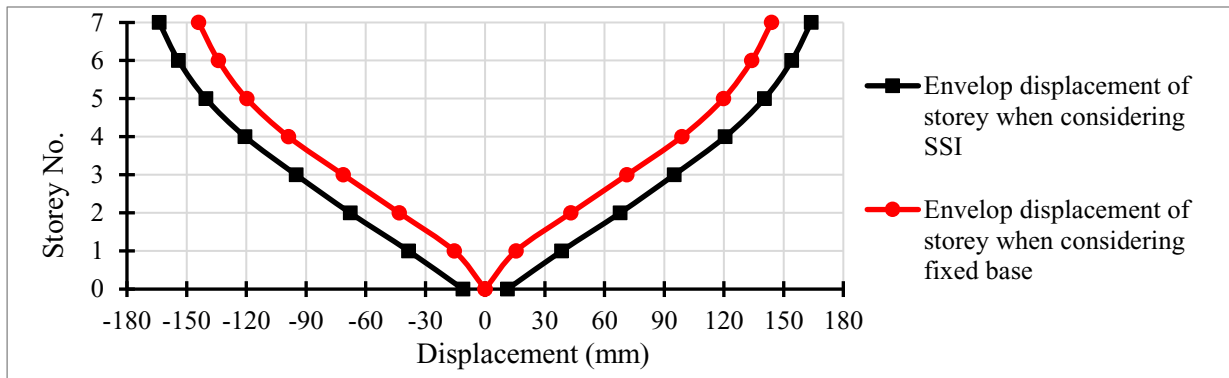


Figure 3. 72. Envelope curve of storey displacement in the x direction

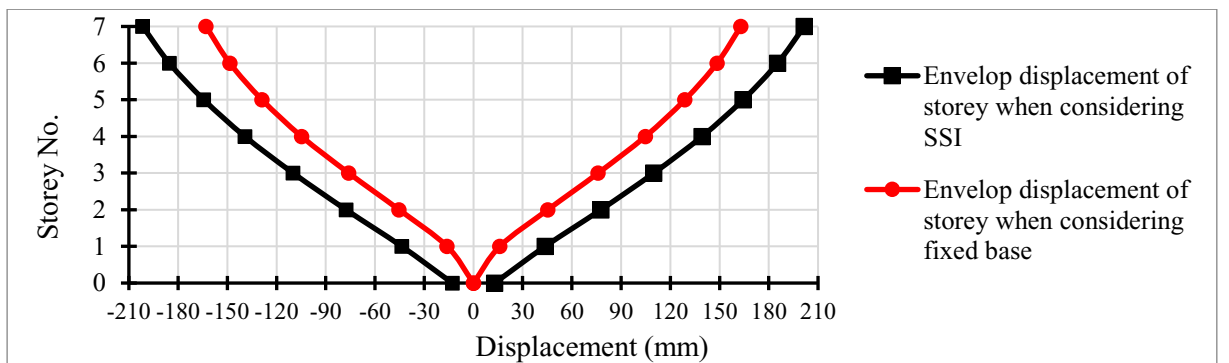


Figure 3. 73. Envelope curve of storey displacement in the y direction

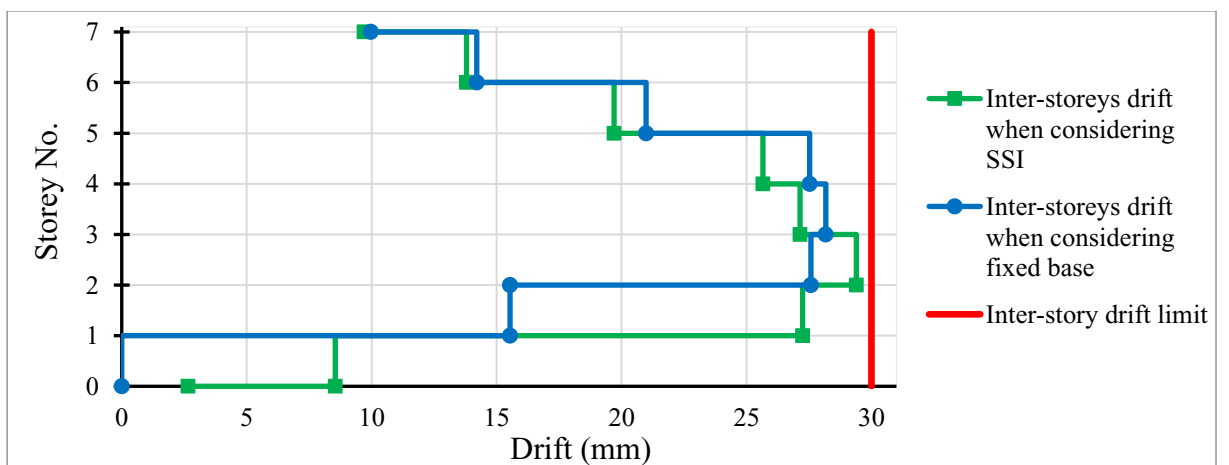


Figure 3. 74. Inter-storey drift in the x direction

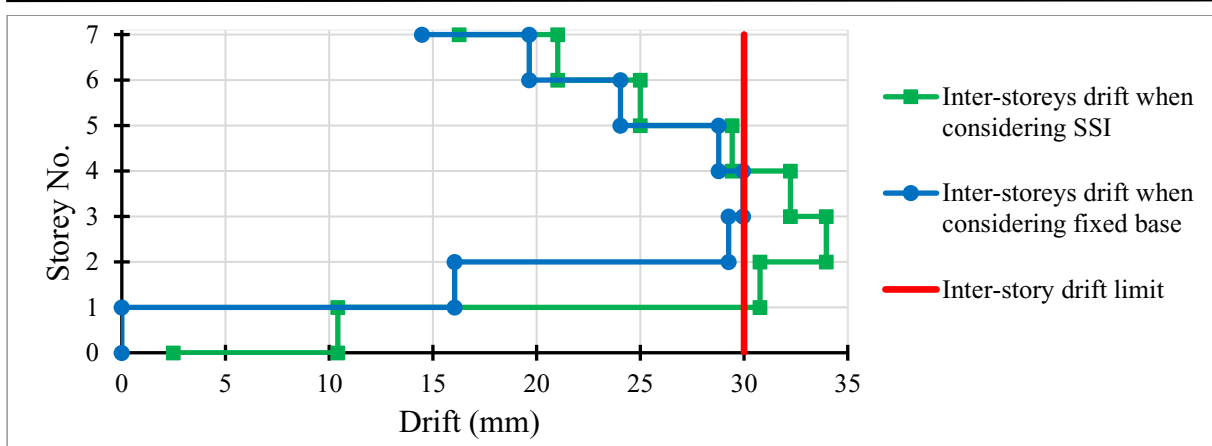


Figure 3. 75. Inter-storey drift in the y direction

Conclusion

The objectives of this chapter were first to present the case study and then to apply the linear static and dynamic analyses described in the methodology chapter. These analyses were used to obtain mainly the cross sections of the structural elements of the building. It was found that the static design is very limited compared to the dynamic design, as it was obtained that the structural elements designed by the static analysis could not support the seismic actions acting on the building and the displacement of the storeys did not comply with the limit prescribed by Eurocode 8, so a new design was needed, taking into account these seismic effects, to obtain a better response of the structure. But this new design was made assuming that the building was a fully elastic structure and on an approximation of its inelastic behaviour under the effect of the earthquake by an approximation of its behaviour factor described in section 2.5.2.2. b. i. This makes the results a little above reality. The next chapter will present the non-linear static analysis, which is an analysis of the same type as the dynamic analysis but which takes into account the non-linearities of the building in order to obtain a more optimised result.

CHAPITRE 4 : PUSHOVER ANALYSIS AND INTERPRETATION OF RESULTS

Introduction

This chapter presents the application of pushover analysis on the studied building to determine its elasto-plastic behaviour and its target displacement when subjected to an earthquake in order to optimise its structural elements. It starts with the modelling of the building and the presentation of the loads patterns that will be used, and ends with the presentation and interpretation of the results obtained from the analysis.

4.1. Modelling of the structure

The modelled building is shown in **Figure 4.1**. It is modelled in the same way as the one used in the elastic analysis, but with some additions:

- Each structural element is modelled with the reinforcing steels determined in linear dynamic analysis.
- Plastic hinges are assigned to the beams and columns to mark the non-linearity of the materials in the structure.

Figure 4.2 shows the properties of the hinges assigned to beams and **Figure 4.3** shows the properties of the hinges assigned to columns.

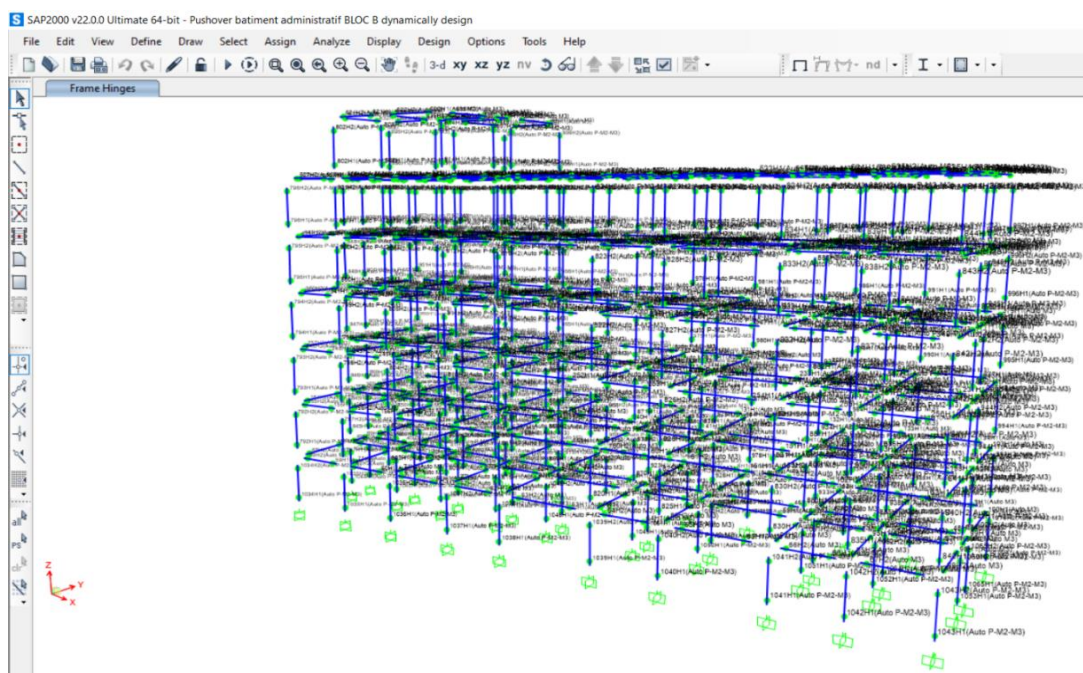


Figure 4. 1. Structural model of the building with affected plastic hinge

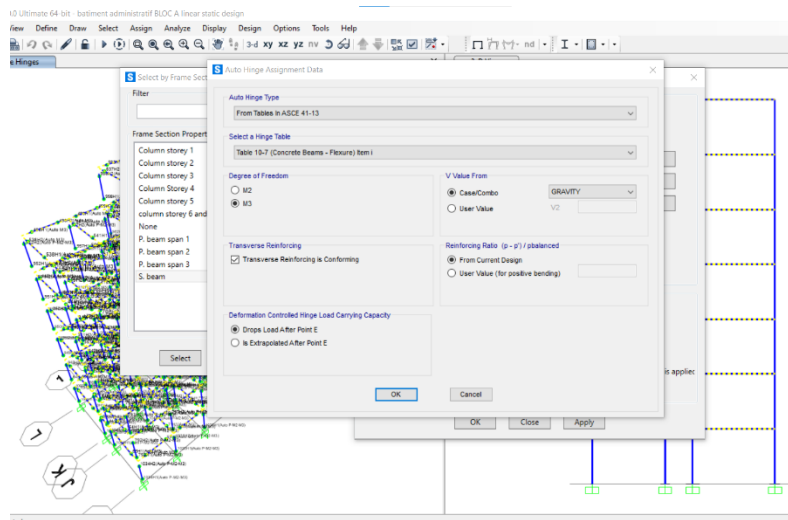


Figure 4. 2. Definition of the properties of the hinge for beams

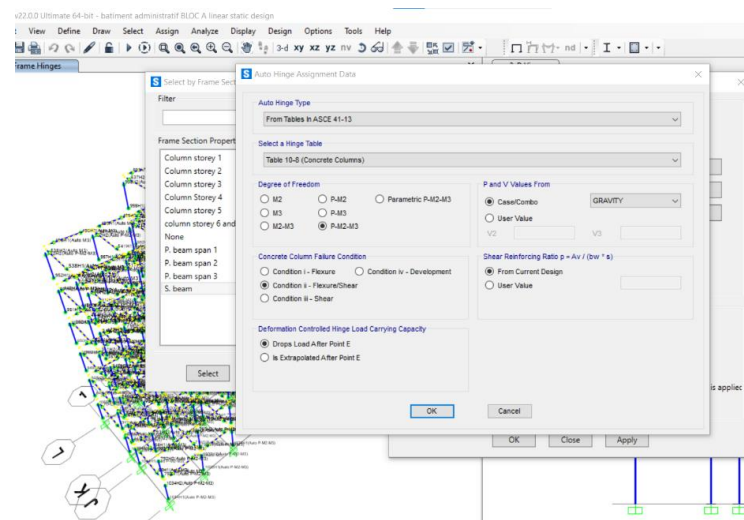


Figure 4. 3. Definition of the properties of the hinge for columns

4.2. Lateral load pattern

As described in section 2.9.3.2. , 3 loading patterns are considered for this analysis:

1) The acceleration loading pattern

Which considers a triangular load distribution which is a function of the acceleration of each storey and their masses.

2) The modal loading patterns

Which considers a modal distribution of the lateral load, which is a function of the effective mass given by each mode of vibration in each storey.

3) The uniform distribution loading pattern.

For which the structure is loaded laterally in the same way at all points.

In order to obtain the behaviour in each orientation of the structure these loads will be applied in the x and y directions of the building.

4.3. Results of the pushover analysis

The results of the pushover analysis allow to obtain the capacity curve of the building and its fragility zones or the collapse mechanisms of the structural elements.

4.3.1. Capacity curve

As we said in section 2.9.4. , the capacity curve describes the behaviour of the building under incremental lateral load. Considering the 3 loading cases described in section 4.2. , the capacity curves were obtained in the x and y directions of the building. They are shown in figures 4.4 and 4.6 respectively.

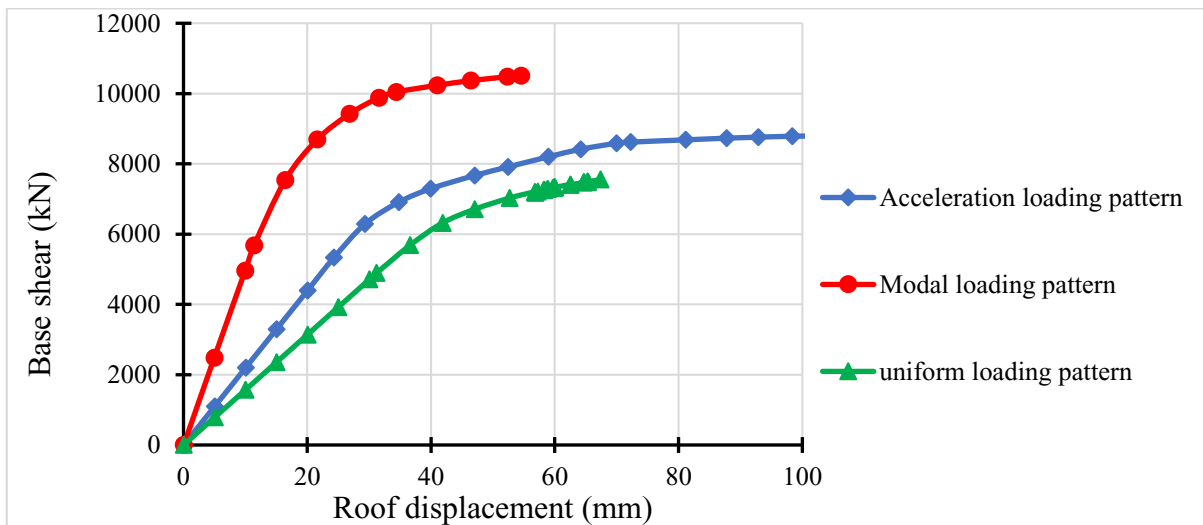


Figure 4. 4. Capacity curve in the x direction of the building

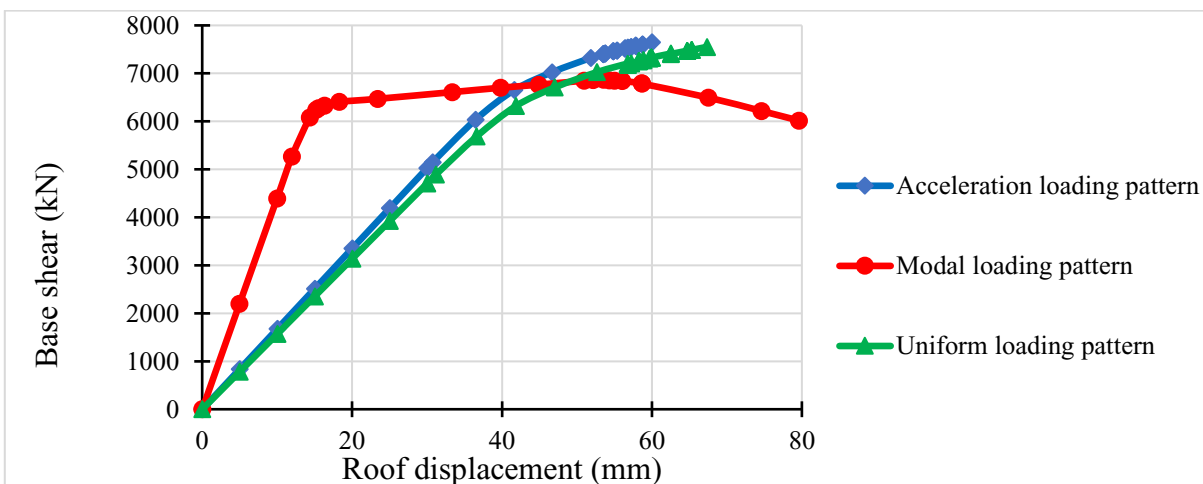


Figure 4. 5. Capacity curve in the y direction of the building

From these figures it can be seen that the building enters the plastic zones more quickly when subjected to modal loading pattern, which is normal and best represents the behaviour of the building when subjected to dynamic loading such as an earthquake because, as we saw in

the dynamic analysis, under dynamic loading the building adopts different modes of vibration, each of these modes generating different accelerations on the building.

The accelerated loading pattern also gives a good approximation of the behaviour of the structure when subjected to seismic loading, but for the regular building in elevation. Indeed, in this case, only the fundamental mode is taken into account, the higher modes are neglected.

4.3.2. Plastic mechanism

Figures 4.6 to 4.13 show the different stages of plastic hinge formation in the building when it is pushed by an accelerated loading model in both x and y orientations.

4.3.2.1. When push along x direction of the building

a. The fifth registration: Formation of the first plastic hinges in beams

Which corresponds to a roof displacement of about **24 mm** and a base shear of **5329.469 kN**. As can be seen in **figure 4.6**, the first plastic hinges appear on the first-floor beams. The color of these plastic hinges indicates that these beams are in the B-IO zone (see **Figure 2. 13**), more precisely in the zone of inelasticity with a linear reduction in beam stiffness. This indicates a very limited occurrence of structural damage, but the cracks are beginning to be significant.

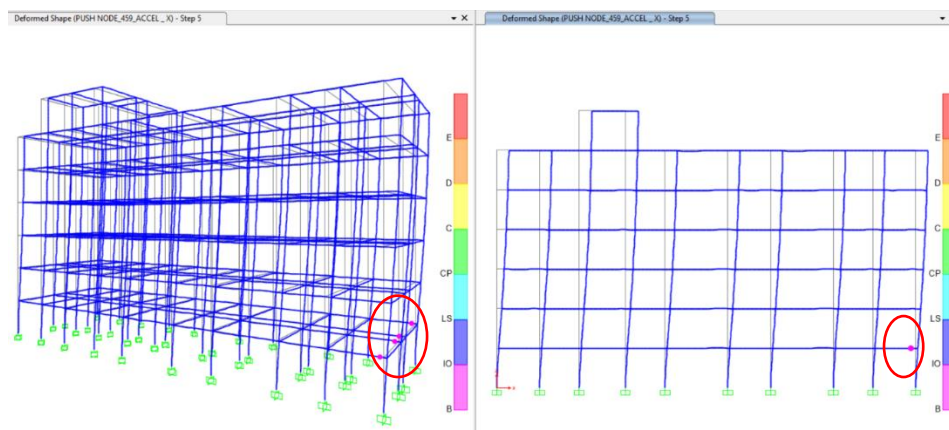


Figure 4. 6. State of the building at the fifth registration of analysis in the x direction

b. The tenth registration: Formation of the first plastic hinges in columns

Which corresponds to a roof displacement of about **52 mm** and a base shear of **7911,603 kN**. As can be seen in **figure 4.7**, the first plastic hinges appear on the first-storey columns. The colour of these plastic hinges indicates that these columns are in the same state as beams shown in the fifth registration.

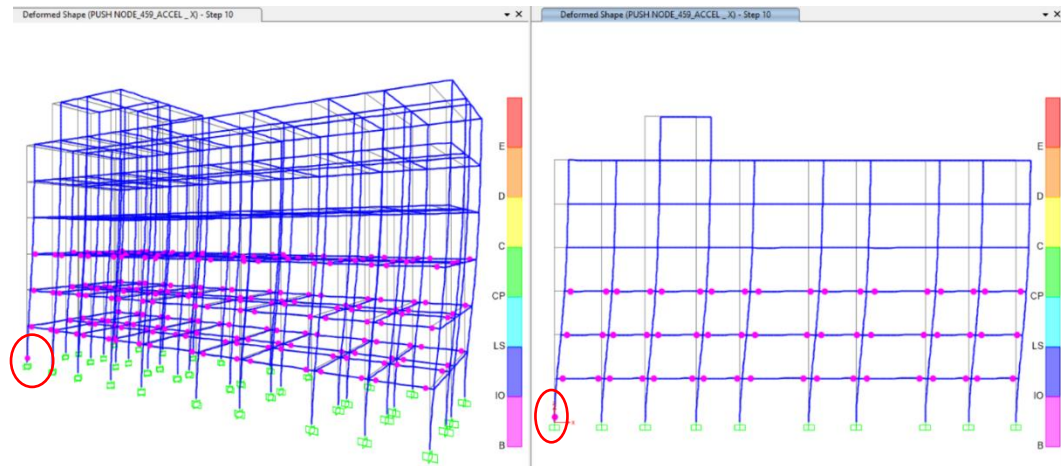


Figure 4. 7. State of the building at the tenth registration of analysis in the x direction

c. The seventeenth registration: The first collapse prevention in columns

Which corresponds to a roof displacement of about **92 mm** and a base shear of **8758,362 kN**. As can be seen in **figure 4.8**, the green colour of the plastic hinges in the columns indicates that the columns are about to collapse.

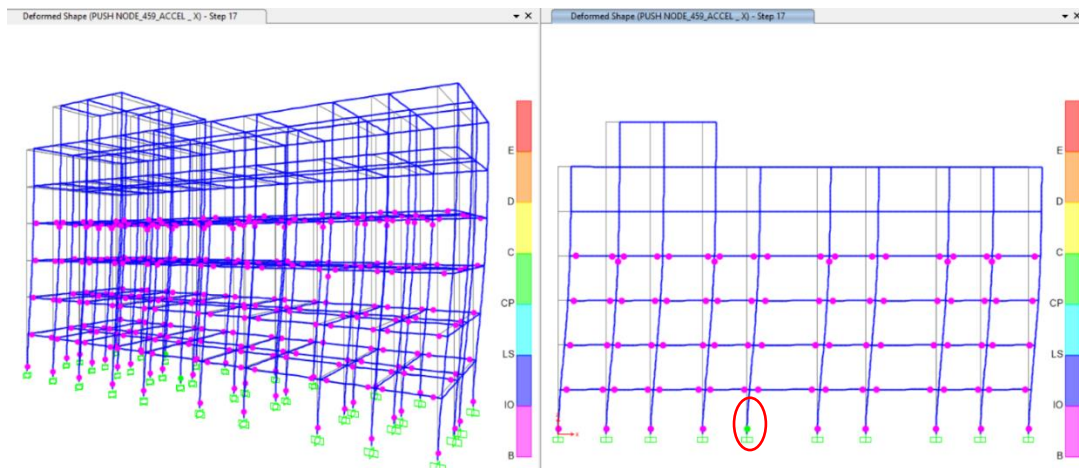


Figure 4. 8. State of the building at the seventeenth registration of analysis in the x direction

d. Twentieth recording: The life safety zone

Which corresponds to a roof displacement of about **115 mm** and a base shear of **8827,785 kN**. As can be seen in **figure 4.9**, the blue colour of the plastic hinges in beams and columns indicates that they are in the LS zone defined in section 1.2.2.2. and in **Figure 2. 13**. Beams have suffered significant damage and shear cracks; minor cracks develop in the columns.

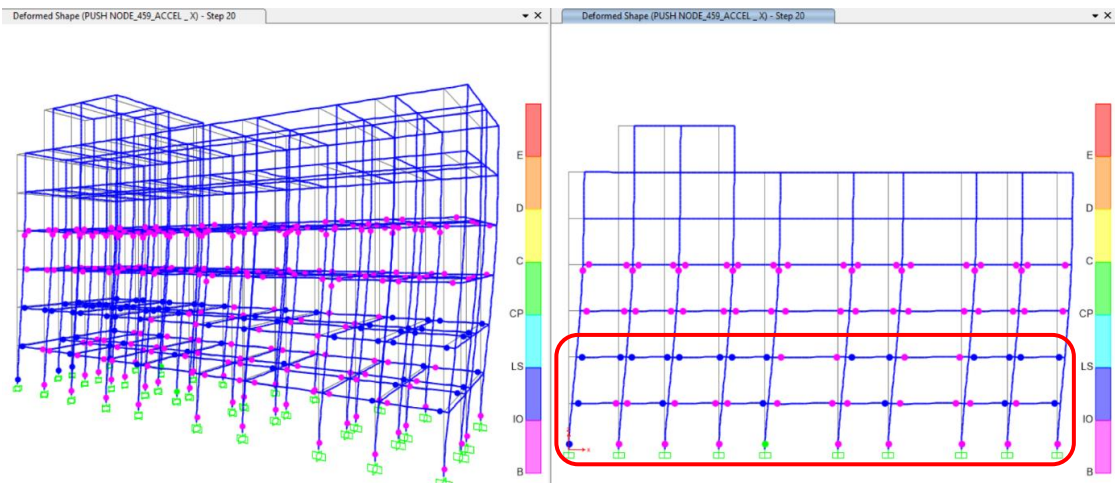


Figure 4. 9. State of the building at the twentieth registration of analysis in the x direction

e. Seventy-seventh registration: The beginning of the collapse

Which corresponds to a roof displacement of about **247 mm** and a base shear of **8893,992 kN**. As can be seen in **Figure 4.10**, the yellow colour of the plastic hinges in the beams indicates that the beams are in the C-D zone (**Figure 2. 13**), which shows a sudden reduction in load resistance and thus the beginning of collapse.

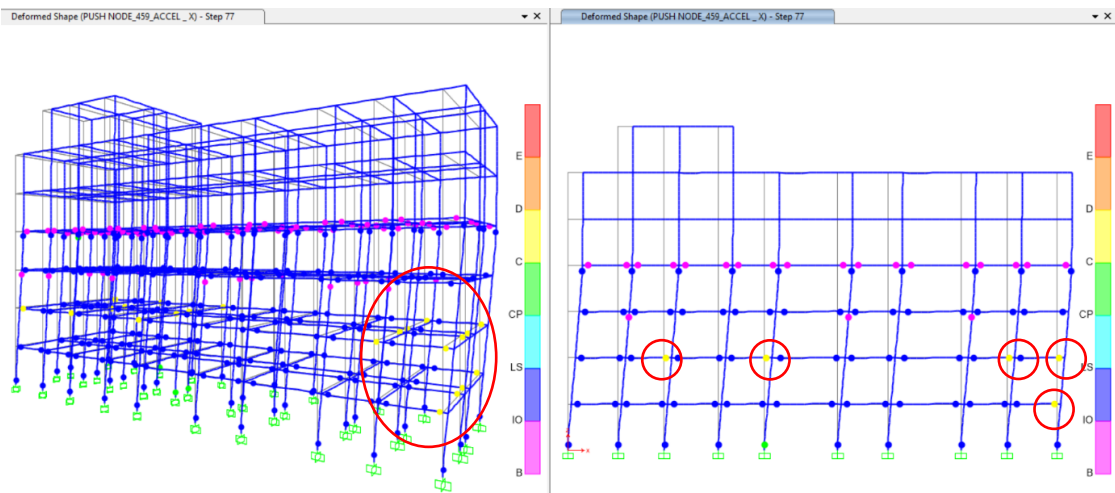


Figure 4. 10. State of the building at the seventy-seventh registration of analysis in the x direction

4.3.2.2. When push along the y direction of the building

a. The seventh registration: Formation of the first plastic hinges in beams

Which corresponds to a roof displacement of about 30 mm and a base shear of 5148,043 kN.

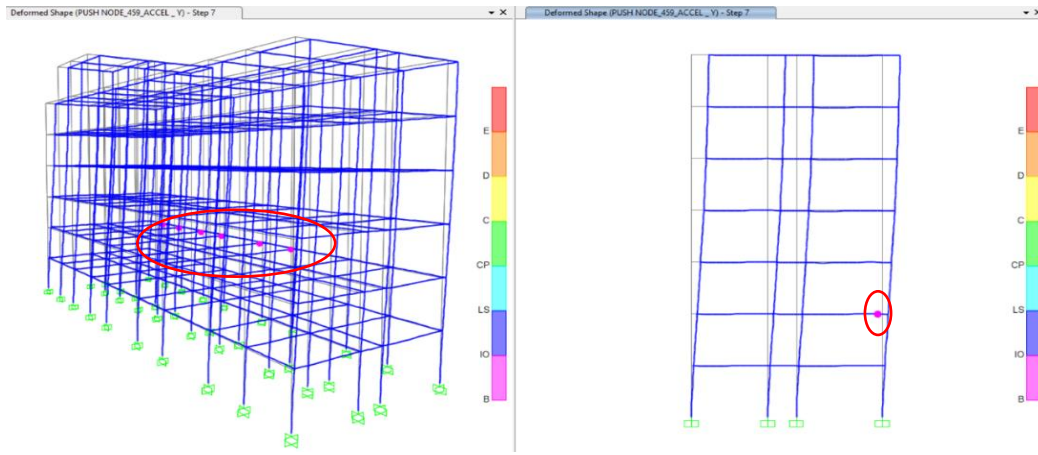


Figure 4. 11. State of the building at the seventh registration of analysis in the y direction

b. The eleventh recording: Formation of the first plastic hinges in columns

Which corresponds to a roof displacement of about 51 mm and a base shear of 7322,531 kN.

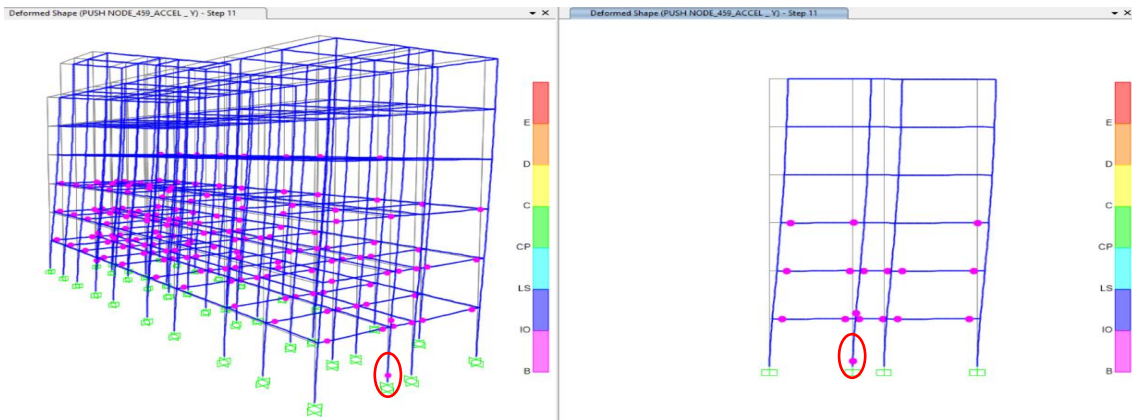


Figure 4. 12. State of the building at the eleventh registration of analysis in the y direction

c. Sixteenth recording: The first collapse prevention in columns

Which corresponds to a roof displacement of about 53 mm and a base shear of 7414,253 kN.

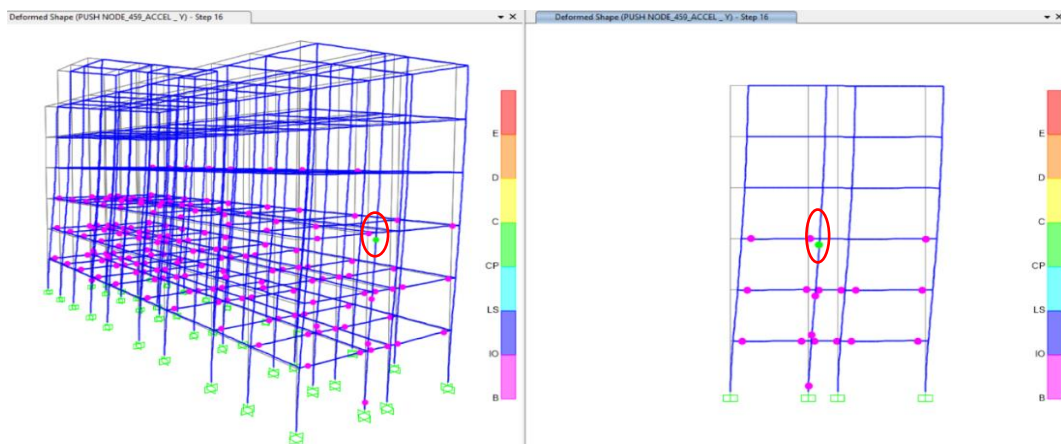


Figure 4. 13. State of the building at the Sixteenth registration of analysis in the y direction

4.4. Target displacement

Following the procedure described in section 2.9.5. for the determination of the target displacement, the first two steps allowed the determination of the bilinear curve and the capacity curve of the equivalent SDOF of the structure along the x and y orientations shown in **Figure 4. 14** and **Figure 4. 15**, using the masses and normalized displacements of each storey presented in **table 4.1**. The transformation factor was determined, its value is presented in **Table 4.2**.

Finally, with the characteristics of these bilinear curves and the characteristics of the elastic spectrum of the earthquake represented in **Figure 3. 36**, the target displacements of the structure along its two orientations x and y have been determined, and are presented in **Table 4.2**

Table 4. 1. Weight and normalized displacement of each storey

Storey	Weight of each storey (kN)		Normalized displacement	
	W_x	W_y	Φ_x	Φ_y
RDC	3877,38	2121,60	0,11	0,10
1	3877,38	2121,60	0,30	0,28
2	3877,38	2121,60	0,50	0,47
3	3577,38	1971,60	0,69	0,64
4	3577,38	1971,60	0,83	0,79
5	3337,38	1851,60	0,93	0,91
6	238,42	192,69	1,00	1,00

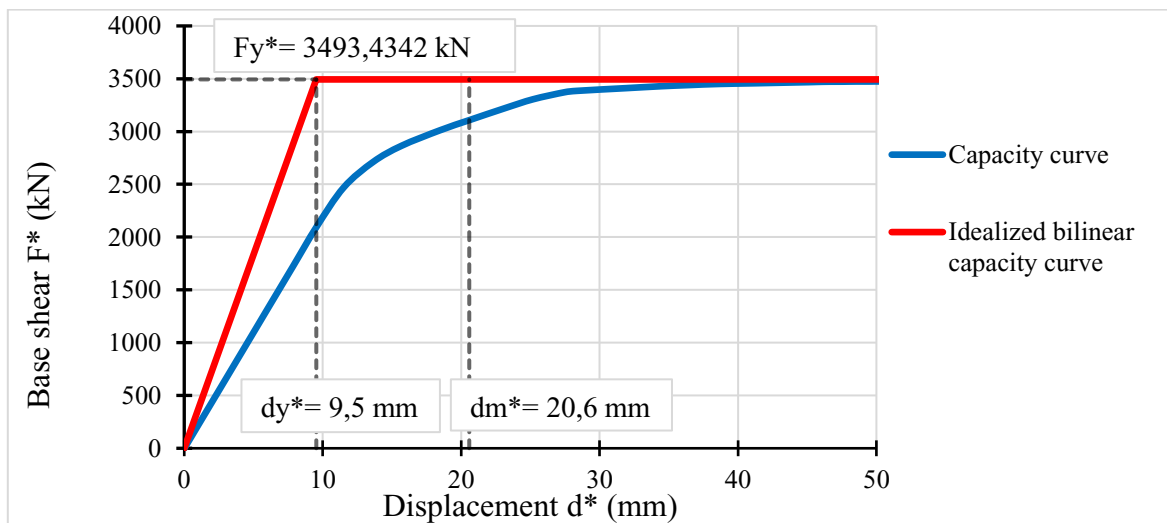


Figure 4. 14. Idealized bilinear capacity curve in the x direction of Equivalent SDOF system

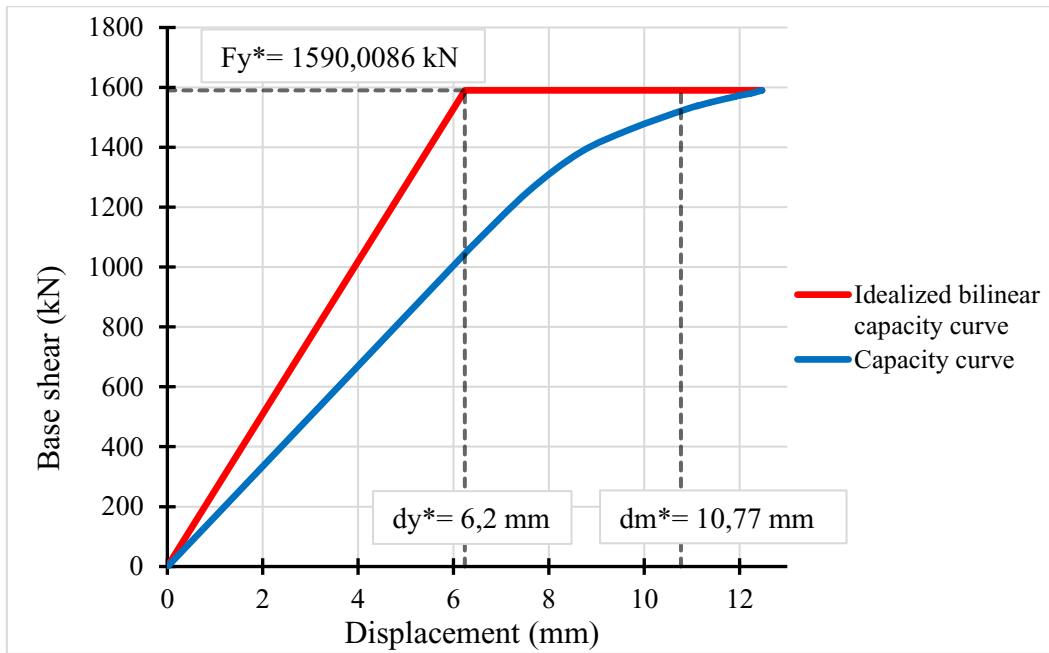


Figure 4. 15. Idealized bilinear capacity curve in the y direction of Equivalent SDOF system

Table 4. 2. Determination of the target displacement

Definitions and units	Properties	Values	
		In the x direction	In the y direction
Total weight of the building (kN)	W	31256,5740	31256,5740
Normalized mass of the building (kg)	m*	1252,7694	662,7448
Transformation factor	Γ	2,5459	4,8125
Yield force of Idealized SDOF (kN)	Fy*	3493,4342	1590,0086
Ultimate displacement of Idealized SDOF (m)	dm*	0,021	0,011
Yield displacement of Idealized SDOF(m)	dy*	0,0095	0,0062
Period of Idealized SDOF (s)	T*	0,3675	0,3204
Spectral acceleration due to T* (m/s ²)	Se(T*)	1,6183	1,6183
Elastic target displacement of Equivalent SDOF (m)	det*	0,0055	0,0042
Type of response		Elastic response	Elastic response
Target displacement of Equivalent SDOF (mm)	dt*	5,5372	4,2078
Target displacement of Building (mm)	dt	14,0972	20,2500
Ductility	μ	2,21	1,77

The base shear corresponding to the target displacement is the maximum response or maximum seismic force that will act on the building. With this force comes optimal solicitations on the vertical structural elements under seismic loading.

4.5. Optimization of the structural element

The target displacement determined for the building in the x-direction corresponds to a base shear of about **3295,587 kN** which corresponds to the 3rd registration step of the analysis in the x-direction, and that in the y-direction corresponds to a base shear of **3351,84 kN** which corresponds to the 4th registration step. With these base shears, we obtain the solicitations on the structural elements that mark the real response.

4.5.1. Beams

Considering the fourth registration step, the bending moment and shear force of the beams were obtained and presented in figure 4.16 for frame 10.

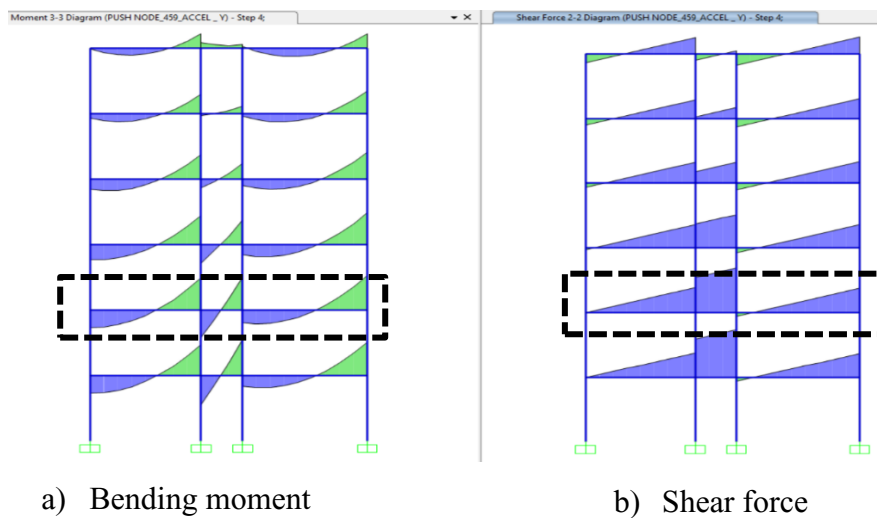


Figure 4. 16. Solicitation on the beams of frame 10 when the load is in the positive x-direction.

Taking into account that the load can be applied in the negative y-direction, the envelope solicitations of the most stressed beam are extracted and plotted in Excel to better show the stress distribution in the beam in each case. (See figure 4.17 and figure 4.18).

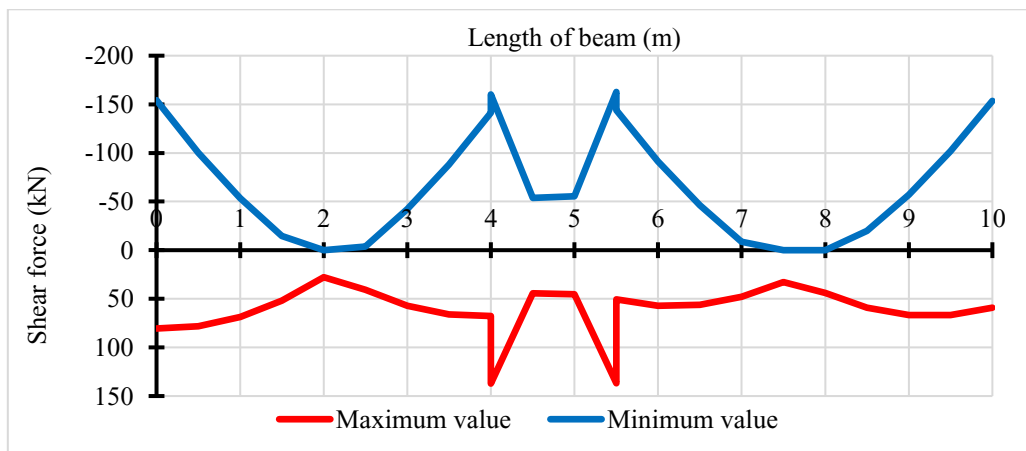


Figure 4. 17. Optimal envelop curve of bending moment of beams

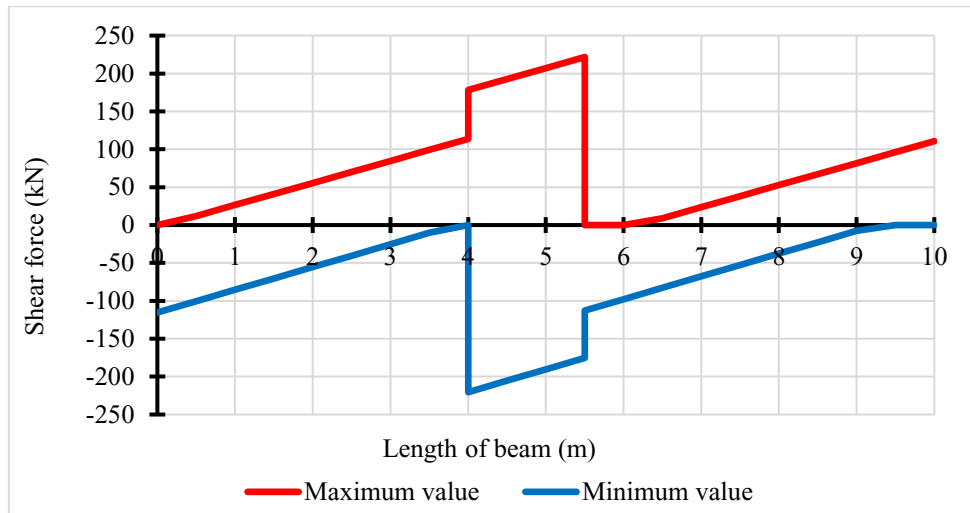


Figure 4.18. Optimal envelop curve of shear force of beams

From these solicitations, the optimal cross-section and reinforcement of the beam are determined. Following the beam design procedure described in section 2.7.1. , the beam cross-section is (25 × 50)cm and the diagrams representing the moment resistance and shear resistance of the beam as a function of the reinforcement characteristics are presented in figures 4.19 and 4.20 respectively.

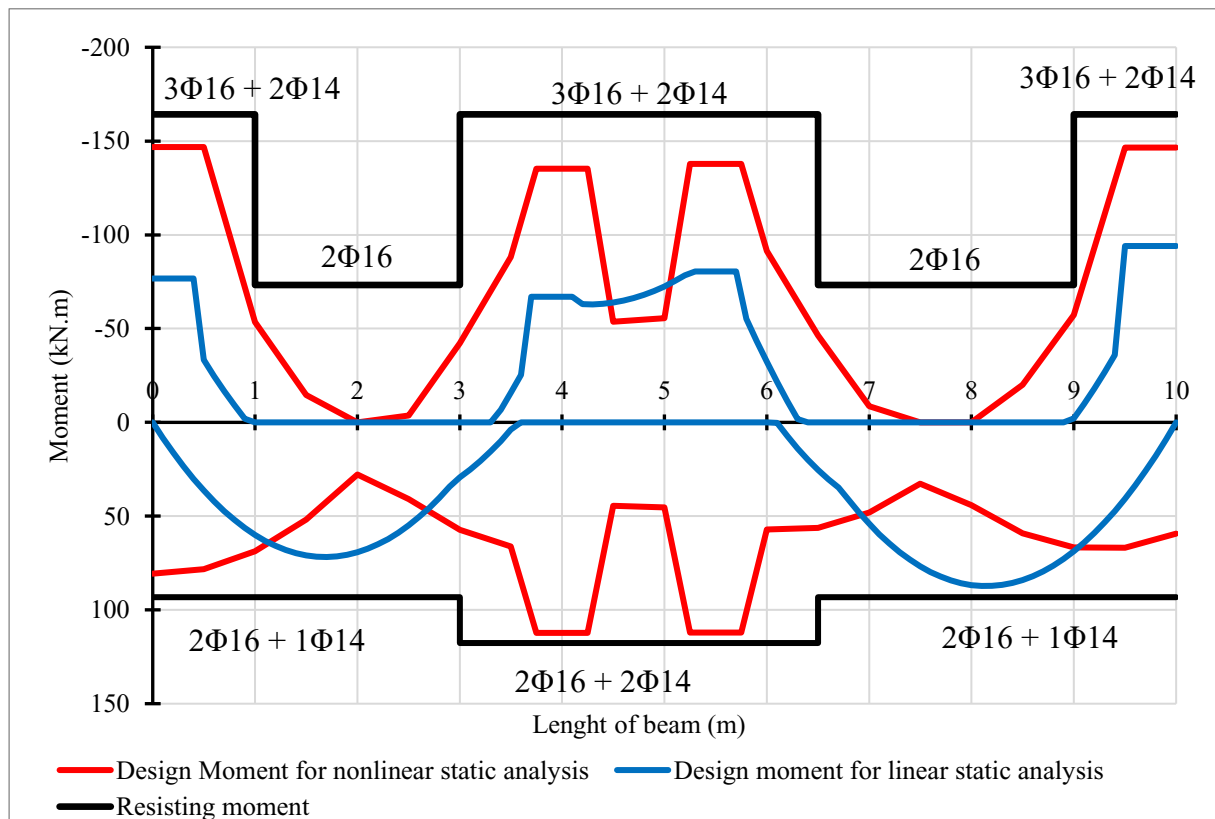


Figure 4.19. Bending moment verification of the designed beam using non-linear static analysis

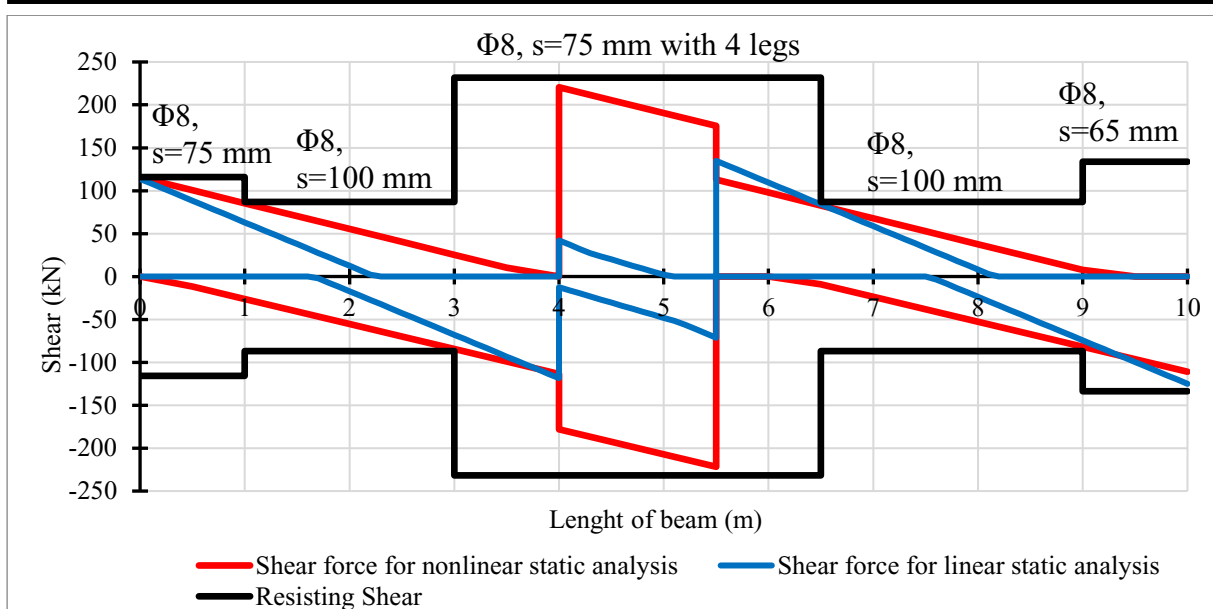


Figure 4. 20. Shear verification of the designed beam using non-linear static analysis

This beam is presented in detail in Appendix C1.

4.5.2. Columns

Considering the third and fourth registration steps according to the analysis in the x and y directions respectively, the solicitations of the columns are determined. The figure 4.21 present the distribution of bending moment in columns in the x and y direction.

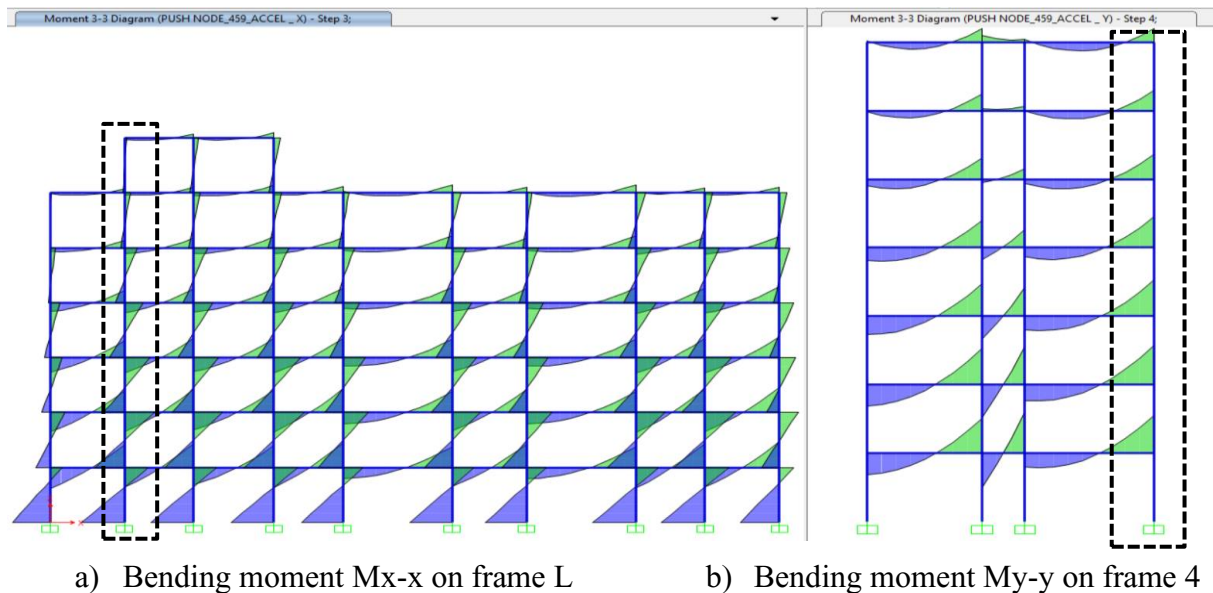


Figure 4. 21. Bending moment on columns of frame 10 when the load is in the positive x and y direction.

Taking into account that the load can be applied in the negative x and negative y direction, the envelope solicitations of the most stressed columns row are extracted and plotted in Excel to better show the stress distribution in columns in each case. (See figure 4.22 to 4.26).

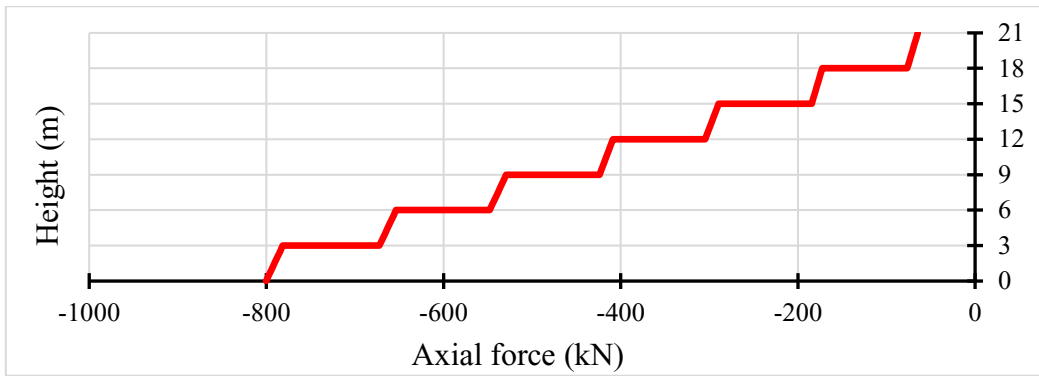


Figure 4.22. Optimal axial forces diagram of the columns in row 4-L

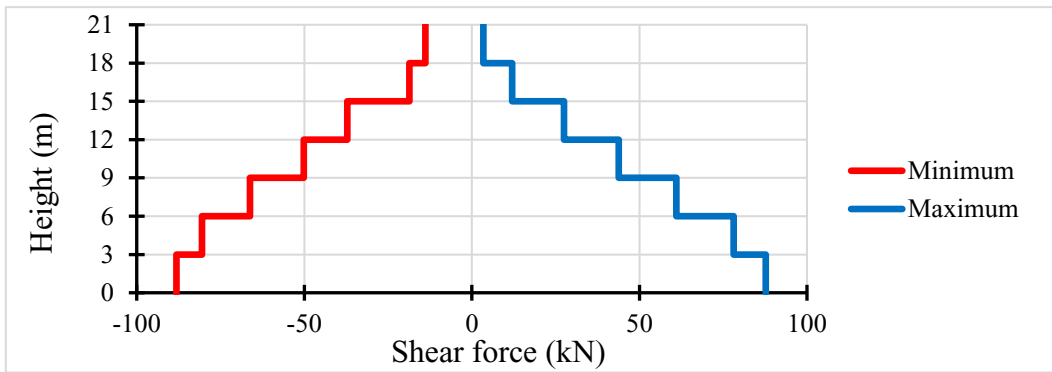


Figure 4.23. Optimal shear force V_{y-y} diagram of the columns in row 4-L in the y-direction

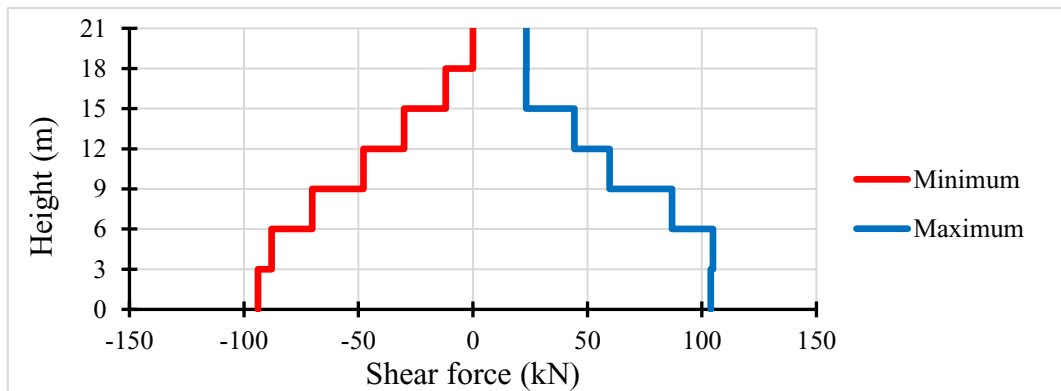


Figure 4.24. Optimal shear force V_{x-x} diagram of the columns in row 4-L in the x-direction

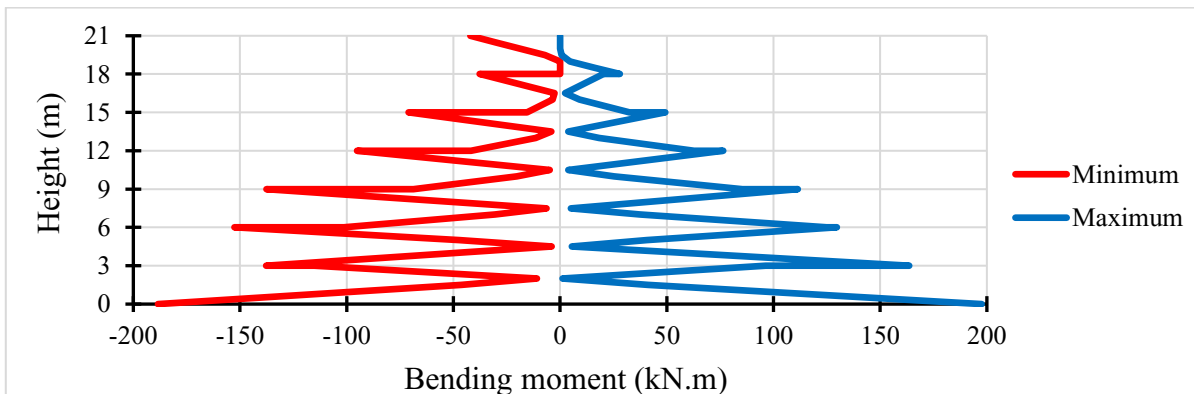


Figure 4.25. Optimal bending moment M_{y-y} diagram of the columns in row 4-L in the y-direction

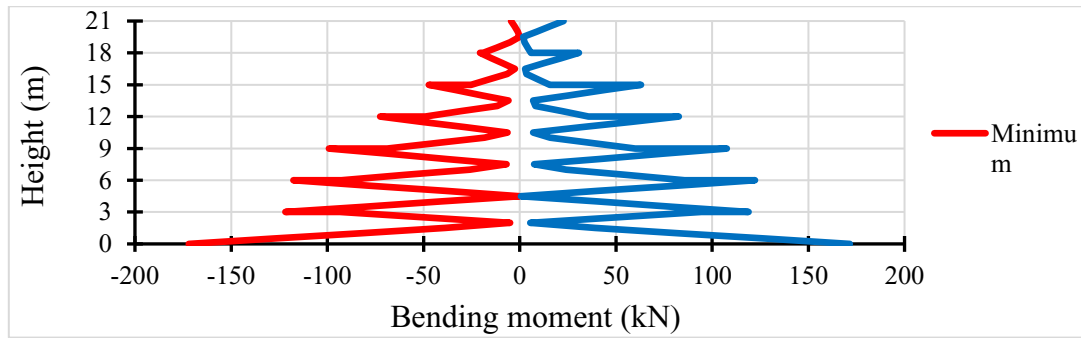


Figure 4. 26. Optimal bending moment M_x - x diagram of the columns in row 4-L in the x -direction

4.5.2.1. The longitudinal reinforcement

From the solicitations presented in figure 4.22, 4.25 and 4.26, the optimal cross-section and the longitudinal reinforcement of the columns are determined following the procedure described in section 2.7.2.3. of the chapter methodology. They are summarised in Table 4.3 and the limit quantity of reinforcement is verified by Table 4.4.

Table 4. 3. Optimised column section with longitudinal reinforcement

level	a	b	dx'	dy'	Asx = Asx'		Asy = Asy'	
	mm	mm	mm	mm	mm ²	Φ	mm ²	Φ
1	500	400	50	40	1010	5Φ16	1010	5Φ16
2	500	400	50	40	866	2Φ16+3Φ14	1010	5Φ16
3	500	400	50	40	866	2Φ16+3Φ14	1010	5Φ16
4	500	400	50	40	770	5Φ14	616	4Φ14
5	500	400	50	40	770	5Φ14	616	4Φ14
6	400	400	40	40	616	4Φ14	616	4Φ14
7	400	400	40	40	616	4Φ14	616	4Φ14

Table 4. 4. Verification of minimum and maximum quantity of steel

Level	As total		Asmin	Asmax	Verification
	(Φ)	mm ²	mm ²	mm ²	
1	16 Φ16	3232	400	80000	Checked
2	10 Φ16+6 Φ14	2944	320	64000	Checked
3	10 Φ16+6 Φ14	2944	320	64000	Checked
4	16 Φ 14	2464	320	64000	Checked
5	16 Φ 14	2464	240	48000	Checked
6	14 Φ 14	2156	180	36000	Checked
7	14 Φ 14	2156	180	36000	Checked

After determining the longitudinal reinforcement, it is necessary to check the M-N interaction.

“Nonlinear static and linear dynamic analysis for reinforced concrete building as complementary method of analysis and design”

4.5.2.2. The M-N interaction diagram

The M-N interaction diagram, described in paragraph 2.7.2.4. of columns designed is presented along X and Y axis in figure 4.27 and 4.28 respectively.

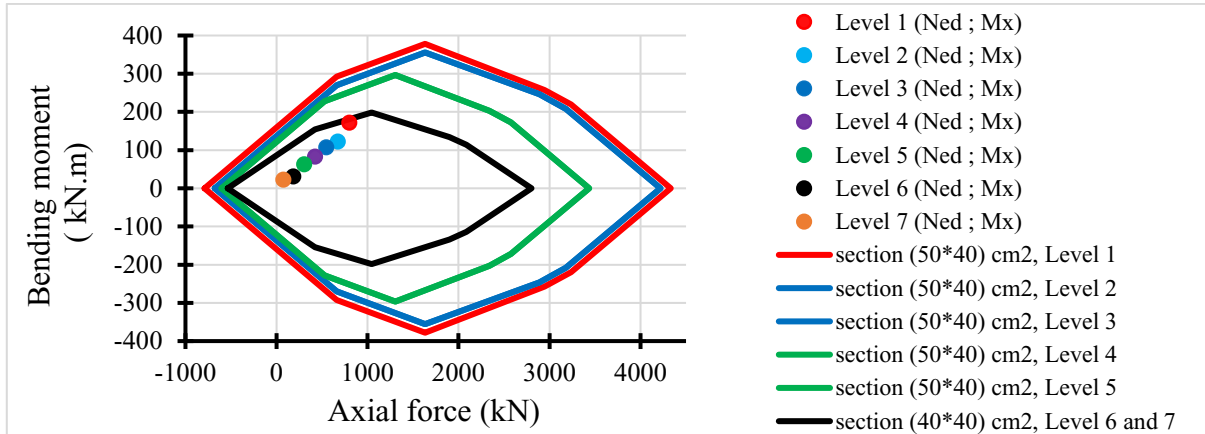


Figure 4. 27. Verification of the M-N interaction in the x direction of the columns

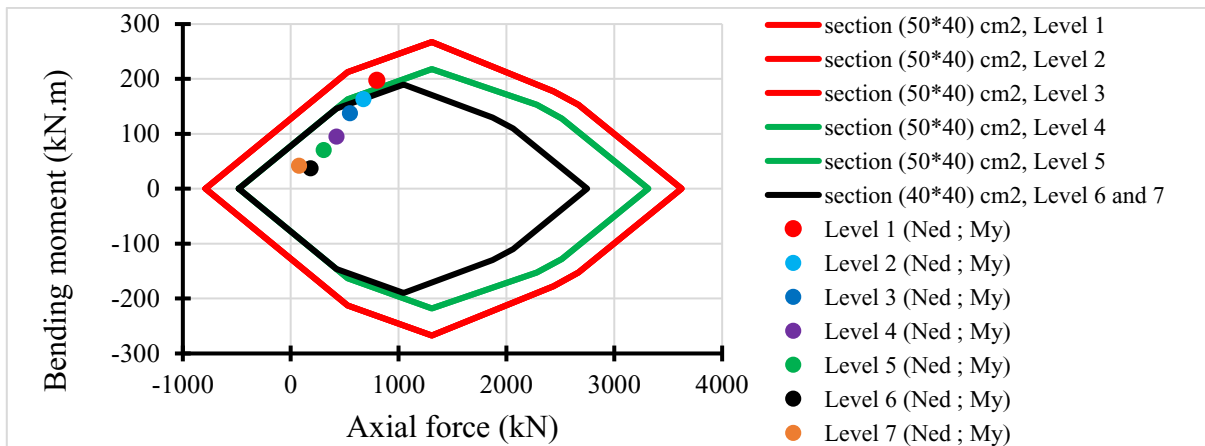


Figure 4. 28. Verification of the M-N interaction in the y direction of the columns

4.5.2.3. The Shear verification

Following the procedure described in section 2.7.2.3. , the distribution of shear reinforcement on the column row is presented in figure 4.29

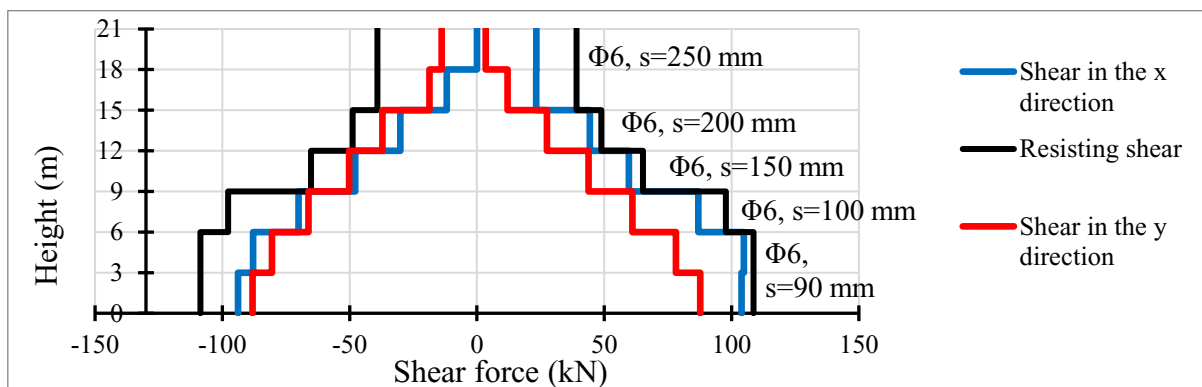


Figure 4. 29. Shear verification on column row 4-L

The columns of level 1 are presented in detail in appendix C2

4.6. The inter-storey drifts

In order to determine the inter-storey drifts of the building, the vertical reference element with the maximum displacement chosen (see **Figure 3. 42**) during the dynamic linear analysis is also considered here. The analysis of its displacements has allowed us to determine the inter-storey drifts presented in **figure 4.30**.

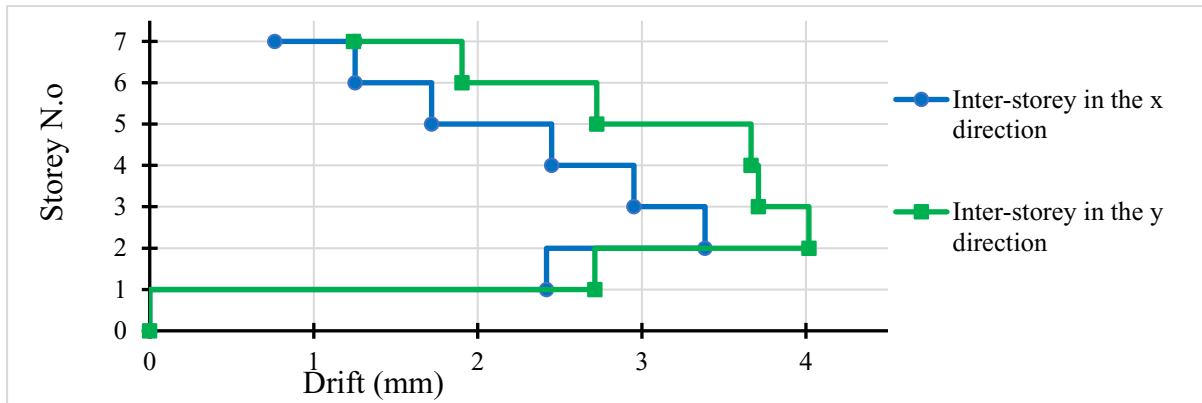


Figure 4. 30. The inter-storeys drift

4.7. When taking into account soil-structure interaction

The behaviour of the structure shown through its capacity curve is evaluated considering only the acceleration loading. This capacity curve is compared to the one obtained at the section 4.3.1. and it is presented in figures 4.31 and 4.32 along the x and y directions respectively.

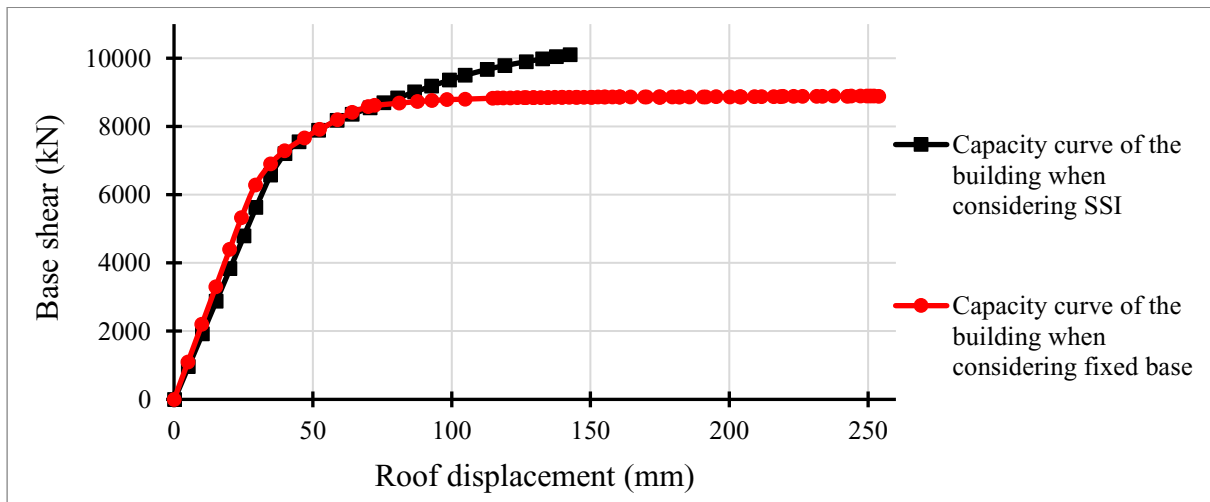


Figure 4. 31. Capacity curve of the building in the x direction

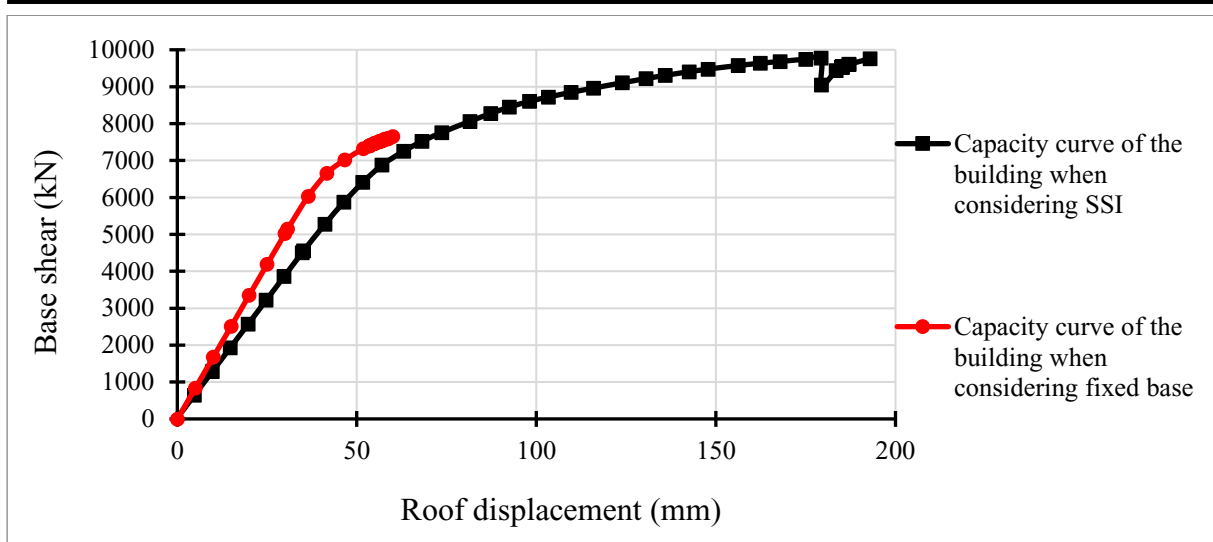


Figure 4. 32. Capacity curve of the building in the y direction

Figure 4.31 shows that in the x-direction, the building is more ductile when the SSI is considered, in fact the roof displacements observed in the plastic zone are lower when the SSI is considered. This is also shown by the fact that the first plastic hinges (see figure 4.33) are formed for a base shear of 5623.17 kN which is higher than that obtained when the base is fixed (see section 4.3.2). However, in the y-direction the structure is less ductile when the SSI is considered, as can be seen in Figure 4.32 which shows that for the same base shear, the roof displacement is greater when the SSI is considered. Here the first plastic hinge (see figure 4.34) is formed for a base shear of 4505.506 kN which is less than that obtained with a fixed base.

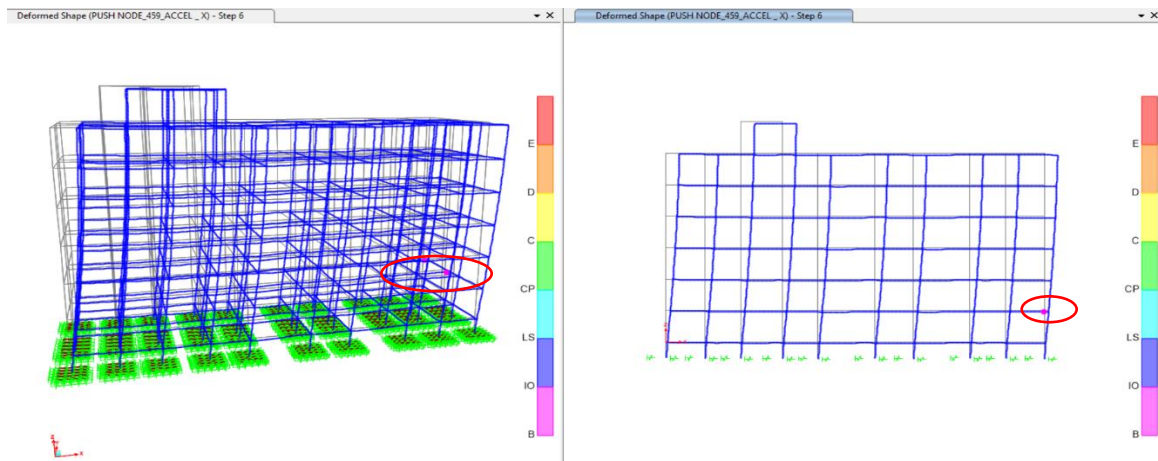


Figure 4. 33. First plastic mechanism in the x-direction

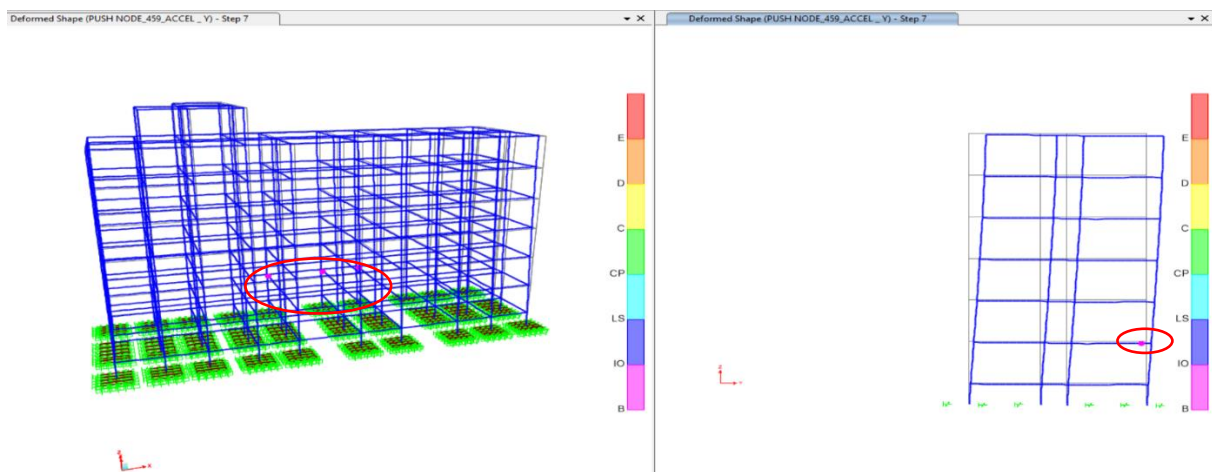


Figure 4. 34. First plastic mechanism in the y-direction

Conclusion

The main objective of this chapter was to design the building taking into account its non-linearities, in order to obtain the real behaviour of the structure under earthquake action. Pushover analysis was used to determine the capacity curve of the building, which was used to determine the target displacement and the ductility of the building under the earthquake using the elastic response spectrum of the seismic action. An optimisation of the cross-sections of the structural elements was carried out, and it was found that the optimisation significantly reduced the amount of reinforcement and the cross-section of the building columns. The cross-sections of the beams remained the same, but there was a slight increase in the amount of reinforcement at the beam-column junctions. The inter-storey drifts have also been considerably reduced and are well below the limit allowed by Eurocode 8. Therefore, it turns out that the linear dynamic analysis oversizes the building because it is assumed to remain in the elastic domain and its real energy dissipation is not taken into account, what is taken into account is just an approximation given by the approximate behaviour factor of the structure.

GENERAL CONCLUSION

This thesis aims to analyse the elastic and inelastic behaviour of reinforced concrete buildings under the effect of a weak earthquake, using linear dynamic analysis and non-linear static analysis, in order to predict its response for better design. The case study is the new administrative building of ENSTP in Yaoundé, Cameroon. The first step was to design the building only under vertical static loads (permanent and operational loads) using linear static analysis. This design provided the concrete and reinforcement sections of the columns and beams required to resist these actions both at the ultimate limit state and at the service limit state.

Through dynamic analysis, and more specifically modal analysis, it was possible to determine the modal properties of the building, i.e., the natural periods and frequencies, the effective modal masses and the participation factors of each mode of vibration that the building would take if subjected to any dynamic loading. Analysis of these modal properties revealed that the minimum vibration modes required to study the linear dynamic behaviour of this building are the first 10 vibration modes whose sum of their effective modal masses is greater than 90% of the total building mass. Using the characteristics of these 10 vibration modes and the design response spectrum derived from the horizontal elastic response spectrum and an approximation of the building's behaviour factor (reflecting the building's ability to dissipate energy), it was possible to determine the response of the structure by means of the response spectrum analysis. The results obtained show large displacements of each floor, inter-storey drifts that exceed the limit prescribed by Eurocode 8, the stresses on the structural elements are huge compared to what the structure can withstand. The statically designed building is therefore not able to resist this seismic action. A new design was therefore carried out, involving an increase in the concrete cross-sections and the amount of reinforcement in the structural elements.

In order to verify the capacity and efficiency of this building, a non-linear static analysis was carried out, which takes into account the non-linearity of the building due to the materials and geometry of the structural elements. This analysis resulted in the capacity curve of the building, showing the real behaviour of the structure, and the different failure mechanisms that the structure could undergo when subjected to horizontal loading and its ductility. Using this curve and the horizontal elastic response spectrum, the real or non-linear response of the structure (target displacement, inter-storeys drift, maximum expected base shear, stresses,) was

determined to be less than those determined by the linear dynamic analysis. This new response allowed the structure to be optimised in terms of the amount of reinforcement and concrete of the structural elements.

With the small study that has been carried out on the soil-structure interaction in the studied analyses, it should be seen that this work is not completely finished because we have seen that the soil-structure interaction impacts on the behaviour of the structure and on its response to the earthquake. Indeed, the natural periods and the displacement of the floors are more important but the ductility of the building is variable (can be higher or less) which could lead to a reduction of the stresses on the structural elements by dissipation at the ground level (Davidovici et al, 2019).

The limitations of this analysis are mainly due to the absence of certain data such as geotechnical and seismic data of the studied construction site. Indeed, the reference acceleration of the soil taken into account during these analyses is obtained according to the French standard and the soil data considered are all assumed from the abacuses presented in the appendices and from the surroundings of the site, no in-situ test was carried out to obtain the real characteristics of the soil.

BIBLIOGRAPHY

BOOKS

1. A. W. Beeby and R. S. Narayanan, *Designers' Guide to EN1992-1-1 and EN1992-1-2. Eurocode 2: Design of concrete structures. General rules and rules for buildings and structural fire design*, H. Gulvanessian, 2005, (Designers' guide to the Eurocodes)
2. ANIL K. Chopra, *Dynamics of structures: Theory and application to earthquake engineering*, Pearson, 1995
3. ATC-40, *Seismic evaluation and retrofit of concrete buildings*, volume 1, November 1996
4. Bill Mosley, John Bungey and Ray Hulse, *Reinforced concrete design to Eurocode 2 seventh edition*, PALGRAVE MACMILLAN, 2012
5. Bungale S. Taranath, *Tall building design*, CRC Press, 2017
6. H. KRAWINKLER, P. FAJFAR, *Nonlinear Seismic Analysis and Design of Reinforced Concrete Buildings*, CRC Press, mars 1992
7. Jack Moehle, *Seismic Design of Reinforced Concrete Buildings*, McGraw-Hill Education, 2015
8. Patricia BALANDIER, *Conception parasismique des bâtiments : Introduction à la dynamique des structures*, Volume 1, Juillet 2001
9. Ray W. Clough and Joseph Penzien, *Dynamics of structures*, 1993
10. R. Park and T. Paulay, *Reinforced concrete structures*, 1975
11. Syed Mehdi Ashraf, P.E., *Practical Design of Reinforced Concrete Buildings*, CRC Press, 2018
12. Victor Davidovici et al., *Pratique du calcul sismique Guide d'application de l'Eurocode 8*, EYROLLES and AFNOR, 2015

NORMS

1. EN 1990, *Basis of structural design*, 2002, (Eurocode 0)
2. BS EN 1991-1-1, *General actions densities, self-weight, imposed loads for buildings*, 2002, (Eurocode 1: Actions on structures)
3. BS EN 1992-1-1, *General rules and rules for buildings*, 2004, (Eurocode 2: Design of concrete structures)
4. BS EN 1998-1, *General rules, seismic actions and rules for buildings*, 2004, (Eurocode 8: Design of structures for earthquake resistance)
5. BS EN 1998-2, *Bridges*, 2005, (Eurocode 8: Design of structures for earthquake resistance)

“Nonlinear static and linear dynamic analysis for reinforced concrete building as complementary method of analysis and design”

Master in civil engineering defended by: TATCHA KANKEU Yvan Loïc, NASPW Yaoundé, 2019-2020

6. FEMA 356, *Prestandard and Commentary for the Seismic Rehabilitation of Buildings*, November 2000
7. FEMA 440, *Improvement of Nonlinear Static Seismic Analysis Procedures*, June 2005.

ARTICLE

1. Bergami, A. V., Forte, A., Lavorato, D., & Nuti, C. (2018). *Non-Linear Static Analysis: Application of Existing Concrete Building*. Lecture Notes in Civil Engineering, 329-340. https://doi.org/10.1007/978-3-319-78936-1_24
2. Chandak, N. R. (2012). *Response Spectrum Analysis of Reinforced Concrete Buildings*. Journal of The Institution of Engineers (India): Series A, 93(2), 121-128. <https://doi.org/10.1007/s40030-012-0012-9>
3. Gowtham, S., Prakash, M., Parthasarathi, N., Satyanarayanan, K., & Thamilarasu, V. (2018). *2D-Linear static and non-linear dynamic progressive collapse analysis of reinforced concrete building*. Materials Today: Proceedings. <https://doi.org/10.1016/j.matpr.2017.12.305>
4. Inel, M., & Ozmen, H. B. (2006). *Effects of plastic hinge properties in nonlinear analysis of reinforced concrete buildings*. Engineering Structures, 28(11), 1494-1502. <https://doi.org/10.1016/j.engstruct.2006.01.017>
5. Ismail, A. (2014). *Nonlinear static analysis of a retrofitted reinforced concrete building*. HBRC Journal, 10(1), 100-107. <https://doi.org/10.1016/j.hbrcj.2013.07.002>
6. Moehle, J. P. (2005). *Nonlinear analysis for performance-based earthquake engineering*. The Structural Design of Tall and Special Buildings, 14(5), 385-400. <https://doi.org/10.1002/tal.334>
7. Pinho, R., Marques, M., Monteiro, R., Casarotti, C., & Delgado, R. (2013). *Evaluation of Nonlinear Static Procedures in the Assessment of Building Frames*. Earthquake Spectra. <https://doi.org/10.1193/100910eqs169m>
8. Rahul Leslie (2002). *The Pushover Analysis, explained in its Simplicity*
9. S. Ojha, A. Mishra, M. Firoj, and K. Narayan (February 2018). *Non-linear static analysis of dual RC frame structure*.

THESIS

1. AIDJOULI Mohamed, KHELOUFI Mohamed (2018). *Etude comparative entre la méthode statique équivalente et la méthode modale spectrale pour l'évaluation des charges*

“Nonlinear static and linear dynamic analysis for reinforced concrete building as complementary method of analysis and design”

Master in civil engineering defended by: TATCHA KANKEU Yvan Loïc, NASPW Yaoundé, 2019-2020

- sismiques*. (Master thesis). UNIVERSITE MOHAMED BOUDIAF - M'SILA Faculté de Technologie Département de Génie Civil
2. DAHMANI Souhaib, RAHMANI Djamel (2014). *Analyse dynamique de la réponse d'une structure*. (Master thesis). Université de TLEMCEM Faculté de Technologie Département de Génie Civil
 3. DJEUKOUA NATHOU Gabrielle Laure (2018). *Comparative analysis of seismic protection systems*. (Master thesis). National Advanced School of Publics works Yaoundé
 4. NGOUO Idriss Michaël. (2015). *Pushover analysis of buildings*. (Master thesis). National Advanced School of Publics works Yaoundé
 5. MOUSTAPHA HOUSSEINI. (2019). *Influence of foundation type on the seismic response of buildings considering soil-structure interaction*. (Master thesis). National Advanced School of Publics works Yaoundé

WEB SITE

1. Arnav Anuj Kasar (September 10, 2013), *Response Spectrum Method Of Analysis – with simplified examples*, <https://civildigital.com/response-spectrum-method-analysis-learn-examples/>, Accessed on 27 April 2021 at 8am
2. Audrey (09 December 2009), *Le Béton Armé: Histoire D'une Invention* <https://www.gralon.net/articles/materiel-et-consommables/materiels-industriels/article-le-beton-arme---histoire-d-une-invention-3431.htm>, Accessed on 16 May 2021 at 7h06
3. Crystal Instruments (2016), *Basics of Modal Testing and Analysis*, <https://www.crystalinstruments.com/basics-of-modal-testing-and-analysis/>, accessed on 30 May 2021 at 8:43
4. CSOA. (May 2, 2020 at 4:38 pm), *Why Concrete is The Most Popular Building Material*, <https://www.contractorsoa.com/concrete-most-popular-building-material/>, accessed on 28 May 2021 at 18:49
5. Engineer's Outlook (October 11, 2011), *History of Reinforced Concrete and Structural Design*, <https://engineersoutlook.wordpress.com/2011/10/11/structural-concrete-design/>, accessed on 28 May 2021 at 22:52
6. Özgün Sunar (1ST March 2021), *What is Linear and Non-Linear Analysis?*, <https://www.mechead.com/what-is-linear-and-nonlinear-analysis/>, accessed on 16 May 2021 at 8:50
7. The constructor, *Concrete Technology*, <https://theconstructor.org/concrete/>, Accessed on 16 May 2021 at 6:08

APPENDIX

APPENDIX A. Tables for Methodology

- Tables for imposed load and reduction factors

Table A. 1. category of use of building (Table 6.1 EN1991-1-1)

Category	Specific Use	Example
A	Areas for domestic and residential activities	Rooms in residential buildings and houses; bedrooms and wards in hospitals; bedrooms in hotels and hostels kitchens and toilets.
B	Office areas	
C	Areas where people may congregate (with the exception of areas defined under category A, B, and D ¹⁾)	<p>C1: Areas with tables, etc. e.g. areas in schools, cafés, restaurants, dining halls, reading rooms, receptions.</p> <p>C2: Areas with fixed seats, e.g. areas in churches, theatres or cinemas, conference rooms, lecture halls, assembly halls, waiting rooms, railway waiting rooms.</p> <p>C3: Areas without obstacles for moving people, e.g. areas in museums, exhibition rooms, etc. and access areas in public and administration buildings, hotels, hospitals, railway station forecourts.</p> <p>C4: Areas with possible physical activities, e.g. dance halls, gymnastic rooms, stages.</p> <p>C5: Areas susceptible to large crowds, e.g. in buildings for public events like concert halls, sports halls including stands, terraces and access areas and railway platforms.</p>
D	Shopping areas	<p>D1: Areas in general retail shops</p> <p>D2: Areas in department stores</p>
<p>¹⁾ Attention is drawn to 6.3.1.1(2), in particular for C4 and C5. See EN 1990 when dynamic effects need to be considered. For Category E, see Table 6.3</p> <p>NOTE 1 Depending on their anticipated uses, areas likely to be categorised as C2, C3, C4 may be categorised as C5 by decision of the client and/or National annex.</p> <p>NOTE 2 The National annex may provide sub categories to A, B, C1 to C5, D1 and D2</p> <p>NOTE 3 See 6.3.2 for storage or industrial activity</p>		

Table A. 2. Imposed loads on floors, balconies and stairs in buildings (Table 6.1 EN1991-1-1)

Categories of loaded areas	q_k [kN/m ²]	Q_k [kN]
Category A		
- Floors	1,5 to <u>2,0</u>	<u>2,0</u> to 3,0
- Stairs	<u>2,0</u> to 4,0	<u>2,0</u> to 4,0
- Balconies	<u>2,5</u> to 4,0	<u>2,0</u> to 3,0
Category B	2,0 to <u>3,0</u>	1,5 to <u>4,5</u>
Category C		
- C1	2,0 to <u>3,0</u>	3,0 to <u>4,0</u>
- C2	3,0 to <u>4,0</u>	2,5 to 7,0 (<u>4,0</u>)
- C3	3,0 to <u>5,0</u>	<u>4,0</u> to 7,0
- C4	4,5 to <u>5,0</u>	3,5 to <u>7,0</u>
- C5	<u>5,0</u> to 7,5	3,5 to <u>4,5</u>
category D		
- D1	<u>4,0</u> to 5,0	3,5 to 7,0 (<u>4,0</u>)
- D2	4,0 to <u>5,0</u>	3,5 to <u>7,0</u>

Table A. 3. The recommended values of factors for buildings (Table A.1.1 of EN 1990.)

Action	ψ_0	ψ_1	ψ_2
Imposed loads in buildings, category (see EN 1991-1-1)			
Category A : domestic, residential areas	0,7	0,5	0,3
Category B : office areas	0,7	0,5	0,3
Category C : congregation areas	0,7	0,7	0,6
Category D : shopping areas	0,7	0,7	0,6
Category E : storage areas	1,0	0,9	0,8
Category F : traffic area, vehicle weight $\leq 30\text{kN}$	0,7	0,7	0,6
Category G : traffic area, $30\text{kN} < \text{vehicle weight} \leq 160\text{kN}$	0,7	0,5	0,3
Category H : roofs	0	0	0
Snow loads on buildings (see EN 1991-1-3)*			
Finland, Iceland, Norway, Sweden	0,70	0,50	0,20
Remainder of CEN Member States, for sites located at altitude $H > 1000$ m a.s.l.	0,70	0,50	0,20
Remainder of CEN Member States, for sites located at altitude $H \leq 1000$ m a.s.l.	0,50	0,20	0
Wind loads on buildings (see EN 1991-1-4)	0,6	0,2	0
Temperature (non-fire) in buildings (see EN 1991-1-5)	0,6	0,5	0
NOTE The ψ values may be set by the National annex. * For countries not mentioned below, see relevant local conditions.			

- **Table for seismic action**

Table A. 4. Reference acceleration at ground level according to the seismicity zone

Seismicity zone	a_{gR}
Very low	0.4
Low	0.7
Moderate	1.1
Medium	1.6
high	3

Table A. 5. Importance coefficient γ_1

building class	importance coefficient γ_1
I	0.8
II	1
III	1.2
IV	1.4

Table A. 6. Soil class

Classe	Description	Paramètres		
		$V_{s,30}$ (m/s)	N (SPT)	Cu (kPa)
A	Rocher, au plus 5 m d'alluvions	> 800	–	–
B	Sable très dense, gravier, argile raide, $h > 10$ m	360-800	> 50	> 250
C	Sable dense, moyennement dense argile raide, $10 \text{ m} < h < 100 \text{ m}$	180-360	15-50	70-250
D	Sable lâche, moyennement dense, argile ferme à molle	< 180	< 15	< 70
E	Alluvion C ou D, $5 \text{ m} < h < 20 \text{ m}$ surmontant rocher A			
S1	Couches contenant states $h > 10 \text{ m}$, argile molle ($IP > 40$) w élevée	< 100 (indicatif)	–	10-20
S2	Sites liquéfiables, tout autre type de site non référencé ci-dessus			

Table A. 7. Soil coefficient

Soil class	S (For seismicity zone 1 to 4)	S (For seismicity zone 5)
A	1	1
B	1.35	1.2
C	1.5	1.15
D	1.6	1.35
E	1.8	1.4

Table A. 8. Values of TB, TC and TD as a function of soil class

Soil class	For seismicity zone 1 to 4			For seismicity zone 5		
	T_B	T_C	T_D	T_B	T_C	T_D
A	0.03	0.2	2.5	0.15	0.4	2
B	0.05	0.25	2.5	0.15	0.5	2
C	0.06	0.4	2	0.2	0.6	2
D	0.1	0.6	1.5	0.2	0.8	2
E	0.08	0.45	1.25	0.15	0.5	2

- **Tables for concrete cover and durability**

Table A. 9. Minimum cover requirements with regard to bond (Table 4.2 of EN 1992-1-1)

Bond Requirement	
Arrangement of bars	Minimum cover $c_{min,b}^*$
Separated	Diameter of bar
Bundled	Equivalent diameter (ϕ_h)(see 8.9.1)

*: If the nominal maximum aggregate size is greater than 32 mm, $c_{min,b}$ should be increased by 5 mm.

Table A. 10. Values of minimum cover requirements with regard to durability for reinforcement steel in accordance with EN 10080 (Table 4.4 of EN 1992-1-1)

Environmental Requirement for $c_{min,dur}$ (mm)							
Structural Class	Exposure Class according to Table 4.1						
	X0	XC1	XC2 / XC3	XC4	XD1 / XS1	XD2 / XS2	XD3 / XS3
S1	10	10	10	15	20	25	30
S2	10	10	15	20	25	30	35
S3	10	10	20	25	30	35	40
S4	10	15	25	30	35	40	45
S5	15	20	30	35	40	45	50
S6	20	25	35	40	45	50	55

Table A. 11. Exposure classes related to environmental conditions in accordance with EN 206-1 (Table 4.1 of EN 1992-1-1)

Class designation	Description of the environment	Informative examples where exposure classes may occur
1 No risk of corrosion or attack		
X0	For concrete without reinforcement or embedded metal: all exposures except where there is freeze/thaw, abrasion or chemical attack For concrete with reinforcement or embedded metal: very dry	Concrete inside buildings with very low air humidity
2 Corrosion induced by carbonation		
XC1	Dry or permanently wet	Concrete inside buildings with low air humidity Concrete permanently submerged in water
XC2	Wet, rarely dry	Concrete surfaces subject to long-term water contact Many foundations
XC3	Moderate humidity	Concrete inside buildings with moderate or high air humidity External concrete sheltered from rain
XC4	Cyclic wet and dry	Concrete surfaces subject to water contact, not within exposure class XC2
3 Corrosion induced by chlorides		
XD1	Moderate humidity	Concrete surfaces exposed to airborne chlorides
XD2	Wet, rarely dry	Swimming pools Concrete components exposed to industrial waters containing chlorides
XD3	Cyclic wet and dry	Parts of bridges exposed to spray containing chlorides Pavements Car park slabs
4 Corrosion induced by chlorides from sea water		
XS1	Exposed to airborne salt but not in direct contact with sea water	Structures near to or on the coast
XS2	Permanently submerged	Parts of marine structures
XS3	Tidal, splash and spray zones	Parts of marine structures
5. Freeze/Thaw Attack		
XF1	Moderate water saturation, without de-icing agent	Vertical concrete surfaces exposed to rain and freezing
XF2	Moderate water saturation, with de-icing agent	Vertical concrete surfaces of road structures exposed to freezing and airborne de-icing agents
XF3	High water saturation, without de-icing agents	Horizontal concrete surfaces exposed to rain and freezing
XF4	High water saturation with de-icing agents or sea water	Road and bridge decks exposed to de-icing agents Concrete surfaces exposed to direct spray containing de-icing agents and freezing Splash zone of marine structures exposed to freezing
6. Chemical attack		
XA1	Slightly aggressive chemical environment according to EN 206-1, Table 2	Natural soils and ground water
XA2	Moderately aggressive chemical environment according to EN 206-1, Table 2	Natural soils and ground water
XA3	Highly aggressive chemical environment according to EN 206-1, Table 2	Natural soils and ground water

- **Tables for SLS verification**

Table A. 12. Recommended values of w_{\max} (mm)

Exposure Class	Reinforced members and prestressed members with unbonded tendons	Prestressed members with bonded tendons
	Quasi-permanent load combination	Frequent load combination
X0, XC1	0,4 ¹	0,2
XC2, XC3, XC4	0,3	0,2 ²
XD1, XD2, XS1, XS2, XS3		Decompression
<p>Note 1: For X0, XC1 exposure classes, crack width has no influence on durability and this limit is set to guarantee acceptable appearance. In the absence of appearance conditions this limit may be relaxed.</p> <p>Note 2: For these exposure classes, in addition, decompression should be checked under the quasi-permanent combination of loads.</p>		

Table A. 13. Maximum bar diameters Φ^* for crack control

Steel stress ² [MPa]	Maximum bar size [mm]		
	$w_k=0,4$ mm	$w_k=0,3$ mm	$w_k=0,2$ mm
160	40	32	25
200	32	25	16
240	20	16	12
280	16	12	8
320	12	10	6
360	10	8	5
400	8	6	4
450	6	5	-

Table A. 14. Maximum bar spacing for crack control

Steel stress ² [MPa]	Maximum bar spacing [mm]		
	$w_k=0,4$ mm	$w_k=0,3$ mm	$w_k=0,2$ mm
160	300	300	200
200	300	250	150
240	250	200	100
280	200	150	50
320	150	100	-
360	100	50	-

APPENDIX B. Structural and architectural plan

- **Architectural plan of the case study**

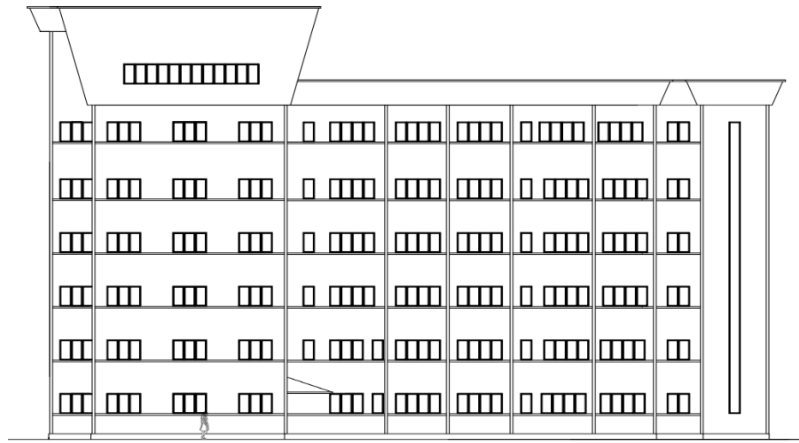


Figure B. 1. Principal side

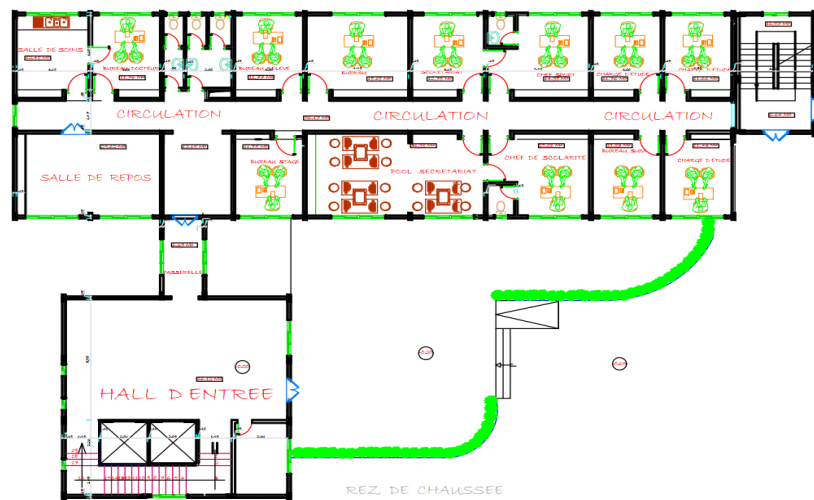


Figure B. 2. Architectural plan of RDC

- **Structural plan of the case study**

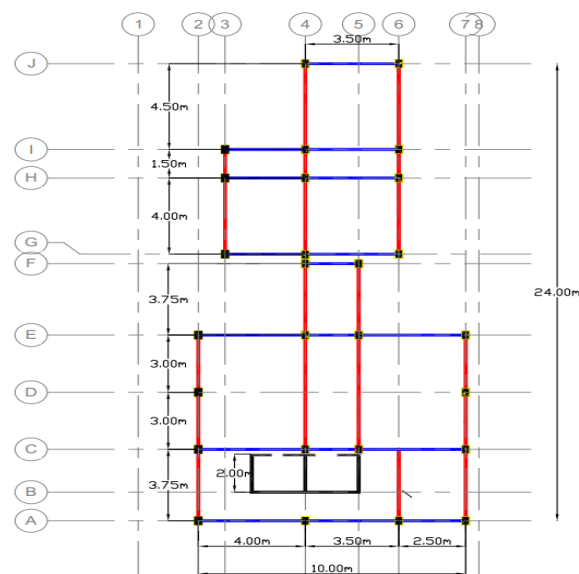
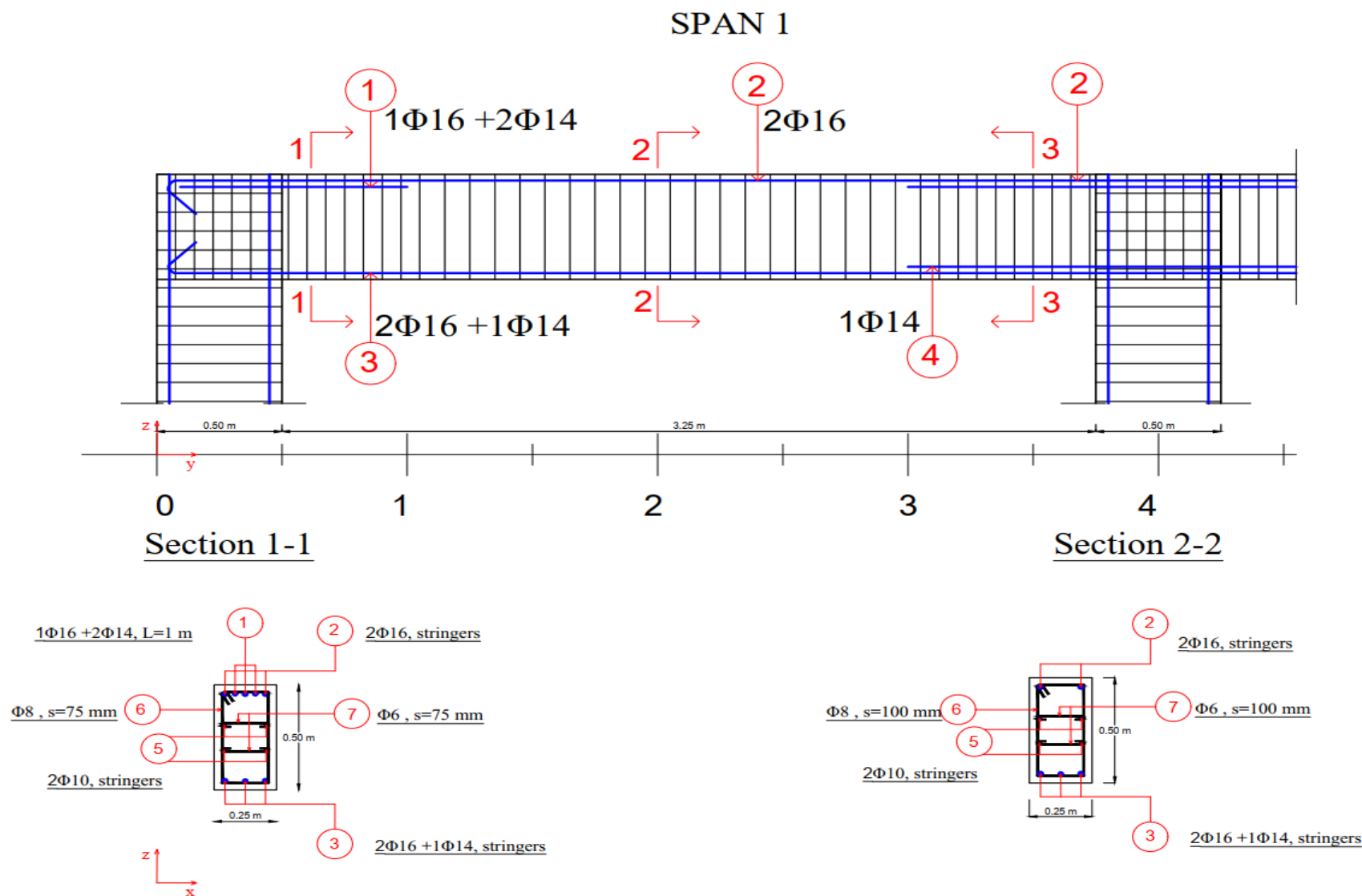


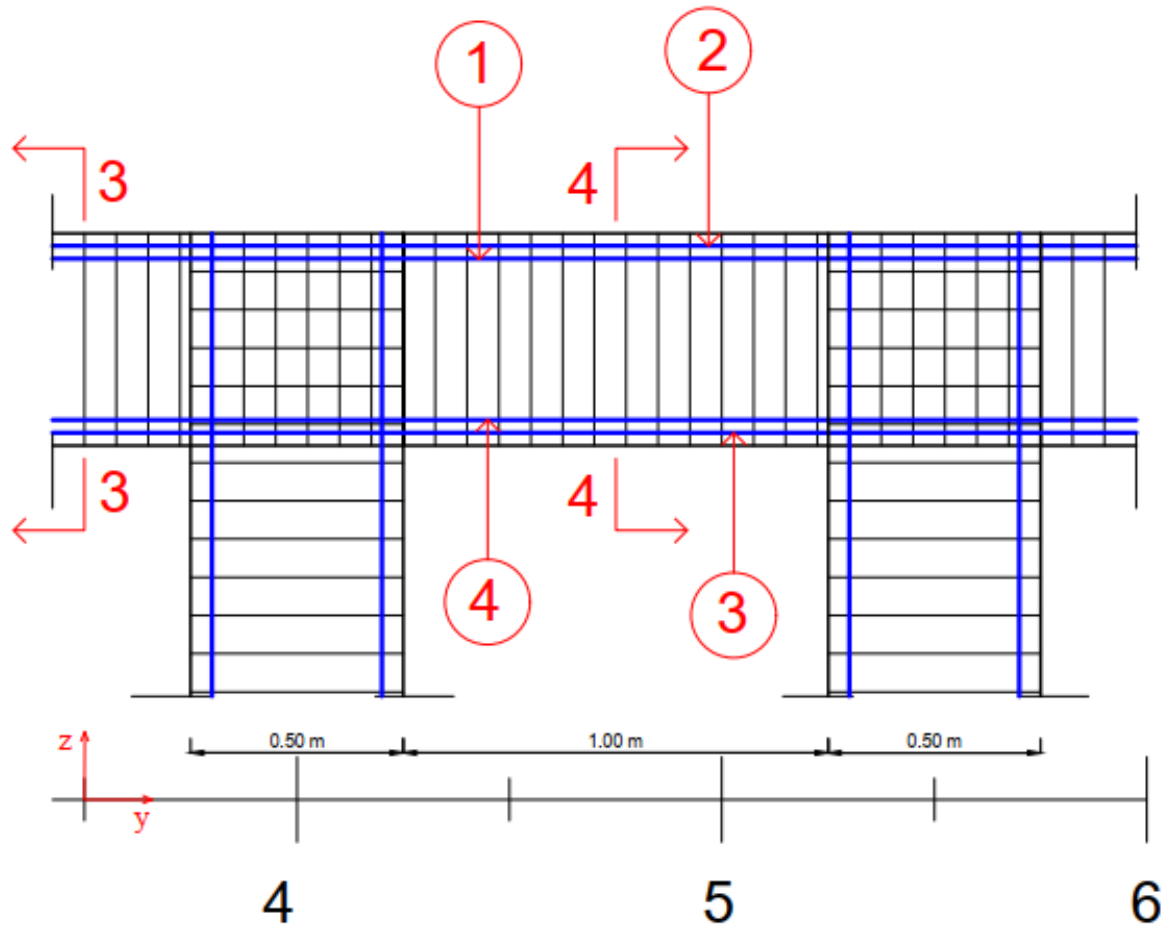
Figure B. 3. Structural plan of storey 6

APPENDIX C. Detailing of structural elements

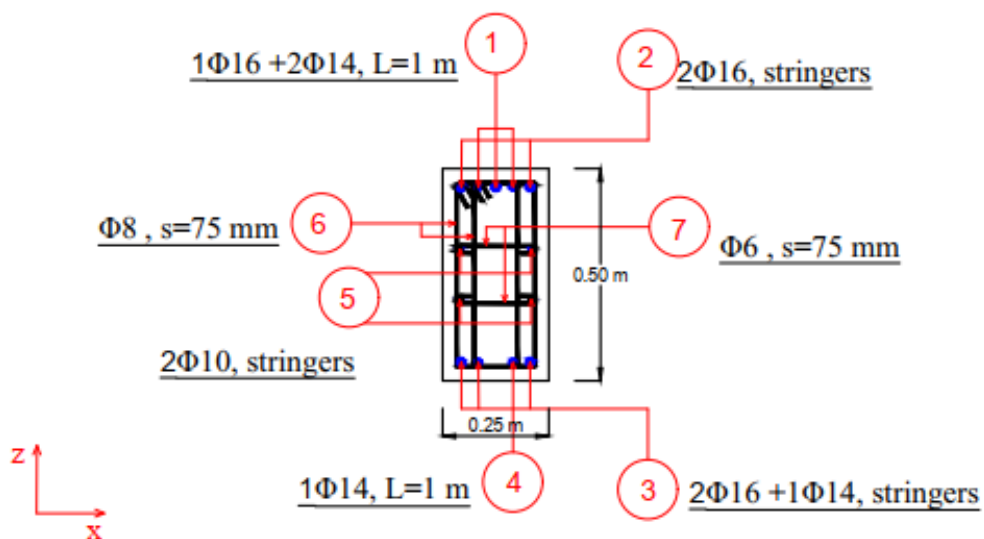
APPENDIX C1. Detailing of the beam



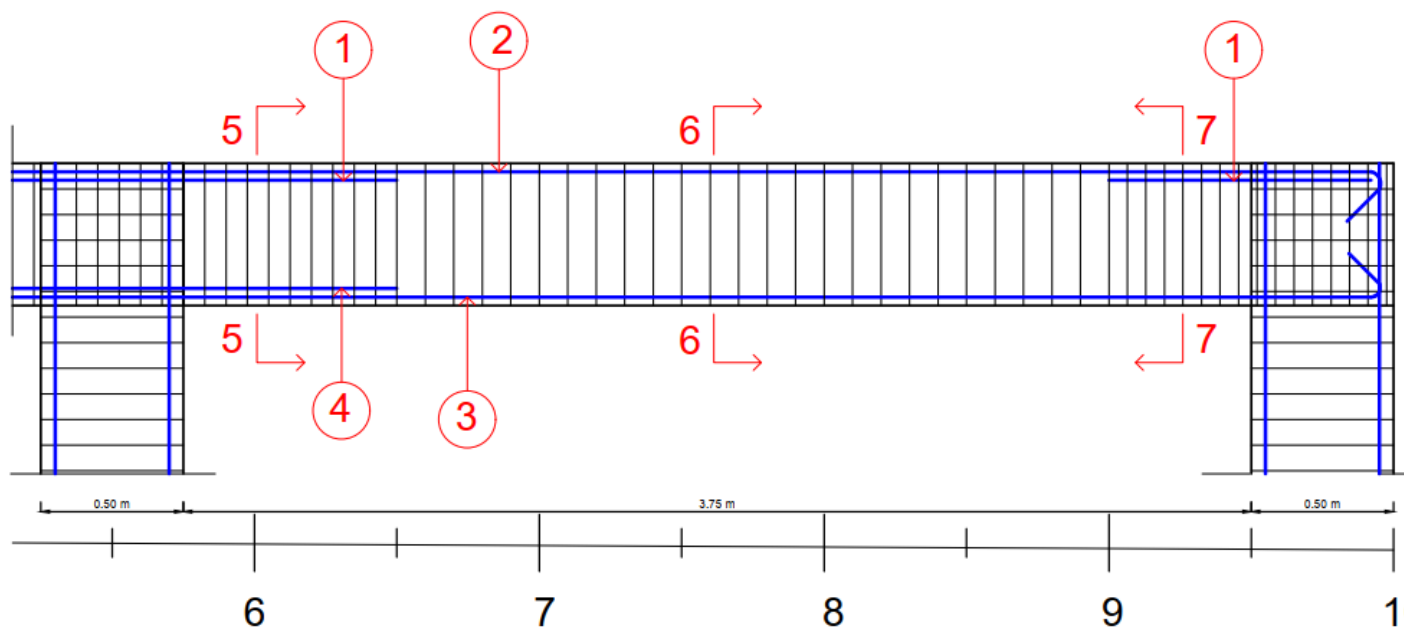
SPAN 2



Section 3-3 = section 4-4



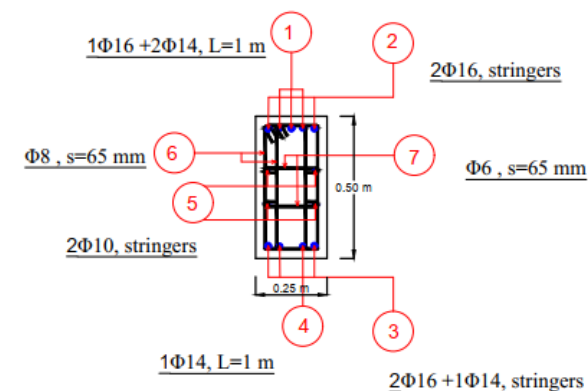
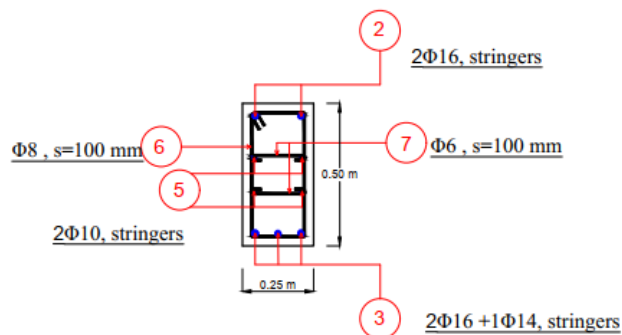
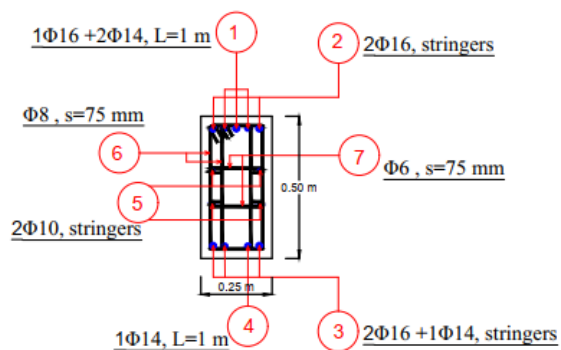
SPAN 3



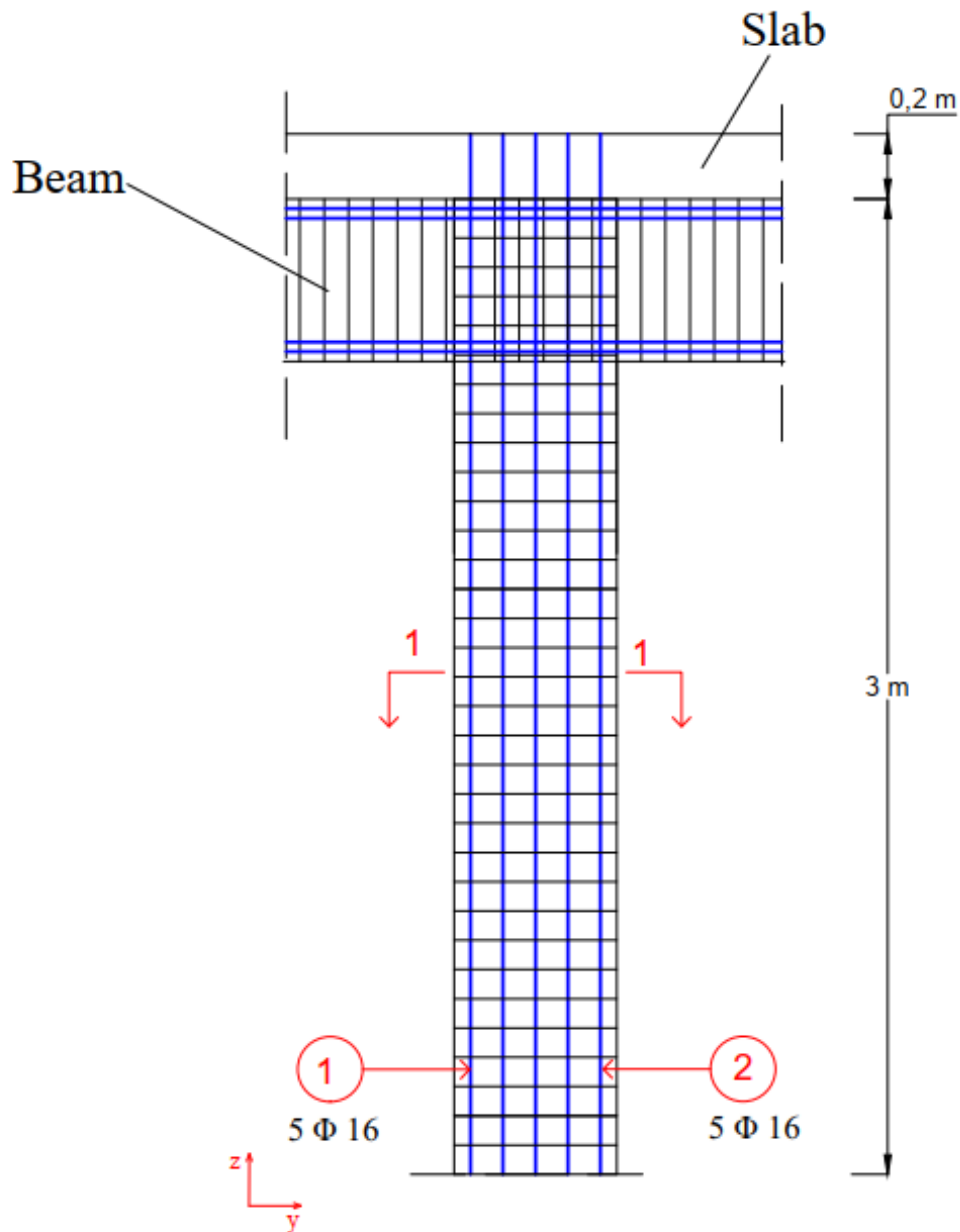
Section 5-5

Section 6-6

Section 7-7



APPENDIX C2. Detailing of column



Section 1-1

